AC-DC LOAD FLOW ANALYSIS FOR DISTRIBUTION SYSTEMS WITH RENEWABLE GENERATIONS

Ph. D. Thesis

by

KRISHNA MURARI

DEPARTMENT OF ELECTRICAL ENGINEERING
INDIAN INSTITUTE OF TECHNOLOGY ROORKEE
ROORKEE – 247667 (INDIA)
JULY, 2019

AC-DC LOAD FLOW ANALYSIS FOR DISTRIBUTION SYSTEMSWITH RENEWABLE GENERATIONS

A THESIS

Submitted in partial fulfilment of the requirements for the award of the degree

of

DOCTOR OF PHILOSOPHY

in

ELECTRICAL ENGINEERING

by

KRISHNA MURARI

DEPARTMENT OF ELECTRICAL ENGINEERING
INDIAN INSTITUTE OF TECHNOLOGY ROORKEE
ROORKEE – 247667 (INDIA)
JULY, 2019

©INDIAN INSTITUTE OF TECHNOLOGY ROORKEE, ROORKEE-2019
ALL RIGHTS RESERVED

INDIAN INSTITUTE OF TECHNOLOGY ROORKEE

STUDENT'S DECLARATION

I hereby certify that the work presented in the thesis entitled "**AC-DC LOAD FLOW ANALYSIS FOR DISTRIBUTION SYSTEMS WITH RENEWABLE GENARTIONS"** is my own work carried out during a period from December, 2014 to July, 2019 under the supervision of Dr. Narayana Prasad Padhy, Professor, Department of Electrical Engineering, Indian Institute of Technology Roorkee, Roorkee.

The matter presented in the thesis has not been submitted for the award of any other degree of this or any other Institute.

(KRISHNA MURARI)

Dated: **August 26, 2019**

SUPERVISOR'S DECLARATION

This is to certify that the above mentioned work is carried out under my supervision.

(Narayana Prasad Padhy)
Supervisor

Dated: **August 26, 2019**

The Ph. D. Viva-Voce Examination of Krishna Murari, Research Scholar, has been held on **August 26, 2019**.

Chairperson, SRC **External Examiner**

This is to certify that the student has made all the corrections in the thesis.

Supervisor **Head of the Department**

Dated:**August 26, 2019**

Abstract

In the late 1880s, two exceptionally brilliant inventors, Nikola Tesla and Thomas Edison embroiled in a battle for establishing the preeminence of alternating current (AC) and direct current (DC) systems respectively. But due to the numerous advantages of AC over DC during that period, the latter was forced out of the competition and AC emerged victorious. Since then, AC system has dominated all the relevant field (viz. generation, transmission and distribution) of the power system. However, with the recent developments in the area of power electronic devices and renewable energy technologies, interest in DC system is revoked. In areas such as long distance transmission, energy storage systems etc., DC has undoubtedly proved its edge over the AC system. Power generation, for which AC was considered to be superior to DC, is now inclining towards DC due to deployment of renewable energy technologies. On the load side of the power system, electronic loads have significantly increased in recent times. The result is a tremendous increase in DC power consuming devices. In the current scenario, there are various advantages of DC over AC system, but the complete reinforcement of existing distribution system into DC seems to be impossible at this stage. The reason is, the existing distribution systems is mostly AC. So researchers are planning a hybrid distribution system (AC-DC distribution system) with both AC and DC grids.

For proper planning, analysis and optimal operation of transmission or distribution system, a power flow or load flow study has to be carried out. Therefore, power-flow/load-flow algorithm for AC-DC distribution system is highly required. However, load flow in such systems is a challenging task due to non linear characteristics of power converters. There are well established algorithms for load flow solution of AC transmission systems, AC-DC transmission systems and for AC distribution systems but for AC-DC distribution systems till date not much work has been reported. The proposed work aims for the development of a load flow algorithm for AC-DC distribution network

To acquire the theme objective of this thesis, firstly a power flow algorithm for AC distribution system has been developed utilising the concept of graph theory and matrix algebra. The developed load flow methodology is capable of handling any kind of AC

distribution network viz. radial, meshed, single phase and three phase distribution network. It requires the conventional bus-branch oriented data as the only input. Seven developed matrices, loads beyond branch matrix (*LB*), load current matrix (*LC*), feeder current matrix (*FC*), path impedance matrix (*PI*), path drop matrix (*PD*), slack bus to other buses drop matrix (*SBOBD*), load flow matrix (*LFM)* and simple matrix operations are utilized to obtain load flow solutions. In contrast with traditional load flow methods for HVDC systems, the proposed technique does not require any lower upper (LU) decomposition, matrix inversion and forward-backward substitution of Jacobian matrix. Because of the aforementioned reasons, the developed technique is computationally efficient. In case of meshed &/or ring network they should be converted to equivalent radial network by breaking the loops. The loop breakpoint matrix/sensitivity matrix has been derived to calculate the net breakpoint injection to mimic the effect of meshed network in the radial scenario. Thus equivalent radial network will have to take into account the loop breakpoint injection. The additional breakpoint injections are reflected in the *LB* or *LC* matrix. Once, the meshed network is converted to radial network, the relevant matrices formulation and load flow procedure are carried out in same manner as the radial distribution network. For three phase unbalanced distribution network, the relevant matrices has been modified as per three phase scenario. The effectiveness of the proposed solution methodology has been tested on several standard distribution systems. Test outcome reveal efficiency and authenticity of the proposed research work.

Subsequently, the developed load flow algorithm has been further extended for solving the load flow problem of AC distribution network with various model of distributed generations. The mathematical model of DG considered as PQ and PV buses are incorporated into the proposed algorithm to imitate the injection of DGs in the distribution systems. The power injected by the DG need to be reflected in the LB matrix of the distribution network. For the PV type buses or distributed generators, the reactive power generation is adjusted between the maximum and minimum limits in order to maintain the constant voltage and constant real power (injected) at the PV bus. The breakpoint matrix has been utilized to obtain the additional reactive power injection/withdrawal to maintain the specified voltage at each PV nodes. In the case of weakly meshed distribution network with PV type distributed generations, the loop breakpoint injections and PV breakpoint injections have been calculated

simultaneously. The net injections is reflected in the *LB* or *LC* matrix of the distribution network. Note that except for some modifications needed to be done for the *LC* or *LB* matrices, the proposed solution techniques require no modification; therefore, the proposed method can obtain the load-flow solution for AC distribution system in the presence of distributed generations efficiently. The remaining supporting matrices will reshape themselves accordingly. The effectiveness of the proposed algorithm has been tested on several standard distribution systems. Test outcome reveal viability and accuracy of the proposed research work.

The AC load flow algorithm developed in this thesis work has been modified in a manner such that it can easily be extended for load flow calculation of AC-DC radial distribution systems with distributed generations. For our purpose, the AC-DC distribution network has been subdivided into a number of sub-distribution systems or sub-regions depending on number of bus-bus interfacing converters present in the distribution system. Each sub-region will act as separate distribution system. These regions or sub distribution systems can be interconnected in different hybrid configuration. The relevant matrices formulation as discussed above has to be carried out for each sub-region separately. The per unit equivalent model of three-phase PWM AC/DC converter, PWM DC-DC converter and three-phase AC-DC LCC converter have been proposed in this section. The mathematical model of DGs considered as P, PQ, PV and V^{dc} buses are incorporated into the proposed algorithm to imitate the injection of DGs in the AC-DC distribution systems. The power injected by the DG need to be reflected in the LBg or LCg matrix of the AC-DC distribution network. The sensitivity or breakpoint matrix has been utilized to obtain the additional reactive power injection/withdrawal to maintain the specified voltage at each PV nodes. Similarly, when V^{dc} nodes are present in DC regions of an AC-DC distribution network, the correct amount of active power injection by the generation units is calculated to compensate the variance between obtained and specified voltage. The V^{dc} sensitivity or breakpoint matrix has been utilized to obtain the additional real power injection/withdrawal to maintain the specified voltage at each V^{dc} nodes. Once the net injection by the DGs is calculated, the load flow solution of active distribution system will be carried out in the same manner as load flow solution of distribution system without DGs.

Subsequently, the developed load flow algorithm has been further extended for solving the load flow problem of AC-DC meshed distribution network with various model of distributed generations. There can exist three kinds of meshes in an AC-DC distribution network.

(a) Mesh consisting of only AC buses in an AC sub-region is called as type 1 mesh.

(b) Mesh consisting of only DC buses in a DC sub-region is called as type 2 mesh.

(c) Mesh consisting of both AC and DC buses or only DC buses with different voltage levels are called as type 3 mesh.

The procedure for calculating injected current/injected power will be different for the different meshed configurations. Suitable procedure has been developed for calculating the loop breakpoint injections for these three kind of loops in the AC-DC distribution network. The additional breakpoint injections are reflected in the LBg or LCg matrix (as per the injected quantity calculated). Once, the meshed AC-DC network is converted to its equivalent radial network, the relevant matrices formulation and load flow procedure are carried out in same manner as the radial AC-DC distribution network. In the case of weakly meshed distribution network with PV and V^{dc} type distributed generations, the loop breakpoint injections and PV breakpoint injections have been calculated simultaneously. Test results signifies the efficacy and accuracy of the developed load flow algorithm.

In order to prove the applicability of the load flow algorithm, a power flow based Distribution use of systems (DUoS) charging methodology has been developed to investigate the impact of protection system reinforcement costs on the consumers associated with renewable integrated distribution network. Conventional distribution network is a radial network with a single power source. Usually overcurrent protection schemes are employed for such system protection for their simplicity and low-cost. With the introduction of renewable generations, the existing protection coordination needs to be upgraded. Provision of directional feature and the requirement of high capacity circuit-breakers at certain points for the protection scheme demands considerable investment. The renovation cost required for upgrading the protection scheme will significantly impact the network cost requirement and consequently distribution use of system (DUoS) charges. This thesis works also aims to investigate the impact of renewable generations on the DUoS charges considering the cost associated in revamping the protection scheme. A power flow based MW+MVAr-Miles

DUoS charging method, that considers used capacity of the network, is proposed to carry out the DUoS charging calculations. The proposed charging mechanism appraise/penalise the users in accordance they are affecting system power factor. Accordingly, the proposed pricing algorithm may encourage users to act based on the economic signal generated at each location. The proposed charging algorithm has been tested on various standard systems to examine the impact of renewable generations on the use of network costs.

Acknowledgements

With GOD's grace I have got this opportunity to thanks all those who have supported me all through this course of work. First and foremost, I would like to express my deepest sense of gratitude towards my supervisor Dr. Narayana Prasad Padhy, Professor, Department of Electrical Engineering, Indian Institute of Technology Roorkee, Roorkee, India for his patience, inspiring guidance, constant encouragement, moral support, and keen interest in minute details of the work. I am sincerely indebted to him for his pronounced individuality, humanistic and warm personal approach, and excellent facility provided to me in the laboratory to carry out this research. It was a great experience working with him.

I also express my sincere gratitude towards my research committee members Dr. C.P. Gupta (Associate Professor, Department of Electrical Engineering & Chairman SRC), Dr. G. B. Kumbhar, (Associate Professor, Department of Electrical Engineering & Internal expert), Dr. N. Sukavanam (Professor, Department of Mathematics & External Expert) for their invaluable direction, encouragement and support, and above all the noblest treatment extended by them during the course of my studies at IIT Roorkee.

I heartily extend my gratitude to Head of the Department of Electrical Engineering, and all faculty members of the department for their help, moral support, and providing the excellent infrastructure, laboratory and computing facility for the research work.

I wish to extend my sincere thanks to Prof. Ashok Kumar Pradhan, Department of Electrical Engineering, Indian Institute of Technology Kharagpur, Kharagpur, India, and Prof. Furong Li, Electronics and Electrical Engineering Department, University of bath, United Kingdom, for their valuable inputs .

I acknowledge my gratitude to Ministry of Human Resource Development, Government of India, for providing the financial support to carry out this research work. I also sincerely acknowledge the support and facilities provided by US-India collAborative for smart diStribution System with STorage (UI-ASSIST) project sponsored by IUSSTF, India to carry out research on present need of globe.

My journey in IIT Roorkee is blessed with many friends who played a major role in maintaining a constantly high level of motivation, and thus in the progress of my work. First

I would like to thank all my seniors especially to Dr. Jitendra Kumar, Dr. Arun Balodi, Dr. Yogesh Sariya, Dr. Om Hari Gupta, Dr. Ankit Singh, Dr. Santosh Singh and Dr. Ksh Milan Singh for supporting me during the whole period. I extend my sincere thanks to my colleagues Dr. Utkarsh Singh, Dr. Pannala Sanjeev, Dr. Yogesh Makwana, Mr. Gaurav, Mr. Chinmaya K.A, Mr. Jose Thankachan, Mr. Kanhaiya Kumar, Mr. Sanjay Kumar, Mr. Potturu Sudharsana Rao, Mr. M.V Gururaj, Mr. Bandla Krishna Chaithanya, Mr. Saran Satsangi, Mr. Subho Paul, Mr. Vishal Gaur, Mr. Soumitri Jena, Ms. Rinalini, Ms. Rashmi, Mr. Narendra Babu, Mr. Nitin, Mr. Arpit, Mr. Abhimanyu, Mr. Phanindra, Mr. Ashish, Mr. Suresh, Mr. Srikanth, Ms. shatabdy Jena, Mr. Subraniam, Ms. Tripti, Mrs. Kartika and many more for supporting me during my research work.

I would also like to thank all the administrative & technical staff of the Department of Electrical Engineering, Indian Institute of Technology Roorkee, Roorkee for their cooperation and necessary facility provided to me to carry out this research work.

I owe a debt of gratitude to my parents, Shri Ram Kishore Pandey and Smt. Ranju Pandey, my brother Sudhanshu Kumar, for their endless support, encouragement, patience and care.

No words can adequately express my deepest gratitude and love to my wife Smt. Kumari Sonam for her unconditional support, encouragement, love and inspiration and always being there for me in good and bad times. Words can hardly express the cooperation and patience of my son, Yuvaan. I could not spare much time for him till now, as I was busy in my research work. His innocent face boosted me up, made me smile and encourage me to work hard.

Last but not the least; I am thankful to lord Shiva who gave me the strength and health for completing the work.

(KRISHNA MURARI)

Contents

List of Figures

List of Tables

List of Symbols

m	Total number of branches.
n	Total number of buses.
b	Branch number (1,2…….m).
k	Node number (1,2…….n).
V(k)	Voltage at node number k.
IL(k)	Load current at bus number k.
IM	Incidence matrix
LB	Loads beyond branch matrix.
BB	Buses beyond branch matrix.
FC	Feeder current matrix.
PI	Path impedance matrix
P	Path matrix.
PD	Path drop matrix
SBOBD	Slack bus to other buses drop matrix.
U	Binary matrix
LFM	Load Flow Matrix
V	Voltage matrix at beginning of a iteration.
V_{new}	Voltage matrix at the end of a iteration.
R(b)	Resistance of branch *b*
Z(b)	Impedance of branch number b.
E	Total number of extreme nodes in the distribution system.
s	Total number of power flow paths.

S(k)	Complex power of load at bus k.
P(k)	Real power of load at bus k.
Q(k)	Reactive power of load at bus k.
ε	Tolerance
DVMAX	Maximum voltage difference.
i	Row number of a matrix.
j	Column number of matrix.
SD	System data matrix
SN	Sending end node
RN	Receiving end node
S(RN)	Complex power at RN node
I(b)	Current through branch number b
PVB	Set of all PV buses
pvb	Total number of PV buses in a distribution network
PVB_K	K^{th} element of set *PVB*
K	Position of PV buses in set PVB (1, 2, 3.....*pvb*)
$V(PVB_K'')^t$	Voltage magnitude (specified) at bus PVB_K associated with PV distributed generation number *K* .
$V(PVB_K)^t$	Voltage magnitude (calculated) at bus PVB_K associated with PV distributed generation number *K* in the beginning of iteration *t.*
$\Delta V(PVB_K)^t$	Voltage magnitude mismatch at bus PVB_K associated with PV distributed generation number *K* in the beginning of iteration *t.*
$\Delta I(PVB_K)^t$	Additional complex current injection at bus PVB_K associated with PV distributed generation number *K* in the beginning of iteration *t.*

$\Delta I^{q}(PVB_K)$	Additional reactive current injection at bus PVB_K associated with PV distributed generation number *K* in the beginning of iteration *t.*
$\Delta I^{r}(PVB_K)$	Additional real current injection at bus PVB_K associated with PV distributed generation number *K* in the beginning of iteration *t.*
$TI(PVB_K)^{t}$	Total reactive current injection at bus PVB_K associated with PV distributed generation number *K* in the beginning of iteration *t.*
$\Delta Q(PVB_K)^{t}$	Additional reactive power injection at bus PVB_K associated with PV distributed generation number *K* in the beginning of iteration *t.*
$TQ(PVB_K)^{t}$	Total reactive power injection at bus PVB_K associated with PV distributed generation number *K* in the beginning of iteration *t.*
MB	Set of all loops
mb	Total number of loop breakpoint in the network
MB_d	d^{th} element of set *MB*
d	Mesh breakpoint number (1, 2, 3.....*mb*)
MB_d and MB_d"	Twp end of mesh breakpoint *d*
$V(MB_d")^{t}$	Voltage magnitude at bus MB_d" associated with mesh breakpoint number *d* in the beginning of iteration *t.*
$V(MB_d)^{t}$	Voltage magnitude at bus MB_d associated with mesh breakpoint number *d* in the beginning of iteration *t.*
$\Delta V(MB_d)^{t}$	Voltage mismatch (real part) between MB_d" and MB_d in the beginning of iteration *t*
$\Delta\delta(MB_d)^{t}$	Voltage mismatch (imaginary part) between MB_d" and MB_d in the beginning of iteration *t*
$\Delta I(MB_d)^{t}$	Additional complex current injection at bus MB_d in the beginning of

	iteration *t.*
$\Delta I^{q}(MB_d)$	Additional reactive current injection at bus MB_d in the beginning of iteration *t.*
$\Delta I^{r}(MB_d)$	Additional real current injection at bus MB_d in the beginning of iteration *t.*
$TI(MB_d)^{t}$	Total complex current injection at bus MB_d in the beginning of iteration *t.*
$\Delta Q(MB_d)^{t}$	Additional reactive power injection at bus MB_d in the beginning of iteration *t.*
$\Delta P(MB_d)^{t}$	Additional real power injection at bus MB_d in the beginning of iteration *t.*
$\Delta S(MB_d)^{t}$	Additional complex power injection at bus MB_d in the beginning of iteration *t.*
$TQ(MB_d)^{t}$	Total reactive power injection at bus at bus MB_d in the beginning of iteration *t.*
$TP(MB_d)^{t}$	Total real power injection at bus at bus MB_d in the beginning of iteration *t.*
VDC	Set of all V^{dc} buses
vdc	Total number of V^{dc} buses in a distribution network
VDC_W	W^{th} element of set *VDC*
W	Position of V^{dc} buses in set VDC (1, 2, 3.....*vdc*)
$V(VDC_W")^{t}$	Voltage magnitude (specified) at bus VDC_W associated with V^{dc} distributed generation number W.
$V(VDC_W)^{t}$	Voltage magnitude (calculated) at bus VDC_W associated with V^{dc} distributed generation number W in the beginning of iteration *t.*
$\Delta V(VDC_W)^{t}$	Voltage magnitude mismatch at bus VDC_W associated with V^{dc}

	distributed generation number W in the beginning of iteration *t.*
$\Delta I(VDC_W)^t$	Additional complex current injection at bus VDC_W associated with V^{dc} distributed generation number W in the beginning of iteration *t.*
$\Delta I^q(VDC_W)$	Additional reactive current injection at bus VDC_W associated with V^{dc} distributed generation number W in the beginning of iteration *t.*
$\Delta I^r(VDC_W)$	Additional real current injection at bus VDC_W associated with V^{dc} distributed generation number W in the beginning of iteration *t.*
$TI(PVB_K)^t$	Total V^{dc} breakpoint current injection at bus VDC_W associated with V^{dc} distributed generation number W in the beginning of iteration *t.*
$\Delta P(VDC_W)^t$	Additional real power injection at bus VDC_W associated with V^{dc} distributed generation number W in the beginning of iteration *t.*
$TP(PVB_K)^t$	Total V^{dc} breakpoint real power injection at bus VDC_W associated with V^{dc} distributed generation number W in the beginning of iteration *t.*
X_{abc}	Three phase vector or matrix of any quantity say X
MI	Modulation index
α	Firing angle
D	Duty Ratio
η	Efficiency of the converter
C	Total sub-regions of an AC-DC distribution network
g	Sub-region number
LB_g	Loads beyond branch matrix of the sub-region g of an AC-DC network
PI_g	Path impedance matrix of the sub-region g of an AC-DC network
LC_g	Load current matrix of the sub-region g of an AC-DC network
FC_g	Feeder current matrix of the sub-region g of an AC-DC network

PD_g	Path drop matrix of the sub-region g of an AC-DC network
PD_g	Slack bus to other buses drop matrix of the sub-region g of an AC-DC network
U_g	Binary matrix of the sub-region g of an AC-DC network
LFM_g	Load flow matrix of the sub-region g of an AC-DC network
V_g	Voltage matrix of the sub-region g at beginning of a iteration *t.*
$V_{g(new)}$	Voltage matrix the sub-region g at the end of a iteration *t*.
c	Facility number (1,2…….m).
m	Total number of facilities/branches in the distribution system.
T	Bus number/customer bus location number/customer number.
C_f	Total cost of facility f .
AF	Annuity factor.
S_f	MVA flow through facility f at its operating capacity.
$S_{\max(f)}$	MVA flow through facility f at its rated capacity.
θ_f	Angle between real and reactive power flowing through facility f operating at its operating capacity.
θ_{mf}	Angle between real and reactive power flowing through facility f at its rated capacity.
U_f	Unit cost to support 1MVA flow in the facility *f.*
$ACR_{P,f}$	The facility f annual chargeable cost owing to actual active power flowing through it.
$ACR_{Q,f}$	The facility f annual chargeable cost owing to actual reactive power flowing through it.
C_P	Total network chargeable cost due to active power flowing in the network
C_Q	Total network chargeable cost due to reactive power flowing in the network .

CC_T	Total annual cost/rate charged to the network user T.
L_f	Length of the facility *f*.
UNC	Total annual unrecovered network cost.
CC(*TP*)	Charges to be paid by network users T for the extent of use of network with respect to their real power.
CC(*TQ*)	Extent of use of network cost for customer T with respect to their reactive power.

List of Abbreviations

DGs	Distributed Generations
RGs	Renewable Generations
DUoS	Distribution Use of System
PM	Proposed Method
BFS	Backward Forward Sweep
LF	Load Flow
AC	Alternating Current
DC	Direct Current
Fig.	Figure
CPLM	Constant Power Load Model
CCLM	Constant Current Load Model
CZLM	Constant Impedance Load Model
ExpLM	Exponential Load Model
LCC	Line Commutated Converter

Chapter-1

Introduction

This chapter begins with an introduction to the AC-DC distribution system, followed by the motivation to the research work carried out in this thesis. It also illustrates the review of prior literature to the work that has been carried out in this thesis. Contribution of author pertinent to formulation of load flow solution algorithm for AC-DC distribution systems are given. Organisation of thesis is explained in the end.

1.1 Background and Motivation

Few decades ago, there was a constant competition between AC and DC systems [1-2]. But owing to the numerous advantages of AC over DC, the latter was forced out of the competition and AC emerged victorious [3]. Owing to the ever increasing demand, declining conventional energy sources and improvements in incorporating deeper penetrations of renewable energy sources into the grid, interest is invoked again towards DC systems [4]. In some area such as transmission at long distances, energy storage systems, etc. DC has undoubtedly proved its edge over the AC system [3]. Power generation, for which AC was considered to be superior to DC, is now inclining towards DC due to deployment of renewable energy technologies such as photovoltaic (PV), wind energy etc [5-6]. On the load side of the power system, DC loads have witnessed a remarkable surge in the recent times [6-7]. The result is a tremendous increase in use of DC power devices. In the current scenario, there are various advantages of DC over AC system [8]:

1. Reactive voltage drop is eliminated in DC distribution system.
2. Synchronization of the multiple loads and sources (phase angles) is not required.
3. Higher power transfer capability is achieved compared to ac distribution system.
4. Greater energy efficiency.
5. Higher power quality.

But the complete reinforcement of existing distribution system into DC seems to be impossible at this stage [9]. The reason is, the existing distribution systems is mostly AC. So

researchers are planning a hybrid distribution system with both AC and DC grids. The merits of using DC power in conjunction with AC power in distribution system have been revealed in some recent studies [10]-[14].

The AC-DC distribution systems have different structural view compared to an AC distribution system. The power converters are one of the major components which compels to realize the possibility of AC-DC distribution systems. It also consists of a variety of AC and DC components, including loads, generating units, lines, and buses. All the buses in an AC-DC distribution network can be either AC or DC, as shown in Fig. 1. In addition to traditional AC loads and AC generators, it can also include DC loads, such as electric vehicles (EVs,) and DC sources, such as PV panels (as evident from Fig. 1.2).

Note- The PWM and DC-DC converters can achieve better control objectives than line commutated bridge converter (LCC) at the distribution level. Hence, these converters can be used between buses (bus-bus interfacing) as well between DG and bus (DG-bus interfacing) for transferring power, fulfilling the requisite control objectives. In the scenario, where control objectives are not highly needed, bridge converter can be used between buses as bus-bus interfacing (but not as DG-bus interfacing) converter.

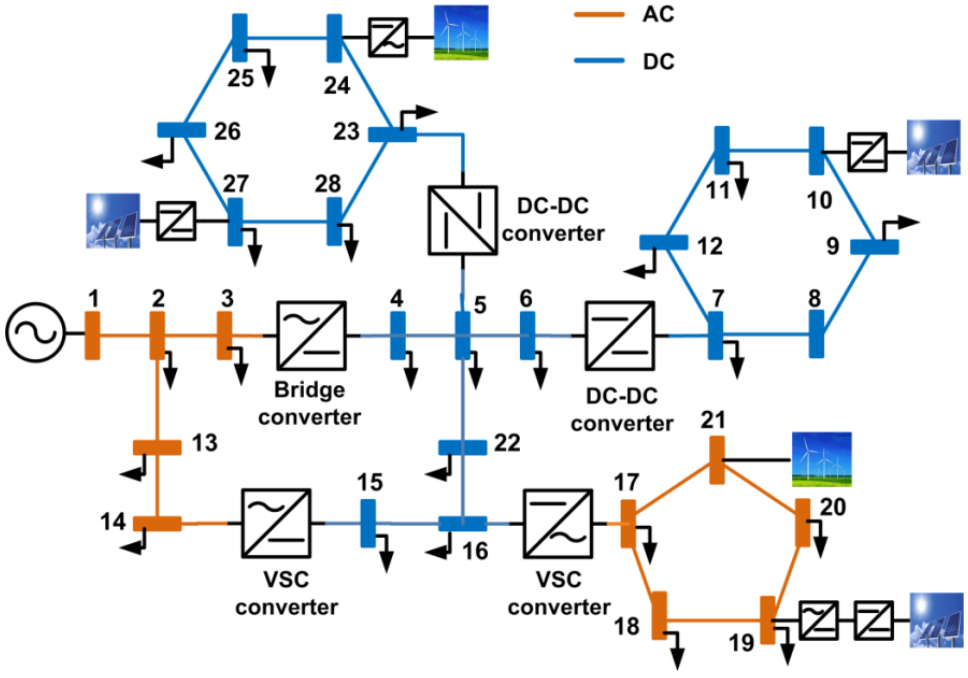

Fig. 1.1: Single line diagram of an AC-DC distribution network.

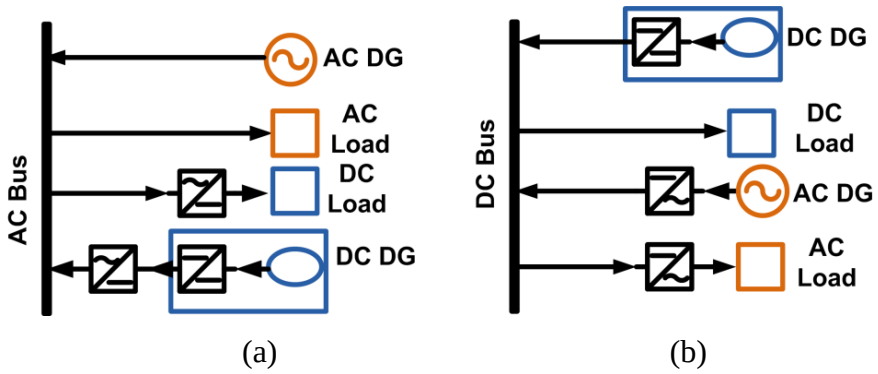

(a) (b)

Fig. 1.2: Various types of loads and generations connection to (a) an AC bus (b) a DC bus.

For proper planning, analysis and optimal operation of transmission or distribution system, a power flow or load flow study has to be carried out. Therefore, power-flow/load-flow algorithm for AC-DC distribution system is highly required. However, load flow in such systems is a challenging task due to non linear characteristics of power converters. There are well established algorithms for load flow solution of AC transmission system, AC-DC transmission systems and for AC distribution system but for AC-DC distribution systems till date not much work has been reported. In this research work, a load flow algorithm for AC-DC distribution system in the presence of distributed generations has been presented. The purpose of this research work is to develop a formulation which embed advantages of the topological aspects of AC-DC distribution system and solves the load flow problem directly utilising the concept of graph theory and matrix algebra.

1.2 Literature Review

The power flow study is, mainly, carried out to obtain the magnitude and the phase angle of the voltage at each bus and the real and the reactive power flow through each line. Applications, especially in the fields of power-system optimization and distribution automation, require repeated, fast power-flow solutions [15]. Due to the large number of interconnections and continuously increasing demand, the size and complexity of the present-day power systems have grown tremendously. Therefore, it is becoming increasingly tedious and time consuming to obtain power-flow solutions.

In the literature survey several conventional methodologies viz. Gauss-Seidel (GS) based iterative method [16-17], the Newton-Raphson (NR) method [16, 18-19], and the fast-decoupled (FDLF) based methods [16, 20-23], have been widely adopted for solving the power flow problem of purely AC transmission network.

Further these conventional methodologies have been modified as per requirement for solving load flow problem of AC-DC transmission or HVDC systems. In general, two basic approaches have been reported for the load flow solution of AC-DC transmission network: sequential [24-28] and unified methods [29-35]. The major difference between the above mentioned approaches lies in the integration procedure of AC and DC system equations. The sequential method solves the DC system equations and AC system equations separately. In the unified method, the DC system equations are incorporated into the equations of the AC system, and then complete set of equations are solved all together.

Various load flow algorithms have prioritized the aforementioned concepts. For example, the load flow techniques developed in [24] and [25] have utilized the sequential approach for solving AC and DC power flow equations independently until boundary conditions of the converters are satisfied. In [26-27], the authors have modified Gauss–Siedel algorithm for solving AC-DC load flow equation sequentially. Furthermore in [28], both Newton-Raphson (NR) algorithm and Broyden approach have been used for solving the nonlinear AC-DC load flow equations. Since, the sequential method is obscure and has a complex computational procedure, an integrated traditional approach was presented in subsequent studies [29]-[35].

The aforementioned approaches (sequential and integrated) have utilized one of the existing traditional load flow methods for solving load flow equations, viz. Gauss–Siedel, Newton Raphson (NR), and Fast decoupled methods. The mentioned power flow algorithms are not suitable for solving AC-DC distribution system load-flow equations [36]. The reasons are: (a) High R/X ratio in the AC sub-regions of the AC-DC distribution network. (b) High loading level of the distribution feeder, (c) Sparse nature of admittance (Y-bus) matrix, (d) Radial and/or weakly meshed structure of the AC-DC distribution network, (e) The assumptions necessary for the simplifications used in the standard fast-decoupled and Newton-Raphson method are often not valid for distribution systems, (f) Lower and upper (LU) decomposition, matrix inversion and forward/backward substitution of admittance matrix requires significant amount of time and thus leading to poor convergence

characteristics of traditional methods.

In view of the above, it is very much clear to the power system researchers that the distribution system has to be handled in a different way. And, as a consequence of continuous research efforts initiated by the previous researchers for many years, numerous load flow solution algorithms are now available in the literature to analyze the distribution system load flow problem.

These reported methods for AC distribution system can be, broadly, classified into three categories:

1. Modified Newton-Raphson and Fast Decoupled based LF methods.
2. Backward/forward sweep based LF methods.
3. Direct LF methods.

Conventional Newton-Raphson and Fast decoupled load flow method are inefficient in handling distribution network load flow problem as the distribution networks are ill-conditioned. However many researchers have proposed modified versions of conventional load flow method for distribution load flow solution has been proposed in [37]. The above mentioned technique is quite simple, devoid of mathematical approximations, and does not require additional storage and calculation time when integrated into the standard Newton-Raphson algorithm. In [38], authors have represented branch voltages in the form of state variables for formulation of constant Jacobian matrix and utilizing the conventional Newton-Raphson method to achieve load flow solution of distribution systems. Authors in [39], introduced a piecewise parallel solution to the Newton-Raphson load flow problem utilising the notion of current mismatches, instead of power mismatches. The provided large distribution network is divided into a number of smaller sub distribution networks. power flow calculations are performed upon the individual sub distribution networks. Then the solution of all the are consolidated to obtain the power flow solution of the original distribution network utilising the Large Change Sensitivity concept. A fast decoupled load flow solution for unbalanced radial distribution systems has been proposed in [40]. In [41] a modified object oriented load flow algorithm suitable for both radial and weakly meshed distribution systems has been developed. This algorithm is modified version of the Newton-Raphson method that allows approximating the full Jacobian matrix. Authors in [42]

proposed a fast decoupled load flow solution method for distribution systems based on transformation of coordinate in Y matrix for Jacobian matrix. This method is computationally more efficient than Newton-Raphson based load flow method [37] for distribution systems as proposed method has a feature of combining the phase angle rotation of Y-matrix and the omission of Jacobian matrix including the real part of Y-matrix. A modified fast decoupled load flow algorithm based on branch current flows is developed in [43]. They have used a sub-Jacobian matrix that need to be factorised only once all through the procedure to achieve power flow solution. In [44], authors have introduced a modified Fast decoupled load flow algorithm for both radial and meshed distribution systems. They have used the theory of complex per unit normalization to enhance the functioning of conventional fast decoupled load flow method. In paper [45] the Newton Raphson power flow solution for three phase unbalanced and multiphase systems has been developed. The aforesaid methodology is capable of handling both radial and meshed configurations of distribution network. Several test cases have been simulated using the developed algorithm to get satisfactory power flow results. A robust and efficient load flow method for the analysis of distribution networks has been developed in paper [46]. The power flow algorithm is considered to be an optimization problem and is split into two sub-problems without using any kind of assumptions. This solution methodology is quite simple and making use of a constant Jacobian matrix. It is solved in similar fashion the fast decoupled load flow method is being solved.

However, these algorithms are found to be computationally burdensome.

The alternative to aforementioned methods is Forward/Backward sweep based load flow methods for distribution systems. In [47], Authors have introduced modified forward backward sweep load flow algorithm for radial distribution networks using simple algebraic expression and only permits the computation of the bus voltages (rms value). A modified version of forward and backward sweep method for load flow solution of 3-phase distribution systems has been introduced in [48] which is quite accurate and efficient. A loop analysis based continuation power flow algorithm has been introduced in [49] and it is valid for both radial and meshed networks. It is a modified version of forward and backward sweep method. In [50], the authors proposed an improved backward/forward sweep load flow method by using breadth-first search graph technique for the formulation of modified

incidence matrix. The modified incidence matrix ensures least number of searching operation for identifying connections between nodes thus assuring faster convergence ability. A backward and forward sweep based distribution load flow algorithm capable of handling transformer of various connection types in unbalanced radial distribution systems has been introduced in [51]. In [52], the Radial Configuration Matrix (RCM) is constructed and utilized in forward and backward sweep iterative step for load flow calculation of 3-phase unbalanced radial distribution network. A new recursive power flow algorithm has been introduced in [53] using the concept of graph theory. They have formulated four generalized matrices to achieve the load flow solution of distribution networks. Authors in paper [54], introduced a fast and competent load flow technique for unbalanced distribution networks by promulgating the idea of traditional backward/forward sweep technique of power flow study. A novel load-impedance matrix (LIM) has been formulated to compute the node voltages in a single stride unlike the conventional backward forward sweep method which involves two distinct steps. In [55], authors utilised load current to bus voltage matrix (LCBV) to compute the node voltages in a single stride unlike the conventional backward forward sweep method which involves two distinct steps. In [56-57] a modified object oriented load flow algorithm suitable for both radial and weakly meshed distribution systems has been developed. Compensation based algorithm, which has both forward sweep and backward sweep, is used to develop the distribution load flow analysis program using the designed objects. Authors in paper [58-59], introduced a fast and competent load flow technique for unbalanced distribution networks by utilising the notion of traditional backward/forward sweep technique of power flow study. In their load flow model they have incorporated various models of distributed generations.

Several other methods of load flow based on BFS based methods are formulated in [60-66].

All of these methods are capable enough to produce accurate LF solutions, However, these methods exhibit some common limitations. In the conventional BFS technique, any receiving end bus voltage of the distribution network has to be calculated as a function of the corresponding sending end bus voltage. This chained calculation procedure limits the convergence speed to a considerable extent. All BFS based LF techniques use time expensive branch numbering scheme to perform both the sweeps.

The direct methods [67-68], have overcome the disadvantages associated with the

traditional load-flow methods and BFS load-flow method. Direct method utilizes three matrices namely branch-current to bus voltage (BCBV) matrix, bus-injection to branch current (BIBC) matrix and distribution load flow (DLF=BCBV×BIBC) matrix are required to achieve the desired load flow solution of radial distribution systems [67-68].

All these distribution load flow methods are developed for solving load flow equations of AC distribution system not for AC-DC distribution system.

Recently, a BIBC matrix method has been formulated for solving load flow equations of AC-DC distribution system [69]. However it's applicability is limited only to radial AC-DC distribution network. This method (BIBC) has not considered the effect of various models of distributed generations.

Apart from BIBC load flow technique, an advanced unified AC-DC load flow procedure has been implemented in general algebraic modeling systems (GAMS) taking care of various hybrid configurations of AC-DC distribution network [36]. This method is applicable to both radial and meshed AC-DC network with various model of distributed generations. However, in this method various operating modes of converters like constant power mode, constant voltage control at the output of converter terminal, constant power factor mode etc. have not been considered.

1.3 Contribution of the Author

Motivated by the above lacuna following studies have been carried out in this thesis:

- Development of a load flow algorithm for AC distribution systems. The proposed method has utilised the concept of graph theory and matrix algebra to obtain the power flow solution of AC distribution systems. This load flow method is applicable for any configuration of AC distribution systems viz. radial, meshed , balanced and unbalanced. A comparative analysis between the proposed method and several other existing methods has been carried out to prove the efficacy of the proposed algorithm.
- The load flow algorithm for AC distribution system in the presence of various models of distributed generations (PQ and PV models) has been formulated. The DGs modelled as PQ bus can be treated as negative load. The breakpoint matrix or sensitivity matrix has been developed to calculate the net injection by the DGs modelled as PV bus into the proposed load flow model. Once the net injection by the

DGs is calculated, the load flow solution of active distribution system will be carried out in the same manner as load flow solution of distribution system without DGs.

- Development of load flow algorithm for AC-DC radial distribution system in the presence of various models of distributed generations (P, PQ, V^{dc} and PV models). The concept of load flow algorithm for AC distribution systems has been modified as per AC-DC scenario for solving radial AC-DC distribution system load flow problem.
- Development of load flow algorithm for AC-DC meshed distribution system in the presence of various models of distributed generations (P, PQ, V^{dc} and PV models). The concept of AC-DC load flow algorithm for radial distribution systems has been modified for solving weakly meshed AC-DC distribution system load flow problem. For converting meshed network to radial network, the loop breakpoint matrix has been derived for calculating loop breakpoint injections in AC-DC scenario. In the case of weakly meshed AC-DC distribution network with PV type and V^{dc} type distributed generations, the loop breakpoint injections, PV breakpoint injections and V^{dc} breakpoint injections have been calculated simultaneously.
- In order to prove the applicability of the load flow algorithm, a power flow based Distribution use of systems (DUoS) charging methodology has been developed to investigate the impact of protection system reinforcement costs on the consumers associated with renewable integrated distribution network. A power flow based MW+MVAr-Miles DUoS charging method, that considers used capacity of the network, is proposed to carry out the DUoS charging calculations. The proposed charging mechanism appraise/penalise the users in accordance they are affecting system power factor. Accordingly, the proposed pricing algorithm may encourage users to act based on the economic signal generated at each location. The proposed charging algorithm has been tested on various standard systems to examine the impact of renewable generations on the use of network costs.

1.4 Thesis Organisation

Apart from this chapter, there are six more chapters in this thesis. In chapter 2 load flow algorithm for AC distribution network (viz. radial, meshed, single phase and three phase distribution network) has been developed. In the chapter 3, the load flow solution algorithm

for AC distribution system in the presence of various model distributed generations has been developed. The chapter 4 provides descriptive analysis of load flow solution algorithm for AC-DC radial distribution system in the presence of distributed generations. The concept developed in chapter 1 and chapter 2 has been modified as per AC-DC scenario to achieve the aforementioned objective. In chapter 5 the load flow algorithm for meshed AC-DC distribution network in the presence of various model of distributed generations is developed. The chapter 6 illustrates the applications of proposed load flow method for investigating the impact of protection system reinforcement on the consumers associated with renewable integrated distribution network. Lastly, chapter 7 lists the major conclusions of this work as well as the future scope of the work.

Chapter-2

Load Flow Solution Algorithm for AC Radial Distribution Systems

In this chapter, a load flow algorithm for AC distribution system (both balanced and unbalanced) has been developed utilising the notion of graph theory and matrix algebra. The proposed algorithm is capable of providing the load flow solution for both radial and meshed configurations of distribution system. Extensive load flow simulation studies are conducted for aforementioned types of distribution systems and corresponding results are examined by comparing with the results obtained by existing load flow methods.

2.1 Introduction

A matrix is a convenient way of depicting a graph to a computer. In this research work a matrix based fast converging graphical load-flow method for distribution networks has been formulated, which works efficiently with both balanced and unbalanced distribution networks. The aforesaid methodology is capable of handling both radial and meshed configurations of distribution network. Importantly, the proposed method applies only simple algebraic matrix operations along with several search techniques to achieve the desired load flow solution of distribution systems. It requires the conventional bus-branch oriented data as the only input. The objective of this work is to develop a method, which incorporates advantages of the topological aspects of distribution networks, and solves the load-flow problem directly. This means that the proposed method does not require time taking LU decomposition and forward/ backward substitution of the admittance matrix or jacobian matrix, required in classical Newton Raphson algorithms. Two developed matrices, loads beyond branch matrix [*LB*], the path impedance matrix [*PI*], and simple matrix multiplication are utilized to obtain load-flow solutions. Rest of the other supporting matrices have been derived from above two mentioned matrices. There is no direct multiplication required between the significant matrices ([*PI*] matrix,[*P*] matrix, [*LB*] matrix, [P*D*] matrix, [*SBOBD*]

matrix and [*LFM*]) that have been formulated for our purpose. The simple algebraic operation and efficient search technique enabling the proposed method to be computationally efficient when compared with the existing direct methods and traditional load-flow methods. Test results reveal the viability and authenticity of the proposed algorithm.

2.2 Load Flow Solution Methodology for Three Phase Balanced AC Radial Distribution Systems

The proposed load-flow technique for AC radial distribution systems is an iterative approach, which uses the concept of graph theory and matrix algebra. For a better insight, the proposed algorithm has been developed first for balanced three phase system and afterward it is extended to work on three-phase unbalanced systems. The detailed derivation of the proposed matrix formulation and complete load flow procedure has been explicitly explained in the subsequent sections.

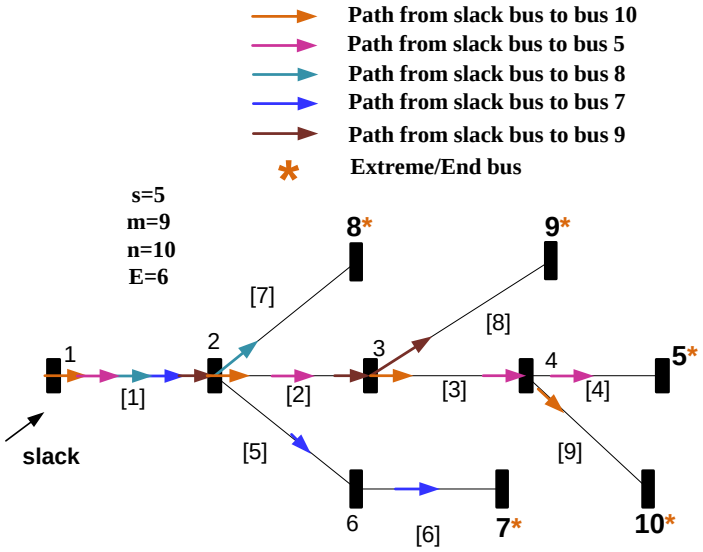

Fig. 2.1: Graphical representation of a radial distribution system.

The proposed technique comprises of the following steps:

i. Identification of total number of paths in the radial distribution system.

ii. Dynamic matrix building algorithm for path matrix as well as path impedance matrix formulation.

iii. Dynamic matrix building algorithm for the formulation of loads beyond Branch matrix.

iv. Node voltage, phase angle and distribution loss calculation by performing matrix algebraic operations on the results obtained from step 2 and step3.

To identify the total number of paths (s) in the radial distribution network, three basic steps need to be followed:

i. Represent the radial distribution network with its equivalent undirected graphical form.

ii. Formulate incidence matrix of the radial distribution network.

iii. Apply a search technique on the incidence matrix to identify the extreme nodes in the radial distribution network

To illustrate all these steps a radial distribution system represented by an undirected graph is shown in Fig. 2.1. The system data of the distribution system can be presented in the matrix form. The system data [*SD*] matrix of the distribution system shown in Fig. 2.1 is given by:

$$\boldsymbol{SD}=\begin{array}{c} \begin{matrix} \boldsymbol{b} & \boldsymbol{SN} & \boldsymbol{RN} & \boldsymbol{Z(b)} & \boldsymbol{S(RN)} \end{matrix} \\ \begin{bmatrix} 1 & 1 & 2 & Z(1) & S(2) \\ 2 & 2 & 3 & Z(2) & S(3) \\ 3 & 3 & 4 & Z(3) & S(4) \\ 4 & 4 & 5 & Z(4) & S(5) \\ 5 & 2 & 6 & Z(5) & S(6) \\ 6 & 6 & 7 & Z(6) & S(7) \\ 7 & 2 & 8 & Z(7) & S(8) \\ 8 & 3 & 9 & Z(8) & S(9) \\ 9 & 4 & 10 & Z(9) & S(10) \end{bmatrix} \end{array} \tag{2.1}$$

In the subsequent step the vertex-edge incidence matrix of the radial distribution network needs to be formulated. In the matrix [*IM*]of a radial distribution system, row number represents the bus number and column number represents the branch number. The matrix [*IM*]of the system shown in Fig. 2.1 is given by:

$$\boldsymbol{IM}=\begin{bmatrix} \mathbf{1} & \mathbf{0} & \mathbf{0} & \mathbf{0} & \mathbf{0} & \mathbf{0} & \mathbf{0} & \mathbf{0} & \mathbf{0} \\ \mathbf{1} & \mathbf{1} & \mathbf{0} & \mathbf{0} & \mathbf{1} & \mathbf{0} & \mathbf{1} & \mathbf{0} & \mathbf{0} \\ \mathbf{0} & \mathbf{1} & \mathbf{1} & \mathbf{0} & \mathbf{0} & \mathbf{0} & \mathbf{0} & \mathbf{1} & \mathbf{0} \\ \mathbf{0} & \mathbf{0} & \mathbf{1} & \mathbf{1} & \mathbf{0} & \mathbf{0} & \mathbf{0} & \mathbf{0} & \mathbf{1} \\ \mathbf{0} & \mathbf{0} & \mathbf{0} & \mathbf{1} & \mathbf{0} & \mathbf{0} & \mathbf{0} & \mathbf{0} & \mathbf{0} \\ \mathbf{0} & \mathbf{0} & \mathbf{0} & \mathbf{0} & \mathbf{1} & \mathbf{1} & \mathbf{0} & \mathbf{0} & \mathbf{0} \\ \mathbf{0} & \mathbf{0} & \mathbf{0} & \mathbf{0} & \mathbf{0} & \mathbf{1} & \mathbf{0} & \mathbf{0} & \mathbf{0} \\ \mathbf{0} & \mathbf{0} & \mathbf{0} & \mathbf{0} & \mathbf{0} & \mathbf{0} & \mathbf{1} & \mathbf{0} & \mathbf{0} \\ \mathbf{0} & \mathbf{0} & \mathbf{0} & \mathbf{0} & \mathbf{0} & \mathbf{0} & \mathbf{0} & \mathbf{1} & \mathbf{0} \\ \mathbf{0} & \mathbf{0} & \mathbf{0} & \mathbf{0} & \mathbf{0} & \mathbf{0} & \mathbf{0} & \mathbf{0} & \mathbf{1} \end{bmatrix} \tag{2.2}$$

The matrix $[IM]$ gives an idea about total number of paths in the distribution network. To identify the total number of paths, end nodes must be identified. End nodes are the extreme point in the network on which only one branch is incident. To identify the end nodes one must apply a search algorithm on the matrix $[IM]$ of the undirected graph in Fig. 2.1. While looking into the matrix $[IM]$ it is being revealed that some rows of incidence matrix will be having only a single non-zero element of unit value. These rows number are the extreme node/end node. In the matrix $[IM]$ of the system shown in Fig. 2.1, there are six such nodes including source node. The rows representing the end nodes are:

$$\text{End nodes} = \{1, 5, 7, 8, 9, 10\} \tag{2.3}$$

As there are six end nodes in the system shown in Fig. 2.1, so total number of paths from slack bus to end nodes will be five. Usually, if a radial distribution network is having E end nodes then, total number of paths (s) will be E-1.

2.2.1 Algorithm for path matrix and path impedance matrix formulation

The $[P]$ matrix of a distribution system having 'n' buses and 'm' branches is a matrix consisting of 's' rows and 'm' columns. This proposed [*P*] matrix is used to establish a relation between the branch number and power flow path (slack bus to end nodes). In this matrix, row number and column number represent path number and branch number respectively in a manner such that:

for, $i=1,2,3\ldots\ldots\ldots\ldots s$

(search for, $j=1,2,3\ldots\ldots\ldots\ldots m$)

if j_{th} branch is traced in i_{th} power flow path

then,

$$P(i, j) = 1$$

else,

$$P(i, j) = 0$$

(2.4)

The repetition of the above procedure for all value of *i* and *j* will lead to the formulation of the matrix [*P*].

where, *i*= Row number. *j*= Column number. *b*= Branch number =*1,2,3.....m.*. s= Total number paths.

The $[PI]$ matrix of a distribution system having 'n' buses and 'm' branches is a matrix consisting of 's' rows and 'm' columns. This proposed [*PI*] matrix is used to establish a relation between the branch impedance and path number. In this matrix, row number and column number represent path number and branch number respectively and impedance value will be stored in the matrix $[PI]$ in a manner such that.

for, $i=1,2,3\ldots\ldots\ldots\ldots s$

(search for, $j=1,2,3\ldots\ldots\ldots\ldots m$)

if j_{th} branch is traced in i_{th} power flow path

then,

$$PI(i,j) = Z(j) = Z(b)$$

else,

$$PI(i,j) = 0 \qquad (2.5)$$

$Z(b)$ =Impedance value of b_{th} branch.

The repetition of the above procedure for all value of *i* and *j* will lead to the formulation of the matrix [*PI*].

In the distribution system shown in Fig. 2.1 there are five paths (slack bus to end nodes) and hence its path matrix and path impedance matrix is-

$$[\boldsymbol{P}]=\begin{bmatrix}\mathbf{1}&\mathbf{1}&\mathbf{1}&\mathbf{1}&\mathbf{0}&\mathbf{0}&\mathbf{0}&\mathbf{0}&\mathbf{0}\\ \mathbf{1}&\mathbf{0}&\mathbf{0}&\mathbf{0}&\mathbf{1}&\mathbf{1}&\mathbf{0}&\mathbf{0}&\mathbf{0}\\ \mathbf{1}&\mathbf{0}&\mathbf{0}&\mathbf{0}&\mathbf{0}&\mathbf{0}&\mathbf{1}&\mathbf{0}&\mathbf{0}\\ \mathbf{1}&\mathbf{1}&\mathbf{0}&\mathbf{0}&\mathbf{0}&\mathbf{0}&\mathbf{0}&\mathbf{1}&\mathbf{0}\\ \mathbf{1}&\mathbf{1}&\mathbf{1}&\mathbf{0}&\mathbf{0}&\mathbf{0}&\mathbf{0}&\mathbf{0}&\mathbf{1}\end{bmatrix} \qquad (2.6)$$

$$[\boldsymbol{PI}]=\begin{bmatrix}\boldsymbol{Z(1)}&\boldsymbol{Z(2)}&\boldsymbol{Z(3)}&\boldsymbol{Z(4)}&\mathbf{0}&\mathbf{0}&\mathbf{0}&\mathbf{0}&\mathbf{0}\\ \boldsymbol{Z(1)}&\mathbf{0}&\mathbf{0}&\mathbf{0}&\boldsymbol{Z(5)}&\boldsymbol{Z(6)}&\mathbf{0}&\mathbf{0}&\mathbf{0}\\ \boldsymbol{Z(1)}&\mathbf{0}&\mathbf{0}&\mathbf{0}&\mathbf{0}&\mathbf{0}&\boldsymbol{Z(7)}&\mathbf{0}&\mathbf{0}\\ \boldsymbol{Z(1)}&\boldsymbol{Z(2)}&\mathbf{0}&\mathbf{0}&\mathbf{0}&\mathbf{0}&\mathbf{0}&\boldsymbol{Z(8)}&\mathbf{0}\\ \boldsymbol{Z(1)}&\boldsymbol{Z(2)}&\boldsymbol{Z(3)}&\mathbf{0}&\mathbf{0}&\mathbf{0}&\mathbf{0}&\mathbf{0}&\boldsymbol{Z(9)}\end{bmatrix} \qquad (2.7)$$

For better understanding, the sequential procedure for the path matrix formulation of the distribution system shown in Fig. 2.2 has been pictorially exemplified below in Fig. 2.2.

$$IM = \begin{array}{c} \begin{matrix} 1 & 2 & 3 & 4 & 5 & 6 & 7 & 8 & 9 \end{matrix} \\ \begin{bmatrix} 1 & 0 & 0 & 0 & 0 & 0 & 0 & 0 & 0 \\ 1 & 1 & 0 & 0 & 1 & 0 & 1 & 0 & 0 \\ 0 & 1 & 1 & 0 & 0 & 0 & 0 & 1 & 0 \\ 0 & 0 & 1 & 1 & 0 & 0 & 0 & 0 & 1 \\ 0 & 0 & 0 & 1 & 0 & 0 & 0 & 0 & 0 \\ 0 & 0 & 0 & 0 & 1 & 1 & 0 & 0 & 0 \\ 0 & 0 & 0 & 0 & 0 & 1 & 0 & 0 & 0 \\ 0 & 0 & 0 & 0 & 0 & 0 & 1 & 0 & 0 \\ 0 & 0 & 0 & 0 & 0 & 0 & 0 & 1 & 0 \\ 0 & 0 & 0 & 0 & 0 & 0 & 0 & 0 & 1 \end{bmatrix} \end{array}$$

$$IM = \begin{array}{c} \begin{matrix} 1 & 2 & 3 & 4 & 5 & 6 & 7 & 8 & 9 \end{matrix} \\ \begin{bmatrix} 1 & 0 & 0 & 0 & 0 & 0 & 0 & 0 & 0 \\ 1 & 1 & 0 & 0 & 1 & 0 & 1 & 0 & 0 \\ 0 & 1 & 1 & 0 & 0 & 0 & 0 & 1 & 0 \\ 0 & 0 & 1 & 1 & 0 & 0 & 0 & 0 & 1 \\ 0 & 0 & 0 & 1 & 0 & 0 & 0 & 0 & 0 \\ 0 & 0 & 0 & 0 & 1 & 1 & 0 & 0 & 0 \\ 0 & 0 & 0 & 0 & 0 & 1 & 0 & 0 & 0 \\ 0 & 0 & 0 & 0 & 0 & 0 & 1 & 0 & 0 \\ 0 & 0 & 0 & 0 & 0 & 0 & 0 & 1 & 0 \\ 0 & 0 & 0 & 0 & 0 & 0 & 0 & 0 & 1 \end{bmatrix} \end{array}$$

$$IM = \begin{array}{c} \begin{matrix} 1 & 2 & 3 & 4 & 5 & 6 & 7 & 8 & 9 \end{matrix} \\ \begin{bmatrix} 1 & 0 & 0 & 0 & 0 & 0 & 0 & 0 & 0 \\ 1 & 1 & 0 & 0 & 1 & 0 & 1 & 0 & 0 \\ 0 & 1 & 1 & 0 & 0 & 0 & 0 & 1 & 0 \\ 0 & 0 & 1 & 1 & 0 & 0 & 0 & 0 & 1 \\ 0 & 0 & 0 & 1 & 0 & 0 & 0 & 0 & 0 \\ 0 & 0 & 0 & 0 & 1 & 1 & 0 & 0 & 0 \\ 0 & 0 & 0 & 0 & 0 & 1 & 0 & 0 & 0 \\ 0 & 0 & 0 & 0 & 0 & 0 & 1 & 0 & 0 \\ 0 & 0 & 0 & 0 & 0 & 0 & 0 & 1 & 0 \\ 0 & 0 & 0 & 0 & 0 & 0 & 0 & 0 & 1 \end{bmatrix} \end{array}$$

$$IM = \begin{array}{c} \begin{matrix} 1 & 2 & 3 & 4 & 5 & 6 & 7 & 8 & 9 \end{matrix} \\ \begin{bmatrix} 1 & 0 & 0 & 0 & 0 & 0 & 0 & 0 & 0 \\ 1 & 1 & 0 & 0 & 1 & 0 & 1 & 0 & 0 \\ 0 & 1 & 1 & 0 & 0 & 0 & 0 & 1 & 0 \\ 0 & 0 & 1 & 1 & 0 & 0 & 0 & 0 & 1 \\ 0 & 0 & 0 & 1 & 0 & 0 & 0 & 0 & 0 \\ 0 & 0 & 0 & 0 & 1 & 1 & 0 & 0 & 0 \\ 0 & 0 & 0 & 0 & 0 & 1 & 0 & 0 & 0 \\ 0 & 0 & 0 & 0 & 0 & 0 & 1 & 0 & 0 \\ 0 & 0 & 0 & 0 & 0 & 0 & 0 & 1 & 0 \\ 0 & 0 & 0 & 0 & 0 & 0 & 0 & 0 & 1 \end{bmatrix} \end{array}$$

$$IM = \begin{array}{c} \begin{matrix} 1 & 2 & 3 & 4 & 5 & 6 & 7 & 8 & 9 \end{matrix} \\ \begin{bmatrix} 1 & 0 & 0 & 0 & 0 & 0 & 0 & 0 & 0 \\ 1 & 1 & 0 & 0 & 1 & 0 & 1 & 0 & 0 \\ 0 & 1 & 1 & 0 & 0 & 0 & 0 & 1 & 0 \\ 0 & 0 & 1 & 1 & 0 & 0 & 0 & 0 & 1 \\ 0 & 0 & 0 & 1 & 0 & 0 & 0 & 0 & 0 \\ 0 & 0 & 0 & 0 & 1 & 1 & 0 & 0 & 0 \\ 0 & 0 & 0 & 0 & 0 & 1 & 0 & 0 & 0 \\ 0 & 0 & 0 & 0 & 0 & 0 & 1 & 0 & 0 \\ 0 & 0 & 0 & 0 & 0 & 0 & 0 & 1 & 0 \\ 0 & 0 & 0 & 0 & 0 & 0 & 0 & 0 & 1 \end{bmatrix} \end{array}$$

Fig. 2.2: Pictorial depiction of proposed search technique for path matrix formulation.

2.2.2 Algorithm for loads beyond branch matrix formulation

The [*LB*] matrix of a distribution system having 'n' buses and 'm' branches is a matrix consisting of 'm' rows and '(n-1)' columns. In this matrix, row number represent branch number and column number represents bus number. The elements located at j_{th} column will store the load value of the bus located at $(j+1)_{th}$ bus number in a manner such that:

for $i=1,2,3\ldots\ldots\ldots\ldots m.$

if loads at bus (j) is located beyond branch i

(search for, $j=2,3,4\ldots\ldots\ldots\ldots n.$)

then

$$LB(i, j-1) = S(j) = S(k)$$

else,

$$LB(i, j-1) = 0$$

(2.8)

Slack bus is not included in this matrix.

$S(k)$ =Complex Load value at k_{th} bus.

k=Bus number=*1, 2, 3*.....*n.*

These matrices play an important role in load flow calculations and the rest of the other supporting matrices have been derived from above mentioned matrices.

The final expression of [*LB*] matrix for the ten-bus test system (refer Fig. 2.1) is shown in equation (2.9).

$$[\boldsymbol{LB}]=\begin{bmatrix} \boldsymbol{S(2)} & \boldsymbol{S(3)} & \boldsymbol{S(4)} & \boldsymbol{S(5)} & \boldsymbol{S(6)} & \boldsymbol{S(7)} & \boldsymbol{S(8)} & \boldsymbol{S(9)} & \boldsymbol{S(10)} \\ \mathbf{0} & \boldsymbol{S(3)} & \boldsymbol{S(4)} & \boldsymbol{S(5)} & \mathbf{0} & \mathbf{0} & \mathbf{0} & \boldsymbol{S(9)} & \boldsymbol{S(10)} \\ \mathbf{0} & \mathbf{0} & \boldsymbol{S(4)} & \boldsymbol{S(5)} & \mathbf{0} & \mathbf{0} & \mathbf{0} & \mathbf{0} & \boldsymbol{S(10)} \\ \mathbf{0} & \mathbf{0} & \mathbf{0} & \boldsymbol{S(5)} & \mathbf{0} & \mathbf{0} & \mathbf{0} & \mathbf{0} & \mathbf{0} \\ \mathbf{0} & \mathbf{0} & \mathbf{0} & \mathbf{0} & \boldsymbol{S(6)} & \boldsymbol{S(7)} & \mathbf{0} & \mathbf{0} & \mathbf{0} \\ \mathbf{0} & \mathbf{0} & \mathbf{0} & \mathbf{0} & \mathbf{0} & \boldsymbol{S(7)} & \mathbf{0} & \mathbf{0} & \mathbf{0} \\ \mathbf{0} & \mathbf{0} & \mathbf{0} & \mathbf{0} & \mathbf{0} & \mathbf{0} & \boldsymbol{S(8)} & \mathbf{0} & \mathbf{0} \\ \mathbf{0} & \mathbf{0} & \mathbf{0} & \mathbf{0} & \mathbf{0} & \mathbf{0} & \mathbf{0} & \boldsymbol{S(9)} & \mathbf{0} \\ \mathbf{0} & \mathbf{0} & \mathbf{0} & \mathbf{0} & \mathbf{0} & \mathbf{0} & \mathbf{0} & \mathbf{0} & \boldsymbol{S(10)} \end{bmatrix} \quad (2.9)$$

The complete procedure for [*LB*] matrix formulation is clearly illustrated through the flow chart shown in Fig. 2.3. These matrices play an important role in load flow calculations and the rest of the other supporting matrices have been derived from above mentioned matrices.

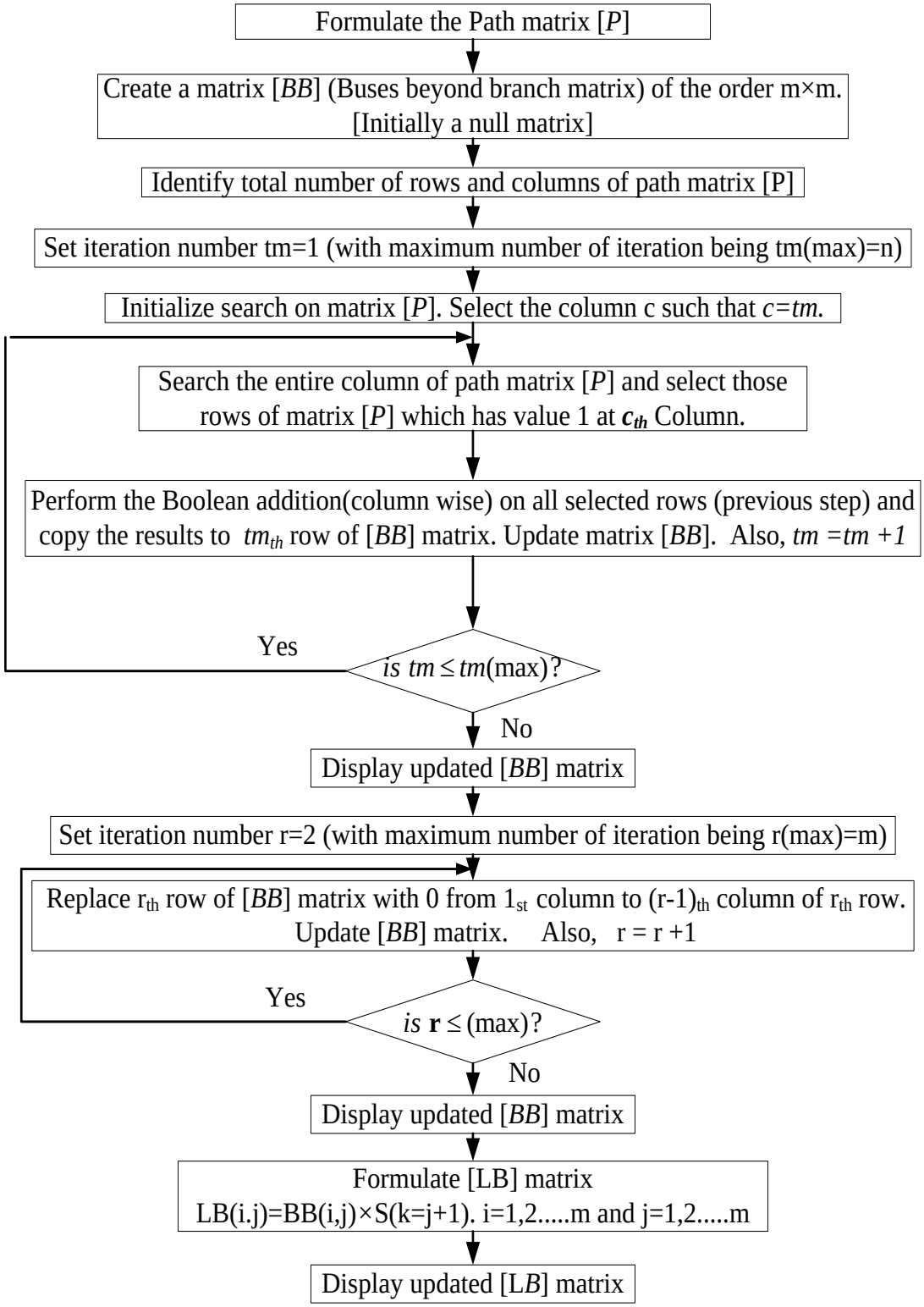

Fig. 2.3: Flowchart for loads beyond branch matrix formulation.

2.2.3 Feeder current matrix formulation algorithm

The procedure to calculate feeder current matrix is listed below in sequential manner.

$$[W] = \text{Conjugate}[LB] \tag{2.10}$$

$$[V1] = \text{Conjugate}[V] \tag{2.11}$$

Where [*V*] is voltage matrix of order 1×m and in this matrix element located at j_{th} column number stores the voltage value of $(j+1)_{th}$ bus number (slack bus is not included). Initially flat voltage profile has to be assumed at every bus location in the distribution system.

for i=*1, 2, 3.....m.*

$$LC(i, j) = \frac{W(i, j)}{V1(1, j)} \tag{2.12}$$

Calculate $LC(i, j)$ for all value of *j*.

Where, j=*1,2.....m.*

The repetition of the above aforementioned procedure for all value of *i* and *j* will lead to the formulation of the matrix [*LC*]. In the matrix $[LC]$,each element represents a load current. On summing up all the load currents of the same row will provide feeder current of the branch represented by that row.

$$FC(i,1) = \sum_{j=1}^{m} LC(i, j) \tag{2.13}$$

Calculate [*FC*] for all value of *i*.

Where, *i=1,2,3.....m.*

The Feeder current matrix $[FC]$ is of order $m \times 1$. The element stored at i_{th} row of $[FC]$ matrix represent the branch current of branch number b of a radial distribution system, such that $b = i$. The [*FC*] matrix of the radial distribution in Fig. 2.1 is -

$$[FC] = \begin{bmatrix} \boldsymbol{I(1)} \\ \boldsymbol{I(2)} \\ \boldsymbol{I(3)} \\ \boldsymbol{I(4)} \\ \boldsymbol{I(5)} \\ \boldsymbol{I(6)} \\ \boldsymbol{I(7)} \\ \boldsymbol{I(8)} \\ \boldsymbol{I(9)} \end{bmatrix} \tag{2.14}$$

The flowchart for $[FC]$ matrix formulation is clearly illustrated through the flow chart shown in Fig. 2.4.

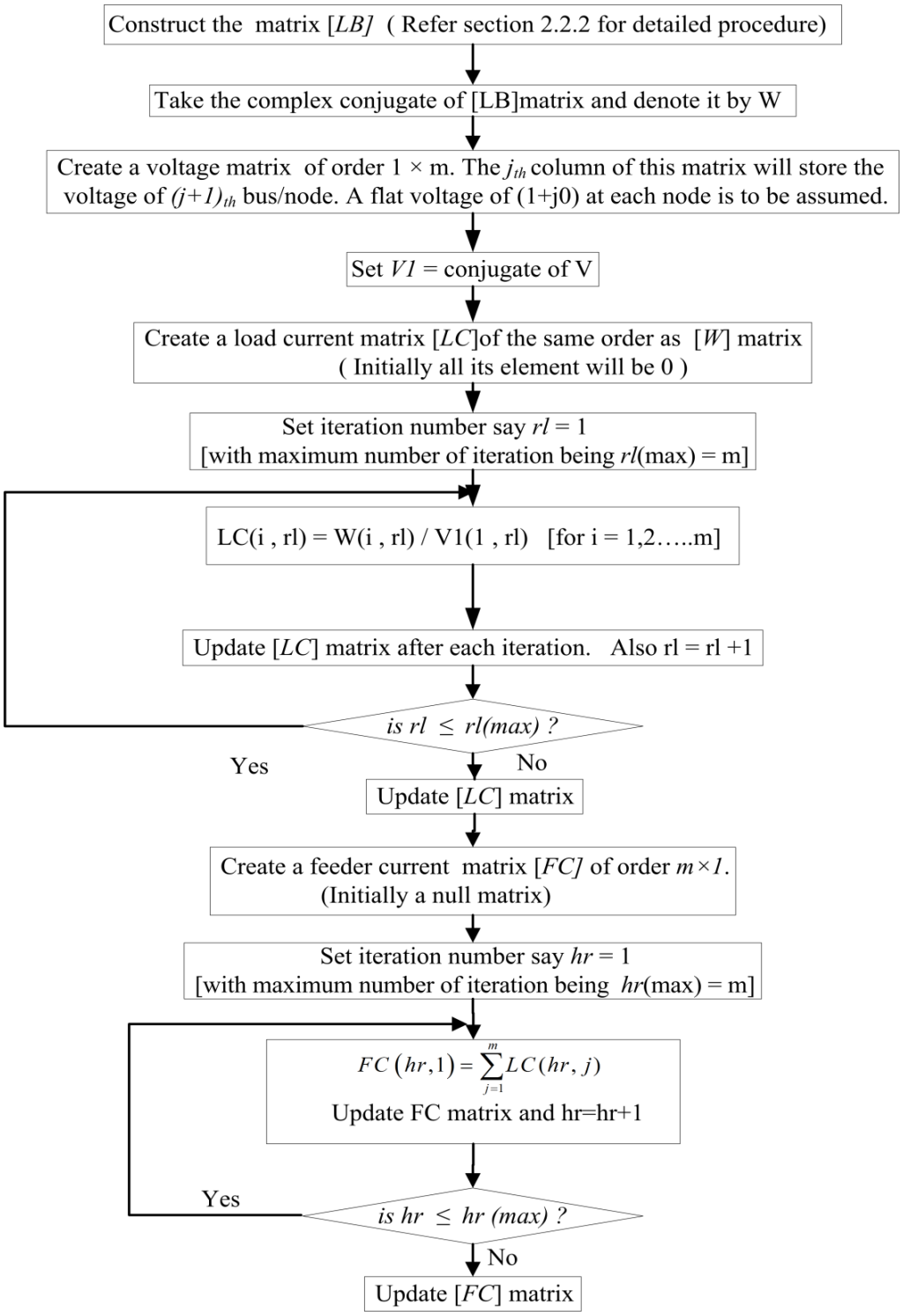

Fig. 2.4: Complete flowchart depicting the procedure for feeder current matrix formulation.

2.2.4 Path drop matrix, Slack bus to other buses drop matrix and Node voltage matrix formulation algorithm

Following steps are required for node voltage matrix calculation:

1) Compute the matrix $[PI]$ (as per section 2.2.1).
2) Compute the Feeder current $[FC]$ matrix (as per section 2.2.3).
3) Create a drop matrix $[PD]$ (initially a null matrix) of the order $s \times m$.
4) Start iteration number $(a = 1)$ with $[a(\max) = \text{m}]$.
5) Multiply all elements located at a_{th} column of matrix $[PI]$ separately with the element located at a_{th} row of $[FC]$ matrix.

$$PD(i,a) = PI(i,a) \times FC(a,1) \qquad [for\ i = 1,2 \ldots . s]$$

Update matrix $[PD]$.

6) $a = a + 1$
7) If $a > a(\max)$ go to step 8, else go to step 5.
8) End of iteration. Display matrix $[PD]$.
9) Create a matrix $[SBOBD]$ (initially a null matrix) of the order $s \times m$.
10) Start iteration count $y = 1$ $[y(\max) = s]$.
11) for $j = 1$ to m, if $D(y, j) = 0$

$$SBOBD(y,j) = 0$$

else

$$SBOBD(y,j) = \sum_{l=1}^{j} D(y,l)$$

12) Update matrix $[SBOBD]$ and $y = y + 1$.
13) If $y > y(\max)$ go to step 14, else go to step 11.
14) End iteration and display $[SBOBD]$.
15) Create a unity matrix $[U]$ of the order $s \times m$.

U(i, j)= 0, if *PI(i,j) is 0.*

U(i, j)= 1, else

16) $[LFM] = [U] - [SBOBD]$

17) Create a matrix $[V_{new}]$(initially a null matrix) of the order $(1\times m)$.

18) Set iteration number $et=1$ [maximum number of iteration being $et(\max)=m$.]

19) $V_{new}(1,et)=\text{maximum}(T(1,et),T(2,et).....T(s,et))$

20) Update $[V_{new}]$matrix and $et=et+1$.

21) If $et>et(\max)$ go to step 22, else go to Step 19.

22) End the iteration. Display $[V_{new}]$ (new voltage matrix)

Several matrices have been formulated in the current section and its structure must be clearly understood to achieve our main objective. The [P*D*] matrix and [*SBOBD*] matrix of the radial distribution system (all are of same order i.e. s×m) shown in Fig.2.1 is -

$[PD]=$

$$\begin{bmatrix} Z(1)\times I(1) & Z(2)\times I(2) & Z(3)\times I(3) & Z(4)\times I(4) & 0\times I(5) & 0\times I(6) & 0\times I(7) & 0\times I(8) & 0\times I(9) \\ Z(1)\times I(1) & 0\times I(2) & 0\times I(3) & 0\times I(4) & Z(5)\times I(5) & Z(6)\times I(6) & 0\times I(7) & 0\times I(8) & 0\times I(9) \\ Z(1)\times I(1) & 0\times I(2) & 0\times I(3) & 0\times I(4) & 0\times I(5) & 0\times I(6) & Z(7)\times I(7) & 0\times I(8) & 0\times I(9) \\ Z(1)\times I(1) & Z(2)\times I(2) & 0\times I(3) & 0\times I(4) & 0\times I(5) & 0\times I(6) & 0\times I(7) & Z(8)\times I(8) & 0\times I(9) \\ Z(1)\times I(1) & Z(2)\times I(2) & Z(3)\times I(3) & 0\times I(4) & 0\times I(5) & 0\times I(6) & 0\times I(7) & 0\times I(8) & Z(9)\times I(9) \end{bmatrix} \quad (2.15)$$

$SBOBD=$

$$\begin{bmatrix} D(1) & D(1)+D(2) & D(1)+D(2)+D(3) & D(1)+D(2)+D(3)+D(4) & 0 & 0 & 0 & 0 & 0 \\ D(1) & 0 & 0 & 0 & D(1)+D(5) & D(1)+D(5)+D(6) & 0 & 0 & 0 \\ D(1) & 0 & 0 & 0 & 0 & 0 & D(1)+D(7) & 0 & 0 \\ D(1) & D(1)+D(2) & 0 & 0 & 0 & 0 & 0 & D(1)+D(2)+D(8) & 0 \\ D(1) & D(1)+D(2) & D(1)+D(2)+D(3) & 0 & 0 & 0 & 0 & 0 & D(1)+D(2)+D(3)+D(9) \end{bmatrix}$$

(2.16)

where,

$$D(1) = Z(1) \times I(1) \qquad D(5) = Z(5) \times I(5)$$
$$D(2) = Z(2) \times I(2) \qquad D(6) = Z(6) \times I(6)$$
$$D(3) = Z(3) \times I(3) \qquad D(7) = Z(7) \times I(7)$$
$$D(4) = Z(4) \times I(4) \qquad D(6) = Z(6) \times I(6)$$

$$[U] = \begin{bmatrix} 1 & 1 & 1 & 1 & 0 & 0 & 0 & 0 & 0 \\ 1 & 0 & 0 & 0 & 1 & 1 & 0 & 0 & 0 \\ 1 & 0 & 0 & 0 & 0 & 0 & 1 & 0 & 0 \\ 1 & 1 & 0 & 0 & 0 & 0 & 0 & 1 & 0) \\ 1 & 1 & 1 & 0 & 0 & 0 & 0 & 0 & 1 \end{bmatrix} \tag{2.17}$$

Initialize a search operation for selecting the maximum (magnitude) value from each column of matrix [*LFM*] leading to formulation of new voltage matrix (as detailed in Section 2.2.4).

$$[LFM] = [U] - [SBOBD] \tag{2.18}$$

[*U*]=Binary matrix of the order $s \times m$.

Described process is iterative. When the mismatch of voltage magnitudes at each node in all the phases in present iteration and previous iteration is lower than tolerance limit, the calculation is stopped. Hence, convergence is being checked for all nodes at the end of each iteration count.

$$\text{Convergence} = \left| V(k)^{t+1} - V(k)^{t} \right| \tag{2.19}$$

$V(k)^{t+1}$ = voltage at the end of $(t+1)_{th}$ iteration number for k_{th} bus.

$V(k)^{t}$ = voltage at the end of $(t)_{th}$ iteration number for k_{th} bus.

The voltage solution at the end of each iteration count is in matrix form, so it is easy to find the convergence at the end of an iteration count in the matrix form.

where, $[V_{new}]$ = voltage matrix at the end of an iteration count

$[V]$ = voltage matrix at the beginning of an iteration count

$$\text{Convergence matrix} = \left| [V_{new}] - [V] \right| \tag{2.20}$$

The generalized algorithm for carrying out load flow solution of radial distribution system (considering all the relevant derivations in this chapter) is shown in Fig. 2.5.

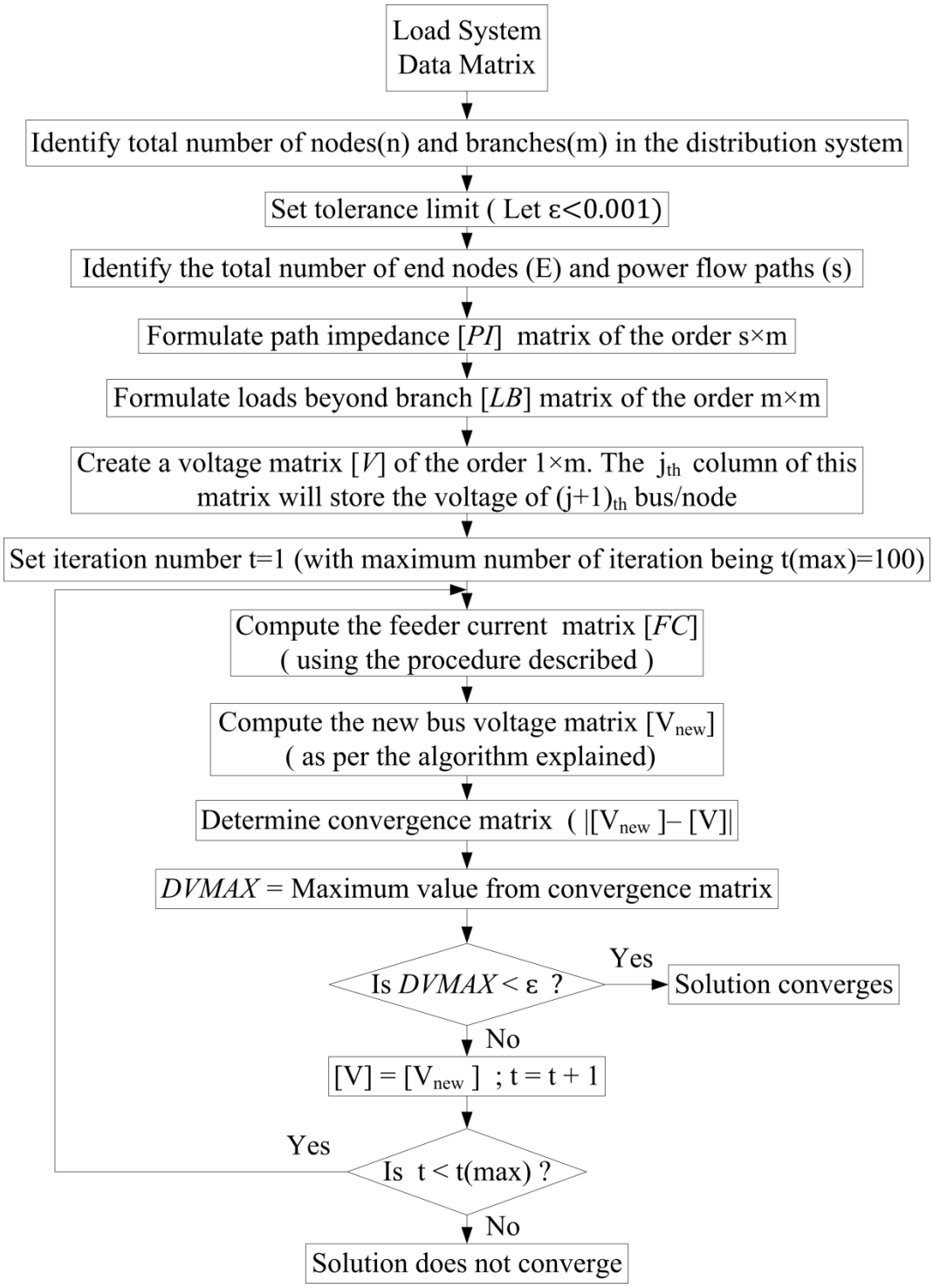

Fig. 2.5: Flowchart of generalized load flow solution algorithm for AC radial distribution systems.

2.3 Load Flow Algorithm for Three Phase Unbalanced Radial Distribution Systems

The important step in modelling unbalance distribution network is line modelling. A precise model of line (both overhead and underground) in three-phase unbalance distribution network has been developed by Kresting [70]. The equivalent primitive circuit of a 3-Φ line segment is shown in Fig. 2.6.

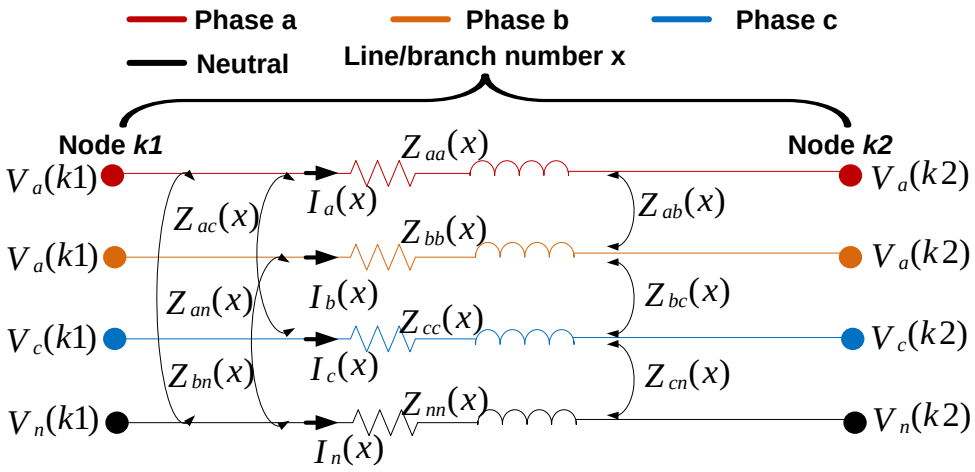

Fig. 2.6: Primitive circuit of a three phase line segment.

The application of Carson's equations will fetch the line parameters of 3-Φ line segment. The primitive impedance matrix of the three phase system shown in Fig. 2.6 can be written as:

$$[Z_{primitive}(x)] = \begin{bmatrix} Z_{aa}(x) & Z_{ab}(x) & Z_{ac}(x) & Z_{an}(x) \\ Z_{ba}(x) & Z_{bb}(x) & Z_{bc}(x) & Z_{bn}(x) \\ Z_{ca}(x) & Z_{cb}(x) & Z_{cc}(x) & Z_{cn}(x) \\ Z_{na}(x) & Z_{nb}(x) & Z_{nc}(x) & Z_{nn}(x) \end{bmatrix} \tag{2.21}$$

One can acquire the phase impedance matrix by applying Kron's reduction technique on the obtained primitive impedance matrix of n-phase system. The effect of the neutral or ground wire is still included in the phase impedance matrix as evident from equation (2.22).

$$[Z_{abc}(x)] = \begin{bmatrix} Z_{aa-n}(x) & Z_{ab-n}(x) & Z_{ac-n}(x) \\ Z_{ba-n}(x) & Z_{bb-n}(x) & Z_{bc-n}(x) \\ Z_{ca-n}(x) & Z_{cb-n}(x) & Z_{cc-n}(x) \end{bmatrix} \tag{2.22}$$

The voltage equation of the mentioned circuit in Fig. 2.7 can be written in terms of obtained phase impedance matrix and branch current matrix of the three phase system.

$$\begin{bmatrix} V_a(k1) \\ V_b(k1) \\ V_c(k1) \end{bmatrix} = \begin{bmatrix} V_a(k2) \\ V_b(k2) \\ V_c(k2) \end{bmatrix} + \begin{bmatrix} Z_{aa-n}(x) & Z_{ab-n}(x) & Z_{ac-n}(x) \\ Z_{ba-n}(x) & Z_{bb-n}(x) & Z_{bc-n}(x) \\ Z_{ca-n}(x) & Z_{cb-n}(x) & Z_{cc-n}(x) \end{bmatrix} \begin{bmatrix} I_a(x) \\ I_b(x) \\ I_c(x) \end{bmatrix} \quad (2.23)$$

If any phase is not present, then corresponding column and row in above mentioned matrix will be zero. To carry out load-flow solution of unbalanced three phase distribution networks using the method developed in section 2.2, several suitable modification/adjustment is eminently required in the proposed algorithm. The proposed algorithm can easily be extended to a multiphase line section or bus. Ex., if the line segment between bus i and bus j is 3-phase, the corresponding feeder/branch current and branch impedance will be a 3×1 matrix and 3×3 matrix respectively. In the path impedance matrix the corresponding branch impedance will be a 3×3 phase impedance matrix as shown in equation (2.26). In the loads beyond branch matrix and load current matrix the corresponding bus/load power/current will be a 3×1 matrix as shown in (2.24). The rest of the other supporting matrices **(***viz.* [*PD*] matrix , [*SBOBD*] matrix and [*LFM*] matrix) will be modified as per given size of bus current vector, bus voltage vector, branch current vector and branch/phase impedance vector/matrix. The [*PD*] matrix and [*U*] matrix will be of same size.

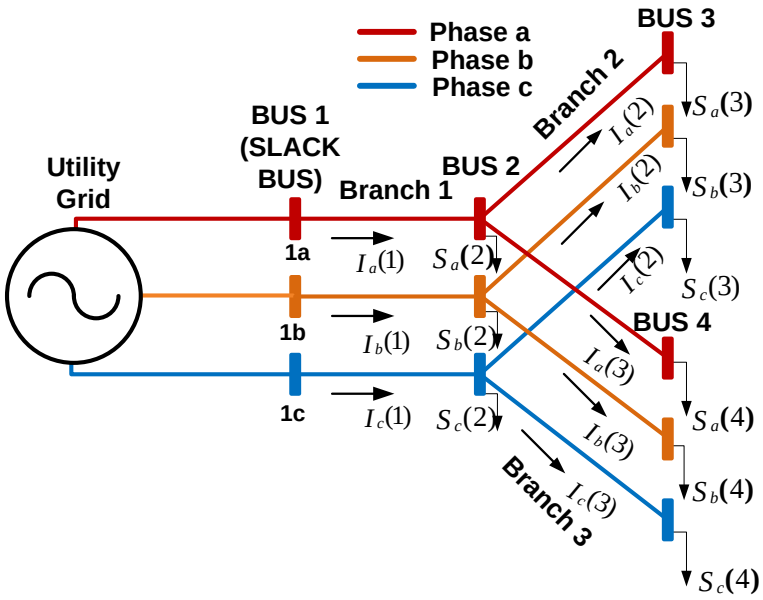

Fig. 2.7: An unbalanced 4-bus radial distribution system.

For example, [*LB*] matrix, [*LC*] matrix, [*PI*] matrix, [*PD*] matrix, [*SBOBD*] matrix and [*LFM*] matrix of the unbalanced distribution system shown in Fig. 2.7 is:

$$[LB]=\begin{bmatrix} \begin{bmatrix} S_a(2) \\ S_b(2) \\ S_c(2) \end{bmatrix} & \begin{bmatrix} S_a(3) \\ S_b(3) \\ S_c(3) \end{bmatrix} & \begin{bmatrix} S_a(4) \\ S_b(4) \\ S_c(4) \end{bmatrix} \\ \begin{bmatrix} 0 \\ 0 \\ 0 \end{bmatrix} & \begin{bmatrix} S_a(3) \\ S_b(3) \\ S_c(3) \end{bmatrix} & \begin{bmatrix} 0 \\ 0 \\ 0 \end{bmatrix} \\ \begin{bmatrix} 0 \\ 0 \\ 0 \end{bmatrix} & \begin{bmatrix} 0 \\ 0 \\ 0 \end{bmatrix} & \begin{bmatrix} S_a(4) \\ S_b(4) \\ S_c(4) \end{bmatrix} \end{bmatrix} \tag{2.24}$$

$$[LC]=\begin{bmatrix} \begin{bmatrix} LC_a(2) \\ LC_b(2) \\ LC_c(2) \end{bmatrix} & \begin{bmatrix} LC_a(3) \\ LC_b(3) \\ LC_c(3) \end{bmatrix} & \begin{bmatrix} LC_a(4) \\ LC_b(4) \\ LC_c(4) \end{bmatrix} \\ \begin{bmatrix} 0 \\ 0 \\ 0 \end{bmatrix} & \begin{bmatrix} S_a(3) \\ S_b(3) \\ S_c(3) \end{bmatrix} & \begin{bmatrix} 0 \\ 0 \\ 0 \end{bmatrix} \\ \begin{bmatrix} 0 \\ 0 \\ 0 \end{bmatrix} & \begin{bmatrix} 0 \\ 0 \\ 0 \end{bmatrix} & \begin{bmatrix} LC_a(4) \\ LC_b(4) \\ LC_c(4) \end{bmatrix} \end{bmatrix} \tag{2.25}$$

$$[PI]=\begin{bmatrix}\begin{bmatrix}Z_{aa-n}(1) & Z_{ab-n}(1) & Z_{ac-n}(1)\\ Z_{ba-n}(1) & Z_{bb-n}(1) & Z_{bc-n}(1)\\ Z_{ca-n}(1) & Z_{cb-n}(1) & Z_{cc-n}(1)\end{bmatrix} & \begin{bmatrix}Z_{aa-n}(2) & Z_{ab-n}(2) & Z_{ac-n}(2)\\ Z_{ba-n}(2) & Z_{bb-n}(2) & Z_{bc-n}(2)\\ Z_{ca-n}(2) & Z_{cb-n}(2) & Z_{cc-n}(2)\end{bmatrix} & \begin{bmatrix}Z_{aa-n}(3) & Z_{ab-n}(3) & Z_{ac-n}(3)\\ Z_{ba-n}(3) & Z_{bb-n}(3) & Z_{bc-n}(3)\\ Z_{ca-n}(3) & Z_{cb-n}(3) & Z_{cc-n}(3)\end{bmatrix}\\ \begin{bmatrix}Z_{aa-n}(1) & Z_{ab-n}(1) & Z_{ac-n}(1)\\ Z_{ba-n}(1) & Z_{bb-n}(1) & Z_{bc-n}(1)\\ Z_{ca-n}(1) & Z_{cb-n}(1) & Z_{cc-n}(1)\end{bmatrix} & \begin{bmatrix}Z_{aa-n}(2) & Z_{ab-n}(2) & Z_{ac-n}(2)\\ Z_{ba-n}(2) & Z_{bb-n}(2) & Z_{bc-n}(2)\\ Z_{ca-n}(2) & Z_{cb-n}(2) & Z_{cc-n}(2)\end{bmatrix} & \begin{bmatrix}Z_{aa-n}(3) & Z_{ab-n}(3) & Z_{ac-n}(3)\\ Z_{ba-n}(3) & Z_{bb-n}(3) & Z_{bc-n}(3)\\ Z_{ca-n}(3) & Z_{cb-n}(3) & Z_{cc-n}(3)\end{bmatrix}\end{bmatrix} \quad (2.26)$$

$$[PD]=\begin{bmatrix}\begin{bmatrix}\begin{bmatrix}Z_{aa-n}(1) & Z_{ab-n}(1) & Z_{ac-n}(1)\\ Z_{ba-n}(1) & Z_{bb-n}(1) & Z_{bc-n}(1)\\ Z_{ca-n}(1) & Z_{cb-n}(1) & Z_{cc-n}(1)\end{bmatrix}\begin{bmatrix}FC_a(1)\\ FC_b(1)\\ FC_c(1)\end{bmatrix} & \begin{bmatrix}Z_{aa-n}(2) & Z_{ab-n}(2) & Z_{ac-n}(2)\\ Z_{ba-n}(2) & Z_{bb-n}(2) & Z_{bc-n}(2)\\ Z_{ca-n}(2) & Z_{cb-n}(2) & Z_{cc-n}(2)\end{bmatrix}\begin{bmatrix}FC_a(2)\\ FC_b(2)\\ FC_c(2)\end{bmatrix} & \begin{bmatrix}Z_{aa-n}(3) & Z_{ab-n}(3) & Z_{ac-n}(3)\\ Z_{ba-n}(3) & Z_{bb-n}(3) & Z_{bc-n}(3)\\ Z_{ca-n}(3) & Z_{cb-n}(3) & Z_{cc-n}(3)\end{bmatrix}\begin{bmatrix}FC_a(3)\\ FC_b(3)\\ FC_c(3)\end{bmatrix}\\ \begin{bmatrix}\begin{bmatrix}Z_{aa-n}(1) & Z_{ab-n}(1) & Z_{ac-n}(1)\\ Z_{ba-n}(1) & Z_{bb-n}(1) & Z_{bc-n}(1)\\ Z_{ca-n}(1) & Z_{cb-n}(1) & Z_{cc-n}(1)\end{bmatrix}\begin{bmatrix}FC_a(1)\\ FC_b(1)\\ FC_c(1)\end{bmatrix} & \begin{bmatrix}Z_{aa-n}(2) & Z_{ab-n}(2) & Z_{ac-n}(2)\\ Z_{ba-n}(2) & Z_{bb-n}(2) & Z_{bc-n}(2)\\ Z_{ca-n}(2) & Z_{cb-n}(2) & Z_{cc-n}(2)\end{bmatrix}\begin{bmatrix}FC_a(2)\\ FC_b(2)\\ FC_c(2)\end{bmatrix} & \begin{bmatrix}Z_{aa-n}(3) & Z_{ab-n}(3) & Z_{ac-n}(3)\\ Z_{ba-n}(3) & Z_{bb-n}(3) & Z_{bc-n}(3)\\ Z_{ca-n}(3) & Z_{cb-n}(3) & Z_{cc-n}(3)\end{bmatrix}\begin{bmatrix}FC_a(3)\\ FC_b(3)\\ FC_c(3)\end{bmatrix}\end{bmatrix}\end{bmatrix} \quad (2.27)$$

$$SBOBD=\begin{bmatrix}[Z_{abc}(1)]\times[FC_{abc}(1)] & [Z_{abc}(1)]\times[FC_{abc}(1)]+[Z_{abc}(2)]\times[FC_{abc}(2)] & 0\\ [Z_{abc}(1)]\times[FC_{abc}(1)] & 0 & [Z_{abc}(1)]\times[FC_{abc}(1)]+[Z_{abc}(3)]\times[FC_{abc}(3)]\end{bmatrix} \quad (2.28)$$

$$[LFM]=\begin{bmatrix}V_{abc}(slack\ bus) & V_{abc}(slack\ bus) & 0\\ V_{abc}(slack\ bus) & 0 & V_{abc}(slack\ bus)\end{bmatrix} - \begin{bmatrix}[Z_{abc}(1)]\times[FC_{abc}(1)] & \left[[Z_{abc}(1)]\times[FC_{abc}(1)]+[Z_{abc}(2)]\times[FC_{abc}(2)]\right] & 0\\ [Z_{abc}(1)]\times[FC_{abc}(1)] & 0 & \left[[Z_{abc}(1)]\times[FC_{abc}(1)]+[Z_{abc}(3)]\times[FC_{abc}(3)]\right]\end{bmatrix} \quad (2.29)$$

Initialize a search operation for selecting the three phase non null vector (any random vector) from each column of matrix [*LFM*] leading to formulation of new voltage matrix (as detailed in section 2.2).

2.4 Load Flow Algorithm for Meshed AC Distribution Systems

Some distribution lines feeding high-density load areas contain loops created by closing normally open tie-lines. The method proposed in section 2.2 can be effectively extended for "weakly-meshed" and "ring" distribution networks with pertinent advancement/modification. A technique for converting weakly meshed network to radial network has been developed and utilised to achieve the load-flow solution of weakly meshed distribution systems. The load-flow solution of the meshed network can be achieved in the same manner as radial distribution systems (after conversion to its equivalent radial network).

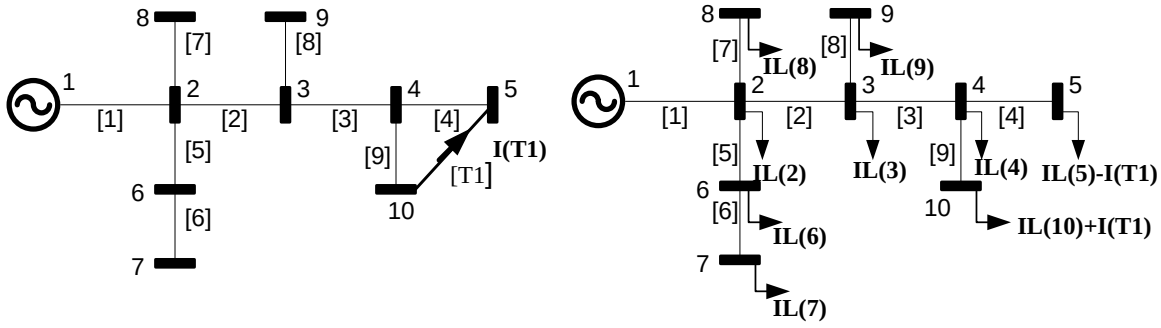

(a) (b)

Fig. 2.8: Distribution systems (a) Schematic diagram with one loop. (b) Equivalent radial system (of Fig. 2.8(a)) for branch current calculation.

The search algorithm and matrix building algorithm developed for radial distribution systems is equally applicable to weakly meshed distribution systems with minor modifications. For example, the load current $[LC]$ matrix of the distribution system in Fig. 2.8 (a) is -

$$[LC]=\begin{bmatrix} IL(2) & IL(3) & IL(4) & IL(5)-I(T1) & IL(6) & IL(7) & IL(8) & IL(9) & IL(10)+I(T1) \\ 0 & IL(3) & IL(4) & IL(5)-I(T1) & 0 & 0 & 0 & IL(9) & IL(10)+I(T1) \\ 0 & 0 & IL(4) & IL(5)-I(T1) & 0 & 0 & 0 & 0 & IL(10)+I(T1) \\ 0 & 0 & 0 & IL(5)-I(T1) & 0 & 0 & 0 & 0 & 0 \\ 0 & 0 & 0 & 0 & IL(6) & IL(7) & 0 & 0 & 0 \\ 0 & 0 & 0 & 0 & 0 & IL(7) & 0 & 0 & 0 \\ 0 & 0 & 0 & 0 & 0 & 0 & IL(8) & 0 & 0 \\ 0 & 0 & 0 & 0 & 0 & 0 & 0 & IL(9) & 0 \\ 0 & 0 & 0 & 0 & 0 & 0 & 0 & 0 & IL(10)+I(T1) \end{bmatrix} \quad (2.30)$$

In general, if a new branch "T" makes the system meshed (the new branch is between bus 'i' and 'j'), then current flowing through branch "T" needs to be calculated. The obtained result

will be added to the elements of i_{th} column of LC matrix (purely radial system -by removing all loops) with non zero value and subtracted from the non zero elements located at j_{th} column of LC matrix. Finally, a modified $[LC]$ matrix will be formulated (2.30). Rest of the matrix will be developed as per proposed algorithm for radial distribution systems (as per section 2).

Note that except for some modifications needed to be done for the [*LC*] matrices, the proposed solution techniques (in case of weakly meshed network) require no modification; therefore, the proposed method can obtain the load-flow solution for weakly meshed distribution systems efficiently.

$$I(T1)^t = \frac{V_{Th(10,5)}}{Z_{Th(10,5)} + Z(T1)} + \sum_{x=1}^{t-1} I(T1)^x \qquad (2.31)$$

$V_{Th(10,5)}$ = Thevenin equivalent voltage across bus 10 and 5.

$Z_{Th(10,5)}$ = Thevenin equivalent impedance across bus 10 and 5.

$Z(T1)$ = Actual impedance of branch T1.

$I(T1)^t$ = Current through branch T1 at the beginning of iteration t.

t = Iteration count.

The Current (I(T1)) through tie branch number T1 as shown in Fig. 2.8(a) can be also calculated using the equation below:

$$I(T1)^t = \frac{V(10)^t - V(5)^t}{\sum_{L \in q} Z(L_p)} + \sum_{x=1}^{t-1} I(T1)^x \qquad (2.32)$$

$Z(L_p)$=impedance of branch L contained in loop p.

q={4,9,T1}=set of branch numbers forming loop p.

$V(10)^t$ and $V(5)^t$= voltage at node 10 and node 5 respectively at the beginning of t_{th} iteration number.

The proposed load-flow algorithm for weakly meshed network can be effectively extended to ring type distribution systems.

Special Case- When two or more loops are having common branches, then the proposed current calculation method cannot be applied in current form. Suitable modification in the loop/tie branch current calculation procedure is required for convenient implementation of the proposed load-flow technique. The loop current can be easily obtained using following

equation-

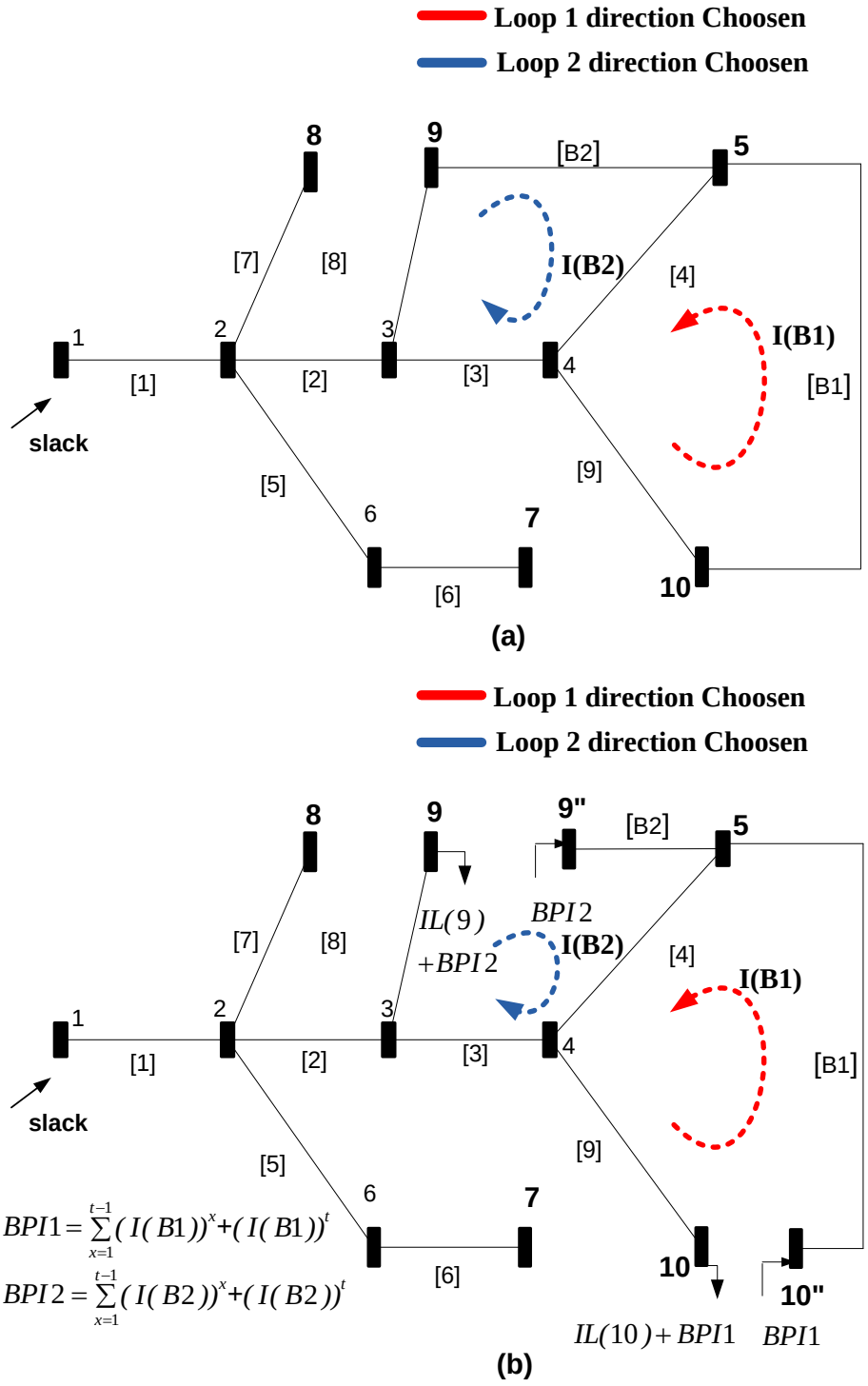

Fig. 2.9: Distribution systems (a) Schematic diagram with two loop. (b) Equivalent radial system (of Fig. 2.9(a)) for branch current calculation.

$$[LZ][LI]^t = [V(Ts)]^t \tag{2.33}$$

$$[LI]^t = [LZ]^{-1}[V(Ts)]^t \tag{2.34}$$

where,

LZ= Loop impedance matrix. *LI*= Loop current matrix. *V(Ts)*= Voltage matrix of tie switch branch. *t*= Iteration number.

Numerically, the diagonal matrix *LZ*(*i*,*i*) is equal to sum of all line sections impedance in a loop. The off-diagonal element, *LZ*(*i*,*j*) is nonzero only if loop *i* and loop *j* share one or more common line sections. The sign of the off-diagonal element depend on the relative direction of the loop currents. The loop current equation of the system shown in Fig. 2.9 can be written as:

$$\begin{bmatrix} Z(9)+Z(4)+Z(B1) & Z(4) \\ Z(4) & Z(8)+Z(3)+Z(4)+Z(B2) \end{bmatrix} \begin{bmatrix} I(B1)^t \\ I(B2)^t \end{bmatrix} = \begin{bmatrix} V(10)^t - V(10'')^t \\ V(9)^t - V(9'')^t \end{bmatrix} \tag{2.35}$$

$V(10)^t, V(10'')^t, V(9)^t$ and $V(9'')^t$ = voltage at node 10, node 10'', node 9 and node 9'' respectively at the beginning of t_{th} iteration number.

$I(B1)^t$ and $I(B2)^t$ = Current through tie switch branch B1 and B2 respectively at the beginning of t_{th} iteration number.

In general, if there exist a meshed structure in the distribution network, then split any of bus say T belonging to that particular mesh in two parts say T and T''. Thus, one additional bus T'' is created called as dummy node (ex. 10'' and 9'' -in Fig. 2.9). Now the system is radial and hence to include the effect of removed line, breakpoint injections are calculated using (2.35). The additional breakpoint injections are reflected in the load current matrix.

For three phase system, since all the loops are likely to be among three phase line sections, hence, all matrix element will be as per requirement of three phase systems. For example, if the line section between bus x and bus y is three-phase, the corresponding bus current, bus power, bus voltage and branch current will be a 3×1 vector, and, loop impedance matrix mainly consist of 3×3 block sub matrices. The developed load-flow algorithm for meshed distribution systems is also applicable to ring systems.

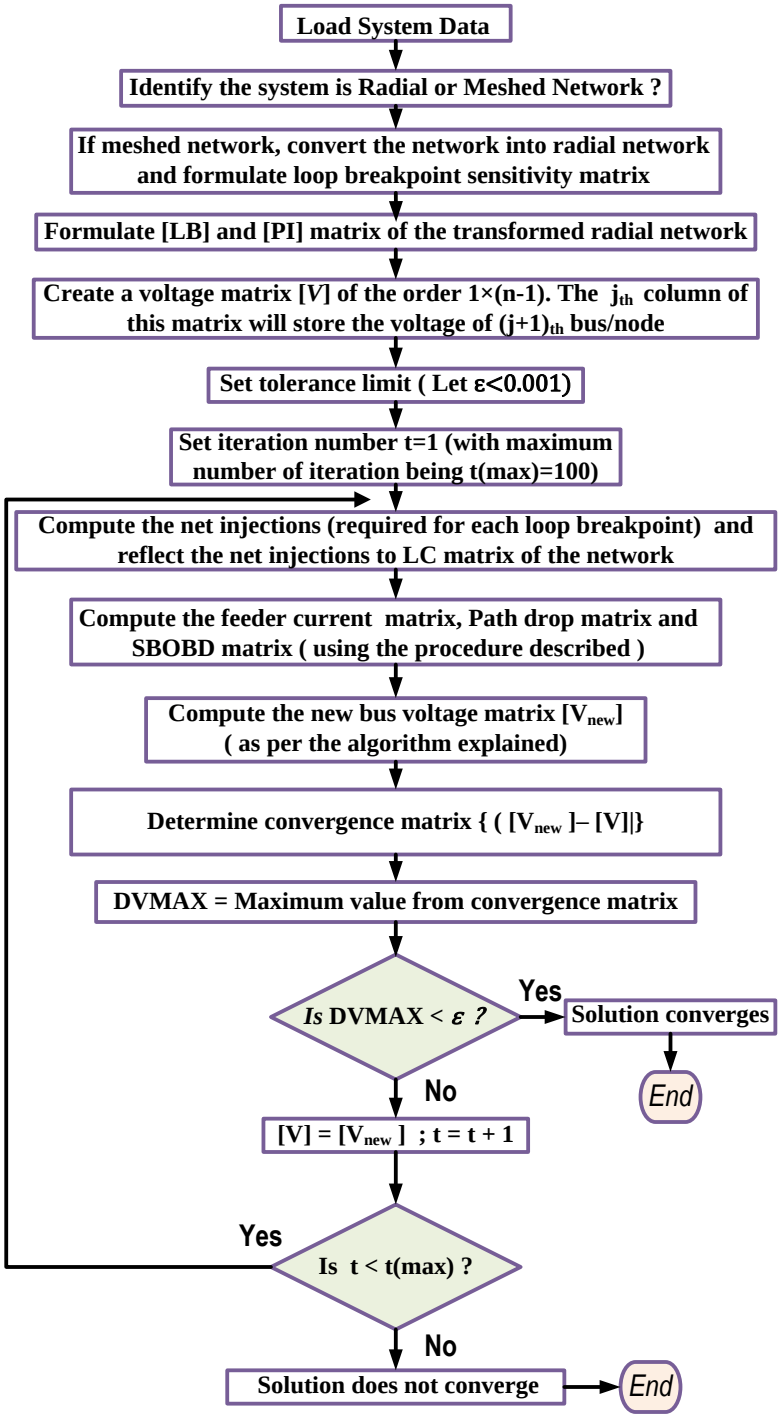

Fig. 2.10: Flowchart of generalized load flow solution algorithm for meshed AC distribution systems.

2.5 Load Modelling

One, two or three phase loads with wye or delta connections can exist. The balanced/unbalanced loads can also be modeled as constant power load, constant current

load, constant impedance load, exponential load and composite load (depending on characteristics of loads) [71]. The mathematical modeling of loads is listed below-

$$P(k) = P(k)_0 \left|V(k)\right|^x \tag{2.36}$$

$$Q(k) = Q(k)_0 \left|V(k)\right|^y \tag{2.37}$$

x & y =0 (in case of constant power load model)

x & y =1 (in case of constant current load model)

x & y =2 (in case of constant impedance load model)

x & y =1.38 & 3.22 respectively (in case of exponential load model)

For composite load model-

$$P(k) = (0.4 \times P(k)_0|V(k)|^0) + (0.3 \times P(k)_0|V(k)|^1) + (0.3 \times P(k)_0|V(k)|^2) \tag{2.38}$$

$$Q(k) = (0.4 \times Q(k)_0|V(k)|^0) + (0.3 \times Q(k)_0|V(k)|^1) + (0.3 \times Q(k)_0|V(k)|^2) \tag{2.39}$$

Where, $P(k)_0 \, and \, Q(k)_0$ is nominal real and reactive power respectively at bus k and $|V(k)|$ is the magnitude of voltage at k_{th} bus.

2.6 Results

The algorithm has been tested using matlab software through a personal computer with CORE i3 processor, 4 GB RAM and 2.66GHz CPU. The developed technique has been implemented on various balanced and unbalanced systems including weakly meshed structure. The load-flow results as acquired by proposed method and the efficacy comparison with that of algorithms prevailing in the literature are presented in this part. Three cases have been taken into consideration to examine the efficacy of the proposed load flow technique.

Case-1: Balanced radial distribution systems.

In this section the AC load-flow algorithm performance is investigated on several standard distribution systems such as: IEEE-15 [66], IEEE-33 [72] and IEEE-69 [73] bus system under different loading condition. The base MVA for all these test cases is same i.e. 100 MVA, the base voltage for IEEE 15 bus system is taken as 11kV and base voltage of 12.66kV for IEEE-33 and IEEE-69 bus system. The system losses and minimum voltage for several IEEE test systems obtained after load-flow simulation is given in Table 2.1. Effect of load modelling on the voltage profile for IEEE-15 bus, IEEE-33 bus and IEEE-69 bus systems are shown in Table 2.2, Table 2.3 and Table 2.4 respectively. The convergence

speed of the proposed method to wide variation of load is detailed in Table 2.5. The efficacy of the proposed method over several other methods for higher accuracy is detailed in Table 2.6. The results show that the proposed load-flow algorithm has very fast convergence ability. The proposed algorithm is robust enough to handle any size of distribution network.

Table 2.1: Real power loss, Reactive power loss and minimum voltage for different load modelling applied to test systems

Test Systems	Type of Load	Power Loss		Minimum Voltage (pu)
		Real(kW)	Reactive(kVAr)	
IEEE-15bus Base value (100 MVA and 11kV) Tolerance(0.0001)	CPLM	61.78	57.28	V(13)=0.9445
	CCLM	56.14	52.04	V(13)=0.9472
	CZLM	51.46	47.70	V(13)=0.9496
	ExpLM	50.28	46.61	V(13)=0.9501
	ComLM	56.73	52.60	V(13)=0.9469
IEEE-33 bus Base value (100 MVA and 12.66kV) Tolerance(0.0001)	CPLM	202.3747	135.0220	V(18)=0.9133
	CCLM	176.5261	117.5183	V(18)=0.9195
	CZLM	156.4608	103.9821	V(18)=0.9248
	ExpLM	157.4017	104.6039	V(18)=0.9241
	ComLM	179.3236	119.4135	V(18)=0.9188
IEEE-69bus Base value (100 MVA and 12.66kV) Tolerance(0.0001)	CPLM	224.5279	101.9812	V(65)=0.9092
	CCLM	191.3300	87.7390	V(65)=0.9167
	CZLM	167.1170	77.3203	V(65)=0.9225
	ExLM	168.0200	77.7056	V(65)=0.9214
	ComLM	194.9950	89.3107	V(65)=0.9158

Table 2.2: Voltage profile of IEEE-15 bus system for different load modelling

Node Number	Types of load				
	CPLM	CCLM	CZLM	ExpLM	ComLM
	Voltage Mag. (pu)	Voltage Mag. (pu)	Voltage Mag. (pu)	Voltage Mag. (pu)	Voltage Mag. (pu)
1	1.0000	1.0000	1.0000	1.0000	1.0000
2	0.9713	0.9726	0.9737	0.9740	0.9725
3	0.9567	0.9587	0.9605	0.9610	0.9585
4	0.9509	0.9532	0.9553	0.9558	0.9530
5	0.9499	0.9523	0.9544	0.9549	0.9521
6	0.9582	0.9601	0.9617	0.9621	0.9599
7	0.9560	0.9580	0.9597	0.9601	0.9578
8	0.9570	0.9589	0.9606	0.9609	0.9587
9	0.9680	0.9694	0.9706	0.9709	0.9692
10	0.9669	0.9684	0.9696	0.9699	0.9682
11	0.9500	0.9524	0.9544	0.9549	0.9521
12	0.9458	0.9485	0.9507	0.9512	0.9482
13	0.9445	0.9472	0.9496	0.9501	0.9469
14	0.9486	0.9511	0.9532	0.9537	0.9508
15	0.9484	0.9509	0.9531	0.9536	0.9506

Table 2.3: Voltage profile of IEEE-33 bus system for different load modelling

Node Number	Types of load				
	CPLM	CCLM	CZLM	ExpLM	ComLM
	Voltage Mag. (pu)	Voltage Mag. (pu)	Voltage Mag. (pu)	Voltage Mag. (pu)	Voltage Mag. (pu)
1	1	1	1	1	1
2	0.9970	0.9972	0.9973	0.9973	0.9972
3	0.9829	0.9839	0.9847	0.9846	0.9838
4	0.9755	0.9769	0.9782	0.9780	0.9768
5	0.9681	0.9701	0.9718	0.9715	0.9699
6	0.9497	0.9530	0.9558	0.9556	0.9527
7	0.9462	0.9498	0.9528	0.9526	0.9494
8	0.9414	0.9453	0.9486	0.9483	0.9449
9	0.9351	0.9395	0.9432	0.9429	0.9390
10	0.9294	0.9343	0.9384	0.9380	0.9338
11	0.9286	0.9335	0.9377	0.9372	0.9330
12	0.9271	0.9322	0.9364	0.9359	0.9316
13	0.9210	0.9266	0.9312	0.9306	0.9259
14	0.9187	0.9245	0.9293	0.9287	0.9238
15	0.9173	0.9232	0.9281	0.9275	0.9225
16	0.9159	0.9219	0.9270	0.9263	0.9213
17	0.9139	0.9201	0.9253	0.9246	0.9194
18	0.9133	0.9195	0.9248	0.9241	0.9188
19	0.9965	0.9967	0.9968	0.9968	0.9966
20	0.9929	0.9931	0.9933	0.9932	0.9931
21	0.9922	0.9924	0.9926	0.9926	0.9924
22	0.9916	0.9918	0.9920	0.9919	0.9918
23	0.9794	0.9804	0.9813	0.9812	0.9803
24	0.9727	0.9739	0.9750	0.9748	0.9738
25	0.9694	0.9707	0.9719	0.9717	0.9706
26	0.9478	0.9512	0.9542	0.9539	0.9509
27	0.9452	0.9489	0.9520	0.9517	0.9485
28	0.9338	0.9383	0.9422	0.9421	0.9378
29	0.9255	0.9308	0.9352	0.9352	0.9302
30	0.9220	0.9275	0.9322	0.9322	0.9269
31	0.9178	0.9237	0.9286	0.9286	0.923
32	0.9169	0.9229	0.9278	0.9278	0.9222
33	0.9166	0.9226	0.9276	0.9276	0.9219

The improvement over widely adopted BFS methods is based on the formulation of incidence matrix, path matrix, path impedance matrix and loads beyond branch matrix incidence matrix. The path search algorithm guarantee minimum number of search operation for identifying the paths between slack buses and end buses. The algorithm is formulated entirely on matrix formulation and computations, even at the juncture of updating the voltage

at each individual node. Therefore the proposed algorithm is computationally efficient when compared with the existing BFS method [47, 60-62].

Table 2.4: Voltage profile of IEEE-69 bus system for different load modelling

Node Number	Types of load				
	CPLM	CCLM	CZLM	ExpLM	ComLM
	Voltage Mag. (pu)	Voltage Mag. (pu)	Voltage Mag. (pu)	Voltage Mag. (pu)	Voltage Mag. (pu)
1	1	1	1	1	1
2	0.999967	0.999968	0.99997	0.99997	0.999968
3	0.999933	0.999936	0.999939	0.99994	0.999936
4	0.99984	0.999848	0.999855	0.999858	0.999847
5	0.999023	0.999086	0.999136	0.999147	0.999079
6	0.990102	0.990764	0.991291	0.991245	0.990689
7	0.980824	0.98211	0.983133	0.983026	0.981964
8	0.978612	0.980048	0.981191	0.981069	0.979885
9	0.977472	0.978988	0.980194	0.980065	0.978815
10	0.972475	0.974169	0.975529	0.975359	0.973978
11	0.971374	0.973108	0.974503	0.974322	0.972913
12	0.968215	0.97007	0.97157	0.97136	0.969862
13	0.965293	0.967271	0.968877	0.968637	0.96705
14	0.962397	0.964497	0.966208	0.965939	0.964263
15	0.95953	0.961751	0.963567	0.963268	0.961504
16	0.958997	0.961241	0.963076	0.962771	0.960991
17	0.958117	0.960398	0.962267	0.961952	0.960145
18	0.958108	0.96039	0.962258	0.961944	0.960136
19	0.957644	0.959946	0.961831	0.961512	0.95969
20	0.957345	0.95966	0.961557	0.961235	0.959403
21	0.956864	0.959199	0.961114	0.960787	0.95894
22	0.956857	0.959193	0.961108	0.960781	0.958933
23	0.956785	0.959124	0.961042	0.960714	0.958864
24	0.956629	0.958974	0.960898	0.960569	0.958714
25	0.95646	0.958813	0.960743	0.960412	0.958552
26	0.95639	0.958746	0.960679	0.960347	0.958485
27	0.956371	0.958727	0.960661	0.960329	0.958466
28	0.999926	0.99993	0.999932	0.999933	0.999929
29	0.999855	0.999858	0.999861	0.999862	0.999858
30	0.999733	0.999737	0.99974	0.999741	0.999736
31	0.999712	0.999716	0.999718	0.99972	0.999715
32	0.999605	0.999609	0.999612	0.999613	0.999608
33	0.999349	0.999353	0.999356	0.999357	0.999352
34	0.999014	0.999018	0.999021	0.999022	0.999017
35	0.998946	0.99895	0.998954	0.998955	0.99895
36	0.999919	0.999923	0.999925	0.999927	0.999922
37	0.999748	0.999751	0.999754	0.999755	0.999751
38	0.999589	0.999593	0.999596	0.999597	0.999592
39	0.999543	0.999547	0.99955	0.999551	0.999547
40	0.999541	0.999545	0.999548	0.999549	0.999544
41	0.998843	0.998848	0.998852	0.998854	0.998848
42	0.998551	0.998556	0.998561	0.998563	0.998556
43	0.998512	0.998518	0.998522	0.998524	0.998517
44	0.998504	0.998509	0.998514	0.998516	0.998509

Node Number	Types of load				
	CPLM	CCLM	CZLM	ExpLM	ComLM
	Voltage Mag. (pu)	Voltage Mag. (pu)	Voltage Mag. (pu)	Voltage Mag. (pu)	Voltage Mag. (pu)
45	0.998406	0.998411	0.998416	0.998418	0.99841
46	0.998405	0.998411	0.998415	0.998417	0.99841
47	0.99979	0.999798	0.999805	0.999808	0.999797
48	0.998545	0.99856	0.998573	0.99858	0.998559
49	0.994705	0.994741	0.994775	0.994793	0.994737
50	0.994161	0.9942	0.994237	0.994257	0.994196
51	0.978576	0.980013	0.981157	0.981035	0.97985
52	0.978567	0.980004	0.981148	0.981026	0.979841
53	0.974685	0.976438	0.97783	0.977679	0.976239
54	0.971442	0.973472	0.97508	0.974903	0.97324
55	0.966968	0.969383	0.971293	0.971079	0.969107
56	0.962603	0.965397	0.967603	0.967354	0.965078
57	0.940146	0.944894	0.948627	0.948001	0.944349
58	0.929096	0.934803	0.939286	0.93847	0.934147
59	0.924821	0.9309	0.935673	0.934782	0.930201
60	0.919801	0.926319	0.931435	0.930446	0.925569
61	0.912409	0.919574	0.925196	0.924139	0.91875
62	0.91212	0.919311	0.924952	0.923893	0.918483
63	0.911732	0.918958	0.924627	0.923563	0.918127
64	0.909834	0.91723	0.923031	0.921949	0.916378
65	0.90926	0.916707	0.922549	0.921462	0.91585
66	0.971317	0.973053	0.974449	0.974268	0.972858
67	0.971317	0.973052	0.974448	0.974268	0.972857
68	0.967886	0.969751	0.97126	0.971048	0.969542
69	0.967884	0.96975	0.971259	0.971047	0.969541

In paper [68], three matrices namely branch-current to bus voltage (BCBV) matrix, bus-injection to branch current (BIBC) matrix and distribution load flow (DLF=BCBV×BIBC) matrix are required to achieve the desired load flow solution of radial distribution systems. These matrices require considerable amount of memory for large sized distribution networks. Because of sparse nature of these three matrices, memory spaces are not being utilized efficiently, particularly for large sized distribution networks. Another drawback of BIBC & BCBV matrix based method is that, in order to obtain load flow solution two direct matrix multiplication is required: (a) between BCBV and BIBC matrices (b) between DLF & 'current Injection column vector' matrices, and hence requires sufficiently large processing time and memory spaces. The proposed method has overcome the disadvantages of BIBC and BCBV matrix based method. There is no direct multiplication required between the matrices ([*PI*] matrix,[*P*] matrix, [*LB*] matrix, [*PD*] matrix, [*SBOBD*] matrix and [*LFM*]) that

have been formulated for our purpose. The simple algebraic operation and efficient search technique enabling the proposed method to be computationally efficient when compared with the existing methods.

Table 2.5: Execution time(s)/ Number of iterations for three radial distribution system (tolerance=0.0001)

Load Type	Test Systems		
	15-Bus	33-Bus	69-Bus
CPLM	0.013726/3	0.03130/3	0.0656/3
CCLM	0.014854/2	0.034029/2	0.0686/3
CZLM	0.015348/3	0.040009/3	0.0988/3
ExpLM	0.015875/3	0.031580/3	0.0990/3
Comp LM	0.016712/2	0.032298/2	0.0930/3

Table 2.6: Convergence speed comparison (Tolerance=0.000001)

Methods	Iteration Number/Execution Time (s)		
	IEEE-15 bus	IEEE-33 bus	IEEE-69 bus
PM	5/0.0203	6/0.0364	6/0.0698
Ref.[68]	6/0.0352	8/0.0425	8/0.0795
Ref [47]	5/0.042	6/0.0692	6/0.0882
Ref [60]	6/0.0628	8/0.0728	8/0.0998
Ref [61]	6/0.0622	8/0.0711	8/0.0993
Ref [62]	9/0.1021	11/0.1254	10/0.1524

Case-2: Unbalanced radial distribution systems.

In a practical distribution system, 1-phase, 2-phase or 3-phase loads may be connected to the system. Also the distribution lines can be 1-phase or multiphase depending upon its requirement. Therefore, distribution system is, predominantly, unbalanced in nature. An efficient load-flow technique should be competent enough to analyze any kind of unbalanced distribution systems with accuracy. In order to check the accuracy and efficacy of the proposed load-flow algorithm for unbalanced loading four test systems have been taken into consideration:

(a) 8-bus test system [68] (b) 19-bus test system [74] (c) 25-bus test system [74] (b) IEEE-13 bus test system [75] (c) IEEE-37 bus test system [75] (d) IEEE-123 bus test system [75].

The convergence tolerance specified is 0.0001 p.u.. The voltage solution of 8-bus distribution system using proposed method and using several existing methods are shown in Table 2.7. The feeders have features that will be predominantly three-phase lateral with unbalanced loads. The voltage profile for 19-bus and 25-bus systems are shown in Table 2.8 and Table 2.9 respectively. The efficacy of the proposed method over several other methods is detailed in Table 2.10.

Table 2.7: Voltage solution for the 8-bus unbalanced distribution system

Bus	Voltage magnitude (pu)			Phase angle (Degree)			Phase
	Proposed Method	Method-2 [61]	Method-3 [68]	Proposed Method	Method-2 [61]	Method-3 [68]	
1	1.0000	1.0000	1.0000	0.0000	0.0000	0.0000	A
1	1.0000	1.0000	1.0000	-120.00	-120.00	-120.00	B
1	1.0000	1.0000	1.0000	120.00	120.00	120.00	C
2	0.9844	0.9840	0.9837	0.1833	0.1833	0.1833	A
2	0.9719	0.9714	0.9712	-119.75	-119.75	-119.75	B
2	0.9702	0.9699	0.9697	119.97	119.97	119.97	C
3	0.9842	0.9699	0.9832	0.1776	0.1776	0.1776	A
4	0.9659	0.9653	0.9652	-119.73	-119.73	-119.73	B
4	0.9679	0.9672	0.9669	119.93	119.93	119.93	C
5	0.9648	0.9644	0.9640	-119.74	-119.74	-119.74	B
6	0.9660	0.9652	0.9650	119.92	119.92	119.92	C
7	0.9692	0.9686	0.9683	119.96	119.96	119.96	C
8	0.9672	0.9674	0.9671	119.95	119.95	119.95	C

Table 2.8: Voltage solution for the 19-bus unbalanced distribution system

Bus	Voltage magnitude (pu)			Phase angle (Degree)		
	Phase A	Phase B	Phase C	Phase A	Phase B	Phase C
1	1.0000	1.0000	1.0000	0.0000	-120.00	120.00
2	0.9875	0.9891	0.988	0.01	−119.98	120.05
3	0.9854	0.9887	0.9863	0.00	−119.98	120.06
4	0.9824	0.9839	0.9830	0.03	−119.97	120.06
5	0.9820	0.9837	0.9828	0.03	−119.97	120.07
6	0.9793	0.9808	0.9801	0.04	−119.96	120.07
7	0.9786	0.9803	0.9796	0.04	−119.96	120.08
8	0.9728	0.9738	0.9735	0.06	−119.94	120.08
9	0.9659	0.9660	0.9657	0.08	−119.91	120.09
10	0.9563	0.9555	0.9550	0.09	−119.86	120.09
11	0.9550	0.9543	0.9533	0.10	−119.86	120.10
12	0.9548	0.9538	0.9536	0.11	−119.87	120.10
13	0.9544	0.9534	0.9521	0.10	−119.85	120.11
14	0.9545	0.9539	0.9528	0.10	−119.86	120.11
15	0.9527	0.9512	0.9513	0.11	−119.83	120.12
16	0.9534	0.9515	0.9522	0.13	−119.86	120.10
17	0.9537	0.9534	0.9523	0.10	−119.90	120.11
18	0.9538	0.9532	0.9521	0.10	−119.82	120.10
19	0.9514	0.9494	0.9501	0.13	−119.86	120.10

From Table 2.10, it is evident that proposed technique outperform method 4, especially for large sized distribution systems. The reason is, the developed technique does not require time consuming LU decomposition and matrix inversion needed in classical Newton Raphson & fast decoupled based algorithms, and, also the ill-conditioned problem prevailing due to factorization of the Jacobian matrix does not exist in the proposed solution method. In fact, the path impedance matrix and path drop matrix are acting as potential support in the proposed method to reduce execution time & memory requirement. It is also evident from

Table 2.10 that proposed algorithm is computationally efficient when compared with the existing BFS method [61] and direct method [68]. The reasons are clearly illustrated in section 2.6. Moreover, the results in Table 2.10 show that the number of iterations required by the proposed method is stable. The load-flow result shows that the proposed algorithm is suitable for power flow calculation in large sized distribution systems.

Table 2.9: Voltage solution for the 25-bus unbalanced distribution system

Bus	Voltage magnitude (pu)			Phase angle (Degree)		
	Phase A	Phase B	Phase C	Phase A	Phase B	Phase C
1	1.0000	1.0000	1.0000	0.0000	-120.00	120.00
2	0.9702	0.9711	0.9755	−0.57	−120.41	119.31
3	0.9632	0.9644	0.9698	−0.70	−120.52	119.15
4	0.9598	0.9613	0.9674	−0.77	−120.57	119.08
5	0.9587	0.9603	0.9664	−0.76	−120.57	119.08
6	0.9550	0.9559	0.9615	−0.55	−120.36	119.29
7	0.9419	0.9428	0.9492	−0.55	−120.30	119.27
8	0.9529	0.9538	0.9596	−0.56	−120.35	119.29
9	0.9359	0.9367	0.9438	−0.55	−120.28	119.26
10	0.9315	0.9319	0.9395	−0.55	−120.26	119.25
11	0.9294	0.9296	0.9376	−0.55	−120.26	119.25
12	0.9285	0.9287	0.9369	−0.55	−120.25	119.26
13	0.9287	0.9287	0.9373	−0.55	−120.26	119.25
14	0.9359	0.9370	0.9434	−0.55	−120.27	119.26
15	0.9338	0.9349	0.9414	−0.55	−120.27	119.25
16	0.9408	0.9418	0.9483	−0.55	−119.86	119.27
17	0.9347	0.9360	0.9420	−0.55	−120.27	119.26
18	0.9573	0.9586	0.9643	−0.70	−120.50	119.15
19	0.9524	0.9544	0.9600	−0.69	−120.49	119.16
20	0.9548	0.9563	0.9620	−0.70	−120.49	119.15
21	0.9537	0.9549	0.9605	−0.69	−120.49	119.16
22	0.9518	0.9525	0.9585	−0.69	−120.48	119.17
23	0.9565	0.9584	0.9648	−0.76	−120.57	119.08
24	0.9544	0.9565	0.9631	−0.76	−120.57	119.07
25	0.9520	0.9547	0.9612	−0.76	−120.57	119.08

Table 2.10: Convergence speed comparison (Tolerance-0.00001)

Test Systems	Iteration Number				CPU Time (s)			
	PM	Method-2 [61]	Method-3 [68]	Method-4 [40]	PM	Method-2 [61]	Method-3 [68]	Method-4 [40]
8 Bus	2	3	3	5	0.012	0.029	0.017	0.089
IEEE-13	3	4	3	7	0.029	0.046	0.035	0.092
19 Bus	2	4	3	6	0.035	0.067	0.040	0.095
25 bus	3	4	3	7	0.038	0.078	0.042	0.089
IEEE-34	3	4	3	8	0.042	0.098	0.050	0.122
IEEE-123	3	5	4	11	0.082	0.114	0.101	0.992

Case-3: Weakly meshed and ring distribution systems.

The applicability of the proposed method for solving load-flow equations of weakly meshed distribution is also tested. The test system consists of 33 buses with five tie lines [72], as shown in Fig. 2.11.

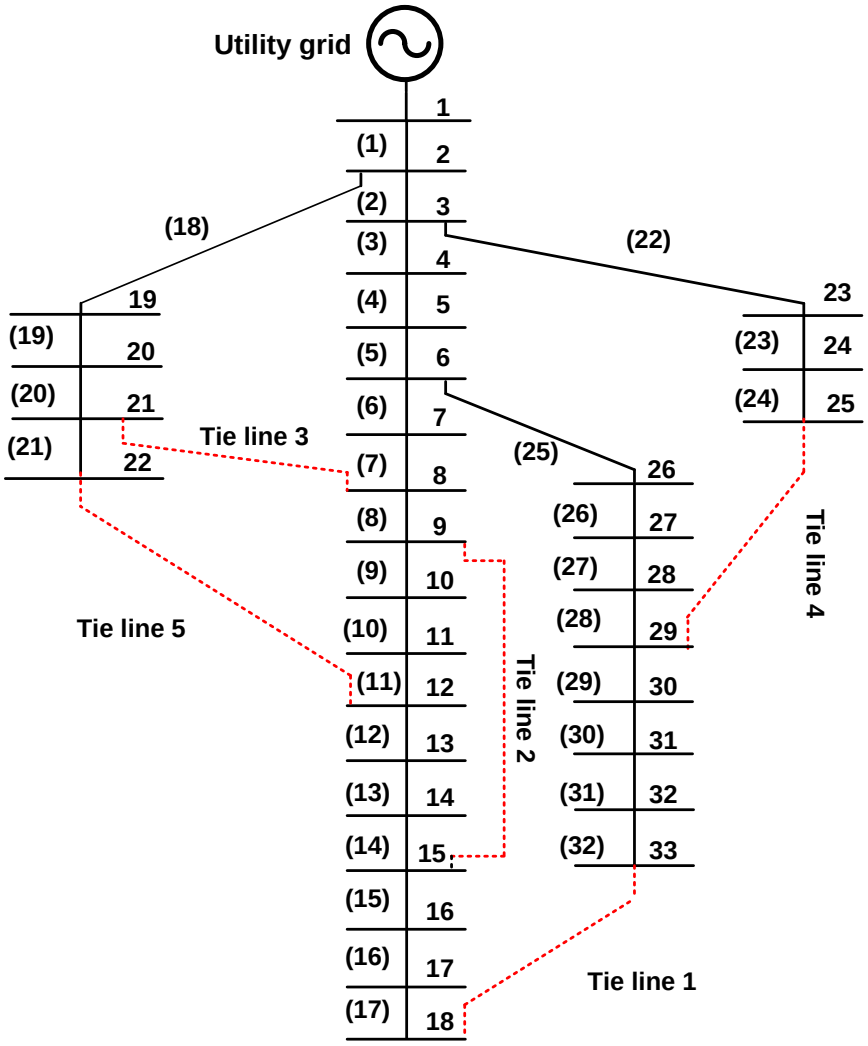

Fig. 2.11: IEEE-33 bus distribution system with five tie lines.

The test results of load flow performed on IEEE-33 bus system with the various combination of tie lines are provide in Table 2.11. The maximum variation between the voltage solution attained by the proposed method(PM) and those obtained by BFS approach [65] and BIBC [68] method is found to be 0.000023 p.u and 0.000018 p.u respectively. It is evident from the Table 2.12 that, with the increase in number of tie-lines, the convergence speed remains approximately unchanged unlike the well accepted BFS algorithm. It is also divulged from the table that the proposed technique is nearly 2–5 times efficient than the conventional BFS

method.

Table 2.11: Voltage profile of meshed IEEE-33 bus system

Node Number	Tie lines				
	1	1 and 2	1, 2 and 3	1, 2, 3 and 4	1, 2, 3, 4 and 5
	Voltage Mag. (pu)	Voltage Mag. (pu)	Voltage Mag. (pu)	Voltage Mag. (pu)	Voltage Mag. (pu)
1	1	1	1	1	1
2	0.9970	0.9970	0.9971	0.9971	0.9971
3	0.9830	0.9830	0.9861	0.9857	0.9863
4	0.9755	0.9756	0.9809	0.9818	0.9826
5	0.9681	0.9682	0.9759	0.9781	0.9792
6	0.9497	0.9499	0.9638	0.9695	0.9712
7	0.9461	0.9456	0.9627	0.9683	0.9703
8	0.9416	0.9404	0.9612	0.9669	0.9692
9	0.9357	0.9371	0.954	0.9608	0.9659
10	0.9304	0.9343	0.9508	0.9580	0.9657
11	0.9296	0.9340	0.9503	0.9576	0.9657
12	0.9283	0.9334	0.9496	0.9570	0.9649
13	0.9226	0.9316	0.9470	0.9551	0.9618
14	0.9204	0.9311	0.9462	0.9545	0.9607
15	0.9191	0.9315	0.9463	0.9548	0.9605
16	0.9180	0.9293	0.9441	0.9535	0.9587
17	0.9160	0.9249	0.9397	0.9510	0.9552
18	0.9156	0.9235	0.9382	0.9503	0.9541
19	0.9965	0.9965	0.9953	0.9955	0.9953
20	0.9929	0.9929	0.9806	0.9828	0.9807
21	0.9922	0.9922	0.9765	0.9792	0.9766
22	0.9916	0.9916	0.9758	0.9786	0.9728
23	0.9794	0.9794	0.9825	0.9800	0.9807
24	0.9727	0.9727	0.9759	0.9687	0.9699
25	0.9694	0.9694	0.9726	0.9608	0.9625
26	0.9477	0.9482	0.9621	0.9685	0.9702
27	0.9450	0.9458	0.9599	0.9672	0.9689
28	0.9333	0.9358	0.9500	0.9619	0.9638
29	0.9249	0.9286	0.9430	0.9584	0.9603
30	0.9211	0.9255	0.9400	0.9549	0.9571
31	0.9167	0.9227	0.9373	0.9511	0.9540
32	0.9158	0.9223	0.9370	0.9503	0.9534
33	0.9155	0.9228	0.9374	0.9502	0.9536

Effect of load modeling on the voltage profile for weakly meshed IEEE-33 bus system is shown in Table 2.13. It is being revealed that if two buses are connected by a tie line then voltage magnitude of the above mentioned buses is not varying much. The proposed algorithm has been further tested on a 4-bus ring network (Fig. 2.12(a)) and the result obtained by the proposed method is clearly depicted in the graph shown in Fig. 2.12(b). The

obtained load-flow result of ring system lies in the proximity of the results obtained by traditional methods.

Table 2.12: Convergence speed comparison (Execution time in sec.)

Method	Number of Tie Lines				
	1	2	3	4	5
PM	0.011986	0.011201	0.011216	0.011218	0.011296
BFS	0.035625	0.055278	0.078226	0.089984	0.090625
BIBC	0.024625	0.026458	0.032469	0.035247	0.037124

Table 2.13: Voltage profile of meshed IEEE-33 bus system for different load modelling

Node Number	Load Models				
	CPLM	CCLM	CZLM	ExpLM	ComLM
	Voltage Mag. (pu)	Voltage Mag. (pu)	Voltage Mag. (pu)	Voltage Mag. (pu)	Voltage Mag. (pu)
1	1	1	1	1	1
2	0.9971	0.9972	0.9973	0.9973	0.9972
3	0.9863	0.9867	0.9871	0.9871	0.9867
4	0.9826	0.9831	0.9837	0.9836	0.9831
5	0.9792	0.9798	0.9805	0.9804	0.9797
6	0.9712	0.9720	0.973	0.9729	0.9719
7	0.9703	0.9711	0.9721	0.9720	0.9710
8	0.9692	0.9700	0.971	0.9710	0.9699
9	0.9659	0.9669	0.968	0.9679	0.9668
10	0.9657	0.9666	0.9677	0.9677	0.9665
11	0.9657	0.9667	0.9678	0.9677	0.9665
12	0.9649	0.9659	0.967	0.9670	0.9658
13	0.9618	0.9629	0.9641	0.9640	0.9627
14	0.9607	0.9618	0.9631	0.9631	0.9617
15	0.9605	0.9616	0.9629	0.9628	0.9615
16	0.9587	0.9599	0.9612	0.9612	0.9597
17	0.9552	0.9566	0.9581	0.9581	0.9564
18	0.9541	0.9555	0.9571	0.9571	0.9554
19	0.9953	0.9955	0.9956	0.9956	0.9955
20	0.9807	0.9814	0.982	0.982	0.9813
21	0.9766	0.9775	0.9782	0.9782	0.9774
22	0.9728	0.9739	0.9748	0.9747	0.9738
23	0.9807	0.9814	0.9820	0.9819	0.9813
24	0.9699	0.9711	0.9720	0.9720	0.9710
25	0.9625	0.9641	0.9653	0.9652	0.9639
26	0.9702	0.9711	0.9720	0.9720	0.9710
27	0.9689	0.9699	0.9709	0.9708	0.9697
28	0.9638	0.9649	0.9661	0.9661	0.9647
29	0.9603	0.9615	0.9628	0.9629	0.9614
30	0.9571	0.9584	0.9599	0.9599	0.9583
31	0.9540	0.9554	0.957	0.9570	0.9553
32	0.9534	0.9549	0.9565	0.9565	0.9547
33	0.9536	0.9551	0.9567	0.9567	0.9549

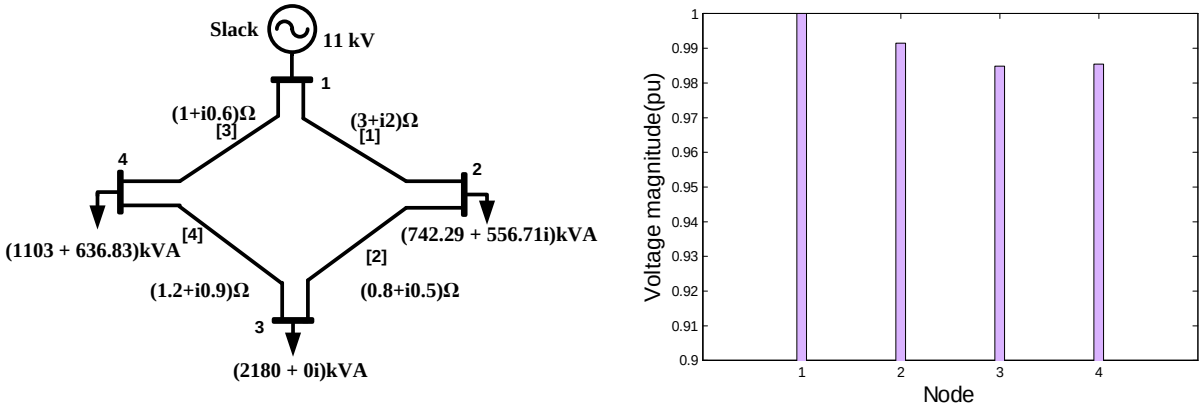

(a) (b)

Fig. 2.12: 4 bus distribution system (a) Schematic diagram, (b) Load flow results.

2.7 Conclusion

A new computationally efficient load-flow algorithm for ac distribution systems based on network graphical information has been introduced in this work. The proposed technique allows dynamic formulation of two matrices: [*PI*] matrix and [*LB*] matrix, which has been used for the load-flow calculation (in matrix form). The most prominent feature of the proposed work lies in construction of the path impedance matrix and loads beyond branch matrix, once formulated, it will remain unaltered for the entire operation. The reconfiguration of these matrices takes place automatically if input data changes. This feature helps the proposed algorithm to be computationally more efficient. Further, by storing all the relevant data in matrix form, it saves immense computer memory. Because of these pronounced reasons, the proposed load-flow technique has found to be competent while working on large sized distribution systems. The developed method has been implemented on various unbalanced, balanced and weakly meshed distribution power networks. However, in case of meshed &/or ring network they should be converted to equivalent radial network by breaking the loops. Furthermore, in case of three phase unbalanced distribution systems each elements of the path impedance matrix, path drop matrix, loads beyond branch matrix, voltage matrix and feeder current matrix should be replaced by their corresponding three phase vector/matrix. The remaining supporting matrices will reshape themselves accordingly. In order to compare the efficacy of the proposed algorithm with those already present in the

literature, it has been applied to acquire load-flow solution of the standard test systems and a comparison with the several existing methods has been observed. The convergence characteristics of the proposed algorithm has been thoroughly investigated for various loading conditions. The comparison of the computational performance, in terms of number of iterations and CPU time, gives detail evidence of the efficacy of the proposed method developed in this work.

Chapter-3

Load Flow Algorithm for AC Distribution Systems in the Presence of Distributed Generations

In this chapter, algorithm developed in chapter 2 has been modified in manner such that it provides load flow solution of AC distribution system (both balanced and unbalanced) in the presence of various model of distributed generations. The proposed algorithm is capable of providing the load flow solution for both radial and meshed configurations of distribution system. Extensive load flow simulation studies are conducted for aforementioned types of distribution systems and corresponding results are examined by comparing with the results obtained by existing load flow methods.

3.1 Introduction

The demand of trustworthy power sources rises along with the ever-increasing demand of power. These power demands result in significant voltage drop at buses/nodes in an existing distribution system. With the insertion of DGs in existing distribution system, the system offers many technical benefits such as active and reactive power loss reduction, improvement of bus voltages, reliability, efficiency and increase in the loadability of system for future expansion [76-81]. Load flow analysis of distribution systems need special models and algorithms to handle multiple sources. The AC load flow algorithm developed in chapter 2 has been modified in a manner such that it is capable of providing the load flow solution of AC distribution network in the presence of distributed generations. The proposed algorithm is equally applicable to balanced and unbalanced distribution systems.

The mathematical model of DG considered as PQ and PV buses are incorporated into the proposed algorithm to imitate the injection of DGs in the distribution systems. The DG modelled as PQ bus is included in the proposed load flow algorithm by considering injection by the DG as the negative load. The power injected by the DG need to be reflected in the *LB* matrix of the distribution network. For the PV type buses or distributed generators, the

reactive power generation is adjusted between the maximum and minimum limits in order to maintain the constant voltage and constant real power (injected) at the PV bus. The sensitivity or breakpoint matrix has been utilized to obtain the additional reactive power injection/withdrawal to maintain the specified voltage at each PV nodes. In the case of weakly meshed distribution network with PV type distributed generations, the loop breakpoint injections and PV breakpoint injections have been calculated simultaneously. The net injections is reflected in the [*LB*] or [*LC*] matrix of the distribution network. Note that except for some modifications that are needed to be done for the [*LC*] or [*LB*] matrices, the proposed solution techniques require no modification; therefore, the proposed method can obtain the load-flow solution for AC distribution system in the presence of distributed generations efficiently. The remaining supporting matrices (path impedance matrix [*PI*], feeder current matrix [*FC*], path drop matrix [*PD*], slack bus to other buses drop matrix [*SBOBD*], load flow matrix [*LFM*] will reshape themselves accordingly. The effectiveness of the proposed solution methodology has been tested on several standard distribution systems. Test outcome show viability and accuracy of the proposed method.

3.2 Load Flow Algorithm for AC Radial Distribution System with Distributed Generations

In general, modelling requires system representation mathematically such that the mathematical model gives sufficient information about actual systems that covers all the necessary system behaviour within certain constraints. A proper model of the DG that can adequately represent a DG type with a view of assessing its impact on the network is of great importance. The model should be represented in such a way that the impact evaluation approach on the network due to the DG presence can easily be conducted. Many models have been developed by researchers on DG for load flow analysis in which the DGs are modelled as either a constant power factor model or constant voltage model or variable reactive power model. The buses with DG connection that yields a small output power are modelled as PQ nodes while those with large DG output are considered as PV nodes.

(a) PQ type distributed generations.

This types of distributed generation has real and reactive power as specified value. The power injected by the DG need to be reflected in the *LB* matrix of the distribution network by

considering injection from the DG as the negative load. For example consider the single phase or balanced three phase distribution network in Fig. 3.1, the modified loads beyond branch matrix will be:

$$[\boldsymbol{LB}]=\begin{bmatrix} \boldsymbol{S(2)} & \boldsymbol{S(3)} & \boldsymbol{S(4)} & \boldsymbol{S(5)} & \boldsymbol{S(6)} & \boldsymbol{S(7)-S(7)_{DG}} & \boldsymbol{S(8)} & \boldsymbol{S(9)} & \boldsymbol{S(10)} \\ \boldsymbol{0} & \boldsymbol{S(3)} & \boldsymbol{S(4)} & \boldsymbol{S(5)} & \boldsymbol{0} & \boldsymbol{0} & \boldsymbol{0} & \boldsymbol{S(9)} & \boldsymbol{S(10)} \\ \boldsymbol{0} & \boldsymbol{0} & \boldsymbol{S(4)} & \boldsymbol{S(5)} & \boldsymbol{0} & \boldsymbol{0} & \boldsymbol{0} & \boldsymbol{0} & \boldsymbol{S(10)} \\ \boldsymbol{0} & \boldsymbol{0} & \boldsymbol{0} & \boldsymbol{S(5)} & \boldsymbol{0} & \boldsymbol{0} & \boldsymbol{0} & \boldsymbol{0} & \boldsymbol{0} \\ \boldsymbol{0} & \boldsymbol{0} & \boldsymbol{0} & \boldsymbol{0} & \boldsymbol{S(6)} & \boldsymbol{S(7)-S(7)_{DG}} & \boldsymbol{0} & \boldsymbol{0} & \boldsymbol{0} \\ \boldsymbol{0} & \boldsymbol{0} & \boldsymbol{0} & \boldsymbol{0} & \boldsymbol{0} & \boldsymbol{S(7)-S(7)_{DG}} & \boldsymbol{0} & \boldsymbol{0} & \boldsymbol{0} \\ \boldsymbol{0} & \boldsymbol{0} & \boldsymbol{0} & \boldsymbol{0} & \boldsymbol{0} & \boldsymbol{0} & \boldsymbol{S(8)} & \boldsymbol{0} & \boldsymbol{0} \\ \boldsymbol{0} & \boldsymbol{0} & \boldsymbol{0} & \boldsymbol{0} & \boldsymbol{0} & \boldsymbol{0} & \boldsymbol{0} & \boldsymbol{S(9)} & \boldsymbol{0} \\ \boldsymbol{0} & \boldsymbol{0} & \boldsymbol{0} & \boldsymbol{0} & \boldsymbol{0} & \boldsymbol{0} & \boldsymbol{0} & \boldsymbol{0} & \boldsymbol{S(10)} \end{bmatrix} \quad (3.1)$$

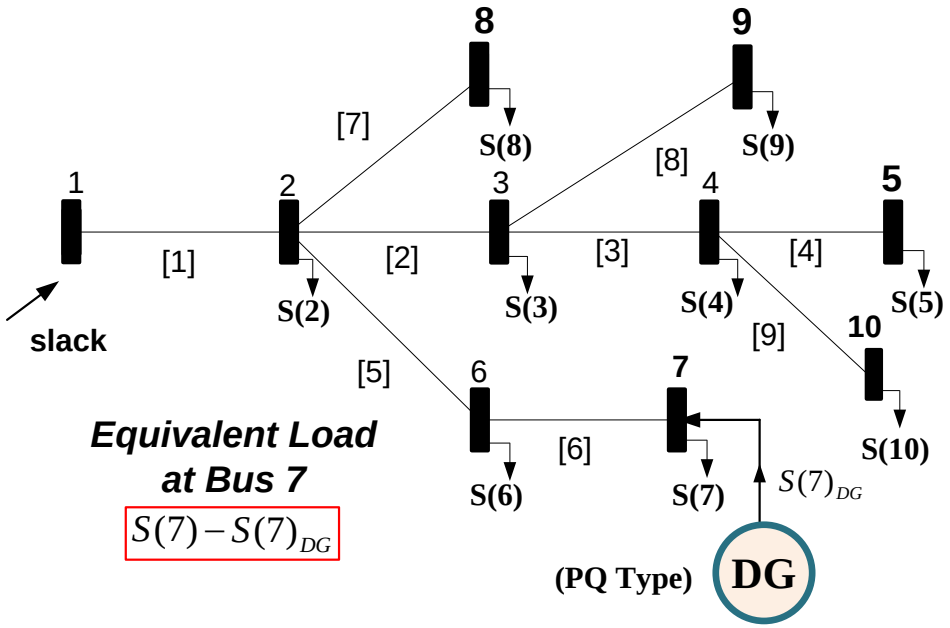

Fig. 3.1: Schematic diagram of a single phase/ balanced distribution network with PQ type DG.

The same concept has been extended for solving three phase unbalanced load flow equations in the presence of PQ type distributed generations. For example consider the three phase unbalanced distribution network in Fig. 3.2, the modified loads beyond branch matrix will be:

$$LB=\begin{bmatrix} S_{abc}(2) & S_{abc}(3) & S_{abc}(4)-\left[S_{abc}(4)\right]_{DG} \\ 0 & S_{abc}(3) & 0 \\ 0 & 0 & S_{abc}(4)-\left[S_{abc}(4)\right]_{DG} \end{bmatrix} \quad (3.2)$$

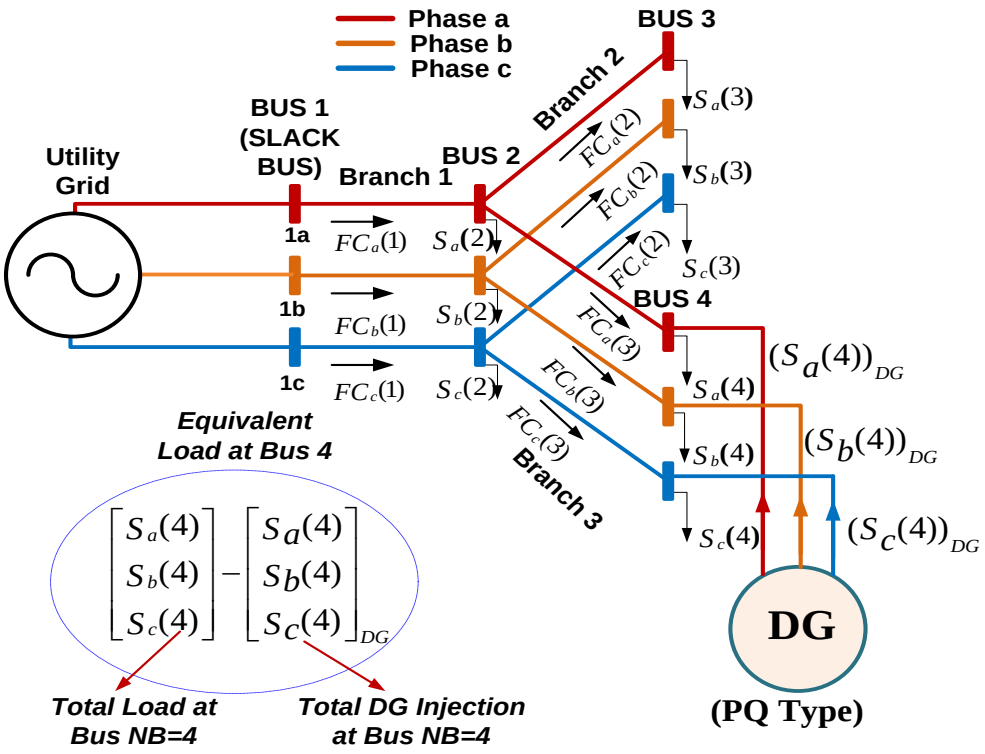

Fig.3.2: Schematic diagram of a three phase unbalanced distribution network with PQ type DG.

Note that except for some modifications needed in [*LB*] matrices, the proposed solution techniques require no modification. The remaining supporting matrices (path impedance matrix [*PI*], Feeder current matrix [*FC*], path drop matrix [*PD*], slack bus to other buses drop matrix [*SBOBD*], load flow matrix [*LFM*] will reshape themselves accordingly. Therefore, the proposed method can obtain the load-flow solution for three phase distribution systems in the presence of PQ type distributed generations efficiently.

(b) PV type distributed generations.

Consider a scenario, where PV nodes are present in a distribution network. PV type buses are mainly generation buses. For the PV type buses or distributed generators, the reactive power generation is adjusted between the maximum and minimum limits in order to maintain the constant voltage and constant real power (injected) at the PV bus. The sensitivity matrix has been utilized to obtain the additional reactive power injection/withdrawal to maintain the specified voltage at each PV nodes.

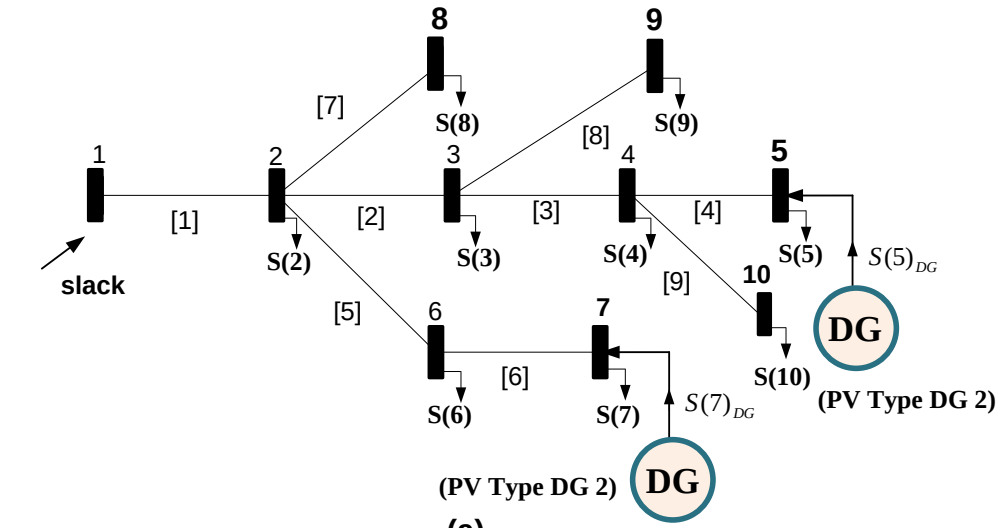

(a)

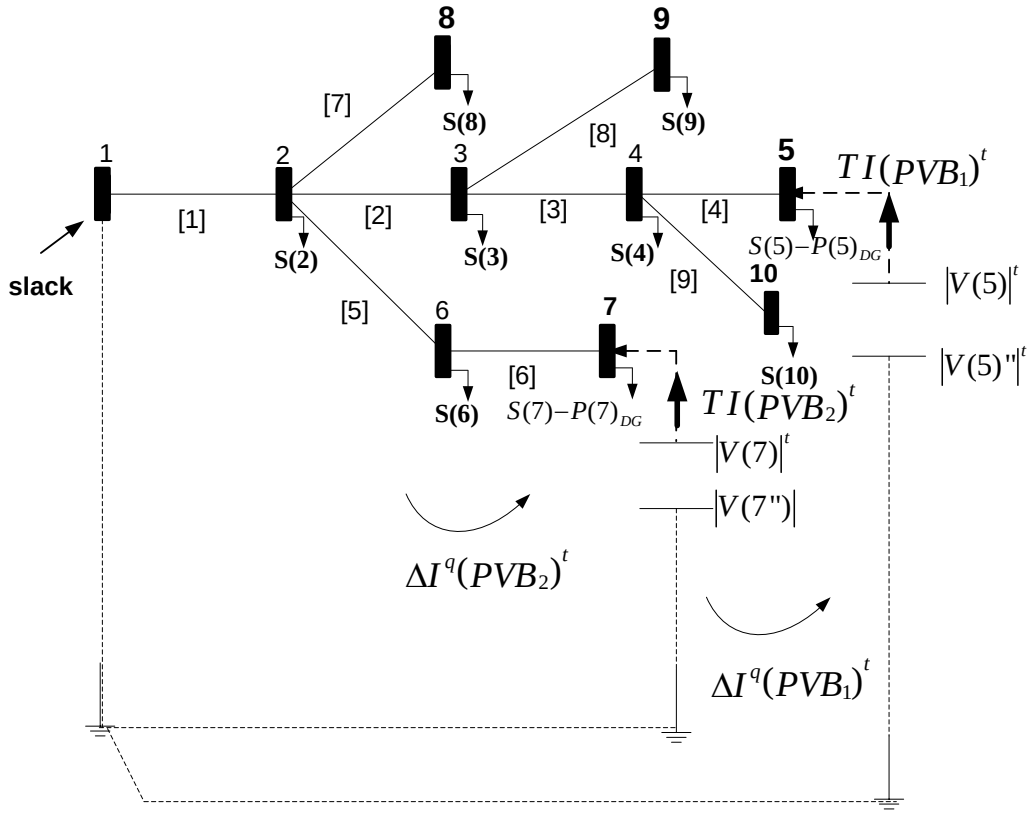

$$TI(PVB_1)^t = \sum_{x=1}^{t-1} \Delta I^q(PVB_1)^x + \Delta I^q(PVB_1)^t$$

$$TI(PVB_2)^t = \sum_{x=1}^{t-1} \Delta I^q(PVB_2)^x + \Delta I^q(PVB_2)^t$$

(b)

Fig. 3.3: Distribution system with PV type DGs (a) Schematic diagram (b) Equivalent circuit for calculating PV bus injections.

For the distribution network that contains PV nodes, one PV breakpoint matrix needs to be formulated. The detailed procedure is explained below:

PVB= Set of all PV buses.

PVB_K= K^{th} element of set PVB

pvb= Total number of PV buses.

K=1,2.....pvb.

For the distribution system shown in Fig. 3.3, the breakpoint equation called as PV breakpoint sensitivity matrix can be written as:

$$\begin{bmatrix} Z(1)+Z(2)+Z(3)+Z(4) & Z(1) \\ Z(1) & Z(1)+Z(5)+Z(6) \end{bmatrix} \times \begin{bmatrix} \Delta I^r(PVB_1)^t - j\Delta I^q(PVB_1)^t \\ \Delta I^r(PVB_2)^t - j\Delta I^q(PVB_2)^t \end{bmatrix} = \begin{bmatrix} \left|V(PVB_1'')^t\right| - \left|V(PVB_1)^t\right| \\ \left|V(PVB_2'')^t\right| - \left|V(PVB_2)^t\right| \end{bmatrix} \quad (3.3)$$

In this particular case,

$$\Delta I^r(PVB_1) = \Delta I^r(PVB_2) = 0$$

PVB= Set of all PV buses={5,7}

pvb=2= Total number of PV buses.

K=1,2

PVB_1= 1st element of set PVB=5.

PVB_2= 1st element of set PVB=7.

$\Delta V(PVB_1)^t$ = Voltage magnitude mismatch at the bus PVB_1 associated with PV distributed generation number 1 in the beginning of iteration t = $V(PVB_1'')^t - V(PVB_1)^t$

$V(PVB_1'')^t$ = Voltage magnitude (specified) at bus PVB_1 associated with PV distributed generation number 1.

$V(PVB_1)^t$ = Voltage calculated (beginning of iteration number t) at bus PVB_1 associated with PV distributed generation number 1.

$\Delta I^q(PVB_1)^t$ = Additional PV breakpoint reactive current injection at bus PVB_1 in the beginning of iteration t.

$\Delta I^r(PVB_1)^t$ = Additional PV breakpoint real current injection at bus PVB_1 in the beginning of iteration t.

$\Delta V(PVB_2)^t$ = Voltage magnitude mismatch at the bus PVB_2 associated with PV distributed generation number 2 in the beginning of iteration *t* = $V(PVB_2'')^t - V(PVB_2)^t$

$V(PVB_2'')^t$ = Voltage magnitude (specified) at bus PVB_2 associated with PV distributed generation number *2.*

$V(PVB_2)^t$ = Voltage calculated (beginning of iteration number t) at bus PVB_2 associated with PV distributed generation number *2.*

$\Delta I^q(PVB_2)^t$ = Additional PV breakpoint reactive current injection at bus PVB_2 in the beginning of iteration t.

$\Delta I^r(PVB_2)^t$ = Additional PV breakpoint real current injection at bus PVB_2 in the beginning of iteration t.

On simplifying equation (3.3), the resulting equation will be:

$$\begin{bmatrix} X(1)+X(2)+X(3)+X(4) & X(1) \\ X(1) & X(1)+X(5)+X(6) \end{bmatrix} \times \begin{bmatrix} \Delta I^q(PVB_1)^t \\ \Delta I^q(PVB_2)^t \end{bmatrix} = \begin{bmatrix} \left|V(PVB_1'')^t\right| - \left|V(PVB_1)^t\right| \\ \left|V(PVB_2'')^t\right| - \left|V(PVB_2)^t\right| \end{bmatrix} \quad (3.4)$$

Equation (3.4) can also be written as:

$$\begin{bmatrix} \Delta I^q(PVB_1)^t \\ \Delta I^q(PVB_2)^t \end{bmatrix} = \begin{bmatrix} X(1)+X(2)+X(3)+X(4) & X(1) \\ X(1) & X(1)+X(5)+X(6) \end{bmatrix}^{-1} \begin{bmatrix} \left|V(PVB_1'')^t\right| - \left|V(PVB_1)^t\right| \\ \left|V(PVB_2'')^t\right| - \left|V(PVB_2)^t\right| \end{bmatrix} \quad (3.5)$$

$$\begin{bmatrix} \Delta I^q(PVB_1)^t \\ \Delta I^q(PVB_2)^t \end{bmatrix} = \begin{bmatrix} X_{11} & X_{12} \\ X_{21} & X_{22} \end{bmatrix}^{-1} \begin{bmatrix} \Delta V(PVB_1)^t \\ \Delta V(PVB_2)^t \end{bmatrix} \quad (3.6)$$

In short equation (3.6) can be written as:

$$\Delta I^q = X^{-1}\Delta V \quad (3.7)$$

The diagonal elements in the sub-matrix X are the sum of positive sequence phase reactance of all the line sections between PV node x and the root node (substation bus). If two PV nodes PVB_k and PVB_l have completely different path to the slack bus then off

diagonal elements $X_{kl} = X_{lk} = 0$. If PV nodes PVB_k and PVB_l share some common branches in their respective path to the slack bus, then $X_{kl} = X_{lk}$ = modulus of the sum of positive sequence phase reactance matrix of all line sections common to two paths. The sign of off-diagonal elements in X depends upon relative direction of breakpoint current in the common branches.

In the subsequent step, calculate the required reactive power generation for each PV bus:

$$\Delta Q(PVB_1)^t = V(PVB_1)^t \times (0 - j\Delta I^q(PVB_1)^t)^* \tag{3.8}$$

$$\Delta Q(PVB_2)^t = V(PVB_2)^t \times (0 - j\Delta I^q(PVB_2)^t)^* \tag{3.9}$$

where,

$\Delta Q(PVB_1)^t$ = Additional PV breakpoint reactive power injection at bus PVB_1 in the beginning of iteration *t*.

$\Delta Q(PVB_2)^t$ = Additional PV breakpoint reactive power injection at bus PVB_2 in the beginning of iteration *t*.

The total reactive power injection by the PV type distributed generation in Figure 4.3 at the beginning of iteration *t* is given by the following equations:

$$TQ(PVB_1)^t = \sum_{x=1}^{t-1} \Delta Q(PVB_1)^x + \Delta Q(PVB_1)^t \tag{3.10}$$

$$TQ(PVB_2)^t = \sum_{x=1}^{t-1} \Delta Q(PVB_2)^x + \Delta Q(PVB_2)^t \tag{3.11}$$

where,

$TQ(PVB_1)^t$ = Total PV breakpoint reactive power injection at bus PVB_1 in the beginning of iteration *t*.

$TQ(PVB_2)^t$ = Total PV breakpoint reactive power injection at bus PVB_2 in the beginning of iteration *t*.

The general breakpoint equation for the distribution system having *pvb* number of PV buses

$$\begin{bmatrix} X_{11} & X_{12} & \cdots & \cdots & X_{1pvb} \\ X_{21} & X_{22} & \cdots & \cdots & X_{2pvb} \\ \vdots & \vdots & \vdots & \vdots & \vdots \\ \vdots & \vdots & \vdots & \vdots & \vdots \\ X_{pvb1} & X_{pvb2} & \cdots & \cdots & X_{(pvb)(pvb)} \end{bmatrix} \begin{bmatrix} \Delta I^q(PVB_1)^t \\ \Delta I^q(PVB_2)^t \\ \vdots \\ \vdots \\ \Delta I^q(PVB_{pvb})^t \end{bmatrix} = \begin{bmatrix} \Delta V(PVB_1)^t \\ \Delta V(PVB_2)^t \\ \vdots \\ \vdots \\ \Delta V(PVB_{pvb})^t \end{bmatrix} \tag{3.12}$$

K=1,2.....PVb.

PVB= Set of all PV buses.

PVB_K= Kth element of set PV.

pvb= Total number of PV buses.

The above equation for calculating PV breakpoint current injection can be modified in terms of PV breakpoint reactive power injection. With the assumption of all bus voltages being close to 1.0 p.u. and the phase angles small, the following equation holds for any PV bus K:

$$\Delta I^{r}(PVB_K)^{t} - j\Delta I^{q}(PVB_K)^{t} = \Delta P(PVB_K)^{t} - \Delta Q(PVB_K)^{t} = \left(\Delta S(PVB_K)^{t}\right)^{*} \tag{3.13}$$

$\Delta P(PVB_K)^{t}$ = Additional PV breakpoint real power injection at bus PVB_K in the beginning of iteration *t*.

$\Delta S(PVB_K)^{t}$ = Additional PV breakpoint complex power injection at bus PVB_K in the beginning of iteration *t*.

Thus, equation (3.12) can be modified as:

$$\begin{bmatrix} X_{11} & X_{12} & \cdots & \cdots & X_{1pvb} \\ X_{21} & X_{22} & \cdots & \cdots & X_{2pvb} \\ \vdots & \vdots & \vdots & \vdots & \vdots \\ \vdots & \vdots & \vdots & \vdots & \vdots \\ X_{pvb1} & X_{pvb2} & \cdots & \cdots & X_{(pvb)(pvb)} \end{bmatrix} \begin{bmatrix} \Delta Q(PVB_1)^{t} \\ \Delta Q(PVB_2)^{t} \\ \vdots \\ \vdots \\ \Delta Q(PVB_{pvb})^{t} \end{bmatrix} = \begin{bmatrix} \Delta V(PVB_1)^{t} \\ \Delta V(PVB_2)^{t} \\ \vdots \\ \vdots \\ \Delta V(PVB_{pvb})^{t} \end{bmatrix} \tag{3.14}$$

$$X\Delta Q = \Delta V \tag{3.15}$$

The net additional injection/withdrawal of reactive power to/from the PV buses need to be reflected in the loads beyond branch matrix of the network. If the calculated reactive power violates the boundary condition, then reactive power generated/absorbed will be positioned at the violated boundary limit and the DG will act as a PQ generator. Note that except for some modifications needed to be done for the [*LB*] matrices, the proposed solution techniques require no modification; therefore, the proposed method can obtain the load-flow solution for three phase distribution systems in the presence of distributed generations efficiently.

Consider the network in Fig. 3.3, the modified loads beyond branch matrix will at the beginning of an iteration *t* is give by:

$$LB = \begin{bmatrix} S(2) & S(3) & S(4) & S(5) - P(PVB_1) - jTQ(PVB_1)^t & S(6) & S(7) - P(PVB_2) - jTQ(PVB_2)^t & S(8) & S(9) & S(10) \\ 0 & S(3) & S(4) & S(5) - P(PVB_1) - jTQ(PVB_1)^t & 0 & 0 & 0 & S(9) & S(10) \\ 0 & 0 & S(4) & S(5) - P(PVB_1) - jTQ(PVB_1)^t & 0 & 0 & 0 & 0 & S(10) \\ 0 & 0 & 0 & S(5) - P(PVB_1) - jTQ(PVB_1)^t & 0 & 0 & 0 & 0 & 0 \\ 0 & 0 & 0 & 0 & S(6) & S(7) - P(PVB_2) - jTQ(PVB_2)^t & 0 & 0 & 0 \\ 0 & 0 & 0 & 0 & 0 & S(7) - P(PVB_2) - jTQ(PVB_2)^t & 0 & 0 & 0 \\ 0 & 0 & 0 & 0 & 0 & 0 & S(8) & 0 & 0 \\ 0 & 0 & 0 & 0 & 0 & 0 & 0 & S(9) & 0 \\ 0 & 0 & 0 & 0 & 0 & 0 & 0 & 0 & S(10) \end{bmatrix} \quad (3.16)$$

The same concept has been extended for solving three phase unbalanced load flow equations in the presence of PV type distributed generations.

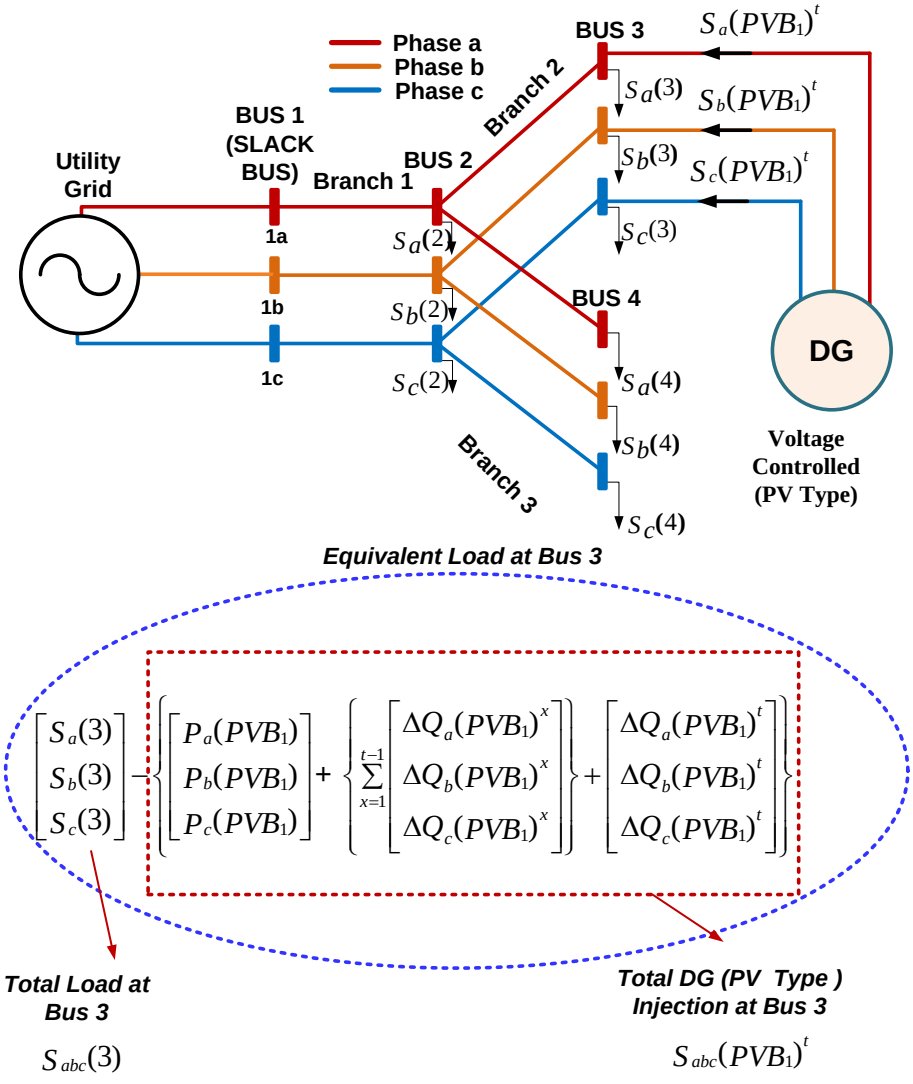

Fig. 3.4: Schematic diagram of an AC unbalanced distribution network with PV type DG.

The general breakpoint equation for the three phase distribution system having *pvb* number of PV buses can be written as:

$$X\Delta Q = \Delta V \tag{3.17}$$

$$\begin{bmatrix} [X_{11}]_{abc} & [X_{12}]_{abc} & \cdots & \cdots & [X_{1pvb}]_{abc} \\ [X_{21}]_{abc} & [X_{22}]_{abc} & \cdots & \cdots & [X_{2pvb}]_{abc} \\ \vdots & \vdots & \vdots & \vdots & \vdots \\ \vdots & \vdots & \vdots & \vdots & \vdots \\ [X_{pvb1}]_{abc} & [X_{pvb2}]_{abc} & \cdots & \cdots & [X_{(pvb)(pvb)}]_{abc} \end{bmatrix} \begin{bmatrix} \Delta Q_{abc}(PVB_1)^t \\ \Delta Q_{abc}(PVB_2)^t \\ \vdots \\ \vdots \\ \Delta Q_{abc}(PVB_{pvb})^t \end{bmatrix} = \begin{bmatrix} \Delta V_{abc}(PVB_1)^t \\ \Delta V_{abc}(PVB_2)^t \\ \vdots \\ \vdots \\ \Delta V_{abc}(PVB_{pvb})^t \end{bmatrix} \tag{3.18}$$

For three phase system, since all the loops are likely to be among three phase line sections, hence, all matrix element will be as per requirement of three phase systems. All element in the X are the sub-matrices of the order 3×3. The diagonal elements in the sub-matrix X are the sum of positive sequence phase reactance matrix of all the line sections between PV node k and the root node (substation bus). If two PV nodes PVB_k and PVB_l have completely different path to the slack bus then off diagonal elements $[X_{kl}]_{abc} = [X_{lk}]_{abc} = 0$. If PV nodes *i* and *j* share some common branches in their respective path to the slack bus, then $[X_{kl}]_{abc} = [X_{lk}]_{abc}$ = modulus of the sum of positive sequence phase reactance matrix of all line sections common to two paths. All element in the ΔQ and ΔV are the sub-matrices or vector of the order 3×1.

The net additional injection/withdrawal of reactive power to/from the PV buses need to be reflected in the loads beyond branch matrix of the network. If the calculated reactive power violates the boundary condition, then reactive power generated/absorbed will be positioned at the violated boundary limit and the DG will act as a PQ generator. Note that except for some modifications needed to be done for the [*LB*] matrices, the proposed solution techniques require no modification; therefore, the proposed method can obtain the load-flow solution for three phase distribution systems in the presence of distributed generations efficiently.

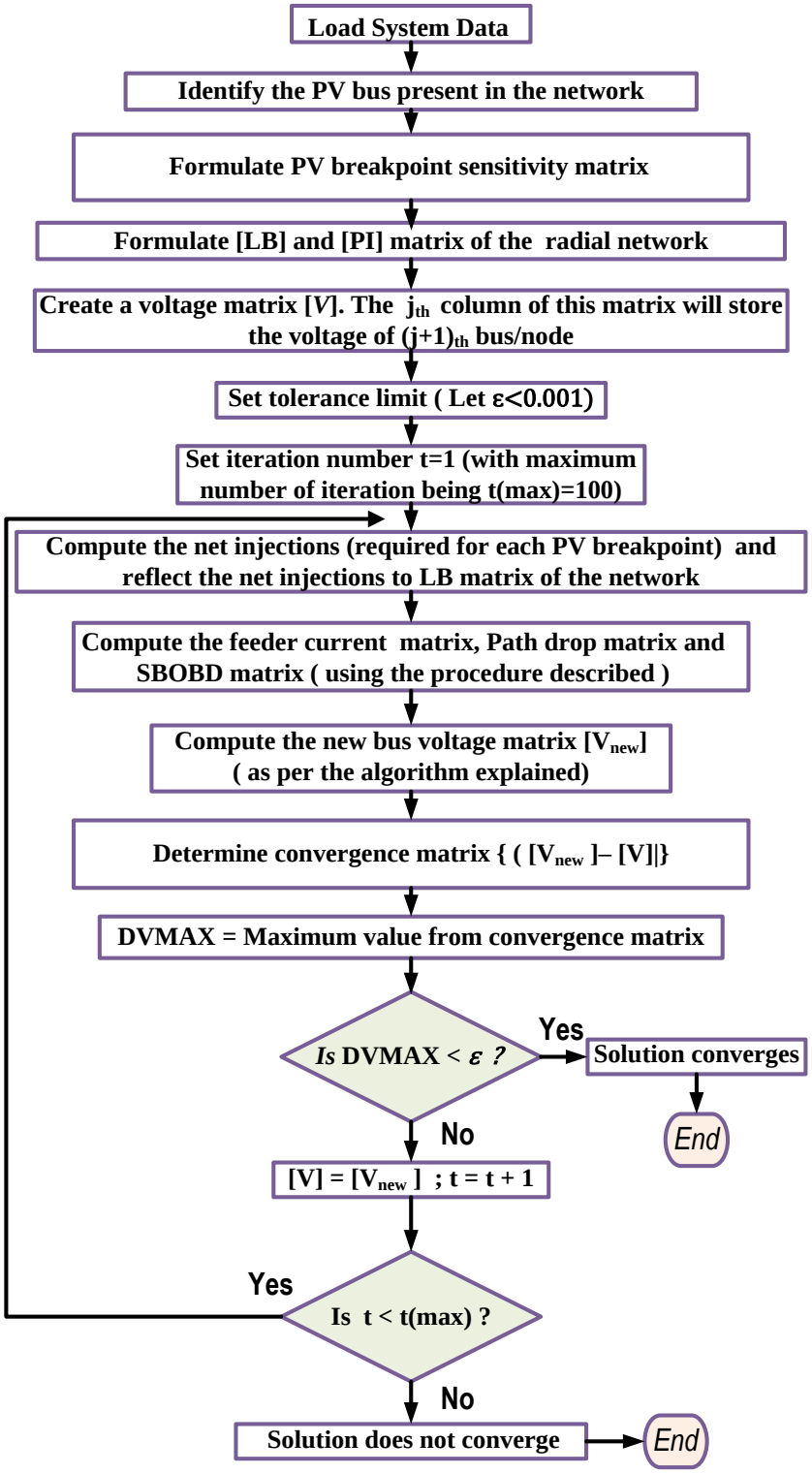

Fig. 3.5: Flowchart for solving load flow problem of AC radial distribution network with PV type DG.

For example consider the three phase unbalanced distribution network in Fig. 3.4, the modified loads beyond branch matrix will be:

$$LB=\begin{bmatrix} S_{abc}(2) & S_{abc}(3)-[P_{abc}(PVB_1)+\{\sum_{x=1}^{t-1}\Delta Q_{abc}(PVB_1)^x\}+\Delta Q_{abc}(PVB_1)^t] & S_{abc}(4) \\ 0 & S_{abc}(3)-[P_{abc}(PVB_1)+\{\sum_{x=1}^{t-1}\Delta Q_{abc}(PVB_1)^x\}+\Delta Q_{abc}(PVB_1)^t] & 0 \\ 0 & 0 & S_{abc}(4) \end{bmatrix} \quad (3.19)$$

The PV breakpoint injection has been calculated utilizing the equations (3.20)-(3.21):

$$\left[\Delta Q_{abc}(PVB_1)^t\right]=\left[X11\right]_{abc}^{-1}\left[\Delta V_{abc}(PVB_1)^t\right] \quad (3.20)$$

$$\left[X_{11}\right]_{abc}=[[X_{abc}(1)]+[X_{abc}(2)]] \quad (3.21)$$

$\Delta Q_{abc}(PVB_1)^t$ = Additional Injection/withdrawal of reactive power by the PV type DG number 1 located at bus number PVB_1=3 (beginning of iteration number *t*).

$\Delta V_{abc}(PVB_1)^t$ = Voltage magnitude mismatch at the bus 3 (i.e PVB_1=3) associated with PV distributed generation 1 (in the beginning of iteration number *t*).

$P_{abc}(PVB_1)$ = Net real power injected by the controlled distributed generation number 1 located at bus 3 (PVB_1=3).

PVB={3}.

PVB_1=3 {First element of set PV}.

K=1.

PVb =1.

The complete algorithm for solving the load flow equations of AC radial distribution system with distributed generations modelled as PV bus has been clearly depicted through the flowchart in Fig. 3.5.

3.3 Load Flow Algorithm for AC Meshed Distribution System with Distributed Generations

Consider a scenario in which PV type buses/distributed generations exists in the three phase meshed distribution network. For such cases, loop breakpoint injections and PV breakpoint injections need to be calculated simultaneously. This requires formulation of one common

matrix called as common breakpoint matrix embedding the properties of loop breakpoint matrix and PV breakpoint matrix.

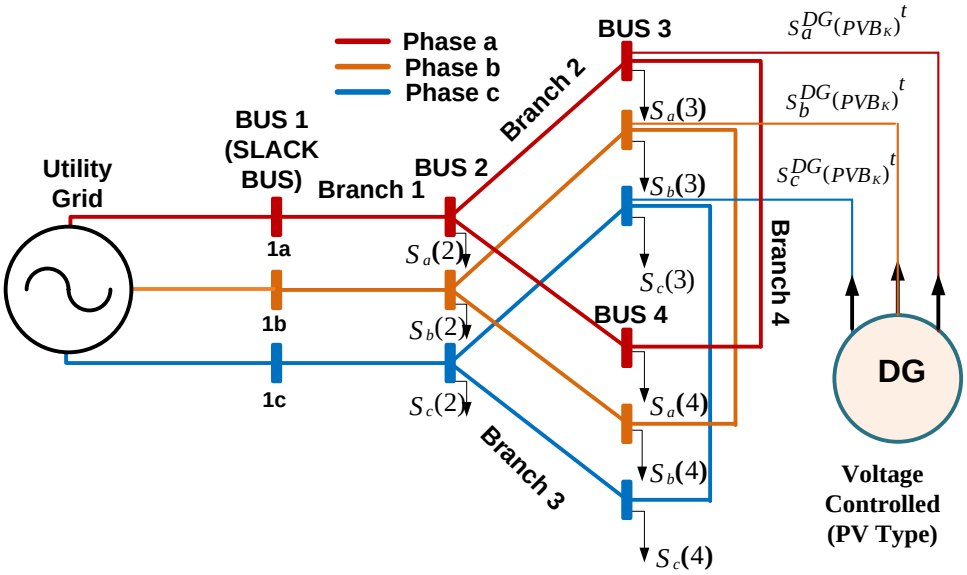

Fig. 3.6: Schematic diagram of a three phase meshed distribution network with PV bus.

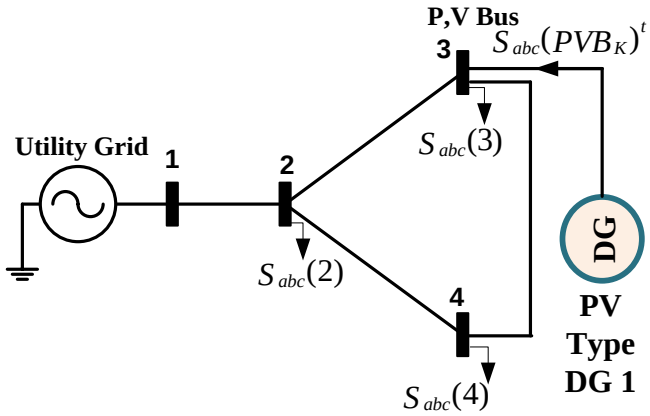

Fig. 3.7: Single line diagram of the three phase distribution network in Fig. 3.6.

For example, consider the three phase meshed distribution network in Fig. 3.6 in which there is existing a PV type bus/distributed generation at bus number 3. Hence, loop breakpoint injections and PV breakpoint injections need to be calculated simultaneously. For better understanding three phase distribution network is represented by a undirected graph (single line representation). Form a loop breakpoint say d by disconnecting the line 4 from bus MB_d and the abovementioned disconnected line 4 should be connected to the artificially

created dummy node say MB_d". Also, create a PV breakpoint K by disconnecting the PV type DG from bus PVB_K and the abovementioned disconnected DG should be connected to the artificially created dummy bus say PVB_K". Where d and K are loop breakpoint number and PV breakpoint number respectively.

$$\Delta I_{abc}(PVB_K)^t = \Delta I^r_{abc}(PVB_K)^t - j\Delta I^q_{abc}(PVB_K)^t$$
$$\Delta I_{abc}(MB_d)^t = \Delta I^r_{abc}(MB_d)^t - j\Delta I^q_{abc}(MB_d)^t$$

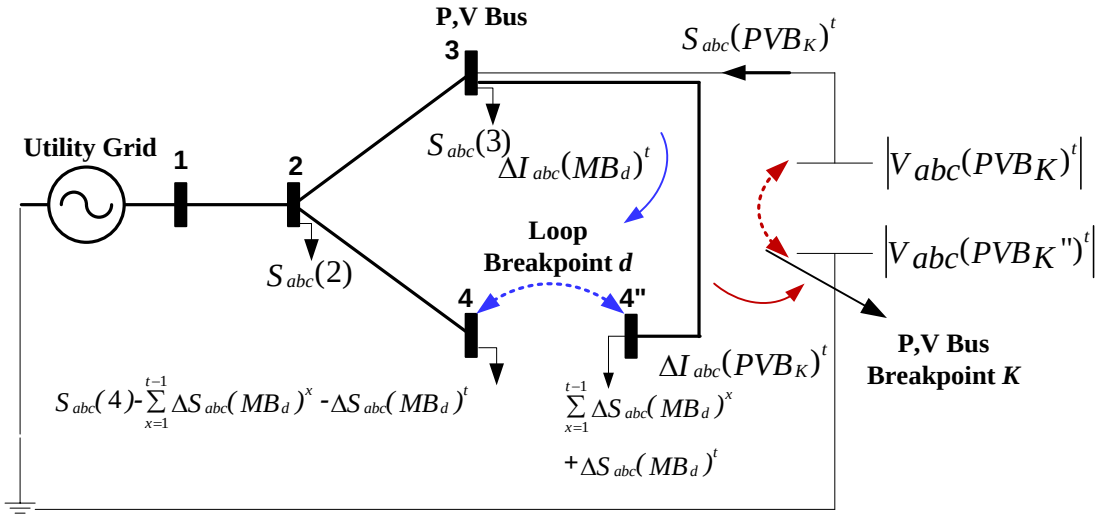

Fig. 3.8: Equivalent diagram of the distribution network in Fig.3.7 for calculating PV bus injections.

For the system shown in Fig. 3.8, the loop breakpoint equation and PV breakpoint equation can be written as:

$$\left[\begin{bmatrix} R_{abc}(1)+R_{abc}(2)+R_{abc}(3) & -R_{abc}(2) \\ -R_{abc}(2) & R_{abc}(1)+R_{abc}(2) \end{bmatrix} + j\begin{bmatrix} X_{abc}(1)+X_{abc}(2)+X_{abc}(3) & -X_{abc}(2) \\ -X_{abc}(2) & X_{abc}(1)+X_{abc}(2) \end{bmatrix}\right]\begin{bmatrix} \Delta I_{abc}(MB_d)^t \\ \Delta I_{abc}(PVB_K)^t \end{bmatrix} = \begin{bmatrix} \Delta V_{abc}(MB_d)^t + j\Delta\delta_{abc}(MB_d)^t \\ \Delta V_{abc}(PVB_K)^t + j\Delta\delta_{abc}(PVB_K)^t \end{bmatrix} \quad (3.22)$$

$$\left[\begin{bmatrix} [R11]_{abc} & [R12]_{abc} \\ [R21]_{abc} & [R22]_{abc} \end{bmatrix} + j\begin{bmatrix} [X11]_{abc} & [X12]_{abc} \\ [X21]_{abc} & [X22]_{abc} \end{bmatrix}\right]\begin{bmatrix} \Delta I^r_{abc}(MB_d)^t - j\Delta I^q_{abc}(MB_d)^t \\ \Delta I^r_{abc}(PVB_K)^t - j\Delta I^q_{abc}(PVB_K)^t \end{bmatrix} = \begin{bmatrix} \Delta V(MB_d)^t + j\Delta\delta(MB_d)^t \\ \Delta V(PVB_K)^t + j\Delta\delta(PVB_K)^t \end{bmatrix} \quad (3.23)$$

On further simplifying the above equation (3.23), the resulting equation will be:

$$\begin{bmatrix} [X11]_{abc} & [X12]_{abc} & [R11]_{abc} & [R12]_{abc} \\ [X21]_{abc} & [X22]_{abc} & [R21]_{abc} & [R22]_{abc} \\ -[R11]_{abc} & -[R12]_{abc} & [X11]_{abc} & [X12]_{abc} \\ -[R21]_{abc} & -[R22]_{abc} & [X21]_{abc} & [X22]_{abc} \end{bmatrix} \begin{bmatrix} \Delta I^{q}_{abc}(MB_d)^{t} \\ \Delta I^{q}_{abc}(PVB_K)^{t} \\ \Delta I^{r}_{abc}(MB_d)^{t} \\ \Delta I^{r}_{abc}(PVB_K)^{t} \end{bmatrix} = \begin{bmatrix} \Delta V_{abc}(MB_d)^{t} \\ \Delta V_{abc}(PVB_K)^{t} \\ \Delta \delta_{abc}(MB_d)^{t} \\ \Delta \delta_{abc}(PVB_K)^{t} \end{bmatrix} \tag{3.24}$$

The above equation for calculating PV breakpoint current injection and mesh breakpoint current injections can be modified in terms of PV breakpoint reactive power injection and loop breakpoint complex power injection. With the assumption of all bus voltages being close to 1.0 p.u. and the phase angles small, the following equation holds:

$$\Delta I^{r}_{abc}(MB_d)^{t} - j\Delta I^{q}_{abc}(MB_d)^{t} = \Delta P_{abc}(MB_d)^{t} - j\Delta Q_{abc}(MB_d)^{t} \tag{3.25}$$

$$\Delta I^{r}_{abc}(PVB_K)^{t} - j\Delta I^{q}_{abc}(PVB_K)^{t} = \Delta P_{abc}(PVB_K)^{t} - j\Delta Q_{abc}(PVB_K)^{t} \tag{3.26}$$

Using equation (3.25) and (3.26) in equation (3.24), the resulting equation will be:

$$\begin{bmatrix} [X11]_{abc} & [X12]_{abc} & [R11]_{abc} & [R12]_{abc} \\ [X21]_{abc} & [X22]_{abc} & [R21]_{abc} & [R22]_{abc} \\ -[R11]_{abc} & -[R12]_{abc} & [X11]_{abc} & [X12]_{abc} \\ -[R21]_{abc} & -[R22]_{abc} & [X21]_{abc} & [X22]_{abc} \end{bmatrix} \begin{bmatrix} \Delta Q_{abc}(MB_d)^{t} \\ \Delta Q_{abc}(PVB_K)^{t} \\ \Delta P_{abc}(MB_d)^{t} \\ \Delta P_{abc}(PVB_K)^{t} \end{bmatrix} = \begin{bmatrix} \Delta V_{abc}(MB_d)^{t} \\ \Delta V_{abc}(PVB_K)^{t} \\ \Delta \delta_{abc}(MB_d)^{t} \\ \Delta \delta_{abc}(PVB_K)^{t} \end{bmatrix} \tag{3.27}$$

The equation (3.27) can also be represented as:

$$\begin{bmatrix} X & R \\ -R & X \end{bmatrix} \begin{bmatrix} \Delta Q \\ \Delta P \end{bmatrix} = \begin{bmatrix} \Delta V \\ \Delta \delta \end{bmatrix} \tag{3.28}$$

where

$$\begin{aligned} X &= \begin{bmatrix} X_{abc}(1) + X_{abc}(2) + X_{abc}(3) & -X_{abc}(2) \\ -X_{abc}(2) & X_{abc}(1) + X_{abc}(2) \end{bmatrix} \\ &= \begin{bmatrix} [X11]_{abc} & [X12]_{abc} \\ [X21]_{abc} & [X22]_{abc} \end{bmatrix} \end{aligned} \tag{3.29}$$

$$\begin{aligned} R &= \begin{bmatrix} R_{abc}(1) + R_{abc}(2) + R_{abc}(3) & -R_{abc}(2) \\ -R_{abc}(2) & R_{abc}(1) + R_{abc}(2) \end{bmatrix} \\ &= \begin{bmatrix} [R11]_{abc} & [R12]_{abc} \\ [R21]_{abc} & [R22]_{abc} \end{bmatrix} \end{aligned} \tag{3.30}$$

$$\Delta Q = \begin{bmatrix} \Delta Q_{abc}(MB_d)^t \\ \Delta Q_{abc}(PVB_K)^t \end{bmatrix} \tag{3.31}$$

$$\Delta P = \begin{bmatrix} \Delta P_{abc}(MB_d)^t \\ \Delta P_{abc}(PVB_K)^t \end{bmatrix} \tag{3.32}$$

$$\Delta V = \begin{bmatrix} \Delta V_{abc}(MB_d)^t \\ \Delta V_{abc}(PVB_K)^t \end{bmatrix} \tag{3.33}$$

$$\Delta \delta = \begin{bmatrix} \Delta \delta_{abc}(MB_d)^t \\ \Delta \delta_{abc}(PVB_K)^t \end{bmatrix} \tag{3.34}$$

$$\Delta \delta_{abc}(PVB_K)^t = \begin{bmatrix} 0 \\ 0 \\ 0 \end{bmatrix} \tag{3.35}$$

$$\Delta P_{abc}(PVB_K)^t = \begin{bmatrix} 0 \\ 0 \\ 0 \end{bmatrix} \tag{3.36}$$

$$\Delta V_{abc}(PVB_K)^t = \left| V_{abc}(PVBK'')^t \right| - \left| V_{abc}(PVB_K)^t \right| \tag{3.37}$$

$$\Delta V_{abc}(MB_d)^t + j\Delta \delta_{abc}(MB_d)^t = V_{abc}(MB_d'')^t - V_{abc}(MB_d)^t \tag{3.38}$$

Using equations (3.35) to (3.36) in equation (3.27), the reduced sensitivity matrix will be formulated. The reduced sensitivity matrix is give by

$$\begin{bmatrix} [X11]_{abc} & [X12]_{abc} & [R11]_{abc} \\ [X21]_{abc} & [X22]_{abc} & [R21]_{abc} \\ -[R11]_{abc} & -[R12]_{abc} & [X11]_{abc} \end{bmatrix} \begin{bmatrix} \Delta Q_{abc}(MB_d)^t \\ \Delta Q_{abc}(PVB_K)^t \\ \Delta P_{abc}(MB_d)^t \end{bmatrix} = \begin{bmatrix} \Delta V_{abc}(MB_d)^t \\ \Delta V_{abc}(PVB_K)^t \\ \Delta \delta_{abc}(MB_d)^t \end{bmatrix} \tag{3.39}$$

Thus utilizing above equations, the loop breakpoint injections and PV breakpoint injections are calculated simultaneously for any three phase distribution system. The net additional injection/withdrawal of reactive power to/from the PV buses and the additional loop breakpoint injections needs to be reflected in the loads beyond branch matrix of the network. The same approach could be extended for solving load flow problem of single phase or balanced distribution network. If any phase is not present, then corresponding

column and row in above mentioned matrices will contain zero.

The complete algorithm for solving the load flow equations of AC meshed distribution system with distributed generations modelled as PV bus has been clearly depicted through the flowchart in Fig. 3.9.

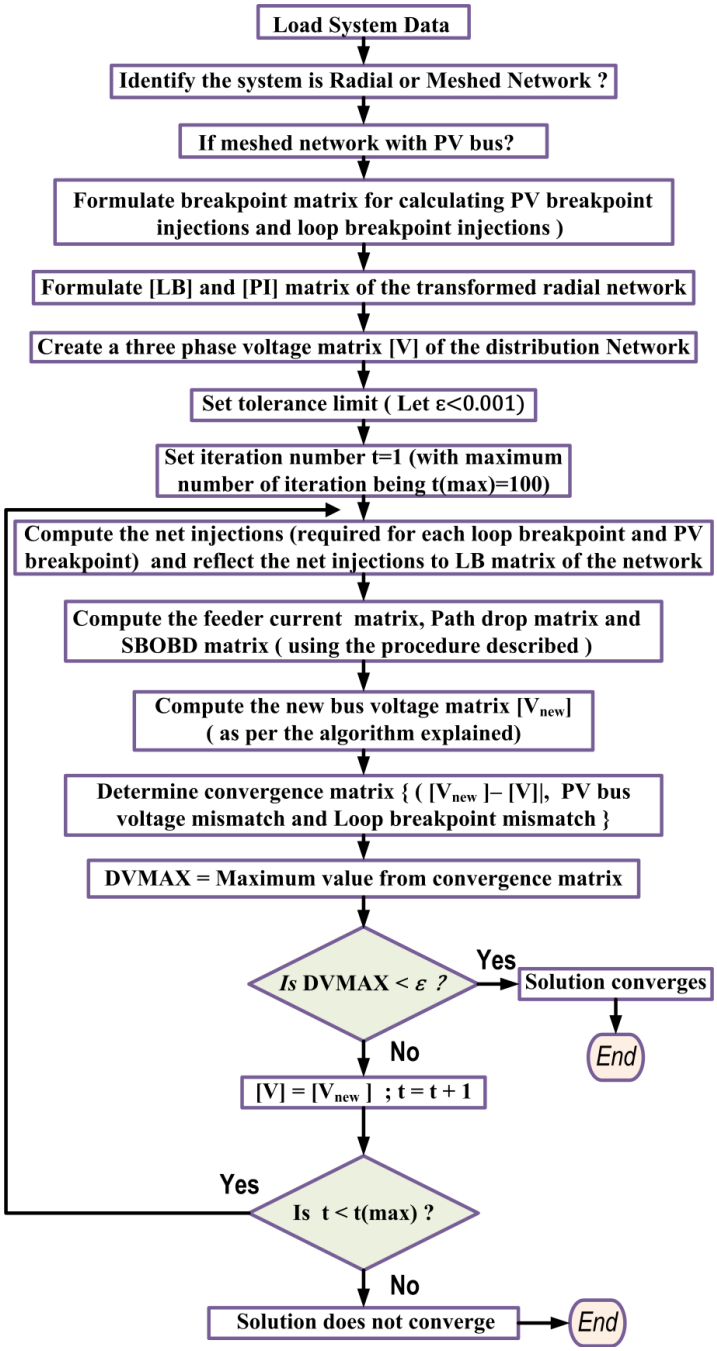

Fig. 3.9: Flowchart depicting complete load flow steps for meshed AC network with PV bus.

3.4 Results

The algorithm has been tested using Matlab software through a personal computer with CORE i3 processor, 4 GB RAM and 2.66GHz CPU. The developed technique has been implemented on various balanced and unbalanced network incorporating PQ and PV model of distributed generations. The load-flow results as acquired by proposed method and the efficacy comparison with that of algorithms prevailing in the literature are presented in this part. The effectiveness of the proposed method has been investigated on various standard test systems.

Case-1: Load flow of radial distribution systems with distributed generation.

In this section the proposed load flow algorithm has been investigated on several standard radial distribution systems such as: IEEE-33 bus [72], IEEE-69 bus [73] and IEEE-13 bus [75] test systems in the presence of PV and PQ model of distributed generations. The base power of 100 MVA and base voltage of 12.66 kV have been considered for IEEE-33 and IEEE-69 test systems. The characteristics of the distributed generations associated with IEEE-33 bus system and IEEE-69 bus test systems are provided in the Table 3.1 and Table 3.2 respectively. The base power of 100 MVA and base voltage of 12.66 kV have been considered for IEEE-13 bus test systems. IEEE 13-node feeder was analyzed for which the data was obtained from IEEE test case archive for Distribution Feeders [14]. The DG node 633 (IEEE-13 bus system) is modelled as PV node. The specified positive sequence voltage at this node is 1.0 p.u. The regulator was removed in order to clearly see the effect of the DG on the system.

For any new method, it is important to make sure that the final solution of the new method is the same as the existent method. The voltage solution for IEEE-33, IEEE-69 and IEEE-13 bus test systems are explicitly presented in Table 3.3, Table 3.5 and Table 3.7 respectively utilizing three algorithms viz. proposed algorithm (PM), backward forward sweep based method [65] and direct load flow method [68]. The load flow solution for the distributed generations associated with IEEE-33 and IEEE-69 bus test systems are provided in Table 3.4, Table 3.6 respectively. The comparison of the results obtained from the proposed load flow model and those obtained by established methods therefore demonstrates the effectiveness and accuracy of the proposed load flow technique.

Table 3.1: Characteristics of distributed generations integrated with IEEE-33 bus radial distribution system

Generator Number	Bus Location	Voltage (pu)	Real Power (kW)		Injected Reactive Power (MVAr)	
			Max.	Min.	Max.	Min.
1	22	PV	200	200	200	50
2	18	PV	90	90	100	20
3	33	PQ	60	60	20	20

Table 3.2: Characteristics of distributed generations integrated with IEEE-69 bus radial distribution system

Generator Number	Bus Location	Voltage (pu)	Real Power (kW)		Injected Reactive Power (MVAr)	
			Max.	Min.	Max.	Min.
1	27	PV	100	100	NL	NL
2	65	PV	100	100	NL	NL
3	52	PQ	50	50	20	20

Table 3.3: Voltage profile of IEEE-33 bus radial distribution system in the presence of distributed generations

Node Number	Voltage Magnitude (pu)			Phase Angle (Degree)		
	PM	BFS	DLF	PM	BFS	DLF
1	1.0000	1.0000	1.0000	0.00000	0.00000	0.00000
2	0.9973	0.9973	0.9973	0.0002	0.0002	0.0002
3	0.9840	0.9840	0.9840	0.0016	0.0016	0.0016
4	0.9770	0.9770	0.9770	0.0026	0.0026	0.0026
5	0.9702	0.9702	0.9702	0.0037	0.0037	0.0037
6	0.9532	0.9532	0.9532	0.0023	0.0023	0.0023
7	0.9502	0.9502	0.9502	-0.0014	-0.0014	-0.0014
8	0.9460	0.9460	0.9460	-0.0011	-0.0011	-0.0011
9	0.9408	0.9408	0.9408	-0.0024	-0.0024	-0.0024
10	0.9362	0.9362	0.9362	-0.0037	-0.0037	-0.0037
11	0.9355	0.9355	0.9355	-0.0036	-0.0036	-0.0036
12	0.9343	0.9343	0.9343	-0.0036	-0.0036	-0.0036
13	0.9297	0.9297	0.9297	-0.0052	-0.0052	-0.0052
14	0.9282	0.9282	0.9282	-0.0064	-0.0064	-0.0064
15	0.9275	0.9275	0.9275	-0.0070	-0.0070	-0.0070
16	0.9269	0.9269	0.9269	-0.0075	-0.0075	-0.0075
17	0.9265	0.9265	0.9265	-0.0084	-0.0084	-0.0084
18	0.9267	0.9267	0.9267	-0.0086	-0.0086	-0.0086
19	0.9971	0.9971	0.9971	0.0001	0.0001	0.0001
20	0.9966	0.9966	0.9966	-0.0006	-0.0006	-0.0006
21	0.9968	0.9968	0.9968	-0.0007	-0.0007	-0.0007
22	0.9978	0.9978	0.9978	-0.0004	-0.0004	-0.0004
23	0.9804	0.9804	0.9804	0.0010	0.0010	0.0010

Node Number	Voltage Magnitude (pu)			Phase Angle (Degree)		
	PM	BFS	DLF	PM	BFS	DLF
24	0.9737	0.9737	0.9737	-0.0005	-0.0005	-0.0005
25	0.9704	0.9704	0.9704	-0.0013	-0.0013	-0.0013
26	0.9514	0.9514	0.9514	0.0029	0.0029	0.0029
27	0.9490	0.9490	0.9490	0.0039	0.0039	0.0039
28	0.9382	0.9382	0.9382	0.0056	0.0056	0.0056
29	0.9304	0.9304	0.9304	0.0072	0.0072	0.0072
30	0.9271	0.9271	0.9271	0.0090	0.0090	0.0090
31	0.9235	0.9235	0.9235	0.0078	0.0078	0.0078
32	0.9228	0.9228	0.9228	0.0075	0.0075	0.0075
33	0.9227	0.9227	0.9227	0.0076	0.0076	0.0076

Table 3.4: Load flow results of distributed generations integrated with IEEE-33 bus radial distribution system

Generator Number	Bus Location	Types of DG	Real Power (kW)			Injected Reactive Power (MVAr)		
			PM	DLF	BFS	PM	DLF	BFS
1	22	PV	200	200	200	131.67	131.66	131.67
2	18	PV	90	90	90	78.95	78.94	78.94
3	33	PQ	60	60	60	20	20	20

Table 3.5: Voltage profile of IEEE-69 bus radial distribution system in the presence of distributed generations

Node Number	Voltage Magnitude (pu)			Phase Angle (Degree)		
	PM	BFS	DLF	PM	BFS	DLF
1	1	1	1	0.00000	0.00000	0.00000
2	0.99997	0.99997	0.99998	-0.00001	-0.00001	-0.00001
3	0.99993	0.99993	0.99994	-0.00003	-0.00003	-0.00003
4	0.99984	0.99984	0.99985	-0.00009	-0.00009	-0.00009
5	0.99902	0.99902	0.99903	-0.00023	-0.00023	-0.00023
6	0.99042	0.99042	0.99043	0.001734	0.001734	0.001734
7	0.98147	0.98147	0.98148	0.003814	0.003814	0.003814
8	0.97934	0.97934	0.97935	0.004317	0.004317	0.004317
9	0.97823	0.97823	0.97824	0.00457	0.00457	0.00457
10	0.97352	0.97352	0.97353	0.006958	0.006958	0.006958
11	0.97248	0.97248	0.97249	0.007494	0.007494	0.007494
12	0.96957	0.96957	0.96958	0.009213	0.009213	0.009213
13	0.96702	0.96702	0.96703	0.011183	0.011183	0.011183
14	0.96449	0.96449	0.9645	0.013174	0.013174	0.013174
15	0.96201	0.96201	0.96202	0.015182	0.015182	0.015182
16	0.96154	0.96154	0.96155	0.015556	0.015556	0.015556
17	0.9608	0.96080	0.96081	0.016232	0.016232	0.016232
18	0.96079	0.96079	0.96080	0.01624	0.01624	0.01624
19	0.96045	0.96045	0.96046	0.016764	0.016764	0.016764

Node Number	Voltage Magnitude (pu)			Phase Angle (Degree)		
	PM	BFS	DLF	PM	BFS	DLF
20	0.96022	0.96022	0.96023	0.017102	0.017102	0.017102
21	0.95986	0.95986	0.95987	0.017649	0.017649	0.017649
22	0.95986	0.95986	0.95987	0.017667	0.017667	0.017667
23	0.95985	0.95985	0.95986	0.017874	0.017874	0.017874
24	0.95982	0.95982	0.95983	0.018323	0.018323	0.018323
25	0.95992	0.95992	0.95993	0.019239	0.019239	0.019239
26	0.95996	0.95996	0.95997	0.019617	0.019617	0.019617
27	0.9600	0.96	0.96001	0.019823	0.019823	0.019823
28	0.99992	0.99992	0.99993	-0.00004	-0.00004	-0.00004
29	0.99985	0.99985	0.99986	-0.00008	-0.00008	-0.00008
30	0.99973	0.99973	0.99974	-0.00005	-0.00005	-0.00005
31	0.99971	0.99971	0.99972	-0.00004	-0.00004	-0.00004
32	0.99960	0.9996	0.99961	-0.00001	-0.00001	-0.00001
33	0.99935	0.99935	0.99936	0.00006	0.00006	0.00006
34	0.99901	0.99901	0.99902	0.000168	0.000168	0.000168
35	0.99894	0.99894	0.99895	0.000187	0.000187	0.000187
36	0.99992	0.99992	0.99993	-0.00004	-0.00004	-0.00004
37	0.99975	0.99975	0.99976	-0.00016	-0.00016	-0.00016
38	0.99959	0.99959	0.9996	-0.00020	-0.0002	-0.0002
39	0.99954	0.99954	0.99955	-0.00021	-0.00021	-0.00021
40	0.99954	0.99954	0.99955	-0.00021	-0.00021	-0.00021
41	0.99884	0.99884	0.99885	-0.00041	-0.00041	-0.00041
42	0.99855	0.99855	0.99856	-0.00049	-0.00049	-0.00049
43	0.99851	0.99851	0.99852	-0.0005	-0.0005	-0.0005
44	0.99850	0.9985	0.99851	-0.0005	-0.0005	-0.0005
45	0.99840	0.9984	0.99841	-0.00053	-0.00053	-0.00053
46	0.99840	0.9984	0.99841	-0.00053	-0.00053	-0.00053
47	0.99979	0.99979	0.9998	-0.00012	-0.00012	-0.00012
48	0.99854	0.99854	0.99855	-0.0009	-0.0009	-0.0009
49	0.99470	0.9947	0.99471	-0.00333	-0.00333	-0.00333
50	0.99416	0.99416	0.99417	-0.00368	-0.00368	-0.00368
51	0.97934	0.97934	0.97935	0.004325	0.004325	0.004325
52	0.97945	0.97945	0.97946	0.004321	0.004321	0.004321
53	0.9755	0.9755	0.97551	0.005131	0.005131	0.005131
54	0.97232	0.97232	0.97233	0.005786	0.005786	0.005786
55	0.96793	0.96793	0.96794	0.006701	0.006701	0.006701
56	0.96366	0.96366	0.96367	0.007607	0.007607	0.007607
57	0.94190	0.9419	0.94191	0.016037	0.016037	0.016037
58	0.93121	0.93121	0.93122	0.020338	0.020338	0.020338
59	0.92707	0.92707	0.92708	0.022051	0.022051	0.022051
60	0.92224	0.92224	0.92225	0.024251	0.024251	0.024251
61	0.91502	0.91502	0.91503	0.02604	0.02604	0.02604
62	0.91476	0.91476	0.91477	0.026201	0.026201	0.026201
63	0.91442	0.91442	0.91443	0.026435	0.026435	0.026435
64	0.91275	0.91275	0.91276	0.02758	0.02758	0.02758
65	0.91250	0.9125	0.91251	0.028901	0.028901	0.028901
66	0.97243	0.97243	0.97244	0.007514	0.007514	0.007514
67	0.97243	0.97243	0.97244	0.007515	0.007515	0.007515

Node Number	Voltage Magnitude (pu)			Phase Angle (Degree)		
	PM	BFS	DLF	PM	BFS	DLF
68	0.96925	0.96925	0.96926	0.009318	0.009318	0.009318
69	0.96924	0.96924	0.96925	0.009318	0.009318	0.009318

Table 3.6: Load flow results of distributed generations integrated with IEEE-69 bus radial distribution system

Generator Number	Bus Location	Types of DG	Real Power (kW)			Injected Reactive Power (MVAr)		
			PM	DLF	BFS	PM	DLF	BFS
1	27	PV	100	100	100	-136.87	-136.87	-136.86
2	65	PV	100	100	100	-106.44	-106.44	-106.44
3	52	PQ	50	50	50	20	20	20

Table 3.7: Load flow results of IEEE-13 bus distribution network in the presence of distributed generations

Node Number	Voltage Magnitude (pu)			Phase Angle (Degree)			Phase
	PM	BFS	DLF	PM	BFS	DLF	
650	1	1	1	0	0	0	A
650	1	1	1	-120	-120	-120	B
650	1	1	1	120	120	120	C
632	0.9915	0.9914	0.9917	-3.65	-3.67	-3.61	A
632	0.9922	0.9921	0.9924	-123.58	-123.57	-123.50	B
632	0.9881	0.9880	0.9885	116.40	116.40	116.41	C
633	1.0000	1.0000	1.0000	-3.91	-3.90	-3.92	A
633	1.0000	1.0000	1.0000	-123.95	-123.94	123.97	B
633	1.0000	1.0000	0.9999	115.95	115.94	115.98	C
634	0.9501	0.9501	0.9501	-3.91	-3.91	-3.91	A
634	0.9498	0.9497	0.9497	-123.97	-123.97	-123.97	B
634	0.9498	0.9498	0.9499	115.95	115.95	115.95	C
645	-	-	-	-	-	-	A
645	0.9786	0.9787	0.9782	-123.92	-123.91	-123.93	B
645	0.9899	0.9898	0.9896	116.36	116.36	116.35	C
646	-	-	-	-	-	-	A
646	0.9733	0.9733	0.9733	-124.11	-124.11	-124.11	B
646	0.9907	0.9908	0.9905	116.36	116.36	116.36	C
671	0.9730	0.9730	0.9731	-7.01	-7.01	-7.01	A
671	0.9993	0.9993	0.9994	-123.58	-123.57	-123.56	B
671	0.9329	0.9329	0.9330	114.53	114.51	114.53	C
680	0.9730	0.9730	0.9730	-6.99	-6.99	-6.99	A
680	0.9993	0.9993	0.9993	-123.57	-123.57	-123.57	B
680	0.9329	0.9329	0.9329	114.53	114.53	114.53	C
684	0.9715	0.9715	0.9715	-7.02	-7.02	-7.02	A
684	-	-	-	-	-	-	B
684	0.9308	0.9308	0.9308	114.49	114.49	114.49	C
611	-	-	-	-	-	-	A

Node Number	Voltage Magnitude (pu)			Phase Angle (Degree)			Phase
	PM	BFS	DLF	PM	BFS	DLF	
611	-	-	-	-	-	-	B
611	0.9298	0.9298	0.9298	114.46	114.46	114.46	C
652	0.9694	0.9694	0.9694	-6.99	-6.99	-6.99	A
652	-	-	-	-	-	-	B
652	-	-	-	-	-	-	C
692	0.9730	0.9730	0.9730	-6.99	-6.99	-6.99	A
692	0.9993	0.9993	0.9993	-123.57	-123.57	-123.57	B
692	0.9329	0.9329	0.9329	114.43	114.43	114.43	C
675	0.9666	0.9666	0.9666	-7.25	-7.25	-7.25	A
675	1.0015	1.0015	1.0015	-123.75	-123.75	-123.75	B
675	0.9306	0.9306	0.9306	114.57	114.57	114.57	C

The efficacy of the proposed method over several other methods for higher accuracy is detailed in Table 3.8. The results show that the proposed load-flow algorithm has very fast convergence ability. The proposed method is robust enough to handle distribution network of any size.

Table 3.8: Convergence speed comparison (Tolerance-0.000001)

Test Systems	Processing Time (sec.)		
	PM	DLF [68]	BFS [65]
IEEE-33	0.0364	0.0425	0.0692
IEEE-69	0.0698	0.0795	0.0998
IEEE-13	0.0420	0.0470	0.0982

The improvement over widely adopted BFS methods is based on the formulation of incidence matrix, path matrix, path impedance matrix and loads beyond branch matrix incidence matrix. The path search algorithm guarantee minimum number of search operation for identifying the paths between slack buses and end buses. The algorithm is formulated entirely on matrix formulation and computations, even at the juncture of updating the voltage at each individual node. Therefore the proposed algorithm is computationally efficient when compared with the existing BFS method [65].

In the papers [68], three matrices namely branch-current to bus voltage (BCBV) matrix, bus-injection to branch current (BIBC) matrix and distribution load flow (DLF=BCBV×BIBC) matrix are required to achieve the desired load flow solution of radial distribution systems. These matrices require considerable amount of memory for large sized distribution networks. Because of sparse nature of these three matrices, memory spaces are

not being utilized efficiently, particularly for large sized distribution networks. Another drawback of BIBC & BCBV matrix based method is that, in order to obtain the load flow solution two direct matrix multiplication is required: (a) between BCBV and BIBC matrices (b) between DLF & 'current Injection column vector' matrices, and hence requires sufficiently large processing time and memory spaces. The proposed method has overcome the disadvantages of BIBC and BCBV matrix based method. There is no direct multiplication required between the matrices ([*PI*] matrix,[*P*] matrix, [*LB*] matrix, [P*D*] matrix , [*SBOBD*] matrix and [*LFM*]) that have been formulated for our purpose. The simple algebraic operation and efficient search technique enabling the proposed method to be computationally efficient when compared with the existing method [68].

Case-2: Load flow of weakly meshed distribution system with distributed generations.

In this section the proposed load flow algorithm has been investigated on IEEE-33 bus test system in the presence of PV and PQ model of distributed generations. The base power of 100 MVA and the base voltage of 12.66 kV have been considered for IEEE-33 bus test systems. The characteristics of the distributed generations associated with IEEE-33 bus system is provided in the Table 3.9. The test system consists of 33 buses with five tie lines, as shown in [72].

Table 3.9: Characteristics of distributed generations integrated with meshed IEEE-33 bus distribution network

Generator Number	Bus Location	Bus Type	Voltage (pu)	Real Power (kW)		Injected Reactive Power (MVAr)	
				Max.	Min.	Max.	Min.
1	10	PQ	-	50	50	20	20
2	25	PV	0.9652	100	100	90	50
3	33	PV	0.9568	60	60	50	10

Table 3.10: Load flow results of meshed IEEE-33 bus distribution network in the presence of distributed generations

Node Number	Voltage Magnitude (pu)			Phase Angle (Degree)		
	PM	BFS	DLF	PM	BFS	DLF
1	1.0000	1.0000	1.0000	0.0000	0.0000	0.0000
2	0.9973	0.9972	0.9972	0.0003	0.0003	0.0003
3	0.9870	0.9872	0.9872	0.001	0.001	0.001
4	0.9836	0.9839	0.9838	0.0011	0.0011	0.0011
5	0.9803	0.9803	0.9801	0.0011	0.0011	0.0011
6	0.9728	0.9727	0.9728	-0.0006	-0.0006	-0.0006
7	0.9719	0.9720	0.9719	-0.0021	-0.0021	-0.0021

Node Number	Voltage Magnitude (pu)			Phase Angle (Degree)		
	PM	BFS	DLF	PM	BFS	DLF
8	0.9709	0.9707	0.9709	-0.0024	-0.0024	-0.0024
9	0.9679	0.9679	0.9679	-0.0028	-0.0028	-0.0028
10	0.9678	0.9678	0.9679	-0.0032	-0.0032	-0.0032
11	0.9677	0.9678	0.9678	-0.0032	-0.0032	-0.0032
12	0.9671	0.9670	0.9672	-0.003	-0.003	-0.003
13	0.9641	0.9647	0.9646	-0.0031	-0.0031	-0.0031
14	0.9630	0.9633	0.9631	-0.0034	-0.0034	-0.0034
15	0.9628	0.9628	0.9629	-0.0033	-0.0033	-0.0033
16	0.9612	0.9612	0.9610	-0.0029	-0.0029	-0.0029
17	0.9581	0.9586	0.9581	-0.0027	-0.0027	-0.0027
18	0.9572	0.9570	0.9572	-0.0021	-0.0021	-0.0021
19	0.9956	0.9958	0.9955	0.0001	0.0001	0.0001
20	0.9817	0.9817	0.9821	-0.0012	-0.0012	-0.0012
21	0.9779	0.9772	0.9780	-0.002	-0.002	-0.002
22	0.9744	0.9746	0.9747	-0.0029	-0.0029	-0.0029
23	0.9819	0.9819	0.9820	0.0009	0.0009	0.0009
24	0.9719	0.9718	0.9720	0.0001	0.0001	0.0001
25	0.9652	0.9655	0.9652	0.0001	0.0001	0.0001
26	0.9719	0.9720	0.9719	-0.0004	-0.0004	-0.0004
27	0.9707	0.9704	0.9707	-0.0001	-0.0001	-0.0001
28	0.9660	0.9661	0.9661	-0.0001	-0.0001	-0.0001
29	0.9629	0.9628	0.9629	0.0002	0.0002	0.0002
30	0.9598	0.9594	0.9598	0.0014	0.0014	0.0014
31	0.9570	0.9572	0.9572	-0.0007	-0.0007	-0.0007
32	0.9565	0.9566	0.9565	-0.0013	-0.0013	-0.0013
33	0.9568	0.9568	0.9569	-0.0017	-0.0017	-0.0017

Table 3.11: Load flow results of distributed generations integrated with meshed IEEE-33 bus distribution system

Generator Number	Bus Location	Real Power (kW)			Injected Reactive Power (MVAr)		
		PM	[65]	[68]	PM	[65]	[68]
1(PQ)	10	50	50	50	10	10	10
2(PV)	25	100	100	100	60	60	60.10
3(PV)	33	60	60	60	20	19.99	20.20

The load flow results for the aforementioned distribution system using proposed algorithm, BFS sweep based load flow algorithm and direct load flow approach is explicitly presented in Table 3.10 and Table 3.11. The maximum difference between the voltage solution obtained by the proposed method(PM) and those obtained by BFS approach[16] and BIBC [15] method is found to be 0.0007 p.u and 0.0005 p.u respectively. The execution time

for the backward forward sweep based method, Direct load flow method and the proposed method is 150 ms, 60ms and 12ms respectively. The comparison of the results obtained from the proposed algorithm and those produced by the existing algorithms viz. BFS and direct load flow method, therefore demonstrates the effectiveness and accuracy of the method developed.

To assess the effect of R/X ratio variation on the convergence characteristics, the proposed methodology has been tested for wide range of R/X ratios of lines belonging to the IEEE-33 bus meshed distribution network (with distributed generations). The test result in Fig. 3.10 justify the convergence ability of the proposed method.

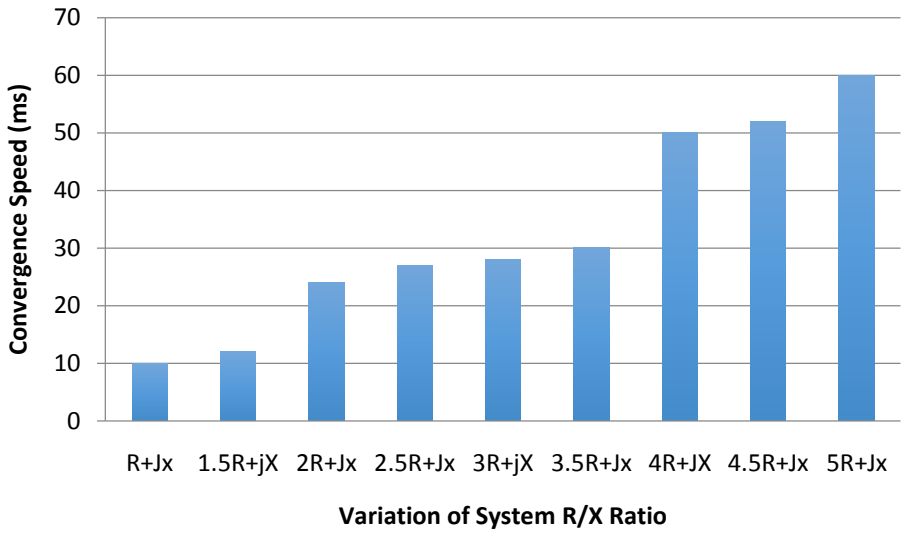

Fig. 3.10: Variation of convergence speed with the change in system R/X ratio.

3.5 Conclusion

The load flow algorithm developed in chapter 1 has been modified in a manner such that it could provide the load flow solution of three phase unbalanced or balanced AC distribution network in the presence of distributed generations. Importantly, the proposed method applies only simple algebraic matrix operations along with several search techniques to achieve the desired load flow solution of distribution systems. The proposed method does not require time taking LU decomposition and forward/ backward substitution of the admittance matrix or jacobian matrix, required in classical Newton Raphson algorithms. The sensitivity or

breakpoint matrix has been utilized to obtain the additional reactive power injection/withdrawal to maintain the specified voltage at each PV nodes. In the case of weakly meshed distribution network with PV type distributed generations, the loop breakpoint injections and PV breakpoint injections have been calculated simultaneously. Thus, saving decent computational time when compared with existing load flow method as they are solving PV and lop breakpoint injections separately. The net injections is reflected in the [*LC*] or [*LB*] matrix of the distribution network. Note that except for some modifications needed to be done for the [*LC*] or [*LB*] matrix, the proposed solution techniques require no modification; therefore, the proposed method can obtain the load-flow solution for AC distribution system in the presence of distributed generations efficiently. The remaining supporting matrices (path impedance matrix [*PI*], Feeder current matrix [*FC*], path drop matrix [*PD*], slack bus to other buses drop matrix [*SBOBD*], load flow matrix [*LFM*] will reshape themselves accordingly. The effectiveness of the proposed solution methodology has been tested on several standard distribution systems. Test outcome show viability and accuracy of the proposed method.

Chapter-4

Load Flow Solution Algorithm for AC-DC Radial Distribution Systems in the Presence of Distributed Generations

In this chapter, the power flow solution algorithm for radial AC-DC distribution network in the presence of distributed generations has been developed. The concept of AC load flow algorithm developed in previous chapters (chapter 2 and chapter 3) has been utilised for solving load flow problem of AC-DC radial distribution systems by making use of proposed per-unit equivalent model of PWM and other power converters (taking care of enactment of control objectives). Various models of distributed generations (P, PQ, PV and V^{dc}) are also incorporated in the proposed load flow study. The proposed load flow algorithm has been tested on several hypothetical AC-DC radial distribution systems to examine its accuracy and efficacy.

4.1 Introduction

For proper planning, analysis and optimal operation of transmission or distribution system, a power flow or load flow study has to be carried out. The AC-DC distribution systems have recently gained huge popularity due to advancements in power converters, high penetration of renewable energy resources and wide usages of DC loads. However, load flow in such systems is a challenging task due to non linear characteristics of power converters. There are well established algorithms for load flow solution of AC-DC transmission systems but for AC-DC distribution systems till date not much work has been reported. In general, two basic approaches have been reported for the load flow solution of AC-DC transmission network: sequential [24]-[28] and unified methods [29]-[35]. The major difference between the above mentioned approaches lies in the integration procedure of AC and DC system equations. The sequential method solves the DC system equations and AC system equations separately. In

the unified method, the DC system equations are incorporated into the equations of the AC system, and then complete set of equations are solved all together.

The aforementioned approaches (sequential and integrated) have utilized one of the existing traditional load flow methods for solving load flow equations, viz. Gauss–Siedel, Newton Raphson (NR), Fast decoupled, and Broyden methods. The mentioned AC-DC power flow algorithms are not suitable for solving AC-DC distribution load-flow equations. The reasons are: (a) High R/X ratio in the AC sub-regions of the AC-DC distribution network. (b) High loading level of the distribution feeder, (c) Sparse nature of admittance (Y-bus) matrix, (d) Radial and/or weakly meshed structure of the AC-DC distribution network, (e) The assumptions necessary for the simplifications used in the standard fast-decoupled and Newton-Raphson method are often not valid for distribution systems, (f) Lower and upper (LU) decomposition, matrix inversion and forward/backward substitution of admittance matrix requires significant amount of time and thus leading to poor convergence characteristics of traditional methods.

The direct method [69], have overcome the disadvantages associated with the traditional load-flow methods. Three matrices namely branch-current to bus voltage (BCBV) matrix, bus-injection to branch current (BIBC) matrix and distribution load flow (DLF=BCBV×BIBC) matrix are required to achieve the desired load flow solution of AC-DC radial distribution systems. These matrices require considerable amount of memory for large sized distribution networks. Because of sparse nature of these three matrices, memory spaces are not being utilized efficiently, particularly for large sized distribution networks. Another drawback of BIBC & BCBV matrix based method is that, in order to obtain load flow solution two direct matrix multiplication is required: (a) between BCBV and BIBC matrices (b) between DLF & 'current Injection column vector' matrices, and hence requires sufficiently large processing time and memory spaces. Also, this method (direct method) has not considered the effect of various models of distributed generations.

With a view to prevail over the shortcomings of the existing methods, a load flow algorithm based on backward forward sweep method is proposed in this chapter for AC-DC distribution network. A matrix is an expedient way of portraying a graph to a computer. The AC load flow algorithm developed in previous chapters (chapter 2 and chapter 3) has been modified in a manner such that it can easily be extended for load flow calculation of AC-DC

radial distribution systems by making use of proposed per-unit equivalent model of PWM and other power converters (taking care of enactment of control objectives). The proposed algorithm requires the conventional bus-branch oriented data as the only input. The objective of this chapter is to develop a load flow algorithm, which incorporates advantages of the topological aspects of distribution systems, and solves the load flow problem directly. Five developed significant matrices, loads beyond branch matrix [*LB*], the path impedance matrix [*PI*], path drop matrix [*PD*], slack bus to load buses drop matrix [*SBOBD*], load flow matrix [*LFM*] and simple matrix operations are utilized to obtain load flow solutions. The matrix building algorithms that have been formulated for AC distribution systems in the previous chapters are equally applicable to AC-DC distribution systems with minor modifications. The relevant matrices formulation as discussed in chapter 1 has to be carried out for each sub-region separately. The distributed generations modelled as PQ, P, V^{dc} and PV buses are incorporated into the proposed algorithm to imitate the injection of DGs in the distribution systems. The DGs modelled as PQ bus and P bus can be included in the proposed load flow algorithm by considering injection by the DGs as the negative load. The power injected by the DGs need to be reflected in the LB matrix of the distribution network. For the DGs modelled as PV type bus and V^{dc} types bus the reactive power generations and real power generations are respectively adjusted between the maximum and minimum limits in order to maintain the constant voltage at their affiliated buses. The breakpoint matrix has been developed to calculate the additional reactive and real power injection/withdrawal to maintain the specified voltage at each PV and V^{dc} buses respectively. Test results reveal the viability and authenticity of the proposed algorithm.

4.2 Load Flow Algorithm for AC-DC Radial Distribution Systems

Power flow study is required for determining the system state under normal and various hypothetical situations. In order to determine the system state of an AC-DC distribution system, AC-DC load flow equations of distribution system are needed to be solved. The single line diagram of an AC-DC distribution system shown in Fig. 4.1 has been used to exemplify the proposed load flow algorithm. The AC-DC distribution systems have different structural view compared to an AC distribution system. It consists of a variety of AC and DC

components, including loads, generating units, lines, and buses. For our purpose, the AC-DC distribution network is subdivided into a number of sub-distribution systems or sub-regions depending on number of bus-bus interfacing converters present in the distribution system.

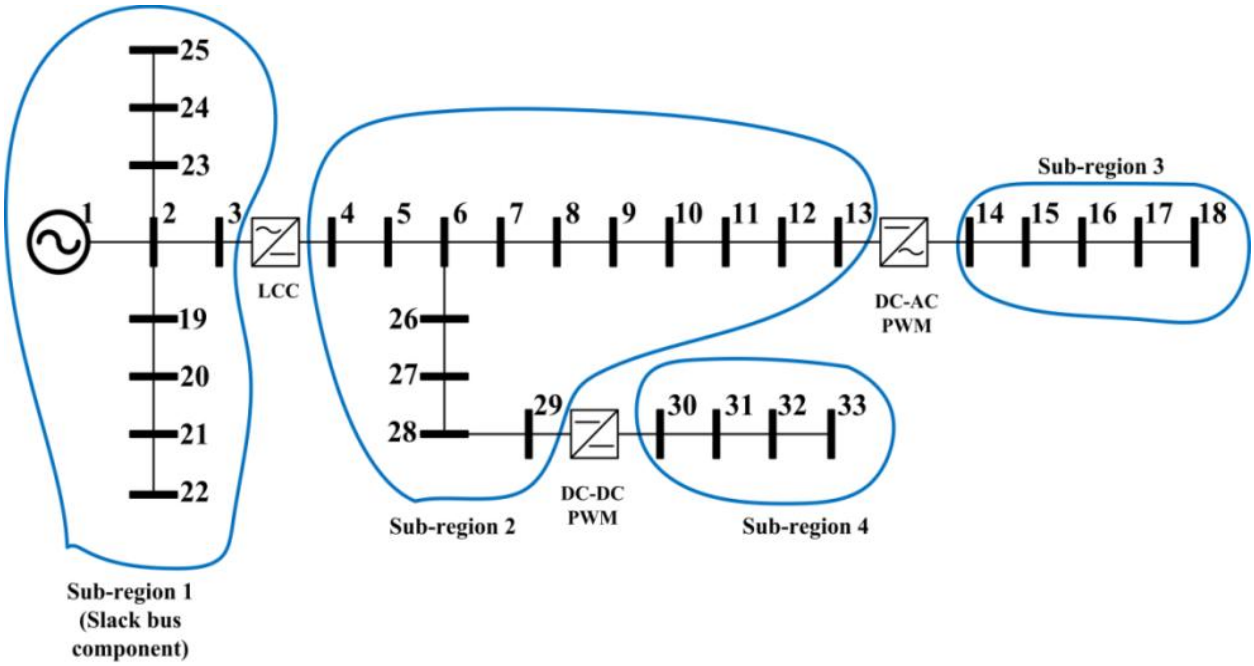

Fig. 4.1: Schematic diagram of a hypothetical 33-bus AC-DC radial distribution system.

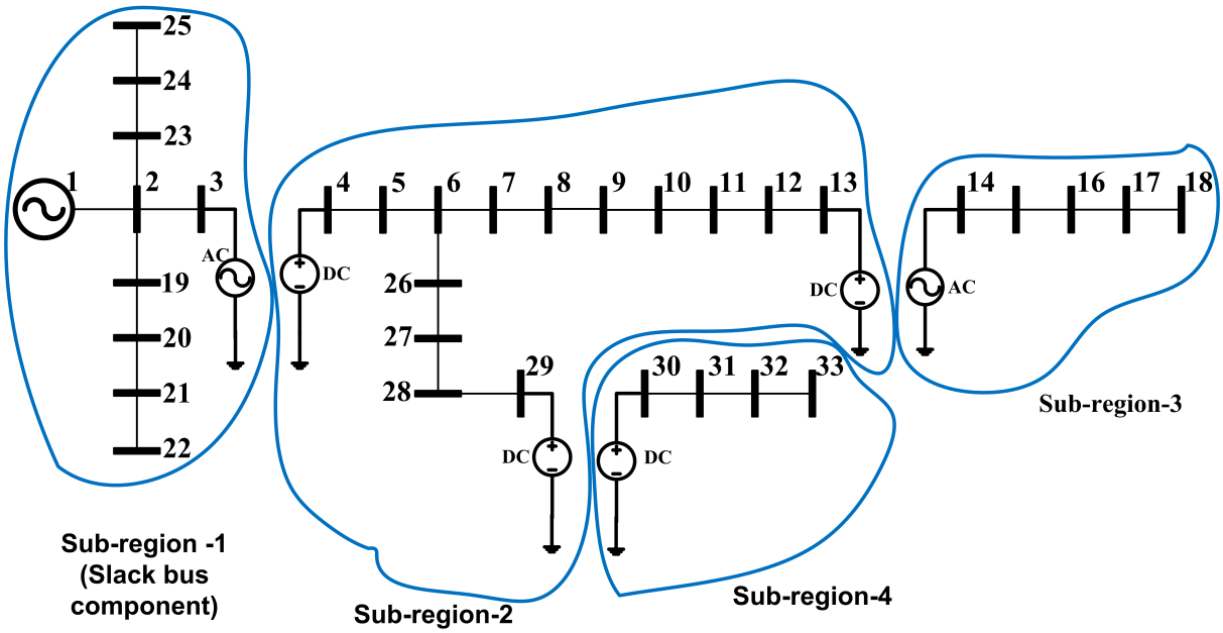

Fig. 4.2: Simplified diagram of a AC-DC radial distribution system shown in Fig. 4.1.

As evident from Fig.4.2, there are four sub-regions of the AC-DC distribution system broadly categorized into AC bus regions and DC bus regions. These regions or sub distribution systems can be interconnected in different hybrid configuration. In the AC-DC distribution system proper modelling of converters will ensure simple load flow equations with quite easier. Thus to ease the load flow problem of AC-DC radial distribution systems, per unit equivalent model of three-phase PWM AC-DC converter, PWM DC-DC converter and three-phase AC-DC bridge LCC converter have been proposed in this section.

4.2.1 Converters modelling

This section illustrates the mathematical modelling of different types of the converters in the AC-DC load-flow calculation considering the balanced network conditions.

(a) Modelling of Three Phase AC-DC Bridge Converters.

The three-phase bridge converter can be treated as an AC-DC transformer (transforming AC to DC and vice versa). As the current through "AC-DC converter" changes, its effective turn's ratio also changes. That is why transformation characteristics of "AC-DC bridge converter" is non-linear. To replace the bridge converter with a circuit node, an AC-DC per unit system has been proposed in this article. The per-unit equivalent circuit of three phase bridge converter is shown in Fig. 4.3 (b).

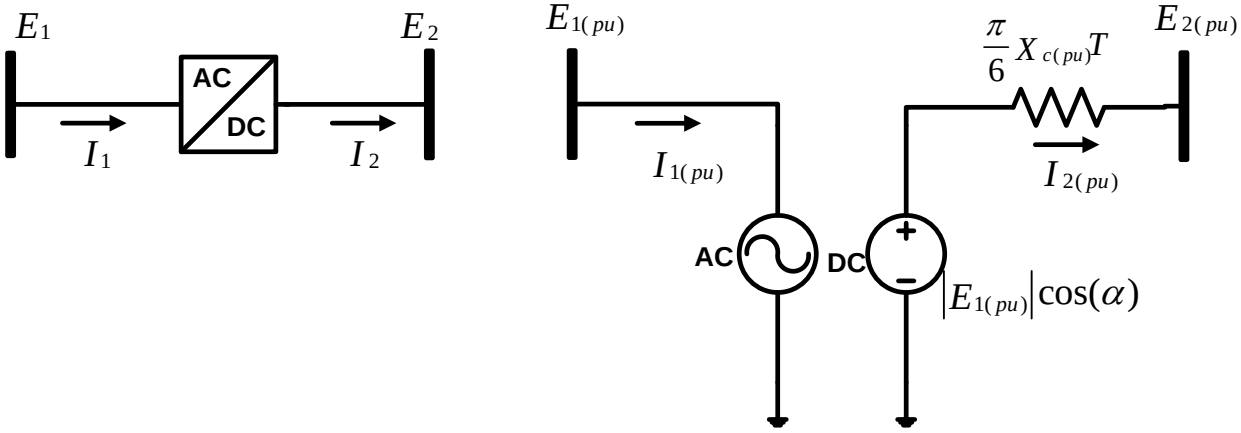

(a) (b)

Fig. 4.3: Three phase bridge converter (a) Schematic diagram, (b) Per-unit equivalent diagram.

The notations/quantities shown in Fig. 4.3(b) are in per-unit and quantities shown in Fig. 4.3(a) are actual phasor value. The per-unit equivalent mathematical model of three phase AC-DC bridge converter can be written as:

$$E_{2(pu)} = \left|E_{1(pu)}\right|\cos(\alpha) - \frac{\pi}{6} X_{c(pu)} I_{2(pu)}\ T \tag{4.1}$$

Another equation which is very useful in analyzing the behavior of bridge rectifier is obtained from equating the real power on both side of full bridge rectifier-

$$\left|E_{1(pu)}\right|\left|I_{1(pu)}\right|\cos(\phi)\eta = E_{2(pu)} I_{2(pu)} \tag{4.2}$$

$\emptyset$= angle between phase voltage and phase current.

η = efficiency of the converter.

The relation between input current (I_1) and output current (I_2) is given by following equation:

$$\left|I_{1(pu)}\right| = \frac{I_{2(pu)}}{\eta} \tag{4.3}$$

$$\cos(\alpha) \approx \cos(\phi) \tag{4.4}$$

In these converters, implementation of four control schemes is possible: constant DC voltage, constant DC current, constant power, and minimum firing angle.

E_1 = Phasor voltage at the ac side

E_2 = Voltage at the dc side

I_1= Phasor current input to converter (Fundamental component)

I_2 = Direct current output from converter

X_c= Commutation reactance

α = Commutation angle

T=1 (rectification mode) and -1(inverting mode)

The subscript *pu* (per unit) associated with the above mentioned symbols or quantities indicates their per unit value.

The base equations are:

$$P_{dc(B)} = VA_{ac(B)} \tag{4.5}$$

$$I_{dc(B)} = \frac{\pi}{\sqrt{6}} I_{ac(B)} \tag{4.6}$$

$$V_{dc(B)} = \frac{3\sqrt{2}}{\pi} V_{ac(B)} \tag{4.7}$$

$$Z_{dc(B)} = \frac{V_{dc(B)}}{I_{dc(B)}} = \frac{18}{\pi^2} Z_{ac(B)} \tag{4.8}$$

Where $VA_{ac(B)}, V_{ac(B)}, I_{ac(B)}$ and $Z_{ac(B)}$ represent the three phase base power, base voltage, base current and base impedance respectively at the AC side of converter and $P_{dc(B)}, V_{dc(B)}, I_{dc(B)}$ *and* $Z_{dc(B)}$ represent the base power, base voltage, base current and base impedance respectively at the DC side of converter.

(b) Modelling of PWM AC/DC Converter

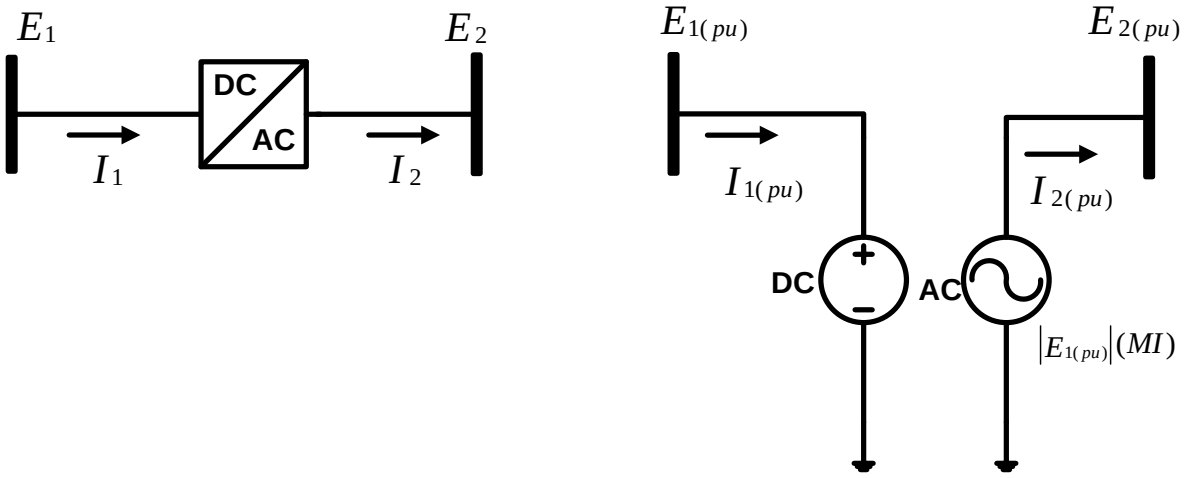

(a) (b)

Fig. 4.4: Three phase PWM DC/AC converter (a) Schematic diagram, (b) Per-unit equivalent diagram.

A schematic diagram of an AC/DC PWM converter and its per-unit equivalent circuit are shown in Fig. 4.4(a) and Fig. 4.4(b) respectively. The notations/quantities shown in Fig. 4.4(b) are in per-unit and quantities shown in Fig. 4.4(a) are actual phasor (line) value. The per-unit equivalent model (Fig. 4.4(b)) of three phase AC-DC PWM converter can be written as:

$$\left|E_{2(pu)}\right| = \left|E_{1(pu)}\right|(MI) \tag{4.9}$$

Another equation which is very useful in analyzing the behavior of PWM AC/DC converter is obtained by equating the real power on both side of PWM converter-

$$\left|E_{2(pu)}\right|\left|I_{2(pu)}\right|\cos(\phi) = E_{1(pu)}I_{1(pu)}\eta \tag{4.10}$$

∅= angle between phase voltage and phase current.

On substituting equation (4.9) in equation (4.10), the resulting equation will provide relation between input (I_1) and output current (I_2).

$$I_{1(pu)} = \frac{\left|I_{2(pu)}\right|\cos(\phi)}{\eta}(MI) \tag{4.11}$$

E_1 = Voltage at the DC side

E_2 = Phasor voltage at the AC side

I_1= DC current input to converter

I_2 = AC phasor current output from converter (Fundamental component)

MI= Modulation index

η = Efficiency of converter

∅= angle between phase voltage (output side) and phase current (output current).

The base values in case of three-phase PWM converter are given as*:*

$$P_{dc(B)} = VA_{ac(B)} \tag{4.12}$$

$$I_{ac(B)} = \frac{2\sqrt{2}}{3} I_{dc(B)} \tag{4.13}$$

$$V_{ac(B)} = \frac{\sqrt{3}}{2\sqrt{2}} V_{dc(B)} \tag{4.14}$$

$$Z_{ac(B)} = \frac{V_{ac(B)}}{I_{ac(B)}} = \frac{3}{8} Z_{dc(B)} \tag{4.15}$$

Where $VA_{ac(B)}, V_{ac(B)}, I_{ac(B)}$ and $Z_{ac(B)}$ represent the three phase base power, base voltage, base current and base impedance respectively at the AC side of converter and $P_{dc(B)}, V_{dc(B)}, I_{dc(B)}$ *and* $Z_{dc(B)}$ represent the base power, base voltage, base current and base impedance respectively at the DC side of converter.

(c) Modelling of PWM DC/DC Converter

DC/DC converter [18] is used for voltage regulation purpose, but enactment of other control schemes such as constant power, constant current, and constant duty cycle (D) is also

possible. In this chapter, solely continuous conduction mode has been considered for operation of these converters.

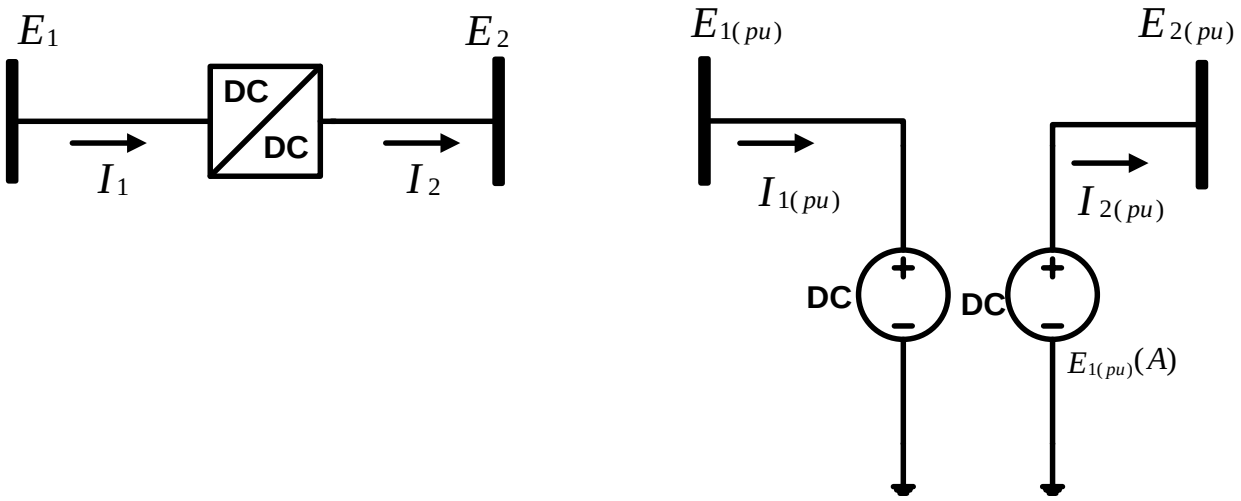

(a) (b)

Fig. 4.5: PWM DC/DC converter (a) Schematic diagram, (b) Per-unit equivalent diagram.

The following mathematical equations have been used to design the Boost, Buck and Buck–Boost converters:

$$\left|E_{2(pu)}\right| = \left|E_{1(pu)}\right|(A) \tag{4.16}$$

Another equation which is very useful in analyzing the behavior of DC-DC converter is obtained by equating the power on both side of DC-DC converter-

$$E_{1(pu)} I_{1(pu)} \eta = E_{2(pu)} I_{2(pu)} \tag{4.17}$$

On substituting (4.16) in (4.17), the resulting equation will provide relation between input (I_1) and output current (I_2).

$$I_{1(pu)} = A \times \frac{I_{2(pu)}}{\eta} \tag{4.18}$$

Where, A is D , $\frac{1}{1-D}$ and $\frac{D}{1-D}$ for buck, boost and buck-boost operations respectively.

E_1 = Converter input voltage

E_2 = Converter output voltage

I_1= DC current input to converter

I_2 = DC current input from converter

D= Duty ratio

η= Efficiency of converter

The base value will remain same on the both sides of the converter irrespective of types of DC-DC converter.

The detailed equations (phase and per-unit equations) of all kind of converters are mentioned in Table 4.1.

Table 4.1: Converters Classification

Equation Types	**Phase Equation**	**Per-unit Equation**
Three Phase Rectifier (LCC)		
Voltage	$E_2 = \frac{3\sqrt{6}}{\pi} \lvert E_{1(ph)} \rvert \cos(\alpha)$	$E_{2(pu)} = \lvert E_{1(pu)} \rvert \cos(\alpha)$
Current	$\lvert I_1 \rvert = \frac{\sqrt{6}}{\eta\pi} I_2$	$\lvert I_{1(pu)} \rvert = \frac{1}{\eta} I_{2(pu)}$
Power Balance	$3 \lvert E_{1(ph)} \rvert \lvert I_1 \rvert \cos(\emptyset)\, \eta = (E_2\, I_2)$	$\lvert E_{1(pu)} \rvert \lvert I_{1(pu)} \rvert \cos(\phi)\eta = E_{2(pu)} I_{2(pu)}$
PWM DC/AC Converter		
Voltage	$\lvert E_{2(ph)} \rvert = \frac{1}{2\sqrt{2}} (MI) E_1$	$\lvert E_{2(pu)} \rvert = E_{1(pu)} (MI)$
Current	$I_1 = \frac{3}{\eta 2\sqrt{2}} (MI) \lvert I_2 \rvert \cos(\emptyset)$	$I_{1(pu)} = \frac{\lvert I_{2(pu)} \rvert \cos(\phi)}{\eta} (MI)$
Power Balance	$3 \lvert E_{2(ph)} \rvert \lvert I_2 \rvert \cos(\emptyset) = (E_1\, I_1\, \eta)$	$\lvert E_{2(pu)} \rvert \lvert I_{2(pu)} \rvert \cos(\phi) = E_{1(pu)} I_{1(pu)} \eta$
PWM DC-DC Converter		
Voltage	$\lvert E_2 \rvert = \lvert E_1 \rvert (A)$	$\lvert E_{2(pu)} \rvert = \lvert E_{1(pu)} \rvert (A)$
Current	$\mathrm{I}_1 = A \times \frac{I_2}{\eta}$	$\mathrm{I}_{1(\mathrm{pu})} = A \times \frac{I_{2(pu)}}{\eta}$
Power Balance	$(E_1\, I_1\, \eta) = (E_2\, I_2)$	$E_{1(pu)} I_{1(pu)} \eta = E_{2(pu)} I_{2(pu)}$

Note- The PWM and DC-DC converters can achieve better control objectives than bridge converter at the distribution level. Hence, these converters can be used between buses (bus-bus interfacing) as well between DG and bus (DG-bus interfacing) for transferring power, fulfilling the requisite control objectives. In the scenario, where control objectives are not highly needed, bridge converter can be used between buses as bus-bus interfacing (but not as DG-bus interfacing) converter.

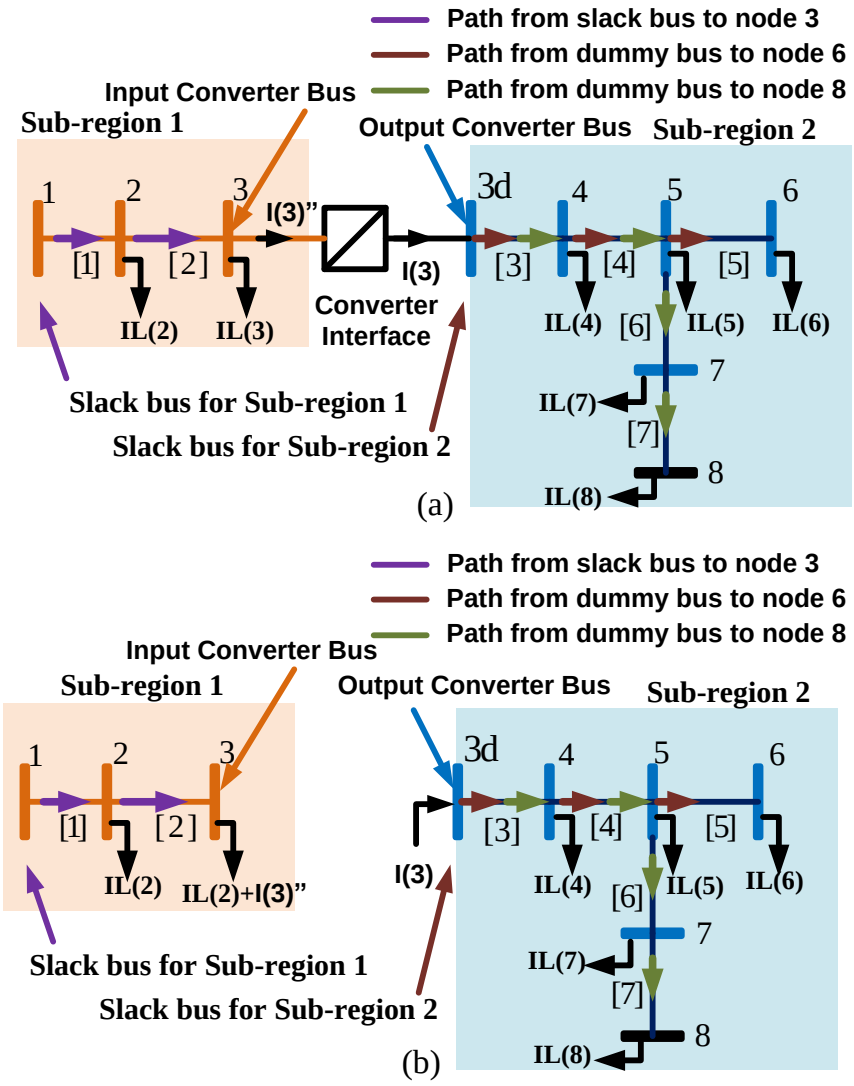

Fig. 4.6: Schematic diagram of an AC-DC radial distribution system.

4.2.2 Solution Methodology

The single line diagram of an AC-DC distribution system shown in Fig. 4.6 has been used to illustrate the proposed load flow algorithm. The converter in Fig. 4.6 can be AC-DC or DC-

AC or DC-DC depending upon the configuration of buses being interfaced (AC-DC, DC-AC and DC-DC bus interfacing respectively) on the both sides of converter terminals.

In the proposed study, the AC-DC distribution system has been subdivided into a number of sub distribution systems or sub-regions. Each sub-region will act as separate distribution system. The converter output bus (*3d* in Fig. 4.6) will be treated as the slack bus of the sub-region that has been numbered later. The relevant matrices formulation as discussed above has to be carried out for each sub-region separately.

Note- **A**. In this section, subscript "g" in the matrices represent the sub-region number otherwise the structural significance of matrix is same as we have described earlier in this section. That means, for each sub-region in an AC-DC distribution system all significant matrices have to be formulated to achieve the desired load flow solution.

B. It is to be noted that anywhere in the article, if a specific symbol has no definition, then it is contemplated merely as a variable that has been used for load flow calculation.

The step by step procedure to implement the proposed load flow algorithm are sequentially listed below:

Step 1. Identify the total number of sub-regions in an AC-DC distribution network. In Fig. 4.6, there are two sub-regions of the AC-DC distribution system.

Step 2. Identify all nodes and branches associated with their respective sub-region in the distribution network. Formulate the loads beyond branch matrix (LB_g) for all sub-regions of AC-DC distribution network separately.

g = sub-region number= 1,2,3,....C.

C=Total number of sub-regions or regions.

The LB_g matrices for the sub-region 1 and sub-region 2 are given as:

$$LB_1 = \begin{bmatrix} S(2) & S(3) \\ 0 & S(3) \end{bmatrix} \tag{4.19}$$

$$LB_2 = \begin{bmatrix} S(4) & S(5) & S(6) & S(7) & S(8) \\ 0 & S(5) & S(6) & S(7) & S(8) \\ 0 & 0 & S(6) & 0 & 0 \\ 0 & 0 & 0 & S(7) & S(8) \\ 0 & 0 & 0 & 0 & S(8) \end{bmatrix} \tag{4.20}$$

Step 3. Formulate the path impedance matrix PI_g for each sub-regions of the AC-DC distribution network. The PI_g matrices of the sub-region 1 and sub-region 2 in Fig. 4.6 are given as:

$$PI_1 = \begin{bmatrix} Z(1) & Z(2) \end{bmatrix} \tag{4.21}$$

$$PI_2 = \begin{bmatrix} Z(3) & Z(4) & Z(5) & 0 & 0 \\ Z(3) & Z(4) & 0 & Z(6) & Z(7) \end{bmatrix} \tag{4.22}$$

Step 4. Set a rated voltage profile at each nodes (including converter interfacing nodes) and formulate the voltage matrices for all the sub-regions of the distribution network. The voltage matrix V_g does not store the voltage value of slack bus and hence its order is $(1 \times (n-1))$. Set tolerance limit $\varepsilon \leq 0.0001$.

n= Total number of buses in a sub-region g of the distribution network.

The formulated voltage matrices for both the sub-regions of AC-DC distribution network in Fig. 4.6 are given as:

$$V_1 = \begin{bmatrix} V(2) & V(3) \end{bmatrix} \tag{4.23}$$

$$V_2 = \begin{bmatrix} V(4) & V(5) & V(6) & V(7) & V(8) \end{bmatrix} \tag{4.24}$$

Step 5. Set iteration number $t = 1$[with *t*(maximum)=100].

Step 6. Compute the controlling parameters of the various converters based on the bus voltage.

Calculate α, if the converter in Fig. 4.6 is three phase bridge converter.

$$\alpha = cos^1 \left(\frac{V(3d)}{|V(3)|} \right) \tag{4.25}$$

Calculate D, if the converter in Fig.4.6 is DC-DC converter.

$$\left.\begin{aligned} D &= \left(\frac{V(3d)}{V(3)} \right) \text{ (buck)} \\ D &= 1 - \left(\frac{V(3)}{V(3d)} \right) \text{ (boost)} \\ \mathrm{D} &= \left(\frac{V(3d)}{V(3) + V(3d)} \right) \text{ (buck-boost)} \end{aligned}\right\} \tag{4.26}$$

Compute MI, if the converter in Fig. 4.6 is three phase VSC converter.

$$MI = \left(\frac{|V(3d)|}{V(3)} \right) \tag{4.27}$$

Step 7. Calculate the load current matrix and feeder current matrix of all the sub-regions. The load current matrix and feeder current matrix of the sub-region farthest from the slack bus sub-region will be evaluated first. The procedure for load current matrix and feeder current matrix calculation are illustrated below:

$W_g = conjugate\left(LB_g\right)$[for AC sub-regions]= LB_g[for DC sub-regions)

$V1_g = conjugate\left(V_g\right)$[for AC sub-regions]= V_g[for DC sub-regions)

for i=1,2.....m.

$$\left.\begin{aligned} LC_g(i,j) &= \frac{W_g(i,j)}{V1_g(i,j)} \text{ (if AC sub-region)} \\ LC_g(i,j) &= \frac{W_g(i,j)}{V1_g(i,j)} \text{ (if DC sub-region)} \end{aligned}\right\} \tag{4.28}$$

Compute LC_g matrix for all value of *n* and *m*.

j=1,2.....*n-1*.

In the matrix LC_g each element represents load current. On summing up all the load currents of the same row will provide feeder current of the branch represented by that row.

$$FC_g(i) = \sum_{l=1}^{n-1} LC_g(i,l) \tag{4.29}$$

i=1,2.....*m*.

m= Total number of branches in a sub-region g of the distribution network.

n= Total number of buses in a sub-region g of the distribution network.

For the AC-DC distribution network in Fig.4.6, the load current matrix and feeder current matrix of sub-region 2 are computed first. The computed results are:

$$LC_2 = \begin{bmatrix} IL(4) & IL(5) & IL(6) & IL(7) & IL(8) \\ 0 & IL(5) & IL(6) & IL(7) & IL(8) \\ 0 & 0 & IL(6) & 0 & 0 \\ 0 & 0 & 0 & IL(7) & IL(8) \\ 0 & 0 & 0 & 0 & IL(8) \end{bmatrix} \tag{4.30}$$

$$FC_2 = \begin{bmatrix} I(3) \\ I(4) \\ I(5) \\ I(6) \\ I(7) \end{bmatrix} \tag{4.31}$$

Step 8. In the subsequent step, calculate the current input to the bus-bus interfacing converter connecting two different sub-regions. In Fig. 4.6, the current input to converter is calculated using equations specified below:

$$|I(3")| = \frac{1}{\eta} I(3) \text{ (If the converter is three phase bridge converter).} \tag{4.32}$$

$$I(3") = \frac{(MI)}{\eta} |I(3)| \cos(\emptyset) \text{ (If the converter is three phase VSC converter).} \tag{4.33}$$

$$I(3") = \frac{A \times I(3)}{\eta} \text{ (If the converter is DC-DC converter).} \tag{4.34}$$

Where, A is D , $\frac{1}{1-D}$ and $\frac{D}{1-D}$ for buck, boost and buck-boost operations respectively.

The phase angle of input current to the converter (only in the case of rectification) is computed using power balance equation.

Step 9. Likewise, compute the load current matrix and feeder current matrix of all sub-regions associated with the AC-DC distribution system. For the AC-DC distribution network in Fig. 4.6, the load current matrix and feeder current matrix are computed for sub-region 1. The computed results are:

$$LC_1 = \begin{bmatrix} IL(2) & IL(3) + I(3") \\ 0 & IL(3) + I(3") \end{bmatrix} \tag{4.35}$$

$$FC_1 = \begin{bmatrix} I(1) \\ I(2) \end{bmatrix} \tag{4.36}$$

Step 10. In next step, calculate path drop matrix of all the sub-distribution networks. The path drop (PD_g) matrices for the two sub-regions of the distribution network in Fig. 4.6 are given as:

$$PD_1 = \begin{bmatrix} Z(1) \times I(1) & Z(2) \times I(2) \end{bmatrix} \tag{4.37}$$

$$PD_2 = \begin{bmatrix} Z(3) \times I(3) & Z(4) \times I(4) & Z(5) \times I(5) & 0 \times I(6) & 0 \times I(7) \\ Z(3) \times I(3) & Z(4) \times I(4) & 0 \times I(5) & Z(6) \times I(6) & Z(7) \times I(7) \end{bmatrix} \tag{4.38}$$

Step 11. In next step, $SBOBD_g$ matrix for all the sub-regions needs to be formulated. For example, $SBOBD_1$ for sub-region 1 of the AC-DC distribution network in Fig. 4.6 is given as:

$$SBOBD_1 = \begin{bmatrix} D(1) & D(1)+D(2) \end{bmatrix} \tag{4.39}$$

where, $D(1) = I(1) \times Z(1)$, $D(2) = I(2) \times Z(2)$

In similar manner, the $SBOBD_g$ matrices for all the remaining sub-regions are calculated.

Step 12. Compute new bus voltage matrix of the AC sub-region connected with slack bus using the procedure described below:

$$LFM_g = (\text{voltage at the slack bus} \times U_g) - SBOBD_g \tag{4.40}$$

U_g=Binary matrix of the same order as $SBOBD_g$.

$U_g(i, j) = 0$, if $PI_g(i, j) =$ *is 0.*

$U_g(i, j) = 1$, else

Initialize a search operation for selecting the maximum value from each column of matrix T_g and store the results in $V_g(new)$ thus leading to formulation of new voltage matrix.

The $V_1(new)$ matrix for the sub-region 1 of the distribution network in Fig. 4.6 is given as:

$$V_{1(new)} = \begin{bmatrix} V(2) & V(3) \end{bmatrix} \tag{4.41}$$

Step 13. Compute the output voltage of the converters connecting two sub-regions of AC-DC distribution systems. To calculate the converters output voltage, first, the controlling parameters of all bus-bus interfacing converters need to be calculated.

For example, if constant voltage magnitude say Q is to be maintained at the converter output terminal $3d$:

$$|V(3d)| = Q$$

$V(3) =$ Newly calculated voltage at bus 3 {refer (4.41}

Then,

Calculate α using (4.25), if the converter in Fig. 4.6 is three phase bridge converter.

Compute MI using (4.27), if the converter in Fig. 4.6 is three phase VSC converter.

Calculate D using (4.26), if the converter in Fig. 4.6 is DC-DC converter.

In the sub-sequent step control limits of calculated controlling parameters are being checked. If the controlling variable transcend the controlled limit (upper bound or lower bound limit),

it will be set to that limit, and this imply that enactment of this control scheme is beyond the bound of possibility (Fig. 4.7).

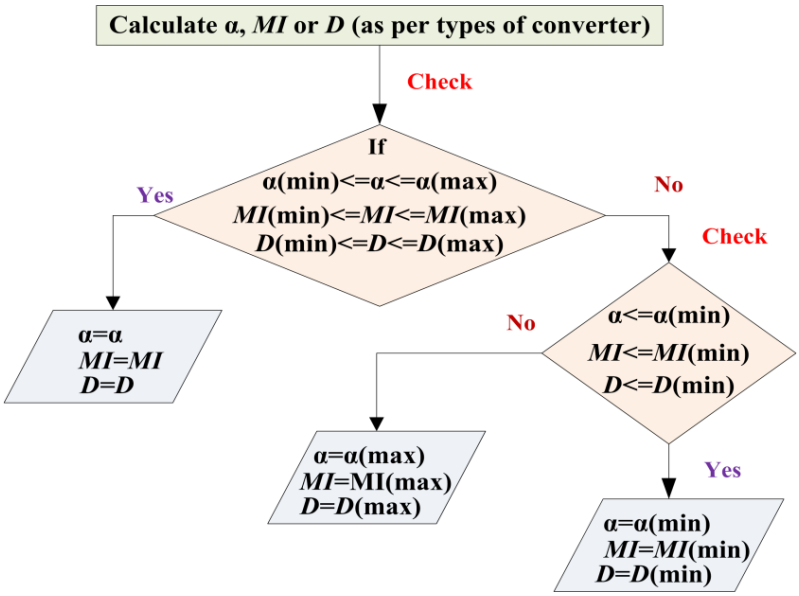

Fig.4.7: Flowchart for controlling parameters calculation.

Once the controlling parameters are calculated, the output converter voltage can easily be calculated using respective converter voltage equation {refer (4.1), (4.4), and (4.7)-(4.9)}. The phase angle of converter output voltage (only in the case of inversion) is computed using the power factor angle difference at the converter terminal calculated at the beginning of iteration and in the current scenario. The difference is new power factor angle of converter output voltage.

Step 14. The converter output buses are treated as slack bus of the sub-region to which it belongs. Hence, the matrix U_g of all sub-regions associated with an AC-DC distribution network should be multiplied by their respective converter output bus voltage.

Step 15. Compute the new bus voltage matrix of all the remaining sub-regions {refer step 12}.

Step 16. Check convergence criterion of all the sub-regions.

Step 17. *DVMAX*=max (convergence of all sub-regions).

Step 18. If $DVMAX < \mathcal{E}$ go to step 22, else go to step 19.

Step 19. Replace the previous voltage matrix of all the sub-regions with their new obtained voltage matrix.

i.e., $V_g = V_{g(new)}$ (4.42)

$g = 1,2 \ldots \ldots \ldots C.$

Step 20. $t = t + 1.$

Step 21. If $t \leq t(\text{maximum})$ go to step 6 else go to step 23.

Step 22. Print "Solution converged".

Step 23. Print "Solution not converged".

The aforementioned algorithm is based on the per unit equivalent model of various types of converters mentioned in this chapter. The load flow algorithm of AC-DC distribution network can also be executed using the phase equivalent model of the converters. The per unit converter equations utilised in Section 4.2 can be replaced with their phase equivalent equations mentioned in Table 4.1 and load flow iteration will be executed in its accordance.

4.3 Load Flow Algorithm for AC-DC Radial Distribution System with Distributed Generations

The distributed generations modelled as PQ, P, V^{dc} and PV buses are incorporated into the proposed algorithm to imitate the injection of DGs in the distribution systems. The DGs modelled as PQ bus and P bus can be included in the proposed load flow algorithm by considering injection by the DGs as the negative load. The power injected by the DGs need to be reflected in the LB matrix of the distribution network. For the PV type buses or distributed generators, the reactive power generation is adjusted between the maximum and minimum limits in order to maintain the constant voltage and constant real power (injected) at the PV bus. Similarly, when $\mathbf{V^{dc}}$ nodes are present in DC regions of an AC-DC distribution network we need to determine the correct amount of active power injection by the generation units to compensate the variance between obtained and specified voltage. Hence, special treatment is required to achieve the load flow solution of AC-DC distribution network with PV and $\mathbf{V^{dc}}$ nodes.

Case 1: The AC-DC distribution system with one V^{dc} node

Consider the AC-DC distribution system shown in Fig. 4.8, a DG modeled as $\mathbf{V^{dc}}$ node is injecting power at bus number 8.

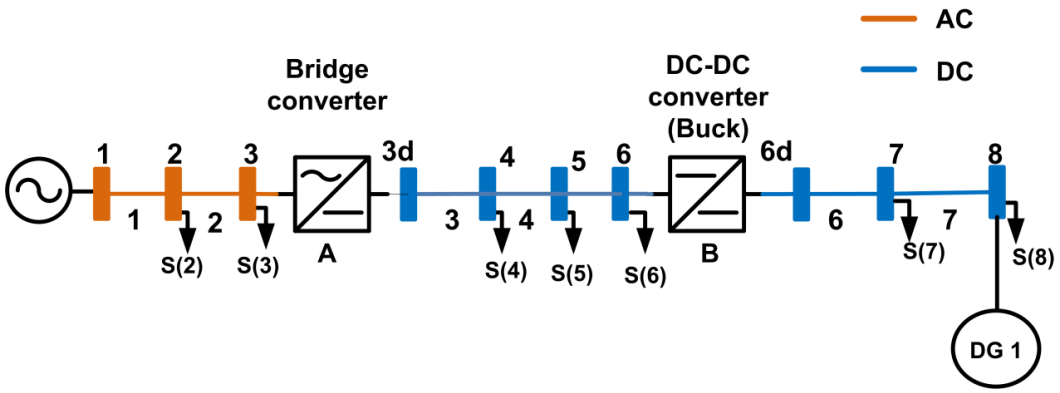

Fig.4.8*:* Schematic diagram of an AC-DC distribution network with V^{dc} bus.

The correct amount of active power injection by the generation units need to be determined to compensate the variance between obtained and specified voltage. The sensitivity matrix or breakpoint matrix has been utilized to obtain the additional real power injection/withdrawal (breakpoint injection) to maintain the specified voltage at each $\mathbf{V^{dc}}$ node. For the distribution network that contains V^{dc} nodes, one breakpoint matrix needs to be formulated. In the distribution system shown in Fig. 4.8, the converter A is operating at commutation angle α and converter B is operating at a duty ratio D. The simplified diagram for calculating V^{dc} breakpoint injection is illustrated in Fig. 4.9. The detailed procedure for calculating V^{dc} breakpoint injection is explained below.

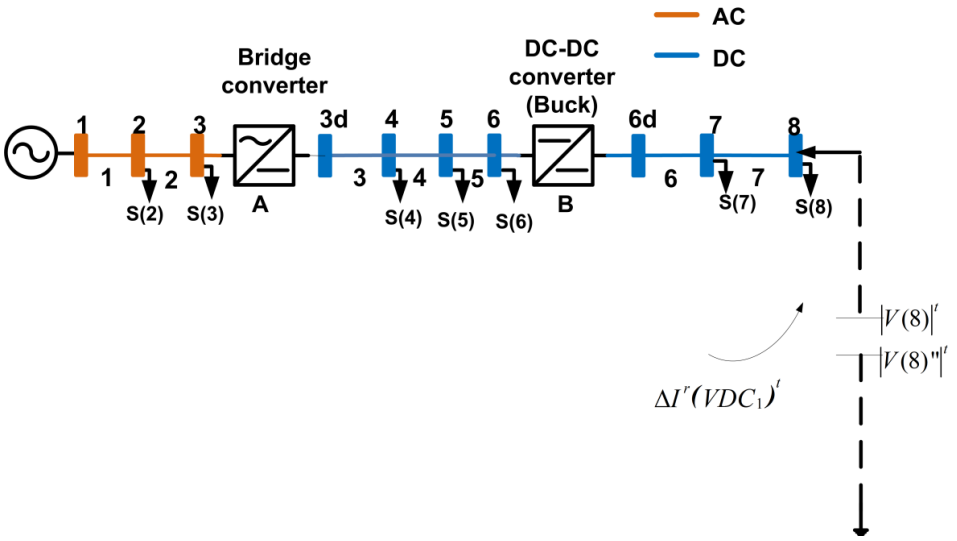

Fig.4.9*:* Simplified diagram of AC-DC distribution network in shown in Fig. 4.8 for V^{dc} breakpoint injection calculations.

VDC= Set of all V^{dc} buses.

VDC_W=Wth element of set VDC

vdc= Total number of V^{dc} buses.

W=1,2.....*vdc*.

For the distribution system shown in Fig. 4.9, the breakpoint equation called as V^{dc} breakpoint matrix can be written as:

$$\left[|Z(1)|\cos(\alpha)D^2+|Z(2)|\cos(\alpha)D^2+|R(3)|D^2+|R(4)|D^2+|R(5)|D^2+(|R(6)|+|R(7)|)\right] \times\left[\Delta I^r(VDC_1)^t\right]=\left[|V(VDC_1'')^t|-|V(VDC_1)^t|\right] \quad (4.43)$$

In this particular case,

$$\Delta I^q(VDC_1)=0$$

VDC= Set of all PV buses={8}

vdc=2= Total number of VDC buses.

W=1

VDC_1= 1st element of set VDC=8.

$\Delta V(VDC_1)^t$ = Voltage magnitude mismatch at the bus VDC_1 associated with V^{dc} distributed generation number 1 in the beginning of iteration *t* = $V(VDC_1'')^t - V(VDC_1)^t$

$V(VDC_1'')^t$ = Voltage magnitude (specified) at bus PVB_1 associated with V^{dc} distributed generation number 1.

$V(VDC_1)^t$ = Voltage calculated (beginning of iteration number t) at bus VDC_1 associated with V^{dc} distributed generation number 1 .

$\Delta I^r(VDC_1)^t$ = V^{dc} real current injection at bus VDC_1 in the beginning of iteration t.

The above equation for calculating V^{dc} breakpoint current injection can be modified in terms of V^{dc} breakpoint real power injection. With the assumption of all bus voltages being close to 1.0 p.u. and the phase angles small, the following equation holds:

$$\Delta I^r(VDC_W)^t=\Delta P(VDC_W)^t \quad (4.44)$$

$\Delta P(VDC_W)^t$ = V^{dc} breakpoint real power injection at bus VDC_1 in the beginning of iteration *t*.

Thus, equation 4.43 can be modified as:

$$\left[|Z(1)|\cos(\alpha)D^2+|Z(2)|\cos(\alpha)D^2+|R(3)|D^2+|R(4)|D^2+|R(5)|D^2+(|R(6)|+|R(7)|)\right] \times\left[\Delta P(VDC_1)^t\right]=\left[|V(VDC_1'')^t|-|V(VDC_1)^t|\right] \quad (4.45)$$

The total real power injection by the V^{dc} type distributed generation in Fig. 4.9 at the beginning of iteration *t* is given by the following equations:

$$TP(VDC_1)^t=\sum_{x=1}^{t-1}\Delta P(VDC_1)^x+\Delta P(VDC_1)^t \quad (4.46)$$

Case 2: The AC-DC distribution system with two V^{dc} node

An AC-DC distribution system shown in Fig. 4.10, DGs modeled as $\mathbf{V^{dc}}$ node/bus is injecting power at bus number 8 and 5.

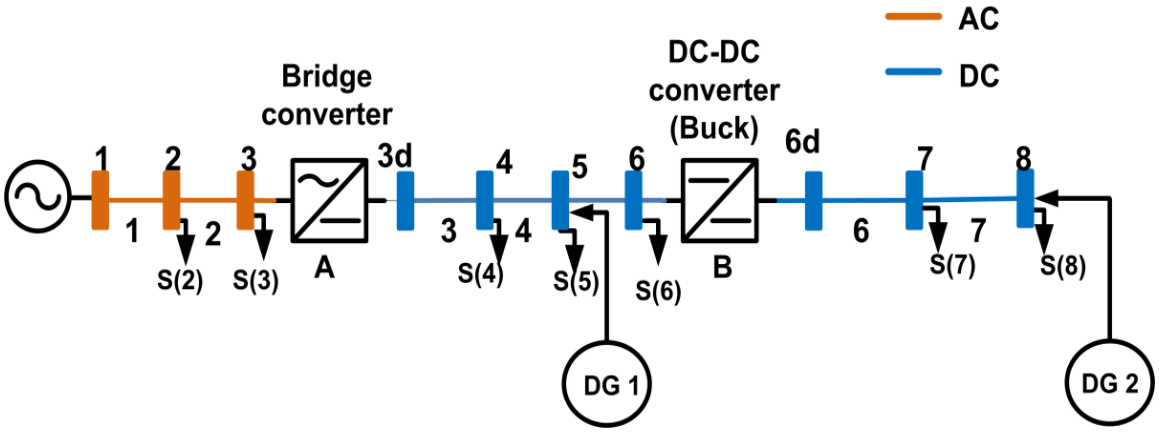

Fig.4.10*:* Schematic diagram of an AC-DC distribution network with two V^{dc} buses.

The correct amount of active power injection by the generation units need to be determined to compensate the variance between obtained and specified voltage. The breakpoint matrix has been developed to obtain the additional real power injection/withdrawal to maintain the specified voltage at each $\mathbf{V^{dc}}$ nodes. The simplified diagram for calculating V^{dc} breakpoint injections is illustrated in Fig. 4.11. The detailed procedure for calculating V^{dc} breakpoint injections is exemplified below.

In the distribution system shown in Fig. 4.10, the converter A is operating at commutation angle α and converter B is operating at a duty ratio D. For the distribution system shown in Fig. 4.10 the breakpoint equation called as V^{dc} breakpoint matrix can be written as:

$$\begin{bmatrix} (|Z(1)|+|Z(2)|)\cos(\alpha)+|Z(3)|+|Z(4)| & (|Z(1)|+|Z(2)|)\cos(\alpha)D+|Z(3)|D+|Z(4)|D \\ (|Z(1)|+|Z(2)|)\cos(\alpha)D+|Z(3)|D+|Z(4)|D & (|Z(1)|+|Z(2)|)\cos(\alpha)D^2+(|Z(3)|+|Z(4)|+|Z(5)|)D^2+|Z(6)|+|Z(7)| \end{bmatrix}$$
$$\times \begin{bmatrix} \Delta I^r(VDC_1)^t \\ \Delta I^r(VDC_2)^t \end{bmatrix} = \begin{bmatrix} |V(VDC_1'')^t|-|V(VDC_1)^t| \\ |V(VDC_2'')^t|-|V(VDC_2)^t| \end{bmatrix} \quad (4.47)$$

In this particular case,

$$\Delta I^q(VDC_1) = \Delta I^q(VDC_2) = 0$$

VDC= Set of all PV buses={5,8}

vdc=2= Total number of V^{dc} buses.

W=2

VDC_1= 1st element of set VDC=5.

VDC_2= 2nd element of set VDC=8.

$\Delta V(VDC_1)^t$ = Voltage magnitude mismatch at the bus VDC_1 associated with V^{dc} distributed generation number 1 in the beginning of iteration *t* = $V(VDC_1'')^t - V(VDC_1)^t$

$V(VDC_1'')^t$ = Voltage magnitude (specified) at bus VDC_1 associated with V^{dc} distributed generation number 1.

$V(VDC_1)^t$ = Voltage calculated (beginning of iteration number t) at bus VDC_1 associated with V^{dc} distributed generation number 1 .

$\Delta V(VDC_2)^t$ = Voltage magnitude mismatch at the bus VDC_2 associated with V^{dc} distributed generation number 2 in the beginning of iteration *t* = $V(VDC_2'')^t - V(VDC_2)^t$

$V(VDC_2'')^t$ = Voltage magnitude (specified) at bus VDC_2 associated with V^{dc} distributed generation number 2.

$V(VDC_2)^t$ = Voltage calculated (beginning of iteration number *t*) at bus VDC_1 associated with V^{dc} distributed generation number 2 .

$\Delta I^r(VDC_1)^t$ =Additional V^{dc} breakpoint real current injection at bus VDC_1 in the beginning of iteration *t*.

$\Delta I^r(VDC_2)^t$ = Additional V^{dc} breakpoint real current injection at bus VDC_2 in the beginning of iteration *t*.

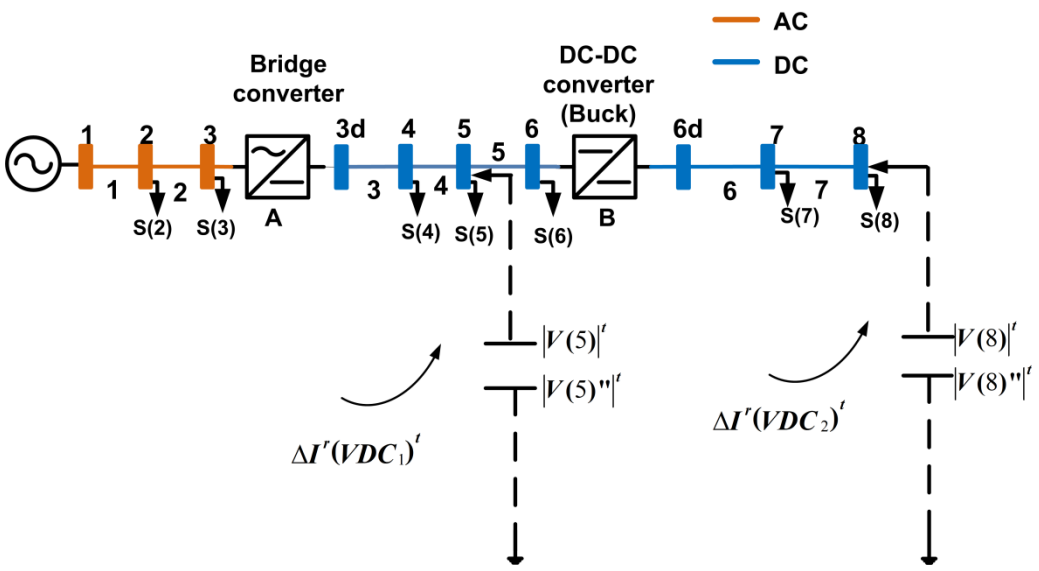

Fig.4.11*:* Simplified diagram of AC-DC distribution network in shown in Fig. 4.10 for V^{dc} breakpoints injection calculation.

The above equation for calculating V^{dc} breakpoint current injection can be modified in terms of V^{dc} breakpoint real power injection. With the assumption of all bus voltages being close to 1.0 p.u. and the phase angles small, the following equation holds:

$$\Delta I^r(VDC_W)^t = \Delta P(VDC_W)^t \tag{4.48}$$

Thus, equation (4.47) can be modified as:

$$\begin{bmatrix} (|Z(1)|+|Z(2)|)\cos(\alpha)+|Z(3)|+|Z(4)| & (|Z(1)|+|Z(2)|)\cos(\alpha)D+|Z(3)|D+|Z(4)|D \\ (|Z(1)|+|Z(2)|)\cos(\alpha)D+|Z(3)|D+|Z(4)|D & (|Z(1)|+|Z(2)|)\cos(\alpha)D^2+(|Z(3)|+|Z(4)|+|Z(5)|)D^2+|Z(6)|+|Z(7)| \end{bmatrix} \times \begin{bmatrix} \Delta P(VDC_1)^t \\ \Delta P(VDC_2)^t \end{bmatrix} = \begin{bmatrix} |V(VDC_1'')^t|-|V(VDC_1)^t| \\ |V(VDC_2'')^t|-|V(VDC_2)^t| \end{bmatrix} \tag{4.49}$$

where

$\Delta P(VDC_1)^t$ =Additional V^{dc} breakpoint real current injection at bus VDC_1 in the beginning of iteration *t*.

$\Delta P(VDC_2)^t$ = Additional V^{dc} breakpoint real power injections at bus VDC_2 in the beginning of iteration *t*.

The total real power injections by the V^{dc} type distributed generations in Fig. 4.10 at the beginning of iteration *t* is given by the following equations:

$$TP(VDC_1)^t = \sum_{x=1}^{t-1} \Delta P(VDC_1)^x + \Delta P(VDC_1)^t \tag{4.50}$$

$$TP(VDC_2)^t = \sum_{x=1}^{t-1} \Delta P(VDC_2)^x + \Delta P(VDC_2)^t \tag{4.51}$$

Case 3: The AC-DC distribution system with one PV node

Consider the AC-DC distribution system shown in Fig. 4.12, a DG modeled as **PV** bus is injecting power at bus number 8.

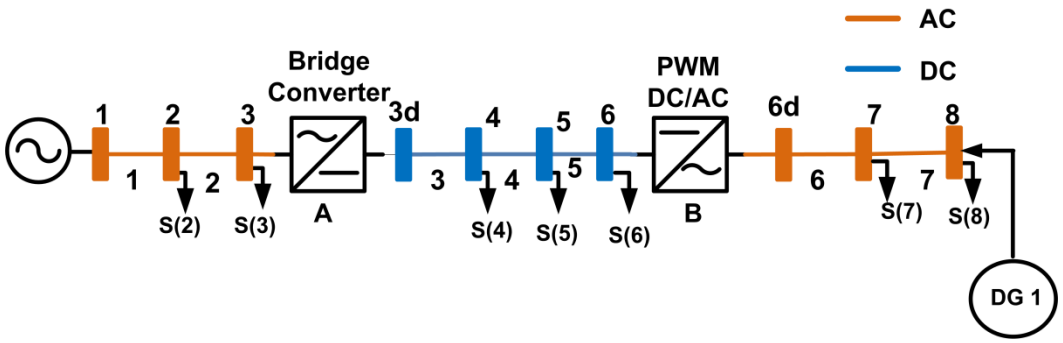

Fig.4.12*:* Schematic diagram of an AC-DC distribution network with PV bus.

The correct amount of reactive power injection by the generation units need to be determined to compensate the variance between obtained and specified voltage. The breakpoint matrix has been developed to obtain the additional real power/current injection/withdrawal to maintain the specified voltage at each $\mathbf{V^{dc}}$ nodes. The simplified diagram for calculating PV breakpoint injection is illustrated in Fig. 4.13. The detailed procedure for calculating V^{dc} breakpoint injection is exemplified below.

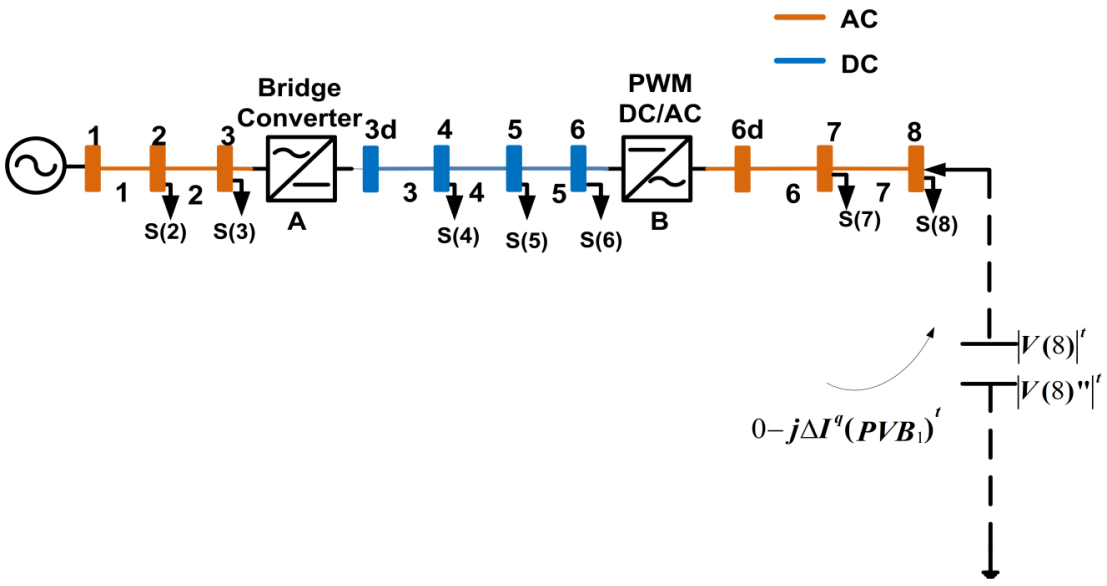

Fig.4.13: Simplified diagram of AC-DC distribution network in shown in Fig. 4.12 for calculating PV breakpoint injection.

In the distribution system shown in Fig. 4.13, the converter A is operating at commutation angle α and converter B is operating at a duty ratio D. For the distribution system shown in Fig. 4.13, the breakpoint equation called as PV breakpoint matrix can be formulated as:

$$\left[\{(|Z(1)|+|Z(2)|)\cos(\alpha)MI+(|Z(3)|+|Z(4)|+|Z(5)|)MI\}\cos(\theta_v)\times\cos(\phi)+(|X(6)|+|X(7)|)\right] \times\left[\Delta I^{q}(PVB_1)^{t}\right]=\left[|V(PVB_1'')^{t}|-|V(PVB_1)^{t}|\right] \quad (4.51)$$

PVB= Set of all PV buses.

PVB_K= K^{th} element of set PVB

pvb= Total number of V^{dc} buses.

K=1,2.....pvb.

In this particular case,

$$\Delta I^{r}(PVB_1)=0$$

PVB= Set of all PV buses={8}

pvb=1= Total number of PV buses.

K=1

PVB_1= 1^{st} element of set PVB=8.

$\Delta V(PVB_1)^{t}$ = Voltage magnitude mismatch at the bus PVB_1 associated with PV distributed generation number 1 in the beginning of iteration t = $V(PVB_1'')^{t}-V(PVB_1)^{t}$

$V(PVB_1'')^{t}$ = Voltage magnitude (specified) at bus PVB_1 associated with PV distributed generation number 1.

$V(PVB_1)^{t}$ = Voltage calculated (beginning of iteration number t) at bus PVB_1 associated with PV distributed generation number 1 .

$\Delta I^{q}(PVB_1)^{t}$ = Additional PV breakpoint reactive current injection at bus PVB_1 in the beginning of iteration t.

θ_v = Phase angle of the converter B terminal voltage.

The above equation for calculating PV breakpoint current injection can be modified in terms of PV breakpoint reactive power injection. With the assumption of all bus voltages being close to 1.0 p.u. and the phase angles small, the following equation holds:

$$\Delta I^{q}(PVB_K)^{t}=\Delta Q(PVB_K)^{t} \quad (4.52)$$

Thus, equation (4.51) can be modified as:

$$\left[\{(|Z(1)|+|Z(2)|)\cos(\alpha)MI+(|Z(3)|+|Z(4)|+|Z(5)|)MI\}\cos(\theta_v)\times\cos(\phi)+(|X(6)|+|X(7)|)\right] \times\left[\Delta Q(PVB_1)^t\right]=\left[|V(PVB_1'')^t|-|V(PVB_1)^t|\right] \tag{4.53}$$

where

$\Delta Q(PVB_1)^t$ = Additional PV breakpoint reactive power injection at bus PVB_1 in the beginning of iteration *t*.

The total reactive power injection by the PV type distributed generation in Fig. 4.12 at the beginning of iteration *t* is given by the following equations:

$$TQ(PVB_1)^t=\sum_{x=1}^{t-1}\Delta Q(PVB_1)^x+\Delta Q(PVB_1)^t \tag{4.54}$$

Case 4: The AC-DC distribution system with both PV and V^{dc} buses

Consider the AC-DC distribution system shown in Fig. 4.14, a DG modeled as $\mathbf{V^{dc}}$ bus is injecting power at bus number 8 and another DG modeled as PV bus is injecting power at bus number 2. For the DG modeled as V^{dc} bus, the correct amount of active power/current injection/withdrawal by the generation units need to be determined to compensate the variance between obtained and specified voltage (V^{dc} bus voltage). In the case of DG modeled as PV bus, the correct amount of reactive power/current injection/withdrawal by the generation units need to be determined to compensate the variance between obtained and specified voltage (PV bus voltage). In order to calculate the injections by both DGs a common breakpoint matrix has been developed. The detailed procedure is exemplified below.

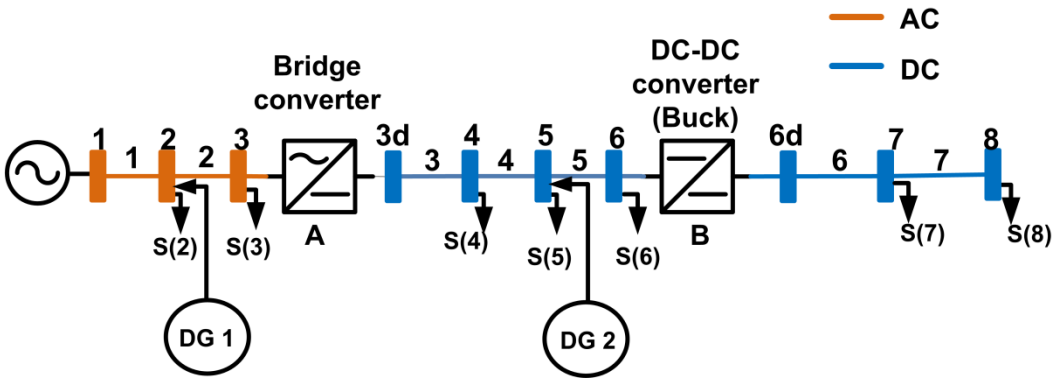

Fig.4.14*:* Schematic diagram of an AC-DC distribution network with both PV and V^{dc} buses.

For the distribution system shown in Fig. 4.14 the common breakpoint matrix for calculating V^{dc} and PV breakpoint injections is given by following equation:

$$\begin{bmatrix} |Z(1)| & |Z(1)| \\ |Z(1)|\cos(\alpha) & (|Z(1)|+|Z(2)|)\cos(\alpha)+|Z(3)|+|Z(4)| \end{bmatrix} \times \begin{bmatrix} \Delta I^{q}(PVB_1)^{t} \\ \Delta I^{r}(VDC_1)^{t} \end{bmatrix} = \begin{bmatrix} \left\| V(PVB_1'')^{t} \right| - \left| V(PVB_1)^{t} \right\| \\ \left| V(VDC_1'')^{t} \right| - \left| V(VDC_1)^{t} \right| \end{bmatrix} \quad (4.54)$$

In this particular case,

$$\Delta I^{q}(VDC_1) = \Delta I^{q}(VDC_2) = 0$$

VDC= Set of all V^{dc} buses={5}

PVB= Set of all PV buses={2}

VDC= Set of all V^{dc} buses={5}

vdc=1= Total number of V^{dc} buses.

pvb=1= Total number of PV buses.

K=1 for PVB

W=1 for VDC

VDC_1= 1st element of set VDC=5.

PVB_1= 1st element of set PVB=2.

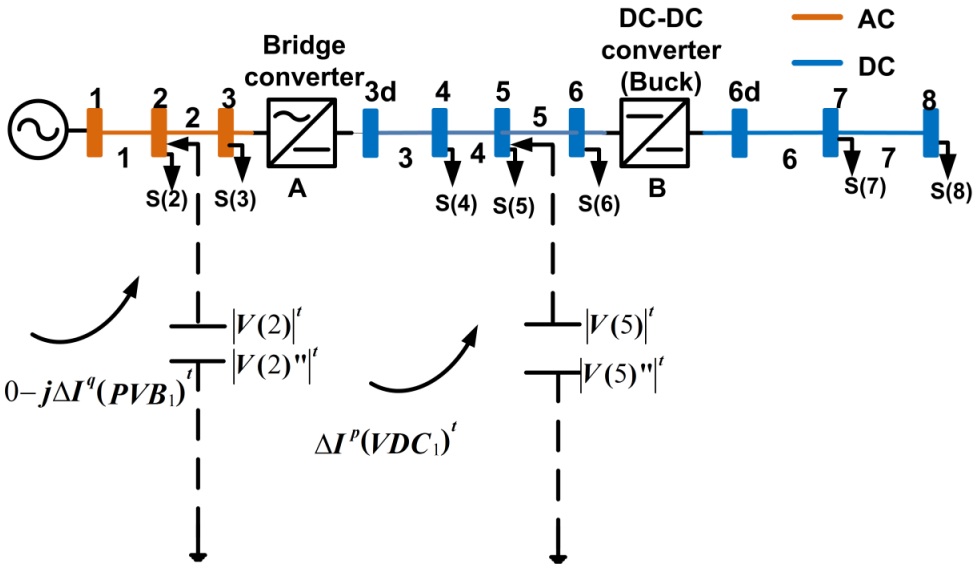

Fig. 4.15: Simplified diagram of AC-DC distribution network in shown in Fig. 4.14 for calculating PV and V^{dc} breakpoint injections.

$\Delta V(VDC_1)^t$ = Voltage magnitude mismatch at the bus VDC_1 associated with V^{dc} distributed generation number 1 in the beginning of iteration *t* = $V(VDC_1'')^t - V(VDC_1)^t$

$V(VDC_1'')^t$ = Voltage magnitude (specified) at bus VDC_1 associated with V^{dc} distributed generation number 1.

$V(VDC_1)^t$ = Voltage calculated (beginning of iteration number t) at bus VDC_1 associated with V^{dc} distributed generation number 1 .

$\Delta I^r(VDC_1)^t$ =Additional V^{dc} breakpoint real current injection at bus VDC_1 in the beginning of iteration *t.*

$\Delta V(PVB_1)^t$ = Voltage magnitude mismatch at the bus PVB_1 associated with PV distributed generation number 1 in the beginning of iteration *t* = $V(PVB_1'')^t - V(PVB_1)^t$

$V(PVB_1'')^t$ = Voltage magnitude (specified) at bus PVB_1 associated with PV distributed generation number 1.

$V(PVB_1)^t$ = Voltage calculated (beginning of iteration number t) at bus PVB_1 associated with PV distributed generation number 1 .

$\Delta I^q(PVB_1)^t$ = Additional PV breakpoint reactive current injection at bus PVB_1 in the beginning of iteration *t*.

The above equation for calculating breakpoint real and reactive current injections can be modified in terms of breakpoint real and reactive power injections respectively. With the assumption of all bus voltages being close to 1.0 p.u. and the phase angles small, the following equation holds:

$$\Delta I^r(VDC_W)^t = \Delta P(VDC_W)^t \tag{4.55}$$

$$\Delta I^q(PVB_K)^t = \Delta Q(PVB_K)^t \tag{4.56}$$

Thus, equation (4.54) can be modified as:

$$\begin{bmatrix} |Z(1)| & |Z(1)| \\ |Z(1)|\cos(\alpha) & (|Z(1)|+|Z(2)|)\cos(\alpha)+|Z(3)|+|Z(4)| \end{bmatrix} \times \begin{bmatrix} \Delta Q(PVB_1)^t \\ \Delta P(VDC_1)^t \end{bmatrix} = \begin{bmatrix} \left\| V(PVB_1'')^t \right| - \left| V(PVB_1)^t \right\| \\ \left| V(VDC_1'')^t \right| - \left| V(VDC_1)^t \right| \end{bmatrix} \tag{4.57}$$

The total real and reactive power injections by the V^{dc} type distributed generation and PV type distributed generation respectively in Fig. 4.14 in the beginning of iteration *t* is given by the following equations:

$$TP(VDC_1)^t = \sum_{x=1}^{t-1} \Delta P(VDC_1)^x + \Delta P(VDC_1)^t \tag{4.58}$$

$$TQ(PVB_1)^t = \sum_{x=1}^{t-1} \Delta Q(PVB_1)^x + \Delta Q(PVB_1)^t \tag{4.59}$$

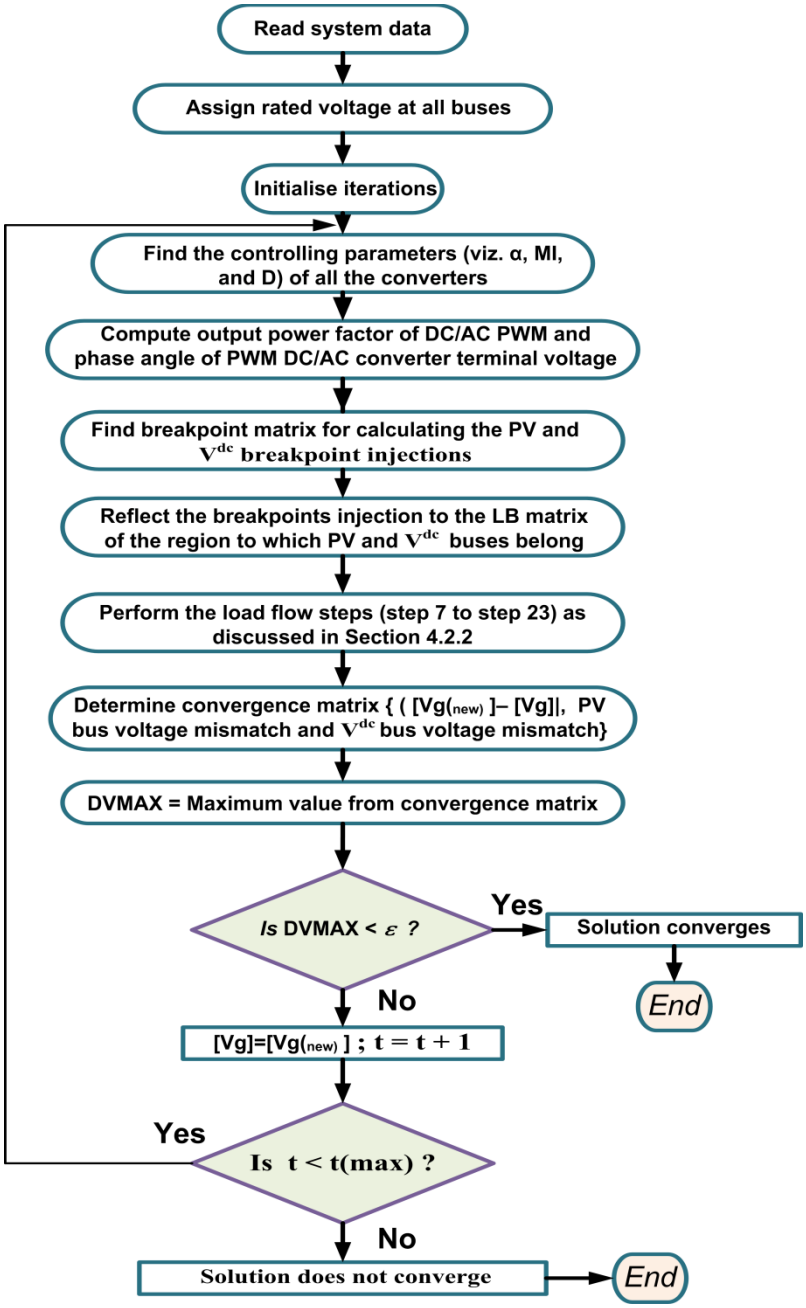

Fig.4.16*:* Load flow algorithm for AC-DC distribution system in the presence of DGs.

4.4 Results

This section presents the case studies that were used for evaluating the effectiveness and accuracy of the proposed LF model. The algorithm has been tested using Matlab software through a personal computer with specifications : Intel core i7 2600@3.4GHz, 64bit, and 8GB RAM. The load-flow results as acquired by proposed method and the efficacy comparison with that of algorithms prevailing in the literature are presented in this part.

Test system 1: 10 bus AC-DC distribution network

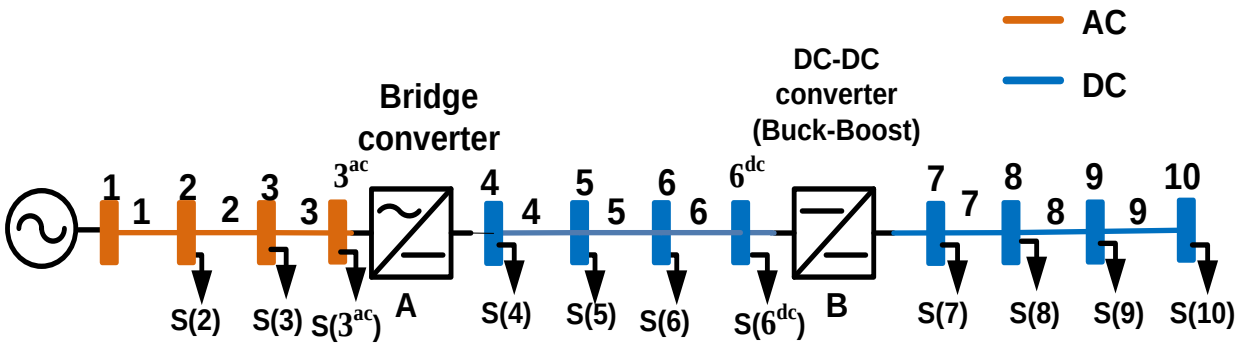

Fig. 4.17*:* Schematic diagram of a hypothetical 10 bus AC-DC distribution network.

As shown in Fig. 4.17, the AC-DC distribution network for the first case study is a 10-bus AC-DC distribution network. The data related to the loads and generators at each bus are presented in Table 4.2 and Table 4.3 respectively. The line data is provided in Table 4.2. In this network, one line commutated converter is connected between buses 3^{ac} and 4. Minimum firing angle limit for this converter is 0°, and its commutation reactance is neglected. The voltage at bus 4 is controlled at 0.9750 pu using three phase bridge converter. The DC-DC buck boost converters connected between buses 6dc and 7 and is being controlled to maintain the constant voltage of the magnitude 0.9801 pu at bus 7. Regarding the bus categorizations, bus 1 represents a slack bus, bus 10 and 5 are V^{dc} buses, bus 4 is generator PQ bus and remaining buses are load buses. The data of various types of converters are provided in Table 4.4. Base MVA=100, Base voltage= 12.66kV (AC side) = 17.09 kV (DC side). All converters are supposed to be working at 100% efficiency. (Tolerance-10^{-6})

Table 4.2: Data of hypothetical 10 bus system shown in Fig. 4.16.

BN	SN	RN	Impedance	Load Data (S(RN)) (kVA/kW)
1	1	2	0.84111+0.82271i	44.1+44.98i
2	2	3	0.84111+0.82271i	44.1+44.98i
3	3	3ac	0.84111+0.82271i	0
-	3ac	4	LCC Converter	264.6
4	4	5	1.6822	132.3
5	5	6	1.6822	44.1
6	6	6dc	1.6822	0
-	6dc	7	DC-DC boost converter	44.1
7	7	8	1.6822	44.1
9	8	9	1.6822	44.1
10	9	10	1.6822	44.1

Table 4.3: Characteristics of controlled generators

Generator Number and Types	Bus Location	Real Power (kW)		Injected Reactive Power (kVAr)		Voltage (pu)
		Max.	Min.	Max.	Min.	
G1 (V^{dc})	5	500	50	-	-	0.9745
G2 (V^{dc})	10	500	50	-	-	0.9782
G4 (PQ)	3	20	20	10	10	-

Table 4.4: Characteristics of converters

Converter Types	Located Between Buses	Control Strategy	Control Limit
3-Φ Full Bridge Converter	3^{ac} & 4	Constant DC Voltage	$\alpha(\min)=7^0$ $\alpha(\max)=18^0$
DC-DC Converter	6^{dc} & 7	Constant Voltage	$D(\min)=0.1$ $D(\max)=0.7$

The load flow results for the aforementioned distribution system (without DGs) using proposed algorithm, the BIBC method and the load flow solution provided by PSCAD software are explicitly presented in Table 4.5. Based on the results acquired, the maximum difference between the bus voltages calculated by the proposed load flow method and the load flow model simulated in PSCAD is 0.0003. The maximum difference between the bus voltages calculated by the proposed load flow method and the BIBC load flow model is 0.0002. The execution time for the proposed method and BIBC method is 20ms and 200ms respectively. The comparison of the results obtained from BIBC method, PSCAD software

and the proposed algorithm demonstrates the effectiveness and accuracy of the method developed.

Table 4.5: Voltage profile for hypothetical 10 bus AC-DC distribution system (without DGs)

Bus Number	Voltage Magnitude (pu)			Phase (Radian)		
	PM	BIBC	PSCAD	PM	BIBC	PSCAD
1	1.0000	1.0000	1.0000	0.0000	0.0000	0.0000
2	0.9965	0.9966	0.9964	-0.0037	-0.0038	-0.0038
3	0.9936	0.9935	0.9936	-0.0075	-0.0090	-0.0091
3^{ac}	0.9910	0.9909	0.9908	-0.0110	-0.0112	-0.0111
4	0.9750	0.9750	0.9750	-	-	
5	0.9729	0.9729	0.9729	-	-	
6	0.9716	0.9716	0.9715	-	-	
6^{dc}	0.9705	0.9705	0.9705	-	-	
7	0.9801	0.9801	0.9801	-	-	
8	0.9780	0.9779	0.9778	-	-	
9	0.9767	0.9765	0.9765	-	-	
10	0.9756	0.9755	0.9754	-	-	

Table 4.6: Voltage profile for hypothetical 10 bus AC-DC distribution system (with DGs)

Bus Number	Voltage Magnitude (pu)		Phase (Radian)	
	PM	PSCAD	PM	PSCAD
1	1.0000	1.0000	0.0000	0.0000
2	0.9977	0.9976	-0.0021	-0.0022
3	0.9958	0.9957	-0.0044	-0.0044
3^{ac}	0.9943	0.9942	-0.0066	-0.0067
4	0.9750	0.9750	-	-
5	0.9745	0.9744	-	-
6	0.9736	0.9735	-	-
6^{dc}	0.9730	0.9729	-	-
7	0.9801	0.9801	-	-
8	0.9795	0.9795	-	-
9	0.9787	0.9788	-	-
10	0.9782	0.9781	-	-

Table 4.7: Distributed generators load flow results

Generator Number and Types	Injected Real Power (kW)		Injected Reactive Power (kVAr)		Voltage (pu)
	PM	PSCAD	PM	PSCAD	
G1 (V^{dc})	80.47	80.48	-	-	0.9745
G2 (V^{dc})	173.90	174	-	-	0.9782
G4 (PQ)	20	20	10	10	-

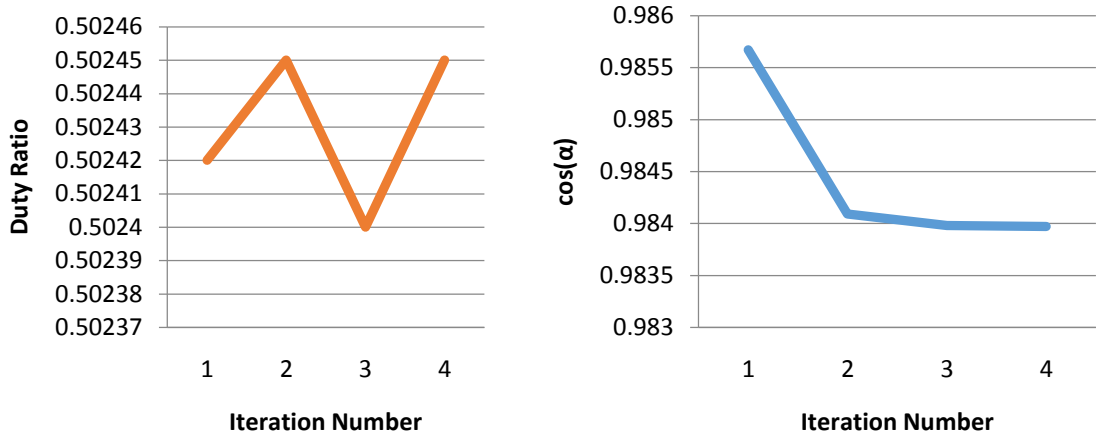

(a) (b)

Fig. 4.18**:** Variation of control variables of the converters in the 10 bus AC-DC distribution network (Fig. 4.17) without DG during load flow iteration (a) Changes in the duty ratio for converter B, (b) Changes in the cos(α) of the converter A.

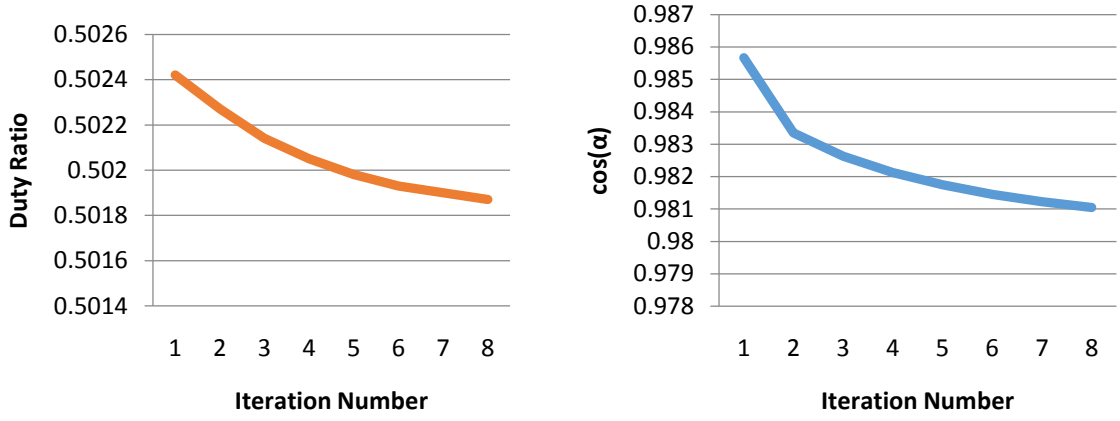

(a) (b)

Fig. 4.19**:** Variation of control variables of the converters in the network (Fig. 4.17) with DG during load flow iteration (a) Changes in the duty ratio for converter B, (b) Changes in the cos(α) of the converter A.

The BIBC matrix method has applicability limited only for simple AC-DC distribution network. This method (BIBC) has not considered the effect of various models of distributed generations. The proposed load flow algorithm has overcome the limitations of existing methodology and is capable of handling mathematical model of various type of distributed generations. A test has been conducted on the AC-DC distribution network shown in Fig.

4.17 in the presence of distributed generations to prove the efficacy of the proposed method. The load flow results for the aforementioned distribution system with DGs using proposed algorithm and the load flow solution provided by PSCAD software is explicitly presented in Table 4.6 and Table 4.7. The comparison of the results obtained from the proposed algorithm and those produced by the PSCAD software therefore demonstrates the effectiveness and accuracy of the method developed.

Changes in the duty cycle of the DC/DC buck boost converter and commutation angle of the rectifier during the load flow iterations of the proposed method are shown in Fig. 4.18 (for base network) and Fig. 4.19 (base network with the inclusion of distributed generations).

Test system 2: 15 bus AC-DC distribution network

The second test system is a 15-bus AC-DC distribution network (Fig. 4.20). The data related to the loads and generators at each bus are presented in Table 4.8 and Table 4.9 respectively. The line data is provided in Table 4.8.

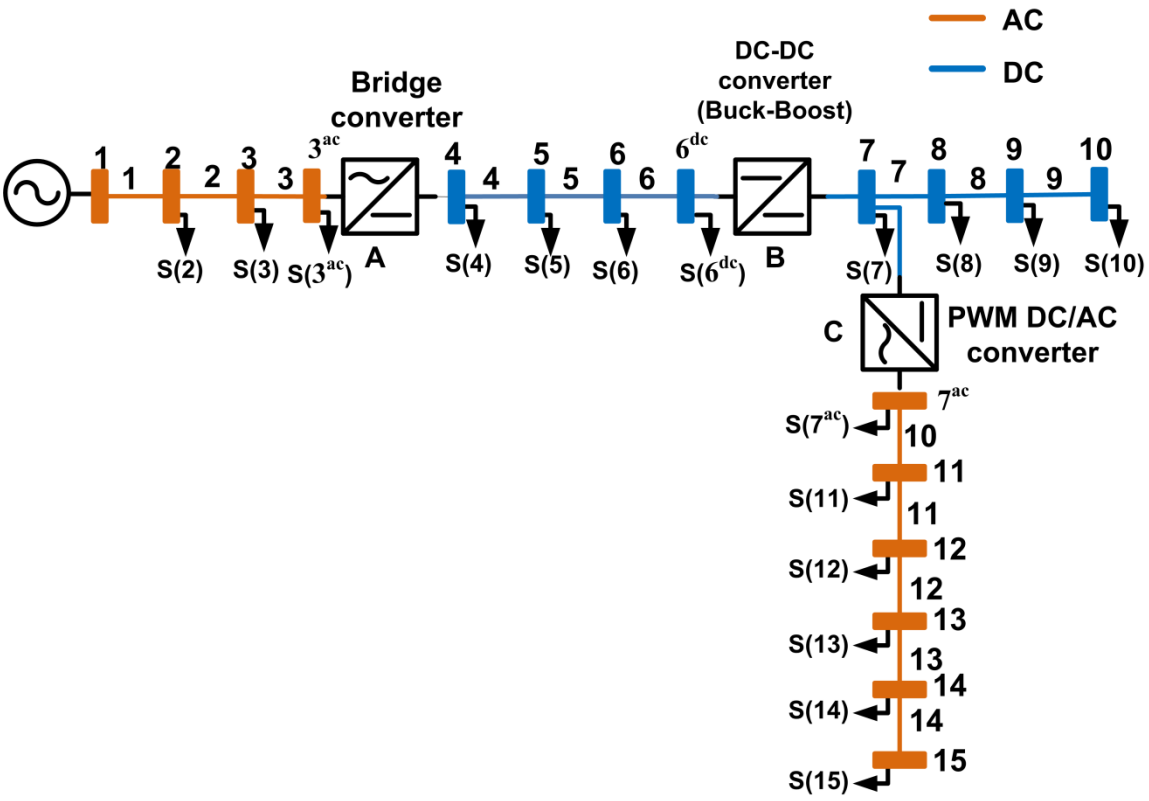

Fig. 4.20*:* Schematic diagram of a hypothetical 15 bus AC-DC distribution network.

In this particular network, one line commutated converter is connected between buses 3^{ac} and 4. Minimum firing angle limit for this converter is 0°, and its commutation reactance is

neglected. The voltage at bus 4 is controlled at 0.9750 pu using three phase bridge converter. The DC-DC buck boost converter connected between buses 6^{dc} and 7 and is being controlled to maintain the constant voltage of the magnitude 0.9801 pu at bus 7. The AC/DC PWM converter connected between buses 7 and 7^{ac} is being controlled to maintain the constant voltage of the magnitude 0.9701 pu at bus 7^{ac}. Regarding the bus categorizations, bus 1 represents a slack bus, bus 5 is P type bus (generator), bus 10 is generator bus modelled as V^{dc} bus, bus 15 is generator bus modelled as PV bus and remaining buses are load buses. The data of various types of converters are provided in Table 4.10. Base MVA=100, Base voltage= 12.66kV (AC side) = 17.09 kV (DC side). All converters are supposed to be working at 100% efficiency. (Tolerance-10^{-6})

Table 4.8: Data of hypothetical 10 bus system shown in Fig. 4.18

BN	SN	RN	Impedance	Load Data (S(RN)) (kVA/kW)
1	1	2	0.84111+0.82271i	44.1+44.98i
2	2	3	0.84111+0.82271i	44.1+44.98i
3	3	3^{ac}	0.84111+0.82271i	0
-	3^{ac}	4	LCC Converter	264.6
4	4	5	1.6822	132.3
5	5	6	1.6822	44.1
6	6	6^{dc}	1.6822	0
-	6^{dc}	7	DC-DC boost converter	44.1
7	7	8	1.6822	44.1
8	8	9	1.6822	44.1
9	9	10	1.6822	44.1
-	7	7^{ac}	DC/AC PWM converter	0
10	7^{ac}	11	0.84111+0.82271i	44.1+44.98i
11	11	12	0.84111+0.82271i	44.1+44.98i
12	12	13	0.84111+0.82271i	132.3 +134.96i
13	13	14	0.84111+0.82271i	88.20+89.97i
14	14	15	0.84111+0.82271i	88.20+89.97i

Table 4.9: Characteristics of controlled generators

Generator Number and Types	Bus Location	Real Power (kW)		Injected Reactive Power (kVAr)		Voltage (pu)
		Max.	Min.	Max.	Min.	
G1 (P)	5	60	60	-	-	-
G2 (V^{dc})	10	500	50	-	-	0.9797
G4(PV)	15	100	100	20	125	0.9600

Table 4.10: Characteristics of converters

Converter Types	Located Between Buses	Control Strategy	Control Limit
3-Φ Full Bridge Converter	3^{ac} & 4	Constant DC Voltage	$\alpha(\min)=7^0$ $\alpha(\max)=18^0$
DC-DC Converter	6^{dc} & 7	Constant Voltage	$D(\min)=0.1$ $D(\max)=0.7$
PWM DC/AC Converter	7 & 7^{ac}	Constant voltage	MI(min)=0.5 MI(max)=1

Table 4.11: Voltage profile for hypothetical 15 bus AC-DC distribution system (without DG).

Bus Number	Voltage Magnitude (pu)			Phase (Radian)		
	PM	BIBC	PSCAD	PM	BIBC	PSCAD
1	1.0000	1.0000	1.0000	0.0000	0.0000	0.0000
2	0.9929	0.9928	0.9929	-0.0047	-0.0046	-0.0049
3	0.9864	0.9863	0.9865	-0.0095	-0.0097	-0.0098
3^{ac}	0.9803	0.9801	0.9804	-0.0144	-0.0146	-0.0147
4	0.9750	0.9750	0.9751	-	-	
5	0.9705	0.9704	0.9707	-	-	
6	0.9668	0.9667	0.9669	-	-	
6^{dc}	0.9633	0.9632	0.9633	-	-	
7	0.9801	0.9801	0.9801	-	-	
8	0.9793	0.9792	0.9793	-	-	
9	0.9787	0.9787	0.9788	-	-	
10	0.9785	0.9784	0.9785	-	-	
7^{ac}	0.9701	0.9701	0.9701	-0.0102	-0.0102	-0.0102
11	0.9658	0.9659	0.9658	-0.0101	-0.0101	-0.0101
12	0.9619	0.9620	0.9619	-0.0100	-0.0100	-0.0100
13	0.9585	0.9586	0.9587	-0.0099	-0.0099	-0.0099
14	0.9566	0.9567	0.9567	-0.0099	-0.0099	-0.0099
15	0.9556	0.9557	0.9558	-0.0098	-0.0098	-0.0098

The load flow results for the aforementioned distribution system (without DGs) using proposed algorithm, the BIBC method and the load flow solution provided by PSCAD software are explicitly presented in Table 4.11. Based on the results acquired, the maximum difference between the bus voltages calculated by the proposed load flow method and the load flow model simulated in PSCAD is 0.0003. The maximum difference between the bus voltages calculated by the proposed load flow method and the BIBC load flow model is 0.0002. The execution time for the proposed method and BIBC method is 30ms and 250ms respectively. The comparison of the results obtained from BIBC method, PSCAD software

and the proposed algorithm demonstrates the effectiveness and accuracy of the method developed.

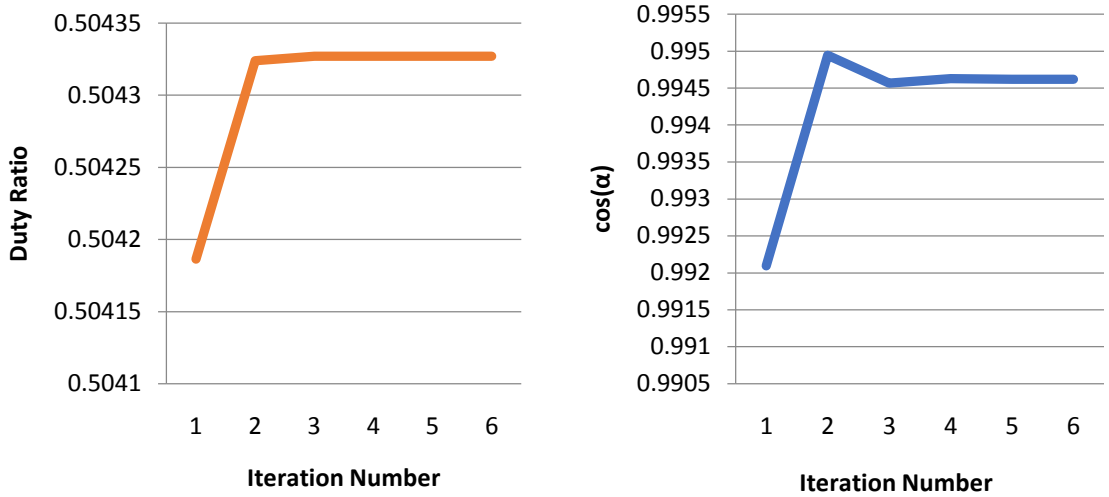

(a) (b)

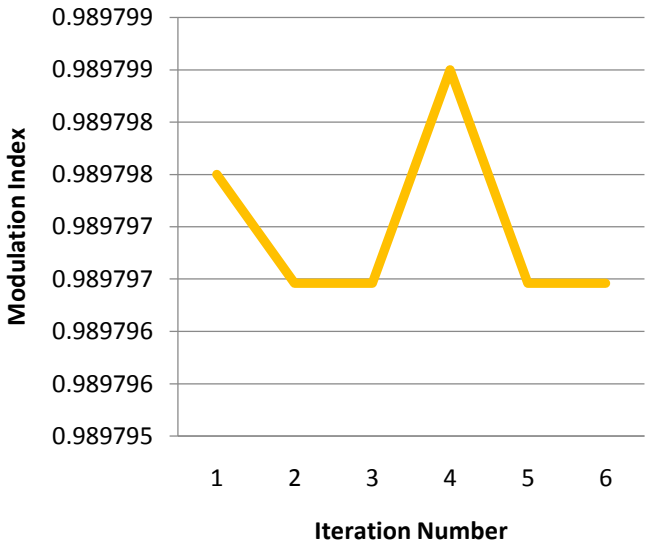

(c)

Fig. 4.21: Variation of control variables of the converters in the network (Fig.4.20) without DG during load flow iteration (a) Changes in the duty ratio for converter B, (b) Changes in the cosine of commutation angle of the converter A, (c) Changes in the duty ratio of the converter C.

For the AC-DC distribution system shown in Fig. 4.20 (without DGs), changes in the duty cycle of the DC/DC buck boost converter, commutation angle of the rectifier and modulation index of PWM DC/AC converter during the load flow iterations of the proposed

method are shown in Fig. 4.21.

The load flow results for the aforementioned distribution system (with DGs) using proposed algorithm and the load flow solution provided by PSCAD software are explicitly presented in Table 4.12 and Table 4.13. Based on the results acquired, the maximum difference between the bus voltages calculated by the proposed load flow method and the load flow model simulated in PSCAD is 0.0001. The comparison of the results obtained from the proposed algorithm and those produced by the PSCAD software therefore demonstrates the effectiveness and accuracy of the method developed.

Table 4.12: Voltage profile for hypothetical 15 bus AC-DC distribution system (with DG).

Bus Number	Voltage Magnitude (pu)		Phase (Radian)	
	PM	PSCAD	PM	PSCAD
1	1.0000	1.0000	0.0000	0.0000
2	0.9942	0.9943	-0.0035	-0.0034
3	0.9889	0.9889	-0.0071	-0.0071
3^{ac}	0.9841	0.9840	-0.0107	-0.0107
4	0.9750	0.9750	-	-
5	0.9719	0.9719	-	-
6	0.9691	0.9690	-	-
6^{dc}	0.9667	0.9666	-	-
7	0.9801	0.9801	-	-
8	0.9797	0.9797	-	-
9	0.9796	0.9796	-	-
10	0.9797	0.9797	-	-
7^{ac}	0.9701	0.9701	-0.0075	-0.0075
11	0.9666	0.9665	-0.0072	-0.0072
12	0.9637	0.9636	-0.0069	-0.0069
13	0.9612	0.9611	-0.0066	-0.0066
14	0.9601	0.9601	-0.0063	-0.0063
15	0.9600	0.9600	-0.0061	-0.0061

Table 4.13: Distributed generators load flow results

Generator Number and Types	Injected Real Power (kW)		Injected Reactive Power (kVAr)		Voltage (pu)
	PM	PSCAD	PM	PSCAD	
G1 (P)	60	60	-	-	-
G2 (V^{dc})	65.29	65.28	-	-	0.9797
G4(PV)	100	100	59.84	59.84	0.9600

For the AC-DC distribution system shown in Fig. 4.20 (with DGs), changes in the duty cycle of the DC/DC buck boost converter, cos(α) of the rectifier and modulation index of

PWM DC/AC converter during the load flow iterations of the proposed method are shown in Fig. 4.22.

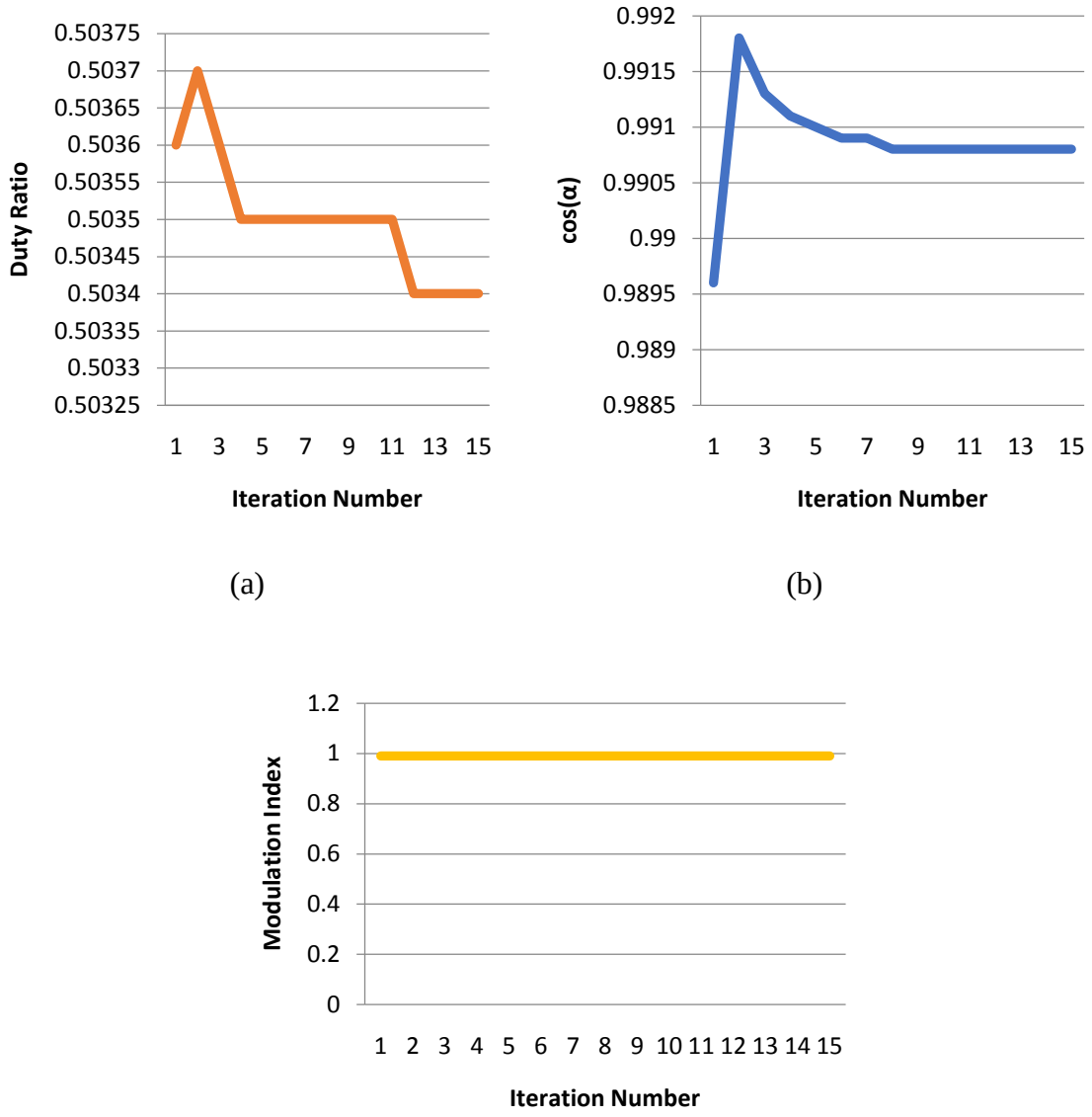

Fig. 4.22: Variation of control variables of the converters in the network (Fig. 4.20) with DG during load flow iteration (a) Changes in the duty ratio for converter B, (b) Changes in the cos(α) of the converter A., (c) Changes in the duty ratio of the converter C.

To assess the effect of R/X ratio variation on the convergence characteristics, the proposed methodology has been tested for wide range of R/X ratios of lines belonging to the

IEEE-33 bus meshed distribution network (with distributed generations). The test result in Fig. 4.23 justify the convergence ability of the proposed method.

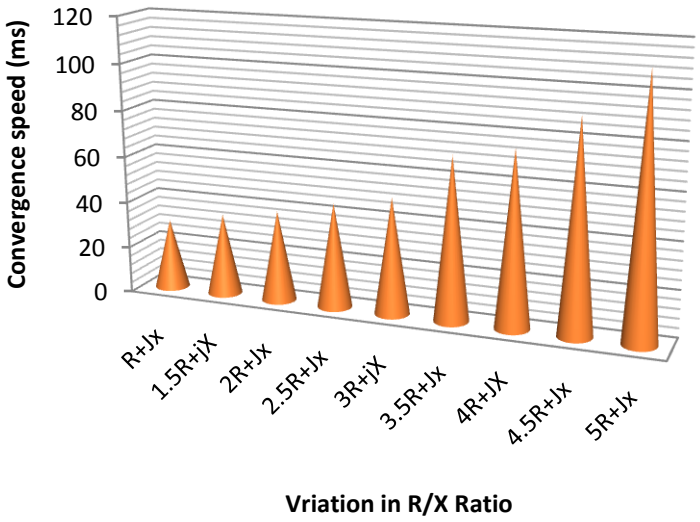

Fig. 4.23: Variation in R/X ratio vs convergence speed graph.

4.5 Conclusion

In this chapter, a power flow algorithm for AC-DC radial distribution network has been proposed. The load flow algorithm developed in chapter 1 and chapter 2 has been modified in a manner such that it will provide the load flow solution of AC-DC radial distribution network in the presence of distributed generations. For bridging the gap between an AC distribution system and a DC distribution system, a per unit model of various power system converters (taking care of the enactment of control scheme) has been introduced. The advantage of introduced converter model enables us to perform the load flow of AC-DC distribution system in per-units. The various operating modes of power converters have also been considered to demonstrate the effectiveness of the proposed method. The sensitivity matrix/ breakpoint matrix has been developed for obtaining the load flow solution of AC-DC distribution network with PV and V^{dc} bus. The simple algebraic operation and efficient search technique enables the proposed method to be computationally efficient. Due to unavailability of a standard AC-DC distribution system at present, hypothetical test cases (10

bus and 15 bus AC-DC distribution system) have been considered and the performance of the AC-DC load flow algorithm is thoroughly investigated. The effectiveness of the proposed model has been verified against the load flow solution produced by PSCAD and BIBC method. The test results demonstrate that the proposed load flow algorithm can provide precise solution while also offering the flexibility and speed required for online applications. For checking the robustness of the method, the system R/X ratio has been varied and convergence ability of the proposed load flow algorithm has been tested. This load flow method converges for a wide range of R/X ratio. However, the convergence speed will decrease with the increase in R/X ratio.

Chapter-5

Load Flow Algorithm for Meshed AC-DC Distribution System with Distributed Generations

In this chapter, the power flow solution algorithm for meshed AC-DC distribution network in the presence of distributed generations has been developed. The concept developed in previous chapters (chapter 2, chapter 3 and chapter 4) has been utilised in a manner such that it provides solution to load flow problem of AC-DC meshed distribution systems by making use of proposed per-unit equivalent model of PWM and other power converters (taking care of enactment of control objectives). Various models of distributed generations (P, PQ, PV and V^{dc}) are also incorporated in the proposed load flow study. The proposed charging algorithm has been tested on several hypothetical AC-DC distribution systems to examine the accuracy and efficacy of the proposed AC-DC load flow algorithm.

5.1 Introduction

Some AC/DC distribution lines feeding high-density load areas contain loops created by closing normally open tie-lines. Such AC-DC distribution system is termed as weakly meshed or meshed network. The load flow solution for such AC-DC systems is a challenging task as converters may exist in those loops. The applicability of direct load flow method [69] is only limited to radial structure of AC-DC distribution network. An advanced unified AC-DC load flow procedure have overcome the disadvantages associated with the direct load flow or BIBC method. The advanced unified AC-DC load flow procedure has implemented an AC-DC power flow model in a general algebraic model system (GAMS) using reduced gradient optimization technique [36]. In this solution method, AC-DC power flow equations have been solved simultaneously considering various hybrid configurations. However, it has certain limitations:

(a) Prohibit applications in problems where the intrinsic intransigence of modelling language does not permit full utilization of the power system properties. For example, the aforementioned method has only utilized AC-DC VSCs model with constant modulation

ratio. The other operating modes (viz. constant power mode, constant voltage control at the output of converter terminal etc.) have been ignored.

(b) The other existing converters such as three phase bridge converter and DC-DC converter have not been considered in the mentioned generic AC-DC power flow solution method.

(c) Blind trust on commercial solvers may not be a good idea since they are completely devoid of special power system properties.

With a view to prevail over the shortcomings of the existing methods, a direct load flow algorithm based on BFS method is proposed in this chapter for AC-DC meshed distribution network with distributed generations. The notion of load flow algorithm developed in previous chapters (chapter 2, chapter 3 and chapter 4) has been utilised in a manner such that it provides the load flow solution of meshed AC-DC distribution system. Generally, if there exist a mesh connection in the AC-DC distribution network then for such system loop or mesh breakpoint injection calculations are required for the conversion of meshed network into radial network. In this chapter, a loop breakpoint matrix has been formulated to compute loop breakpoint injection of meshed distribution network. Once the loop breakpoint injections are computed, then meshed network can be converted into its equivalent radial form by suitably injecting the breakpoint injections on both side of the loop breakpoint. The DGs modelled as PQ bus and P bus is included in the proposed load flow algorithm by considering injection by the DG as the negative load. The power injected by the DG need to be reflected in the LBg matrix of the distribution network. In the case of weakly meshed distribution network with PV or V^{dc} type distributed generations, the loop breakpoint injections and PV breakpoint injections have been calculated simultaneously. The net injections is reflected in the LBg or LCg matrix of the distribution network. Note that except for some modifications needed to be done for the LBg or LCg matrices, the solution techniques developed in chapter 4 require no modification.

5.2 Load Flow Solution Methodology for AC-DC Meshed Distribution Systems

A technique for converting meshed network to radial network has been developed and utilized to achieve the load-flow solution of meshed distribution systems. The load-flow

solution of the meshed network can be achieved in the same manner as radial distribution systems (after converting to its equivalent radial network).

There can exist three kinds of meshes in an AC-DC distribution network.

(a) Mesh consisting of only AC buses in an AC sub-region is called as type 1 mesh.

(b) Mesh consisting of only DC buses in a DC sub-region is called as type 2 mesh.

(c) Mesh consisting of both AC and DC buses or only DC buses with different voltage levels is called as type 3 mesh.

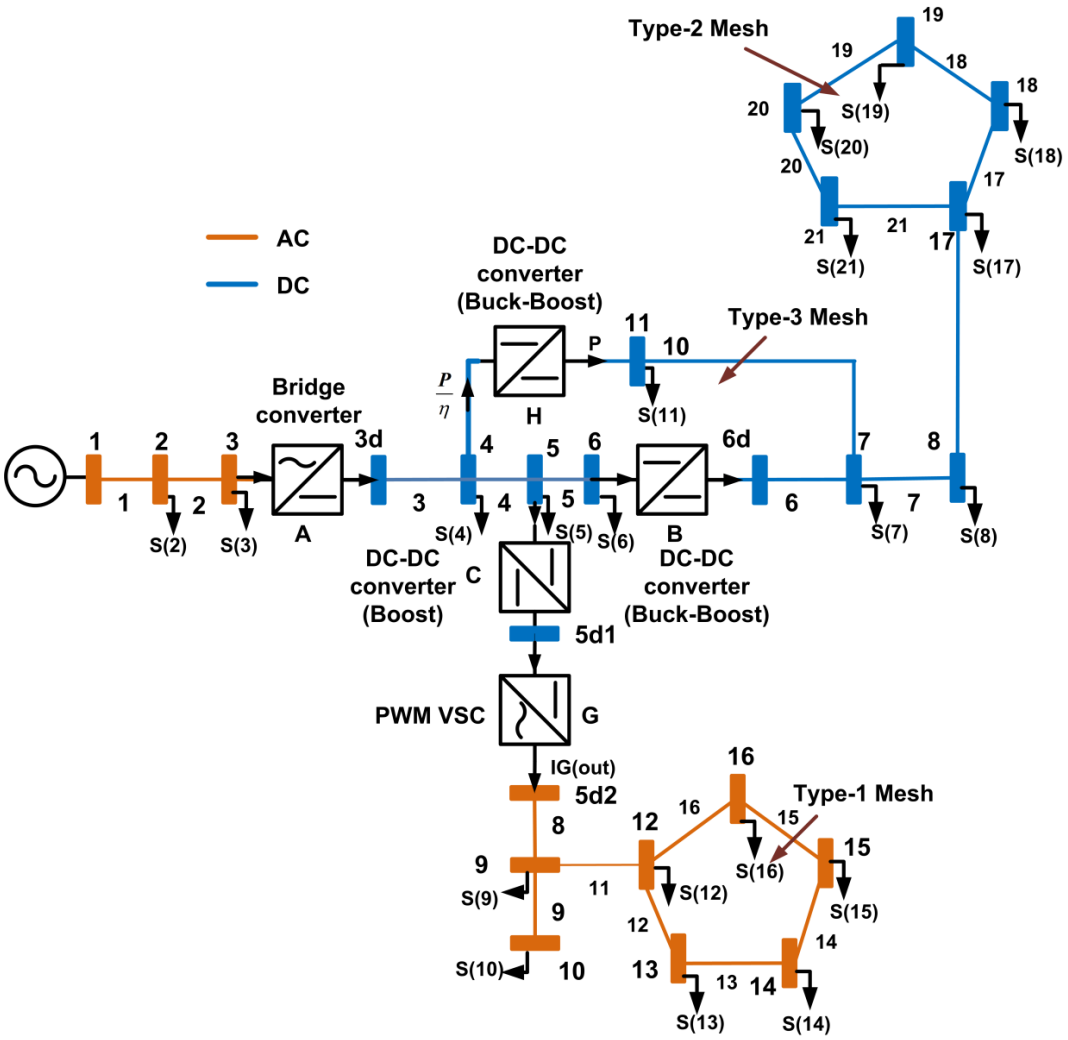

Fig. 5.1: Single line diagram of a meshed AC-DC distribution system.

These three mesh configurations are clearly illustrated in Fig. 5.1. The procedure for calculating breakpoint injected current/injected power will be different for the different meshed configurations. Following are the steps required for converting meshed network to radial network:

Step 1: If there exists a type-1 mesh (a mesh with only AC buses) in an AC sub-network, this mesh will be opened from any line section of type 1 mesh, and then sensitivity matrix is formulated to calculate the loop breakpoint injections. In the AC-DC distribution network, AC sub-regions are connected via DC links, therefore they are independent from each other. Hence, corresponding element in the sensitivity matrix will be zero. For each AC sub-network which contains a type-1 mesh, only one sensitivity matrix is required.

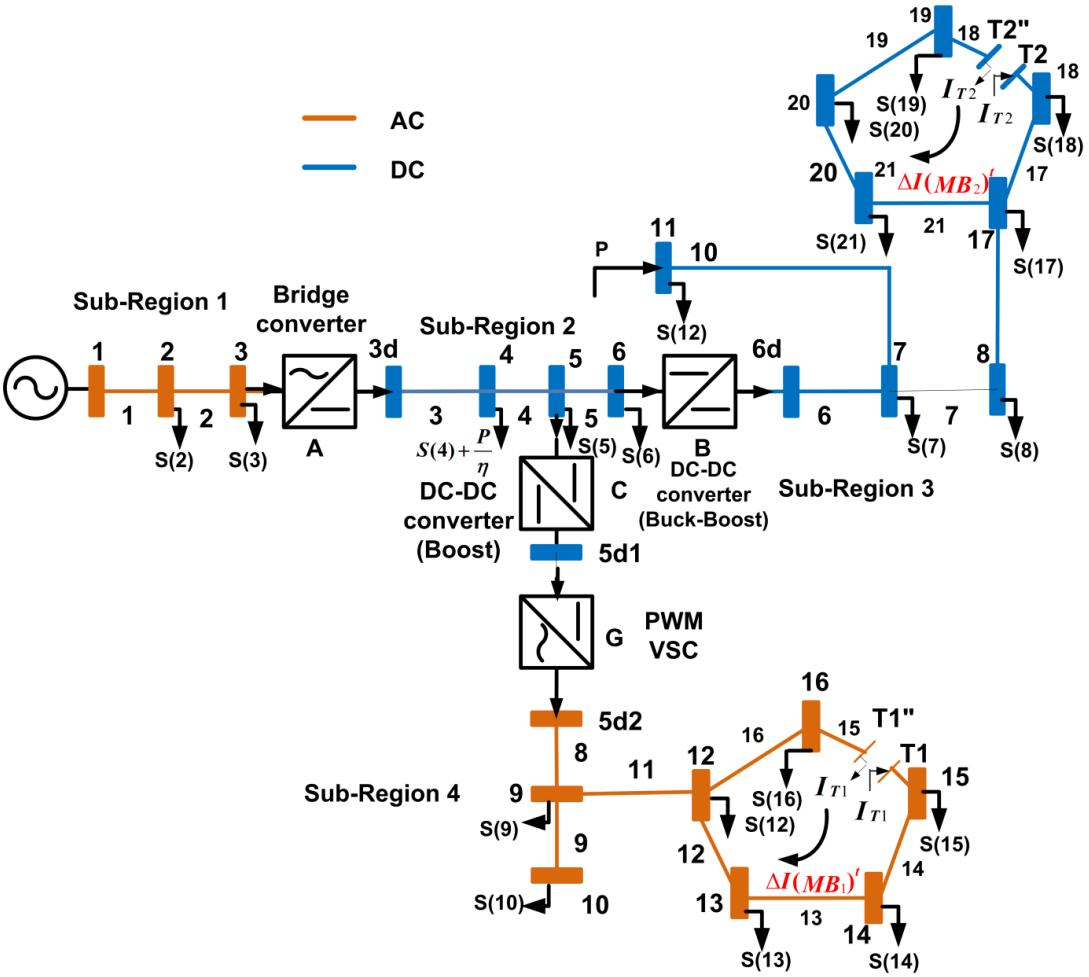

Fig. 5.2: Equivalent radial system of Fig. 5.1 for loads beyond branch matrix calculation.

In the Fig.5.1, type-1 mesh is present and hence loop breakpoint matrix needs to be formulated. For this purpose, split any branch belonging to that mesh in two parts and two additional nodes are created (say T1 and T1"-as evident from Fig. 5.2). In the sub-sequent step, calculate the loop breakpoint injections.

For the system shown in Fig. 5.1, the loop breakpoint equation for type 1 mesh can be written as:

$$\left[Z(12)+Z(13)+Z(14)+Z(15)+Z(16)\right]\times\left[\Delta I(MB_1)^t\right]=\left[V(MB_1'')^t-V(MB_1)^t\right] \tag{5.1}$$

Representing the above equation in rectangular coordinates:

$$\begin{aligned}\left[\left[R(12)+R(13)+R(14)+R(15)+R(16)\right]+j\left[X(12)+X(13)+X(14)+X(15)+X(16)\right]\right]\\ \times\left[\Delta I^r(MB_1)^t-j\Delta I^q(MB_1)^t\right]=\left[\Delta V(MB_1)^t+j\Delta\delta(MB_1)^t\right]\end{aligned} \tag{5.2}$$

On further simplifying the above equation (5.2), the resulting equation will be:

$$\begin{aligned}&\begin{bmatrix}\left[X(12)+X(13)+X(14)+X(15)+X(16)\right] & \left[R(12)+R(13)+R(14)+R(15)+R(16)\right]\\ -\left[R(12)+R(13)+R(14)+R(15)+R(16)\right] & \left[X(12)+X(13)+X(14)+X(15)+X(16)\right]\end{bmatrix}\\ &\times\begin{bmatrix}\Delta I^q(MB_1)^t\\ \Delta I^r(MB_1)^t\end{bmatrix}=\begin{bmatrix}\Delta V(MB_1)^t\\ \Delta\delta(MB_1)^t\end{bmatrix}\end{aligned} \tag{5.3}$$

The total breakpoint injections in term of currents at the beginning of iterations *t* is given by:

$$TI(MB_1)^t=\sum_{x=1}^{t-1}\Delta I(MB_1)^x+\Delta I(MB_1)^t \tag{5.4}$$

where, $$\Delta I(MB_1)^t=\Delta I^r(MB_1)^t-j\Delta I^q(MB_1)^t$$

The equation (5.3) can also be represented as:

$$\begin{bmatrix}X & R\\ -R & X\end{bmatrix}\times\begin{bmatrix}\Delta I^q\\ \Delta I^r\end{bmatrix}=\begin{bmatrix}\Delta V\\ \Delta\delta\end{bmatrix} \tag{5.5}$$

The diagonal elements in sub-matrices X and R are the self reactance and self resistance of the breakpoints respectively. The off-diagonal elements in sub-matrices X and R denote the mutual reactance and resistance respectively of two break points (of the same sub-region).

The above equation for calculating mesh breakpoint current injection can be modified in terms of loop breakpoint complex power injection. With the assumption of all bus voltages being close to 1.0 p.u. and the phase angles small, the following equation holds:

$$\Delta I^r(MB_1)^t-j\Delta I^q(MB_1)^t=\Delta P(MB_1)^t-j\Delta Q(MB_1)^t=\left(\Delta S(MB_1)^t\right)^* \tag{5.6}$$

Using equation (5.5) in equation (5.3), the resulting equation will be:

$$\begin{aligned}&\begin{bmatrix}\left[X(12)+X(13)+X(14)+X(15)+X(16)\right] & \left[R(12)+R(13)+R(14)+R(15)+R(16)\right]\\ -\left[R(12)+R(13)+R(14)+R(15)+R(16)\right] & \left[X(12)+X(13)+X(14)+X(15)+X(16)\right]\end{bmatrix}\\ &\times\begin{bmatrix}\Delta Q(MB_1)^t\\ \Delta P(MB_1)^t\end{bmatrix}=\begin{bmatrix}\Delta V(MB_1)^t\\ \Delta\delta(MB_1)^t\end{bmatrix}\end{aligned} \tag{5.7}$$

The equation (5.7) can also be represented as:

$$\begin{bmatrix} X & R \\ -R & X \end{bmatrix} \times \begin{bmatrix} \Delta Q \\ \Delta P \end{bmatrix} = \begin{bmatrix} \Delta V \\ \Delta \delta \end{bmatrix} \tag{5.8}$$

where, $\Delta V + j\Delta\delta = \Delta V(MB_1)^t + j\Delta\delta(MB_1)^t = V(T1")^t - V(T1)^t$ (5.9)

$V(T1)^t$=Voltage at node T1 in the beginning of iteration number *t*.

$V(T1")^t$= Voltage at node T1" in the beginning of iteration number *t*.

X=[X(12)+X(13)+X(14)+X(15)+X(16)]

R= [R(12)+R(13)+R(14)+R(15)+R(16)]

All relevant matrices required for calculating loop breakpoint injections have been explicitly detailed above. The type-1 mesh is converted into radial network and corresponding injections are being inducted to the dummy nodes (T1 and T1") as shown in Fig. 5.2. The corresponding injections are reflected in LB_g matrices (as per injected quantity) of the sub-regions to which mesh belongs.

The total breakpoint injections in terms of real and reactive power at the beginning of iterations *t* is given by:

$$TP(MB_1)^t = \sum_{x=1}^{t-1} \Delta P(MB_1)^x + \Delta P(MB_1)^t \tag{5.10}$$

$$TQ(MB_1)^t = \sum_{x=1}^{t-1} \Delta Q(MB_1)^x + \Delta Q(MB_1)^t \tag{5.11}$$

Step 2: If there exists a type-2 mesh (a mesh with only DC buses) in a DC sub-network, this mesh will be opened from any line section of type 1 mesh, and then sensitivity matrix or loop breakpoint matrix is formulated to calculate the loop breakpoint injections.

In the Fig. 5.1, type-2 mesh is present and hence loop breakpoint matrix needs to be formulated. For this purpose, split any branch belonging to that mesh in two parts and two additional nodes are created (say T2 and T2"-as evident from Fig. 5.2). In the sub-sequent step, calculate the loop breakpoint injections.

For the system shown in Fig. 5.1, the loop breakpoint equation for type 2 mesh can be written as:

$$\left[R(17)+R(18)+R(19)+R(20)+R(21)\right] \times \left[\Delta I(MB_2)^t\right] = \left[V(MB_2")^t - V(MB_2)^t\right] \tag{5.12}$$

$$\left[R(17)+R(18)+R(19)+R(20)+R(21)\right] \times \left[\Delta I^r(MB_2)^t - j\Delta I^q(MB_2)^t\right] = \left[\Delta V(MB_2)^t + j\Delta\delta(MB_2)^t\right] \tag{5.13}$$

where,

$$\Delta I^{q}(MB_2)^{t} = 0 \tag{5.14}$$

$$\Delta \delta(MB_2)^{t} = 0 \tag{5.15}$$

Using equations (5.14) and (5.15) in equation (5.13), the resulting equation will be:

$$\left[R(17)+R(18)+R(19)+R(20)+R(21)\right]\times\left[\Delta I^{r}(MB_2)^{t}\right]=\left[\Delta V(MB_2)^{t}\right] \tag{5.16}$$

The total breakpoint injections in term of currents at the beginning of iterations *t* is given by:

$$TI(MB_2)^{t} = \sum_{x=1}^{t-1}\Delta I(MB_2)^{x} + \Delta I(MB_2)^{t} \tag{5.17}$$

where,
$$\Delta I(MB_2)^{t} = \Delta I^{r}(MB_2)^{t} \tag{5.18}$$

The equation (5.13) can also be represented as:

$$\begin{bmatrix} X & R \\ -R & X \end{bmatrix}\times\begin{bmatrix} \Delta I^{q} \\ \Delta I^{r} \end{bmatrix}=\begin{bmatrix} \Delta V \\ \Delta \delta \end{bmatrix} \tag{5.19}$$

In this case,

$$X=0 \tag{5.20}$$

$$\Delta I^{q}=\left[\Delta I^{q}(MB_2)^{t}\right]=0 \tag{5.21}$$

$$\Delta \delta=\left[\Delta \delta(MB_2)^{t}\right]=0 \tag{5.22}$$

$$\Delta V + j\Delta\delta = \left[\Delta V(MB_2)^{t}\right] = V(T2")^{t}\text{-}V(T2)^{t} \tag{5.23}$$

$V(T2)^{t}$=Voltage at node T2 in the beginning of iteration number *t*.

$V(T2")^{t}$= Voltage at node T2" in the beginning of iteration number *t*.

On simplifying equation (5.19), the resulting will be:

$$\begin{bmatrix} 0 & R \\ -R & 0 \end{bmatrix}\times\begin{bmatrix} 0 \\ \Delta I^{r} \end{bmatrix}=\begin{bmatrix} \Delta V \\ 0 \end{bmatrix} \tag{5.24}$$

The above equation for calculating mesh breakpoint current injection can be modified in terms of loop breakpoint complex power injection. With the assumption of all bus voltages being close to 1.0 p.u., the following equation holds:

$$\Delta I^{r}(MB_2)^{t} - j\Delta I^{q}(MB_2)^{t} = \Delta P(MB_2)^{t} - j\Delta Q(MB_2)^{t} = \left(\Delta S(MB_2)^{t}\right)^{*} \tag{5.25}$$

where,

$$\Delta I^{q} = \left[\Delta I^{q} (MB_2)^{t} \right] = \Delta Q (MB_2)^{t} = 0 \tag{5.26}$$

Using equation (5.26) in equation (5.25), the resulting equation will be:

$$\Delta I^{r} (MB_2)^{t} = \Delta P (MB_2)^{t} \tag{5.27}$$

Using equation (5.27) in equation (5.16), the resulting equation will be:

$$\left[\left[R(17) + R(18) + R(19) + R(20) + R(21) \right] \right] \times \left[\Delta P (MB_2)^{t} \right] = \left[\Delta V (MB_2)^{t} \right] \tag{5.28}$$

The equation (5.28) can also be represented as:

$$\begin{bmatrix} 0 & R \\ -R & 0 \end{bmatrix} \times \begin{bmatrix} 0 \\ \Delta P \end{bmatrix} = \begin{bmatrix} \Delta V \\ 0 \end{bmatrix} \tag{5.29}$$

All relevant matrices required for calculating loop breakpoint injections have been explicitly detailed above. The type-2 mesh is converted into radial network and corresponding injections are being inducted to the dummy nodes (T2 and T2") as shown in Fig. 5.2. The corresponding injection are reflected in LB_g / LC_g matrix (as per injected quantity) of the sub-region to which type 2 mesh belongs.

The total breakpoint injections in terms of real power at the beginning of iterations *t* is given by:

$$TP(MB_2)^{t} = \sum_{x=1}^{t-1} \Delta P (MB_2)^{x} + \Delta P (MB_2)^{t} \tag{5.30}$$

Step 3: In this step, presence of a type-3 mesh is examined. If a type-3 mesh is present in the AC-DC network, one of the converter interface within the mesh or line subsequent to the converter is opened. Note that the selection of converter or line selection depends on the converter control scheme. In a constant power/ current scheme, a type-3 mesh is opened through the converter and the specified power/ current is injected on both sides of the converter terminal. The converter control limits must be verified after calculating terminal voltages in the forward phase.

In the Fig. 5.2, type 3 mesh is present in the AC-DC distribution network. In this mesh, the converters H and B are supposed to be operating in constant power mode and constant voltage control mode respectively. As per the procedure of converting the type 3 mesh into radial, the converter H is opened and the specified power (P) and (P/η) is injected on the both sides of converter terminal (as evident from Fig. 5.2). Once, the meshed network is converted to radial network, the relevant matrices formulation are carried out in same manner as the

radial distribution network. The corresponding injection are reflected in LB_g matrix of the sub-regions to which type-3 mesh belongs.

If the converters H and B are operating at a constant duty ratio say D, then selection of breakpoint will be in different manner. In this case, split any branch belonging to that mesh in two parts and two additional nodes are created (say T3 and T3"-as evident from Fig. 5.3). In the sub-sequent step, calculate the loop breakpoint injections.

Assumption: All converters are supposed to working at its 100% efficiency.

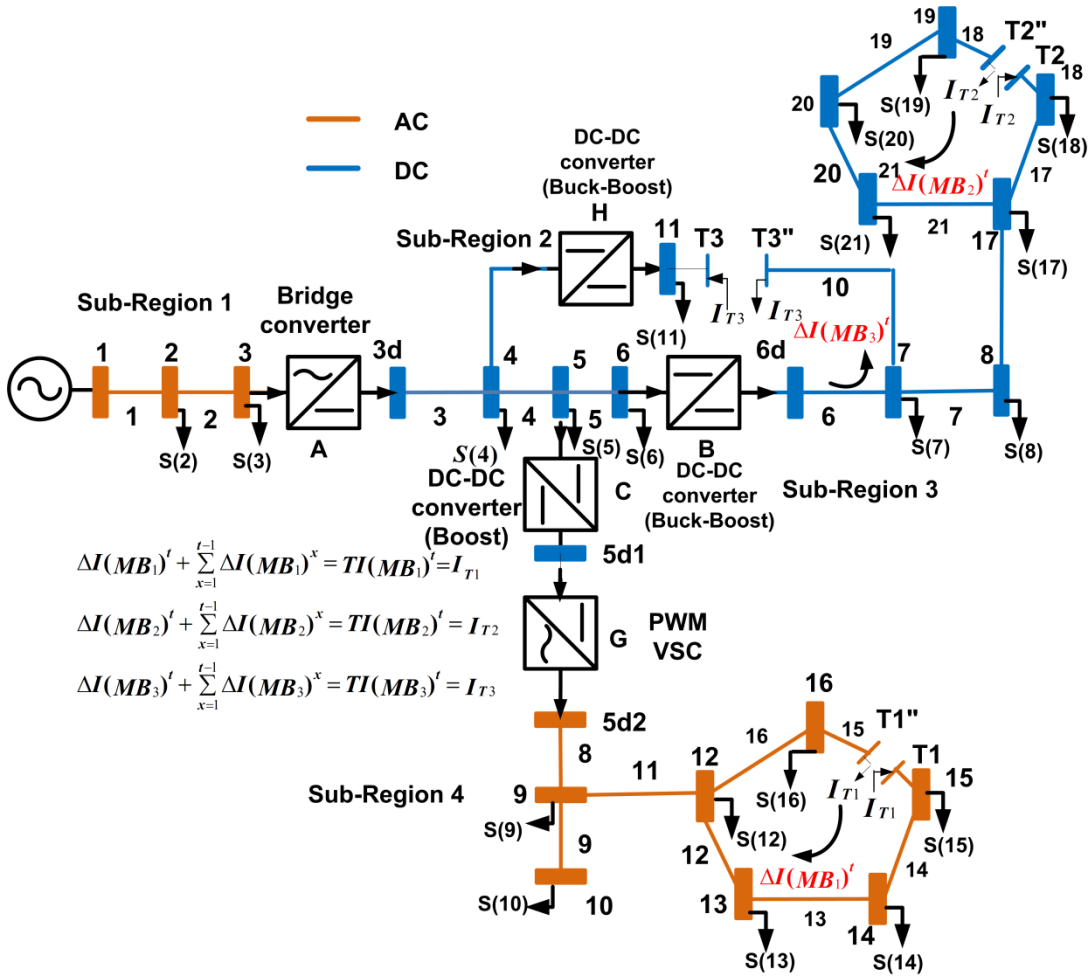

Fig. 5.3: Equivalent radial system of Fig. 5.1 for loads beyond branch matrix calculation.

For the system shown in Fig. 5.3, the loop breakpoint equation for type 3 mesh can be written as:

$$\left[R(6)+R(10)+\left((R(4)+R(5))\times\left(\frac{D}{1-D}\right)^2\right)\right]\times\left[\Delta I(MB_3)^t\right]=\left[V(MB_3")^t-V(MB_3)^t\right] \quad (5.31)$$

Equation (5.28) can also be represented as:

$$\left[R(6)+R(10)+\left((R(4)+R(5))\times\left(\frac{D}{1-D}\right)^2\right)\right] \times\left[\Delta I^r(MB_3)^t - j\Delta I^q(MB_3)^t\right]=\left[\Delta V(MB_3)^t + j\Delta\delta(MB_3)^t\right] \quad (5.32)$$

where,

$$\Delta I^q(MB_3)^t = 0 \quad (5.33)$$

$$\Delta\delta(MB_3)^t = 0 \quad (5.34)$$

Using equations (5.33) and (5.34) in equation (5.32), the resulting equation will be:

$$\left[R(6)+R(10)+\left((R(4)+R(5))\times\left(\frac{D}{1-D}\right)^2\right)\right] \times\left[\Delta I^r(MB_3)^t\right]=\left[\Delta V(MB_3)^t\right] \quad (5.35)$$

The equation (5.32) can also be represented as:

$$\begin{bmatrix} X & R \\ -R & X \end{bmatrix}\times\begin{bmatrix}\Delta I^q \\ \Delta I^r\end{bmatrix}=\begin{bmatrix}\Delta V \\ \Delta\delta\end{bmatrix} \quad (5.36)$$

In this case,

$$X=0 \quad (5.37)$$

$$\Delta I^q=\left[\Delta I^q(MB_3)^t\right]=0 \quad (5.38)$$

$$\Delta\delta=\Delta\delta(MB_3)^t=0 \quad (5.39)$$

$$\Delta V + j\Delta\delta = \left[\Delta V(MB_3)^t\right] = V(T3")^t - V(T3)^t \quad (5.40)$$

$V(T3)^t$=Voltage at node T3 in the beginning of iteration number *t*.

$V(T3")^t$= Voltage at node T3" in the beginning of iteration number *t*.

On simplifying equation (5.36), the resulting will be:

$$\begin{bmatrix} 0 & R \\ -R & 0 \end{bmatrix}\times\begin{bmatrix}0 \\ \Delta I^r\end{bmatrix}=\begin{bmatrix}\Delta V \\ 0\end{bmatrix} \quad (5.40)$$

The total breakpoint injections in term of currents at the beginning of iterations *t* is given by:

$$TI(MB_3)^t=\sum_{x=1}^{t-1}\Delta I(MB_3)^x+\Delta I(MB_3)^t \quad (5.41)$$

where, $$\Delta I(MB_3)^t=\Delta I^r(MB_3)^t \quad (5.42)$$

The above equation for calculating mesh breakpoint current injection can be modified in terms of loop breakpoint complex power injection. With the assumption of all bus voltages

being close to 1.0 p.u., the following equation holds:

$$\Delta I^{r}(MB_3)^{t} - j\Delta I^{q}(MB_3)^{t} = \Delta P(MB_3)^{t} - j\Delta Q(MB_3)^{t} = \left(\Delta S(MB_3)^{t}\right)^{*} \tag{5.43}$$

where,

$$\Delta I^{q} = \left[\Delta I^{q}(MB_3)^{t}\right] = \Delta Q(MB_3)^{t} = 0 \tag{5.44}$$

Using equation (5.44) in equation (5.43), the resulting equation will be:

$$\Delta I^{r}(MB_3)^{t} = \Delta P(MB_3)^{t} \tag{5.45}$$

Using equation (5.45) in equation (5.35), the resulting equation will be:

$$\left[R(6)+R(10)+\left((R(4)+R(5))\times\left(\frac{D}{1-D}\right)^{2}\right)\right]\times\left[\Delta P(MB_3)^{t}\right]=\left[\Delta V(MB_3)^{t}\right] \tag{5.46}$$

The equation (5.46) can also be represented as:

$$\begin{bmatrix} 0 & R \\ -R & 0 \end{bmatrix}\times\begin{bmatrix} 0 \\ \Delta P \end{bmatrix}=\begin{bmatrix} \Delta V \\ 0 \end{bmatrix} \tag{5.47}$$

The total breakpoint injections in terms of real power at the beginning of iterations *t* is given by:

$$TP(MB_3)^{t} = \sum_{x=1}^{t-1}\Delta P(MB_3)^{x} + \Delta P(MB_3)^{t} \tag{5.48}$$

All relevant matrices required for calculating loop breakpoint injections have been explicitly detailed above. The type-3 mesh is converted into radial network and corresponding injections are being inducted to the dummy nodes (T3 and T3") as shown in Fig. 5.3. The corresponding injection are reflected in LB_g/LC_g matrix (as per injected quantity) of the sub-region to which type 2 mesh belongs.

If the converter has minimum firing angle or constant voltage or any other scheme (apart from constant power or current scheme), then any line section subsequent to the converter is opened. The equivalent injected current is now calculated by considering the voltages of the opened line terminals and its Thevenin resistance/impedance.

5.3 Load Flow Solution Methodology for AC-DC Meshed Distribution System with Distributed Generations

Consider a scenario in which PV and V^{dc} type buses/distributed generations exists in the meshed AC-DC distribution network. For such cases, loop breakpoint injections, PV

breakpoint injections and V^{dc} breakpoint injections need to be calculated simultaneously. This requires formulation of one common matrix called as common breakpoint matrix embedding the properties of loop breakpoint matrix and PV breakpoint matrix.

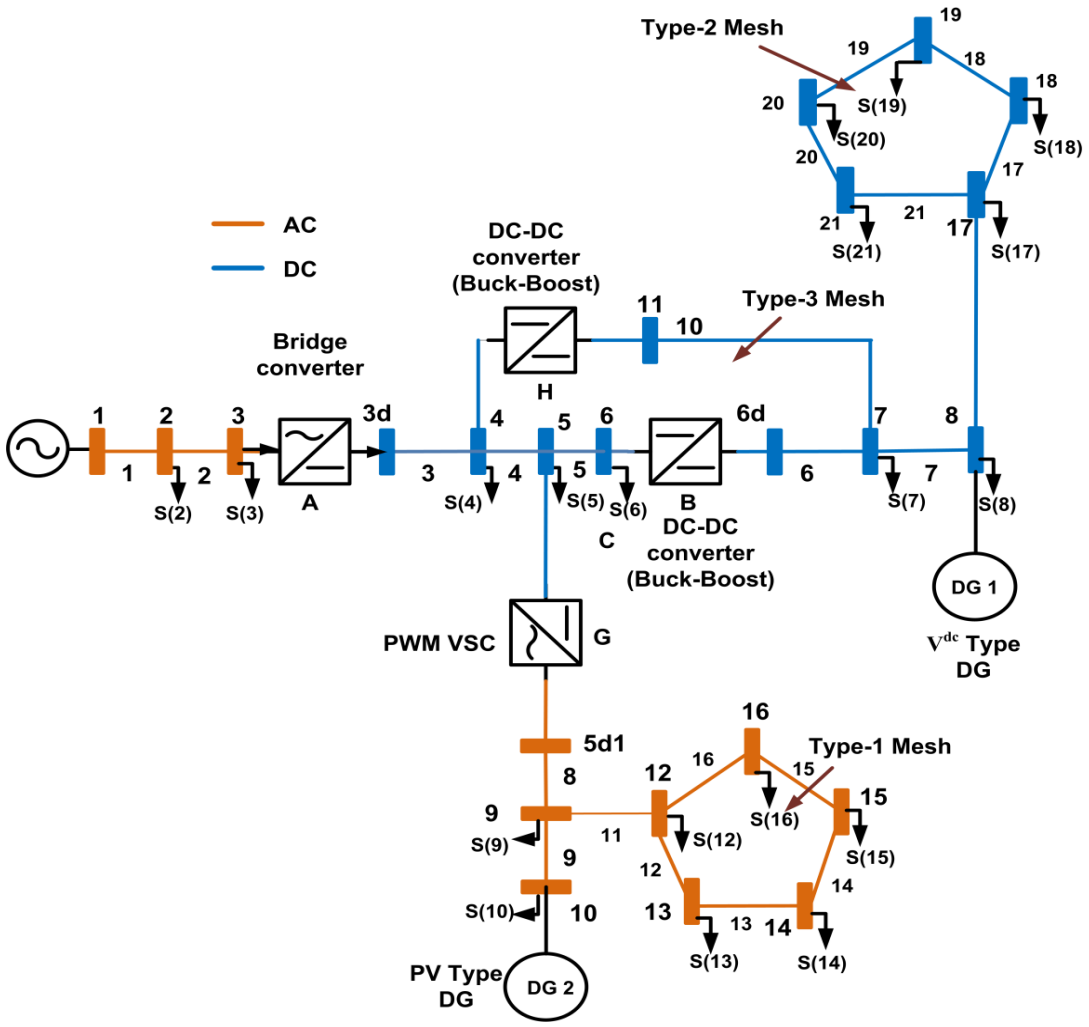

Fig. 5.4: Single line diagram of a meshed AC-DC distribution system with PV and V^{dc} buses.

For example, consider the AC-DC meshed distribution network in Fig. 5.4 in which there is existing a PV type bus/distributed generation at bus number 10 and a V^{dc} type bus/DG at bus number 8. Hence, loop breakpoint injections and PV breakpoint injections need to be calculated simultaneously. The equivalent diagram for calculating loop breakpoint injections, PV breakpoint injection and V^{dc} breakpoint injection simultaneously is depicted in Fig. 5.5.

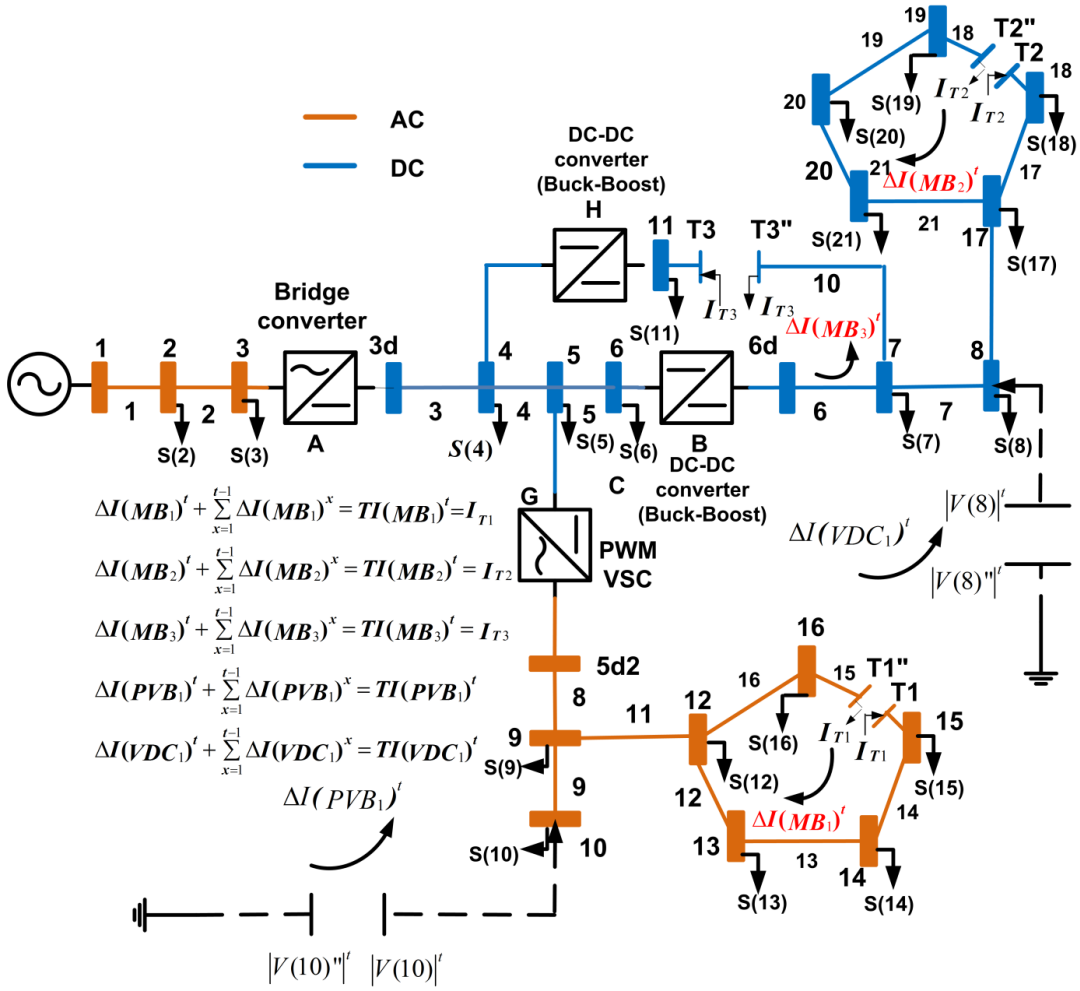

Fig. 5.5: Equivalent radial system of Fig. 5.4 for loads beyond branch &/or load current matrix calculation.

For the system shown in Fig. 5.5, the loop breakpoint equation, V^{dc} breakpoint equation and PV breakpoint equation is formulated as follows:

For type 1 mesh, the loop breakpoint equation is:

$$\left[Z(12)+Z(13)+Z(14)+Z(15)+Z(16)\right]\times\left[\Delta I(MB_1)^t\right]=\left[V(MB_1'')^t-V(MB_1)^t\right] \quad (5.49)$$

Equation (5.49) can also be represented as:

$$\left[\left[R(12)+R(13)+R(14)+R(15)+R(16)\right]+j\left[X(12)+X(13)+X(14)+X(15)+X(16)\right]\right] \times\left[\Delta I^r(MB_1)^t - j\Delta I^q(MB_1)^t\right]=\left[\Delta V(MB_1)^t + j\Delta\delta(MB_1)^t\right] \quad (5.50)$$

On separating the real and imaginary parts of equation (5.50):

$$\begin{bmatrix} \left[X(12)+X(13)+X(14)+X(15)+X(16)\right] & \left[R(12)+R(13)+R(14)+R(15)+R(16)\right] \\ -\left[R(12)+R(13)+R(14)+R(15)+R(16)\right] & \left[X(12)+X(13)+X(14)+X(15)+X(16)\right] \end{bmatrix} \times \begin{bmatrix} \Delta I^{q}(MB_1)^{t} \\ \Delta I^{r}(MB_1)^{t} \end{bmatrix} = \begin{bmatrix} \Delta V(MB_1)^{t} \\ \Delta\delta(MB_1)^{t} \end{bmatrix} \quad (5.51)$$

where,

$$\Delta V(MB_1)^{t} + j\Delta\delta(MB_1)^{t} = V(T1'')^{t} - V(T1)^{t}$$

$$\Delta I(MB_1)^{t} = \Delta I^{r}(MB_1)^{t} - j\Delta I^{q}(MB_1)^{t}$$

For type 2 mesh, the loop breakpoint equation is:

$$\left[R(17)+R(18)+R(19)+R(20)+R(21)\right]\times\left[\Delta I(MB_2)^{t}\right] = \left[V(MB_2'')^{t} - V(MB_2)^{t}\right] \quad (5.52)$$

Equation (5.52) can also be represented as:

$$\left[R(17)+R(18)+R(19)+R(20)+R(21)\right]\times\left[\Delta I^{r}(MB_2)^{t} - j\Delta I^{q}(MB_2)^{t}\right] = \left[\Delta V(MB_2)^{t} + j\Delta\delta(MB_2)^{t}\right] \quad (5.53)$$

where,

$$\Delta V(MB_2)^{t} + j\Delta\delta(MB_2)^{t} = V(T2'')^{t} - V(T2)^{t} \quad (5.54)$$

$$\Delta I(MB_2)^{t} = \Delta I^{r}(MB_2)^{t} - j\Delta I^{q}(MB_2)^{t} \quad (5.55)$$

$$\Delta I^{q}(MB_2)^{t} = 0 \quad (5.56)$$

$$\Delta\delta(MB_2)^{t} = 0 \quad (5.57)$$

Using equations (5.54) and (5.57) in equation (5.53), the resulting equation will be:

$$\left[R(17)+R(18)+R(19)+R(20)+R(21)\right]\times\left[\Delta I^{r}(MB_2)^{t}\right] = \left[\Delta V(MB_2)^{t}\right] \quad (5.58)$$

For type 3 mesh, the loop breakpoint equation is:

$$\left(\left(\left(R(4)+R(5)\right)\left(\frac{D}{1-D}\right)^{2} + \left(R(6)+R(10)\right)\right)\times\left(\Delta I(MB_3)^{t}\right)\right) - \left(\left(R(4)\left(\frac{D}{1-D}\right)(MI)(\cos(\phi))\right)\times\left(\left|\Delta I(PVB_1)^{t}\right|\right)\right) - \left(\left(\left(R(4)+R(5)\right)\left(\frac{D}{1-D}\right)^{2} + R(6)\right)\times\left(\Delta I(VDC_1)^{t}\right)\right) = \left(V(MB_3'')^{t} - V(MB_3)^{t}\right) \quad (5.59)$$

On further simplifying equation (5.59):

$$\left(\begin{array}{l}\left(\left(R(4)+R(5)\right)\left(\frac{D}{1-D}\right)^2+\left(R(6)+R(10)\right)\right)\\ \times\left(\Delta I^r(MB_3)^t-j\Delta I^q(MB_3)^t\right)\end{array}\right)-\left(\begin{array}{l}\left(R(4)\left(\frac{D}{1-D}\right)(MI)\left(\cos(\phi)\right)\right)\\ \times\left(\left|\Delta I^r(PVB_1)^t-j\Delta I^q(PVB_1)^t\right|\right)\end{array}\right) \tag{5.60}$$

$$-\left(\left(\left(R(4)+R(5)\right)\left(\frac{D}{1-D}\right)^2+R(6)\right)\times\left(\Delta I^r(VDC_1)^t-j\Delta I^q(VDC_1)^t\right)\right)=\left(\Delta V(MB_3)^t+j\Delta\delta(MB_3)^t\right)$$

where,

$$\Delta V(MB_3)^t+j\Delta\delta(MB_3)^t=V(T3")^t-V(T3)^t \tag{5.61}$$

$$\Delta I(MB_3)^t=\Delta I^r(MB_3)^t-j\Delta I^q(MB_3)^t \tag{5.62}$$

$$\Delta I(PVB_1)^t=\Delta I^r(PVB_1)^t-j\Delta I^q(PVB_1)^t \tag{5.63}$$

$$\Delta I(VDC_1)^t=\Delta I^r(VDC_1)^t-j\Delta I^q(VDC_1)^t \tag{5.64}$$

$$\Delta I^q(MB_3)^t=0 \tag{5.65}$$

$$\Delta\delta(MB_3)^t=0 \tag{5.66}$$

$$\Delta I^q(VDC_1)^t=0 \tag{5.67}$$

$$\Delta I^r(PVB_1)^t=0 \tag{5.68}$$

cos(Φ)= Power factor at the converter output terminal.

$\cos(\theta_v)$ = cosine of phase angle of the voltage at converter terminal.

Using equations (5.61) to (5.68) in equation (5.60), the resulting breakpoint equation will be:

$$\left(\begin{array}{l}\left(\left(R(4)+R(5)\right)\left(\frac{D}{1-D}\right)^2+\left(R(6)+R(10)\right)\right)\\ \times\left(\Delta I^r(MB_3)^t-j\Delta I^q(MB_3)^t\right)\end{array}\right)-\left(\begin{array}{l}\left(R(4)\left(\frac{D}{1-D}\right)(MI)\left(\cos(\phi)\right)\right)\\ \times\left(\left|\Delta I^r(PVB_1)^t-j\Delta I^q(PVB_1)^t\right|\right)\end{array}\right) \tag{5.69}$$

$$-\left(\left(\left(R(4)+R(5)\right)\left(\frac{D}{1-D}\right)^2+R(6)\right)\times\left(\Delta I^r(VDC_1)^t-j\Delta I^q(VDC_1)^t\right)\right)=\left(\Delta V(MB_3)^t\right)$$

For the PV type bus, the PV breakpoint equation is written as:

For the system shown in Fig. 5.5, the PV breakpoint equation can be written as:

$$\left\{\left(\left(\left(|Z(1)|+|Z(2)|\right)\cos(\alpha)+\left(R(4)+R(3)\right)\right)\left(\left(\cos(\theta_v)\right)(MI)\left(\frac{D}{1-D}\right)\right)\right)\right\} \times\left(\left(\Delta I^{r}(VDC_1)^{t}-j\Delta I^{q}(VDC_1)^{t}\right)\right)$$
$$+\left\{\left(\left(\left(\left(|Z(1)|+|Z(2)|\right)\cos(\alpha)+\left(R(4)+R(3)\right)\right)\left(\left(\cos(\theta_v)\right)\left(MI^{2}\right)\left(\cos(\phi)\right)\right)+\left(X(8)+X(9)\right)\right)\right\} \times\left(\left|\Delta I^{r}(PVB_1)^{t}-j\Delta I^{q}(PVB_1)^{t}\right|\right)$$
$$+\left\{\left(\left(R(4)\right)\left(\cos(\theta_v)\right)(MI)\left(\frac{D}{1-D}\right)\right)\times\left(-\left(\Delta I^{r}(MB_3)^{t}-j\Delta I^{q}(MB_3)^{t}\right)\right)\right\}=\left(\left|V(PVB_1'')^{t}\right|-\left|V(PVB_1)^{t}\right|\right) \tag{5.70}$$

On further simplifying equation (5.70)

$$\left\{\left(\left(\left(|Z(1)|+|Z(2)|\right)\cos(\alpha)+\left(R(4)+R(3)\right)\right)\left(\left(\cos(\theta_v)\right)(MI)\left(\frac{D}{1-D}\right)\right)\right)\right\} \times\left(\left(\Delta I^{r}(VDC_1)^{t}-j\Delta I^{q}(VDC_1)^{t}\right)\right)$$
$$+\left\{\left(\left(\left(\left(|Z(1)|+|Z(2)|\right)\cos(\alpha)+\left(R(4)+R(3)\right)\right)\left(\left(\cos(\theta_v)\right)\left(MI^{2}\right)\left(\cos(\phi)\right)\right)+\left(X(8)+X(9)\right)\right)\right\} \times\left(\left|\Delta I^{r}(PVB_1)^{t}-j\Delta I^{q}(PVB_1)^{t}\right|\right)$$
$$+\left\{\left(\left(R(4)\right)\left(\cos(\theta_v)\right)(MI)\left(\frac{D}{1-D}\right)\right)\times\left(-(\Delta I^{r}(MB_3)^{t}-j\Delta I^{q}(MB_3)^{t})\right)\right\}=\left(\Delta V(PVB_1)^{t}+j\Delta\delta(PVB_1)^{t}\right) \tag{5.71}$$

where,

$$\Delta V(PVB_1)^{t}+j\Delta\delta(PVB_1)^{t}=V(10'')^{t}\text{-}V(10)^{t} \tag{5.72}$$

$$\Delta\delta(PVB_1)^{t}=0 \tag{5.73}$$

Using equations (5.61) to (5.68) and (5.72) to (5.73) in equation (5.71), the resulting breakpoint equation will be:

$$\left\{\left(\left(\left(|Z(1)|+|Z(2)|\right)\cos(\alpha)+\left(R(4)+R(3)\right)\right)\left(\left(\cos(\theta_v)\right)(MI)\left(\frac{D}{1-D}\right)\right)\right)\right\}\times\left(\Delta I^{r}(VDC_1)^{t}\right)\right\}$$
$$+\left\{\left(\left(\left(\left(|Z(1)|+|Z(2)|\right)\cos(\alpha)+\left(R(4)+R(3)\right)\right)\left(\left(\cos(\theta_v)\right)\left(MI^{2}\right)\left(\cos(\phi)\right)\right)+\left(X(8)+X(9)\right)\right)\right\} \times\left(\Delta I^{q}(PVB_1)^{t}\right)$$
$$+\left\{\left(\left(R(3)\right)\left(\cos(\theta_v)\right)(MI)\left(\frac{D}{1-D}\right)\right)\times\left(-\Delta I^{r}(MB_3)^{t}\right)\right\}=\left(\Delta V(PVB_1)^{t}\right) \tag{5.74}$$

For the V^{dc} type bus, the V^{dc} breakpoint equation is written as:

$$\left(\left(\left(\left(\left(|Z(1)|+|Z(2)|\right)\cos(\alpha)+\left(R(4)+R(3)+R(5)\right)\right)\times\left(\frac{D}{1-D}\right)^2\right)+(R(6)+R(7))\right)\times\left(\left(\Delta I^r(VDC_1)^t-j\Delta I^q(VDC_1)^t\right)\right)\right)$$
$$-\left(\left(\left(R(4)+R(5)\right)\left(\frac{D}{1-D}\right)^2+R(6)\right)\times\left(\Delta I^r(MB_3)^t-j\Delta I^q(MB_3)^t\right)\right)$$
$$+\left(\left(\left(\left(|Z(1)|+|Z(2)|\right)\cos(\alpha)+R(3)+R(4)\right)\left(\left(\frac{D}{1-D}\right)(MI)(\cos(\phi))\right)\right)\times\left(\Delta I^r(PVB_1)^t-j\Delta I^q(PVB_1)^t\right)\right)$$
$$=\left(\Delta V(VDC_1)^t+j\Delta\delta(VDC_1)^t\right) \tag{5.75}$$

where,

$$\Delta V(VDC_1)^t+j\Delta\delta(VDC_1)^t=V(8'')^t-V(8)^t \tag{5.76}$$

$$\Delta\delta(VDC_1)^t=0 \tag{5.77}$$

Using equations (5.61) to (5.68), (5.72) to (5.73) and (5.76) to (5.77) in equation (5.75), the resulting breakpoint equation will be:

$$\left(\left(\left(\left(\left(|Z(1)|+|Z(2)|\right)\cos(\alpha)+\left(R(4)+R(3)+R(5)\right)\right)\times\left(\frac{D}{1-D}\right)^2\right)+(R(6)+R(7))\right)\times\left(\left(\Delta I^r(VDC_1)^t\right)\right)\right)$$
$$-\left(\left(\left(R(4)+R(5)\right)\left(\frac{D}{1-D}\right)^2+R(6)\right)\times\left(\Delta I^r(MB_3)^t\right)\right)$$
$$+\left(\left(\left(\left(|Z(1)|+|Z(2)|\right)\cos(\alpha)+R(3)+R(4)\right)\left(\left(\frac{D}{1-D}\right)(MI)(\cos(\phi))\right)\right)\times\left(\Delta I^q(PVB_1)^t\right)\right)=\left(\Delta V(VDC_1)^t\right) \tag{5.78}$$

The simultaneous solution of equations (5.51), (5.58), (5.69), (5.74) and (5.78) will provide the loop or mesh breakpoint injections, PV breakpoint injection and V^{dc} breakpoint injection for all the loops and controlled buses of the distribution system in Fig. 5.5. The corresponding injection are reflected in LB_g/LC_g matrix (as per injected quantity).

The above equation for calculating breakpoint current injection can be modified in terms of breakpoint power injection (as per procedure described in chapter 4). The detailed steps for

carrying out the load flow solution for meshed AC-DC distribution system with distributed generations is provided in Fig 5.6.

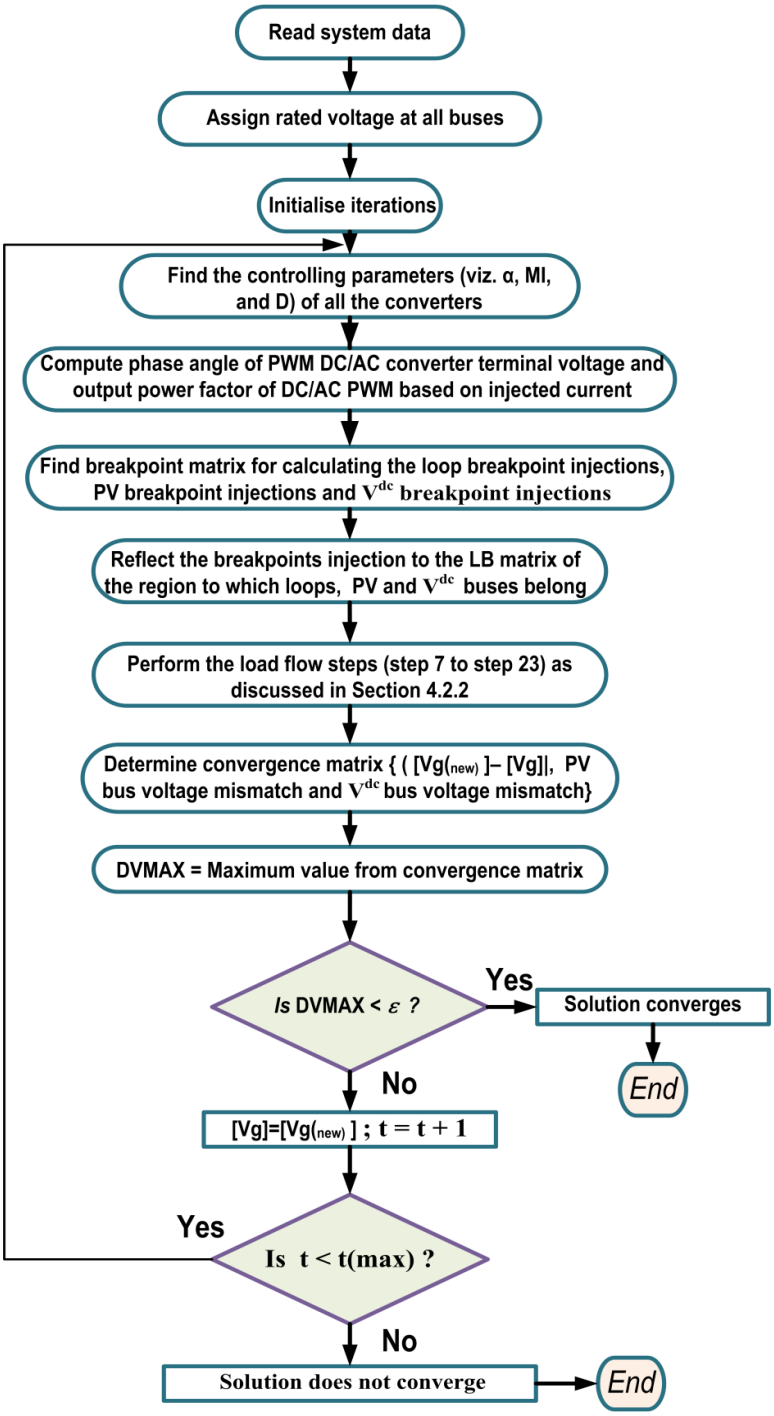

Fig. 5.6: Load flow algorithm for meshed AC-DC distribution system with DGs.

5.4 Results

This section presents the case studies that were used for evaluating the effectiveness and accuracy of the proposed LF model. The algorithm has been tested using Matlab software through a personal computer with specifications : Intel core i7 2600@3.4GHz, 64bit, and 8GB RAM. The load-flow results as acquired by proposed method and the efficacy comparison with that of algorithms prevailing in the literature are presented in this part.

Test system 1: 33 bus AC-DC distribution network

For any new method, it is important to make sure that the final solution of the new method is the same as the existent method. The 33 bus AC-DC distribution network has been used for the case study [36] and comparison. The load flow results for the aforementioned distribution system using proposed algorithm (PM) and reduced gradient optimization approach [36] is explicitly presented in Table 5.1. Based on the results acquired, the maximum difference between the bus voltages calculated by the proposed load flow method and the reduced gradient approach is 0.00008. In this case convergence tolerance rate is taken as 0.00001.The execution time for the reduced gradient optimization approach and the proposed method is 201ms, and 78ms respectively. The comparison of the results obtained from the proposed load flow model and those obtained by the reduced gradient approach therefore demonstrates the effectiveness and accuracy of the proposed load flow technique.

The authors [36], have implemented an AC-DC power flow model in a general algebraic model system (GAMS) using reduced gradient optimization technique. In this solution method, AC-DC power flow equations have been solved simultaneously considering various hybrid configurations. However, it has certain limitations:

(a) Prohibit applications in problems where the intrinsic intransigence of modelling language does not permit full utilization of the power system properties. For example, the aforementioned method has only utilized AC-DC VSCs model with constant modulation ratio. The other operating modes (viz. constant power mode, constant voltage control at the output of converter terminal etc.) have been ignored.

(b) The other existing converters such as three phase bridge converter and DC-DC converter have not been considered in the mentioned generic AC-DC power flow solution method.

(c) Blind trust on commercial solvers may not be a good idea since they are completely devoid of special power system properties.

The method developed in this article has flexibility to include all kind of power converters. Various operating mode of power converters have also been considered to demonstrate the effectiveness of the proposed method.

Table 5.1: Load flow solution of hypothetical 33 bus AC-DC distribution system

Bus Number	Voltage Magnitude (pu)		Phase (Radian)	
	PM	[36]	PM	[36]
1	1.05000	1.05000	0.00000	0.00000
2	1.04715	1.04709	-0.00952	-0.00972
3	1.03782	1.03776	-0.02653	-0.02781
4	1.03363	1.03360	-0.03725	-0.03683
5	1.03000	1.03000	-0.05203	-0.05114
6	1.01920	1.01912	-0.27694	-0.27694
7	1.01872	1.01869	-0.29568	-0.29890
8	1.02920	1.02920	-	-
9	1.02674	1.02674	-	-
10	1.02480	1.02479	-	-
11	1.02431	1.02430	-	-
12	0.99319	0.99317	-0.62574	-0.62317
13	0.99218	0.99215	-0.66665	-0.66568
14	0.99226	0.99225	-0.66524	-0.66363
15	0.99452	0.99449	-0.62944	-0.62944
16	1.03695	1.03692	-	-
17	1.03884	1.03884	-	-
18	1.03932	1.03930	-	-
19	1.04505	1.04503	-0.05980	-0.05930
20	1.02872	1.02871	-0.43589	-0.43950
21	1.03707	1.03702	-	-
22	1.03716	1.03715	-	-
23	1.03478	1.03477	-0.05565	-0.05338
24	1.03000	1.03000	-0.11923	-0.11852
25	1.02242	1.02238	-0.21775	-0.21870
26	1.04951	1.04951	-	-
27	1.04810	1.04808	-	-
28	1.04372	1.04371	-	-
29	1.02000	1.02000	-0.22623	-0.22492
30	1.01406	1.01404	-0.24914	-0.24914
31	1.00229	1.00228	-0.50627	-0.50558
32	1.00012	1.00006	-0.57383	-0.57217
33	0.99825	0.99823	-0.63485	-0.63485

Test system 2: 13 bus AC-DC distribution network

As shown in Fig. 5.7, the AC-DC distribution network for the second case study is a 13-bus network. The data related to the loads and generators at each bus are presented in Fig. 9 and Table 5.2. In this network, one line commutated converter is connected between buses 8 and 9. Minimum firing angle limit for this converter is 7°, and its commutation reactance is

neglected. The voltage at bus 9 is controlled at 5.0 kV using three phase bridge converter. Constant power flow (0.5MW) between buses 11 and 6 is being maintained using DC-DC converter connected between buses 11 and 6. Two DC-DC converters, one connected between buses 12 and 13 and another connected between buses 10 and 11, are controlled to maintain the constant voltage at buses 13 and 11 respectively. The voltage at bus 11 and bus 13 are controlled at 5.3 kV and 5.4 kV respectively. Another DC-DC converter connected between buses 4 and 5 is operating in constant duty ratio mode (D=0.97). Constant power flow (0.5+0.4i MVA) between buses 3 and 2 is being controlled using the three phase PWM converter connected between bus 2 and 3. Regarding the bus categorizations, bus 1 represents a slack bus, bus 8 is P-V bus, buses 4 and 6 are DC voltage controlled bus **(**V^{dc} bus**),** bus 10 is constant real power generating bus (P bus) and the remaining buses are load bus. The data of various types of converter is provided in Table 5.3. Base MVA=10, Base voltage= 4.16kV (AC side) = 5.1 kV (DC side).

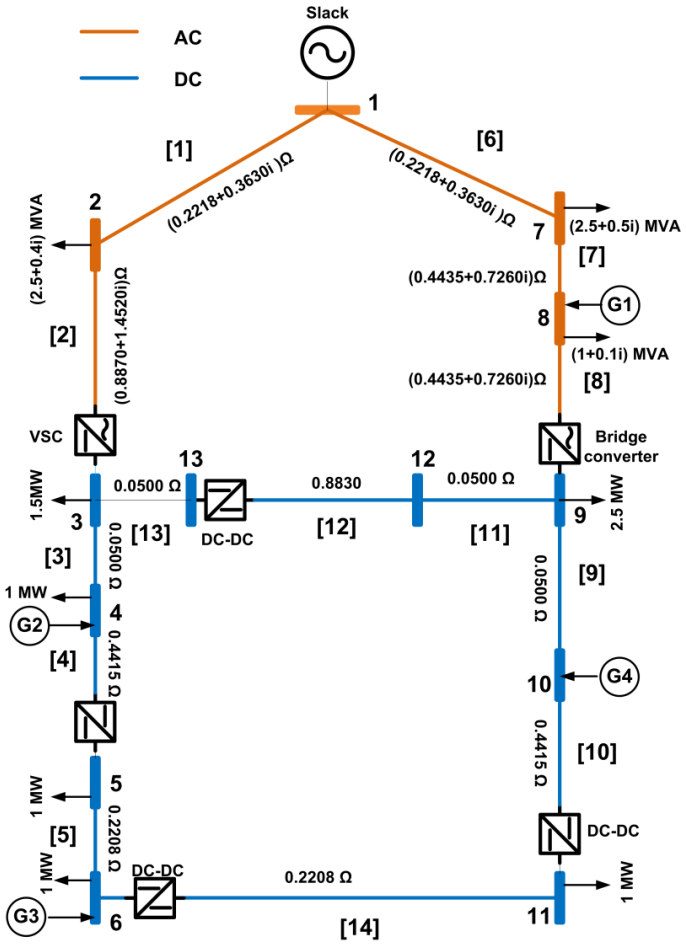

Fig. 5.7: Single line diagram of a hypothetical 13 bus AC-DC distribution network.

Table 5.2: Characteristics of distributed generations in Fig. 5.7

Generator Number and Types	Real Power (MW)		Injected Reactive Power (MVAr)		Voltage (pu)
	Max.	Min.	Max.	Min.	
G1 (PV)	3.5	3.5	1.5	0.2	1.03490
G2 (V^{dc})	3	1.2	-	-	1.06500
G3 (V^{dc})	3	1.2	-	-	1.07480
G4 (P)	3	3	-	-	-

Table 5.3: Characteristics of converters in Fig. 5.7

Converter Types	Located Between Buses	Control Strategy	Control Limit
3-Φ Full Bridge Converter	8 & 9	Constant DC Voltage	$\alpha(\min)=7^0$ $\alpha(\max)=18^0$
3-Φ VSC Converter	2 & 3	Constant Power	$MI(\min)=0.7$ $MI(\max)=1$
DC-DC Converter	4 & 5	Constant Duty Ratio	-
DC-DC Converter	10 & 11	Constant Voltage	$D(\min)=0$ $D(\max)=0.8$
DC-DC Converter	12 & 13	Constant Voltage	$D(\min)=0$ $D(\max)=0.8$
DC-DC Converter	11 & 6	Constant Power	$D(\min)=0$ $D(\max)=0.8$

Table 5.4: Voltage profile of 13 bus AC-DC system

Bus Number	Voltage Magnitude (pu)		Phase (Radian)	
	PM	PSCAD	PM	PSCAD
1	1.0000	1.0000	0.00000	0.00000
2	0.99370	0.99370	0.03868	0.03867
3	1.05971	1.05977	-	-
4	1.06500	1.06498	-	-
5	1.05552	1.05556	-	-
6	1.07480	1.07480	-	-
7	0.99030	0.99028	-0.01098	-0.01095
8	1.03490	1.03490	0.001418	0.001420
9	0.98039	0.98046	-	-
10	0.98350	0.98357	-	-
11	1.03920	1.03921	-	-
12	0.98140	0.98146	-	-
13	1.05880	1.05877	-	-

The load flow results for the aforementioned distribution system using proposed algorithm and the load flow solution provided by PSCAD software is explicitly presented in Table 5.4

and Table 5.5. Based on the results acquired, the maximum difference between the bus voltages calculated by the proposed load flow method and the load flow model simulated in PSCAD is 0.00003. The maximum difference between the active and reactive line flows calculated by the proposed load flow method and the load flow model simulated in PSCAD is 3×10^{-6} and 6×10^{-6} pu respectively (Fig. 5.8). The execution time for the proposed method is 60ms. The comparison of the results obtained from the proposed algorithm and those produced by the PSCAD software therefore demonstrates the effectiveness and accuracy of the method developed.

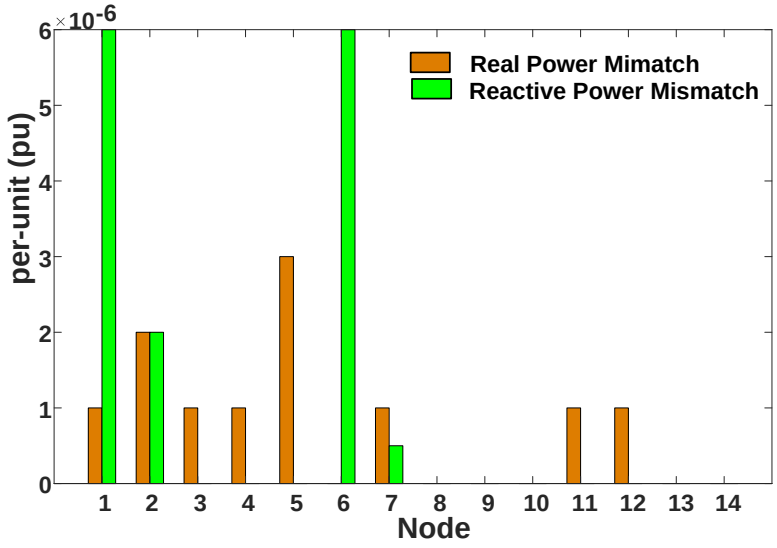

Fig. 5.8: Real power and reactive power mismatch in each line sections.

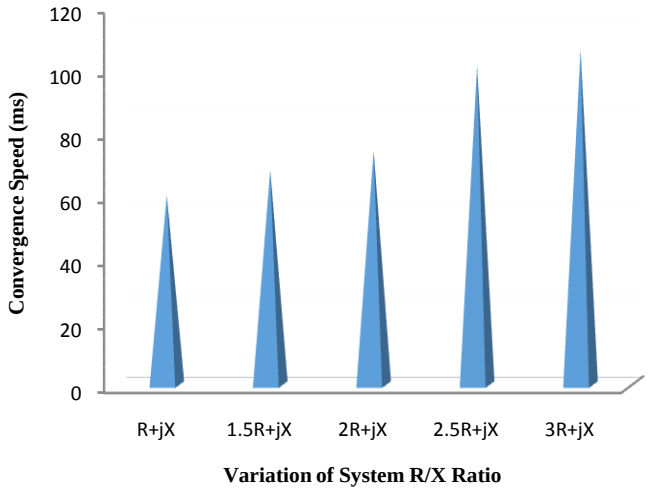

Fig. 5.9: Variation of convergence speed with the change in system R/X ratios.

Table 5.5: Distributed generators load flow results

Generator Number	Real Power (MW)		Injected Reactive Power (MVAr)	
	PM	PSCAD	PM	PSCAD
G1	3.5	3.5	0.5	0.5
G2	2.5	2.49	-	-
G3	2.5	2.51	-	-
G4	3.0	3.0	-	-

To assess the effect of R/X ratio variation on the convergence characteristics, the proposed methodology has been tested for wide range of R/X ratios of AC lines belonging to the 13-bus AC-DC distribution network. The test result in Fig. 5.9 justify the convergence ability of the proposed method.

5.5 Conclusion

In this chapter load flow algorithm for meshed AC-DC distribution network with various models of distributed generations has been formulated. A technique for converting the meshed AC-DC network into radial network has been thoroughly derived. For converting meshed network to radial network, the loop breakpoint matrix has been derived for calculating loop breakpoint injections in AC-DC scenario. In the case of weakly meshed distribution network with PV type and V^{dc} type distributed generations, the loop breakpoint injections, PV breakpoint injections and V^{dc} breakpoint injections have been calculated simultaneously. The net injections is reflected in the loads beyond branch matrix or load current matrix of the distribution network. Note that except for some modifications needed to be done for the LB_g or LC_g matrices, the proposed solution techniques require no modification; therefore, the proposed method can obtain the load-flow solution for AC-DC distribution system in the presence of distributed generations efficiently. Due to unavailability of a standard AC-DC distribution system at present, hypothetical test cases (33 bus and 13 bus AC-DC distribution system) have been considered and the performance of the AC-DC load flow algorithm is thoroughly investigated. The effectiveness of the proposed model has been verified against the load flow solution produced by PSCAD and reduced gradient approach (implemented in GAMS). The test results demonstrate that the proposed load flow algorithm can provide precise solution while also offering the flexibility and speed required for online applications. For checking the robustness of the method, the system R/X

ratio has been varied and convergence ability of the proposed load flow algorithm has been tested. This load flow method converges for a wide range of R/X ratio. However, the convergence speed will decrease with the increase in R/X ratio.

Chapter-6

Investigating the Impact of Protection System Reinforcement Cost on the Consumers Associated with Renewable Integrated Distribution Network

This chapter aims to investigate the impact of renewable generations on the DUoS charges considering the cost associated in revamping the protection scheme. A power flow based MW+MVAr-Miles DUoS charging method, that considers used capacity of the network, is proposed to carry out the DUoS charging calculations. The proposed charging algorithm has been tested on IEEE-33 and IEEE-69 bus distribution systems to examine the impact of renewable generations on the use of network costs.

6.1 Introduction

Conventional distribution systems are radial in nature, that is, the power flows from higher voltage level down to consumers connected to the radial feeder. This simple configuration has enabled straightforward protection strategies (Fig.6.1). Typically, overcurrent protection schemes are deployed for protecting such kind of system because of their simplicity and low-cost [82-84].

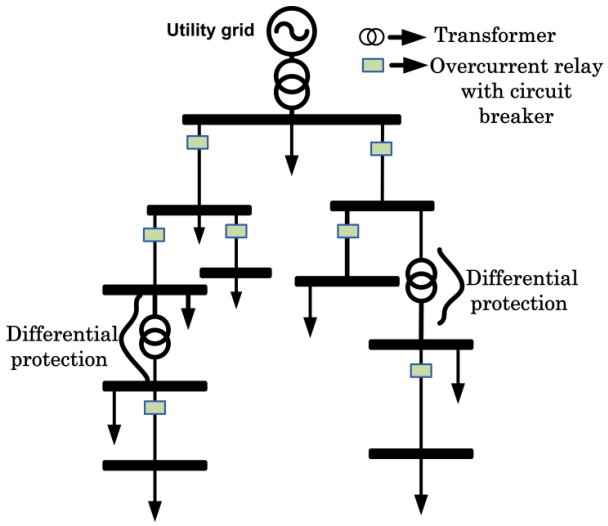

Fig. 6.1: Conventional distribution system with overcurrent protection scheme.

The promise of a future world dominated by rapid population growth and unparalleled energy demand presents many challenges to the global energy industry and indeed society as a whole. The renewable energy sources are the promising solution to combat the challenge of sustainable development [85]-[86]. With the connection of renewable generations (RG), radial distribution network may become multiple power supply system. The inclusion of renewable generations into the distribution network will affect the amplitude, direction, and distribution of fault current when short-circuit fault occurs [87]-[90]. Thus, exiting overcurrent protection coordination may be affected, or entirely lost in some cases. Therefore, conventional overcurrent protection schemes that are intended for protection of distribution system without considerations of the renewable generation impacts are inadequate for supporting wider renewable energy-based DG penetration [8]. The type, position and capacity of DG will affect protection coordination of distribution network. For such systems, overcurrent relay must be supplemented with directional components and circuit breakers ought to meet desired current interruption limit prerequisite (Fig. 6.2) [89-90].

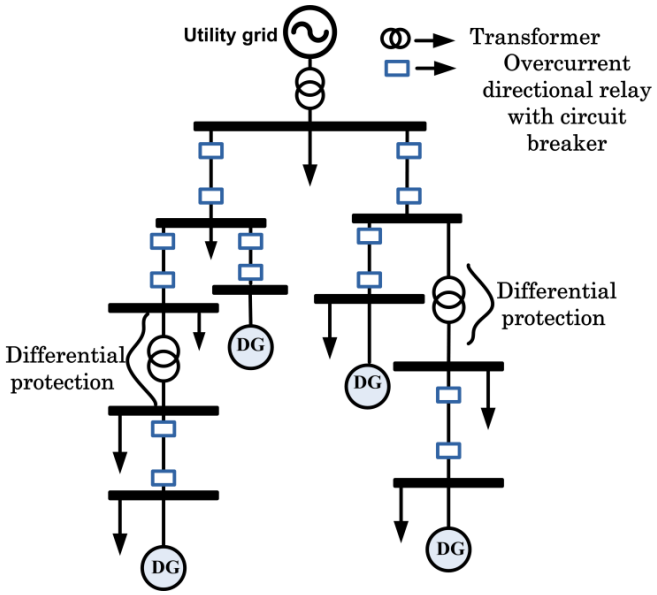

Fig. 6.2: Distribution system with overcurrent directional protection scheme.

The renovation required for an existing distribution system to meet the desired protection coordination in the presence of renewable generation demands considerable investment. The reasons are:

1) Directional overcurrent relay with associated circuit breaker are required for both ends of a feeder connecting two buses where there is possibility of bidirectional fault current flow {Fig. 6.2}. In conventional distribution system (without DG), overcurrent relay along with associated circuit breaker is connected only toward the substation end of the feeder {Fig. 6.1}.
2) In addition all existing circuit breakers may have to be replaced by higher capacity breaker as short circuit level of the distribution system may rise with the inclusion of distributed generations [91].
3) Further, a protection system require current transformers (CTs) and potential transformers (PTs), battery supply and other accessories as per requirement.

The additional protection renovation cost will have significant impact on the distribution network annuity cost requirement and will also have significant economic impact on the network users. Distribution use of system (DUoS) charge is a key factor for scrutinizing the economic impact of renewable generation on distribution network users.

The distribution networks deal with the components such as overhead lines, underground cables, substations, transformers and other related equipment. DUoS charges contribute towards the cost of installing, operating and maintaining the regional distribution network, so that a safe and reliable electricity supply is available to all. These charges vary from region to region but normally account for 15-19 percent of a typical non-domestic electricity bill which indeed is a significant figure [92]. The design of a distribution pricing scheme can usually be separated into two steps: establishing the regulatory revenues (the allowed revenue over a certain period of time) and allocating this allowed revenue from network users; revenue recovery comes through the connection and the use of system pricing and tariff structure [92]. It is a complicated issue, given the huge size and diverse nature of power system networks all over the world. Various power companies around the world are undergoing significant changes, with an objective of efficient and economic solutions to electricity supply. A simple and efficient pricing strategy can ensure better utilization of resources, supply to consumers and a considerable amount of profit [93]. New regulatory mechanisms are being proposed in an effort to serve the consumers in a better way. A methodology for setting DUoS charges is expected to serve mainly two purposes: (i) good return on investment to the network companies. (ii) to facilitate efficient utilization of network assets.

Existing DUoS charging schemes are not much advanced as required by the rapid development in networks. The local charging mechanisms were non-existent prior to year 2007 and the yardstick approach had been adopted for allocating fixed costs with differing sophistication [94-97]. The majority of conventional DUoS charging methodologies for distribution network are not cost reflective— that is, they do not reflect the costs/benefits that distributed generations might bring to the distribution network and power supply [98-99]. Hence, the conventional DUoS charging model cannot efficiently influence how and when network users should use the system.

A natural method for pricing of distribution systems is to embrace a traditional pricing model for that of transmission systems [100-109]. The MW-miles method relies on the effective network assets usage by the customers. The distribution systems are generally operated at a lower power factor relative to that of transmission system. Furthermore, a considerable proportion of distributed generators are wind farms, where the reactive power drawn can be significant. As a result, if only active power flow is considered in a DUoS charging method, it will credit wind generator for its active power injection, but fails to penalize for its reactive power drawn from the network, leading to misleading locational signal. An improved MW-Mile method has been proposed by Nojeng et al. considering not only the MW flows but also the quality of the load [110].

The MVA-miles method is considered as a better alternative to MW-miles method [111]. It works well in scenarios where there is simultaneous energy generation and consumption at various levels. It also keeps track of the net real and reactive power flows in the system. However, the direction of flows cannot be ascertained by this method e.g. in the case of wind generators, where real power is injected and reactive power is simultaneously withdrawn, it fails to detect the direction of power flows which may result in false pricing.

The MW-Miles method and MVA-Miles method only take into account unidirectional power flow. If the DUoS is only obtained from the degree of facility utilization, it may not be able to distinguish multidirectional power flow. Hence these pricing mechanisms are not cost reflective when wind generations are part of distribution network. But, for other renewable sources with unidirectional power flow these pricing mechanisms may be cost reflective.

The MW+MVAr-Miles method [112] is used for pricing real and reactive power separately taking into consideration the distance, direction and magnitude they travel to

support the customers and customers impact on system power factor. Hence to analyse the impact of wind generations on the DUoS charges, this method is most appropriate when compared with above mentioned methods. However, for large power system with deeper penetration of distributed generations, the existing MW+MVAr-miles method finds it very difficult in obtaining the desired DUoS calculations by tracing power flow path and facility supporting it. Although, there are various power tracing algorithms are available in literatures [113-117] (for transmission system not for distribution system), it will bring more complexity and computational burden to the mentioned DUoS charging algorithms. Hence, a smart DUoS charging algorithm based on MW+MVAr-Miles method is required for reflecting the impact of renewable generations on DUoS charges.

The proposed work aims to investigate the impact of renewable generations on the network protection cost requirement and its subsequent economic effect on the network users. Distribution use of system (DUoS) charge is a key factor for scrutinizing the economic impact of renewable generation on distribution network users. For this purpose, a MW+MVAr-Miles DUoS charging methodology for charging network users has been formulated. The impact of renewable generations (especially wind) on the distribution use of system (DUoS) charges for the network users has been thoroughly investigated by utilizing the concept of proposed network charging methodology. The proposed charging methodology has following advantages as compared to existing literatures [100-112]:

(a) The developed charging methodology is used for separately pricing real and reactive power, taking into consideration not only the distance and magnitude they travel to support the customers but also customers impact on system power factor.

(b) Two triangle concept (maximum capacity triangle and used capacity triangle) has been proposed for fair network charging among distribution network users. With the proposed charging model for use of network cost calculation, the customers are charged in accordance with the exactly used capacity of the network.

(c) The proposed pricing algorithm may encourage users to act based on the economic signal generated at each location.

(d) In this algorithm, the charging calculations can be carried out without detecting the power flow path and hence can save a significant computational burden.

6.2 Distribution Use of Systems (DUoS) Charges

The distribution networks deal with the components such as overhead lines, underground cables, substations, transformers and other related equipment. DUoS charges contribute towards the cost of installing, operating and maintaining the regional distribution network, so that a safe and reliable electricity supply is available to all. These charges vary from region to region but normally account for 15-19 percent of a typical non-domestic electricity bill which indeed is a significant figure [92], [118-119]. The design of a distribution pricing scheme can usually be separated into two steps: establishing the regulatory revenues (the allowed revenue over a certain period of time) and allocating this allowed revenue from network users; revenue recovery comes through the connection and the use of system pricing and tariff structure [92], [118-119]. In this section, the mathematical formulation of a power flow based MW+MVAr-Miles method has been derived for charging network users. The proposed charging method allocate the embedded system costs i.e., fixed cost among distribution system users for their extent of use of network. The proposed algorithm has made use of maximum capacity triangle and used capacity triangle of facility for allocating the chargeable cost to the network facility and distributing the net chargeable facility cost among network users in accordance with the extent by which they have utilized the network facility.

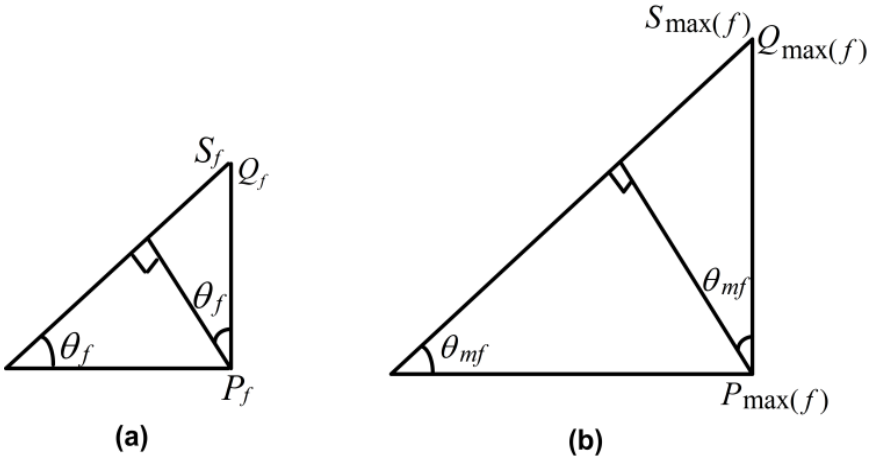

Fig. 6.3: Facility *f* power flow triangle at its (a) Operating capacity, (b) Rated capacity.

Consider a facility f having maximum capacity $|S_{\max(f)}|$ (MVA). The annuity cost or annual cost of facility f associated with its maximum capacity is AC_f. Annuity cost or

Annual cost is the Series of payments at fixed intervals, guaranteed for a fixed number of years or till lifetime of the assets or the network.

Let's say, if the network has m number of facilities or branches then the total annuity or annual cost of the network is given by:

$$\text{Total network annuity cost}=\sum_{f=1}^{m} AC_f \tag{6.1}$$

where, m=Total number of facilities/branches in the distribution network.

AC_f has been obtained using the following equation:

$$AC_f = AF \times C_f \tag{6.2}$$

where C_f = total cost of facility f (which includes total cost of installing, operating and maintaining the facility f).

AF= annuity factor.

Assuming the life of the assets or facilities to be y years and the interest rate to be paid to the bank or financing agency is r% per year, the annuity factor is calculated as:

$$AF = \frac{r}{1-(1+r)^{-y}} \tag{6.3}$$

r = Rate per annum=10% (in this work)

y =Number of year=30 (in this work)

With the application of pertinent distribution load flow algorithm developed in chapter 2 and chapter 3, power flow through each facility/branch in the distribution system is calculated. The MVA flow (S_f) in each facility can be represented as:

$$S_f = P_f + jQ_f \tag{6.4}$$

$$|S_f|^2 = {P_f}^2 + {Q_f}^2 \tag{6.5}$$

On simplifying equation (6.5), we will get contribution of actual real and reactive power to actual apparent power flow in the facility *f*.

$$|S_f| = \frac{{P^2}_f}{|S_f|} + \frac{{Q^2}_f}{|S_f|} \tag{6.6}$$

$$|S_f| = |S_f|\cos^2(\theta_f) + |S_f|\sin^2(\theta_f) \tag{6.7}$$

Let's consider a situation in which facility f is operating at its maximum MVA capacity ($|S_{\max(f)}|$) with power factor angle θ_{mf}. The maximum MVA capacity of each branch/facility

can also be represented in terms of its real and reactive power components:

$$S_{\max(f)} = P_{\max(f)} + jQ_{\max(f)} \tag{6.8}$$

$$\left|S\max(f)\right|^2 = P^2{}_{\max(f)} + Q^2{}_{\max(f)} \tag{6.9}$$

The contribution of real and reactive power to apparent power at the rated capacity can be obtained by simplifying equation (6.9).

$$\left|S_{\max(f)}\right| = \left|S_{\max(f)}\right|\cos^2(\theta_{mf}) + \left|S_{\max(f)}\right|\sin^2(\theta_{mf}) \tag{6.10}$$

Equations (6.1) through (6.10) are the basic amenities for network charging formulation for users/customers associated with a distribution system.

The unit cost to support 1MVA flow in the facility f is given by:

$$U_f = \frac{AC_f}{\left|S_{\max(f)}\right|} \tag{6.11}$$

The extent of facility f cost ($C_{P,f}$) due to real power flow in the facility f at the rated capacity is calculated as:

$$C_{P,f} = (P_{\max(f)} \times \cos(\theta_{mf})) \frac{AC_f}{\left|S_{\max(f)}\right|} \tag{6.12}$$

The extent of facility f cost ($C_{Q,f}$) due to reactive power flow in the facility f at the rated capacity is calculated as:

$$C_{Q,f} = (Q_{\max(f)} \times \sin(\theta_{mf})) \frac{AC_f}{\left|S_{\max(f)}\right|} \tag{6.13}$$

Facility f annual chargeable network cost ($ACR_{P,f}$) (based on its used capacity) for its actual active power flow contribution to apparent power (actual) flow in the facility is calculated as:

$$ACR_{P,f} = \frac{P_f \times \cos(\theta_f)}{P_{\max(f)} \times \cos(\theta_{mf})}\ C_{P,f} \tag{6.14}$$

$$ACR_{P,f} = \frac{P_f \times \cos(\theta_f)}{\left|S_{\max(f)}\right|}\ AC_f \tag{6.15}$$

$$ACR_{P,f} = \frac{\left|S_f\right| \times \cos^2(\theta_f)}{\left|S_{\max(f)}\right|}\ AC_f \tag{6.16}$$

Facility f annual chargeable network cost $(ACR_{Q,f})$ (based on its used capacity) for its actual reactive flow contribution to apparent power (actual) flow in the line is calculated as:

$$ACR_{Q,f} = \frac{Q_f \times \sin(\theta_f)}{Q_{\max(f)} \times \sin(\theta_{mf})}\ C_{Q,f} \tag{6.17}$$

$$ACR_{Q,f} = \frac{Q_f \times \sin(\theta_f)}{\left|S_{\max(f)}\right|}\ AC_f \tag{6.18}$$

$$ACR_{Q,f} = \frac{\left|S_f\right| \times \sin^2(\theta_f)}{\left|S_{\max(f)}\right|}\ AC_f \tag{6.19}$$

AC_f , $C_{P,f}$, $C_{Q,f}$ S_f , $ACR_{Q,f}$ and $ACR_{P,f}$ are computed for all existing facilities in the distribution system. Equations (6.16) and (6.19) are the key development in the proposed charging methodology; they provide simple formulae for obtaining the network chargeable cost.

Therefore, the total network/system chargeable cost (based on utilized capacity) due to active and reactive power contribution to the apparent power flow is:

$$C_P = \sum_{f=1}^{m} ACR_{P,f} \tag{6.20}$$

$$C_Q = \sum_{f=1}^{m} ACR_{Q,f} \tag{6.21}$$

where m= total number of the facilities in the distribution system.

Once the system costs for reactive and real power are assigned, the total network usage cost associated with a customer T is given by following equation:

$$CC_T = \frac{\sum_f (MW\,f)_T \times L_f}{\sum_T (\sum_f (MW\,f)_T \times L_f)} \times C_P + \frac{\sum_f (MVAr\,f)_T \times L_f}{\sum_T (\sum_f (MVAr\,f)_T \times L_f)} \times C_Q \tag{6.22}$$

where

CC_T = total annual cost/rate for network user T.

L_f = length of facility *f.*

f=1,2,.....m.

T= 1,2.....C.

Total annual recovered cost=$\sum_{T=1}^{C} CC_T$ (6.23)

The total unrecovered cost (UNC) due to underutilized capacity of facilities supporting power flow in the distribution network is calculated by:

$$UNC = \sum_{f=1}^{m} AC_f - \sum_{T=1}^{C} CC_T \tag{6.24}$$

where, C=total number of users associated with a distribution system.

It is apparent from the developed DUoS charging algorithm equations, network users will be charged for the utilised network capacity, additionally, there is a provision to penalize the associated customers operating at poor power factor by charging for the amount of reactive power they are drawing from the network. This particular feature encourages users to act in a manner for the betterment of system condition.

For large power system network with deeper penetration of renewable energy sources, it is very difficult to get the desired nodal pricing by checking power flow path and facility supporting it and hence a suitable modification in the proposed DUoS charging method is need of the hour. The proposed algorithm has been further modified to achieve the aforementioned objectives. The sequential steps are listed below:

1) Obtain the power flowing through each branch in the distribution network.
2) In the subsequent step, facilities annuity cost at their rated capacity are computed.
3) Calculate $ACR_{P,f}$ and $ACR_{Q,f}$ for all existing facilities of the distribution system using equations (6.15) and (6.18) respectively considering base case branch flows.
4) Sub sequentially, compute C_P and C_Q using computed value of $ACR_{P,f}$ (for all facilities) and $ACR_{Q,f}$ (for all facilities) respectively {refer step 3} using equations (6.19) and (6.20) respectively considering base case branch flows.
5) Add 1MW of load at any single bus (T) except slack bus to the existing base system (one bus at a time) and obtain the power flow results of modified system.
6) Calculate new value of $ACR_{P,f}$ and $ACR_{Q,f}$ for all existing facilities in the distribution network considering the newly obtained power flow results.
7) Using the newly computed value of $ACR_{P,f}$ and $ACR_{Q,f}$ for all existing facilities in the network, calculate C_P and C_Q .
8) The total annual DUoS charges to be paid by network user T for drawing 1MW of real power from the network is given by the following equation:

$$CC(TP) = \Delta C_P + \Delta C_Q \quad (6.25)$$

$$\Delta C_P = C_P \; obtained \; for \; base \; case - C_P \; obtained \; after \; 1 \; MW \; load \; addition$$

$$\Delta C_Q = C_Q \; obtained \; for \; base \; case - C_Q \; obtained \; after \; 1 \; MW \; load \; addition$$

9) Repeat step 5, 6, 7 and 8 for the entire utility centres/bus locations in the network.

10) The cost due to reactive power is obtained by adding 1MVAr of load at a bus T (one bus at a time) and obtain the power flowing through each facility in the distribution network.

11) Calculate new value of $ACR_{P,f}$ and $ACR_{Q,f}$ for all existing facilities in the distribution network considering the newly obtained power flow results.

12) Using the newly computed value of $ACR_{P,f}$ and $ACR_{Q,f}$ for all existing facilities in the network, calculate C_P and C_Q .

13) The total annual DUoS charges to be paid by network user T for drawing 1MVAr of reactive power from the network is given by the following equation:

$$CC(TQ) = \Delta C_P + \Delta C_Q \quad (6.26)$$

$$\Delta C_P = C_P \; for \; base \; case - C_P \; after \; 1 \; MVAr \; load \; addition$$

$$\Delta C_Q = C_Q \; for \; base \; case - C_Q \; after \; 1 \; MVAr \; load \; addition$$

14) Repeat step 10, 11, 12 and 13 for the entire utility centres/bus locations in the distribution system.

6.3 Results

This Section is divided into three parts. In the first part of this section, the proposed DUoS charging methodology has been validated by comparing with the already established methods on a small test systems. In the second part, the impact of renewable generations on the network protection cost requirement has been thoroughly investigated. The aforesaid analysis will provide the net additional cost required for upgrading the protection system of conventional distribution system for its successful operation in the presence of renewable generations. The additional protection renovation cost will significantly impact the total installation costs of distribution network and consequently, it will have a considerable economic impact on the distribution network users (loads, industrial consumers, generators etc.). Distribution use of system (DUoS) charge is a key factor for scrutinizing the economic

impact of renewable generation on distribution network customers. The next sub-section will elaborate the impact of renewable generations on DUoS charges due to additional protection cost requirement. The test systems are IEEE-33 bus system [72] and IEEE-69 bus system [73].

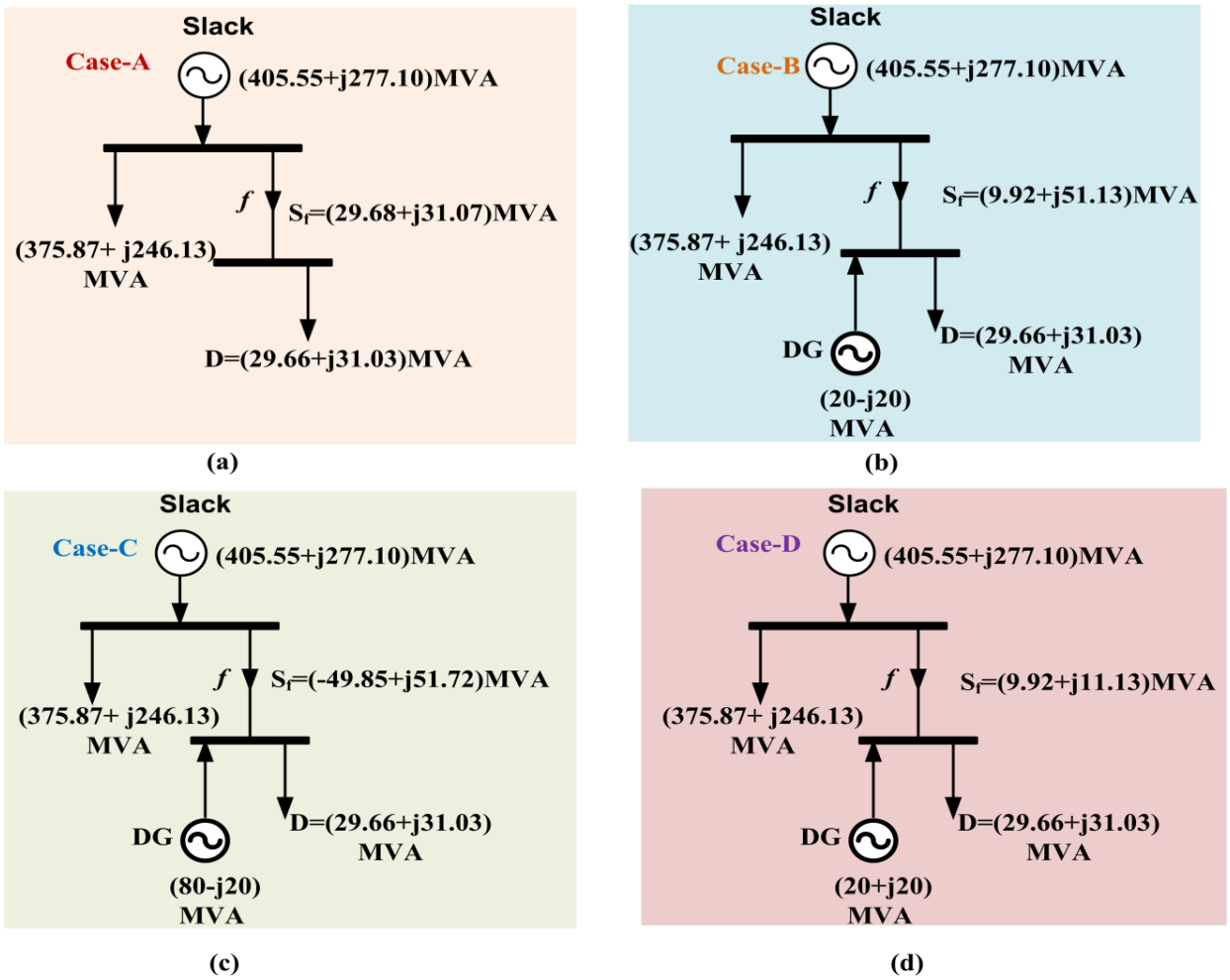

Fig. 6.4: Load flow results of a reduced 2-bus bar system (a) Without distributed generations (base case power flow), (b) In the presence of distributed generations injecting (20-j20)MVA, (c) In the presence of distributed generations injecting (80-j20)MVA, (d) In the presence of distributed generations injecting (20+j20)MVA.

6.3.1 Validation of the proposed distribution network charging methodology

In this section the efficacy comparison of the proposed charging method with other existing methods have been carried out on a small test system. The test system is an eight bus system

which is a part of practical Western Power Distribution network [112]. The system has been further reduced to 2-bus network, as shown in Fig. 6.4(a).

For better understanding, the study illustrates the proposed DUoS charging method by only allocating facility *f* cost to customers at bus 2 according to their extent of the use of the facility. Table 6.1 provides the charges to both generation and demand customers considering four different cases utilising the concept of proposed DUoS charging methodology. For each case, the assumed generator's ratings, its associated reactive power outputs, and resultant power flow over line *f* for supporting its associated customers are provided in Fig. 6.4. The comparison between different methodologies has been carried out considering four test cases (Table 6.2).

- **Case A: Distribution system with demand customer only**

In this case only demand customers are connected to bus 2 as shown in Fig. 6.4(a). The charges are levied on the customer associated with bus 2 in accordance with the extent to which they utilise the network facility *f*. The distribution use of system charges utilizing the proposed method (PM), MW-Miles method, MVA-Miles method, and existing MW+MVAr-Miles method are presented in Table 6.2. As evident from the test results that the net recovery using MW-Miles model is a small proportion of total network annuity cost as it considers real power only, leaving large unrecovered revenue to be allocated in an uneconomical approach. Both MVA-miles and MW+MVAr-Miles (existing and proposed) recover significantly higher revenue as both real and reactive power are taken into consideration.

- **Case B: Distribution system with wind generation injecting (20-j20) MVA power to the network**

In this case, the distributed generation is injecting 20MW real power to the network and withdrawing 20 from the network. It is quite obvious from the load flow result that , the real power flowing through the facility *f* has been reduced, hence, DG should be credited for its active power injection to the network. On the other hand, the system loading has been increased by 21% due to reactive power drawn by the DG from the network and hence charges should be levied on the DG for its reactive power withdrawal. Table 6.2 provides the charges to both generation and demand customers from the four charging models. The MW-

Miles method credits the DG for its real power injection but fails to penalise for its reactive power drawn from the network, leading to a favourable appraisal for the DG. The MVA-Miles method is an advanced pricing scheme as compared to MW-Miles. It accounts for the amount of network usage by consumers and also considers the real and reactive powers, whether injected or consumed. This method however fails to distinguish between the direction of real and reactive power flow and as a result, it credits the DG for both its real power injection to and reactive power drawn from the network. Hence, leads to false network charging. In contrast, the MW+MVAr-Miles method is capable to admire both cost and benefit of network users, especially DGs. As the DG has reduced active power withdrawn from the system, the DG has been praised for its active power injection but charged for its use of the network for withdrawing reactive power.

Table 6.1: Use of network charges

Test Case	Demand Charges (Unit Price)		Generation Charges (Unit Price)		Net Recovery £/yr
	CC(TP) £/MWh	*CC(TP)* £/MVArh	*CC(TP)* £/MWh	*CC(TP)* £/MVArh	
Case-A	0.2075	0.2174	-	-	113035
Case-B	0.0587	0.2954	-0.0587	0.2954	137015
Case-C	-0.2064	0.2191	0.2064	0.2191	188961
Case-D	0.2052	0.2261	-0.2052	-0.0061	39212

Table 6.2: Recovery of network cost using proposed method and other existing methods

Test Case	Net Recovery (£/yr)			
	PM	MW-Miles Method	MVA-Miles Method	Existing MW+MVAr-Miles Method
Case-A	**113035**	78131	112995	112728
Case-B	**137015**	25518	38589	100375
Case-C	**188961**	132349	103935	188018
Case-D	**39212**	25518	38589	38536

- **Case C: Distribution system with wind generation injecting (80-j20) MVA power to the network**

In this case, the distributed generation is injecting 80MW real power to the network and withdrawing 20 from the network. The loading level of the supporting facility *f* is increased by 40% owing to the DG's real power injection as well as reactive power withdrawn.

Consequently, remunerations should be paid by DG to the distribution network operator for its active power injection. In addition, charges should be levied on DG for its reactive power drawn from the test network. As evident from the Table 6.2 that the MW-Miles DUoS charging scheme did not penalize customer for its reactive power drawn from the network. Hence, the revenue recoveries from both demand and generating customer is low. The MVA-Miles scheme fails to detect the direction of power flows, leading to over-credit the demand consumers. On the contrary, the proposed network charging methodology is proficient in charging the DG for its active power injection and reactive power withdrawal.

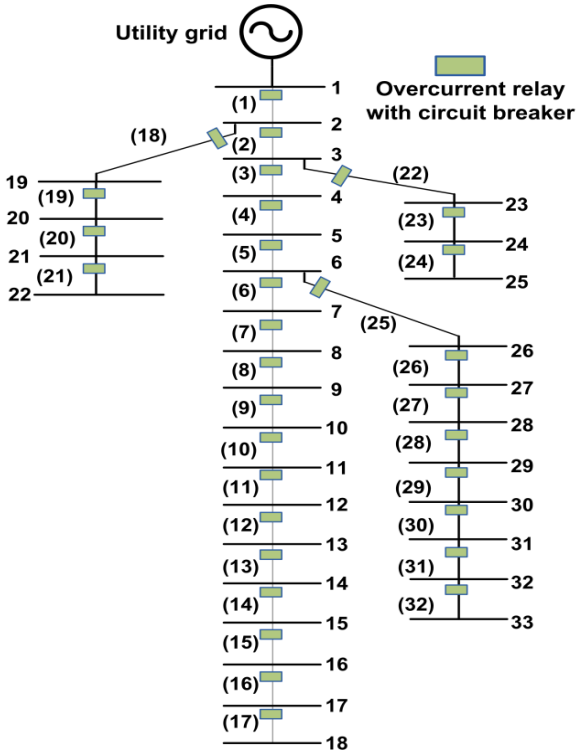

Fig. 6.5: Conventional protection scheme for IEEE-33 bus distribution network with unidirectional power flow.

- **Case D: Distribution system with wind generation injecting (20+j20) MVA power to the network**

In this case, the DG is injecting (20+20) MVA to the network, supporting the load customer for its active and reactive power perquisite leading to drop in system loading level. Consequently, remuneration has been paid to DG for both active and reactive power injection when using MVA-Miles and MW+MVAr-Miles (existing and proposed) where as using MW-Miles method DG has been credited for its real power injection to the network only. In

Table 6.2, the comparative cost analysis of all charging methods has been clearly exemplified. It is quite evident from the Table 6.2, that the proposed charging methodology accounts for higher network cost recovery compared to other existing charging methods.

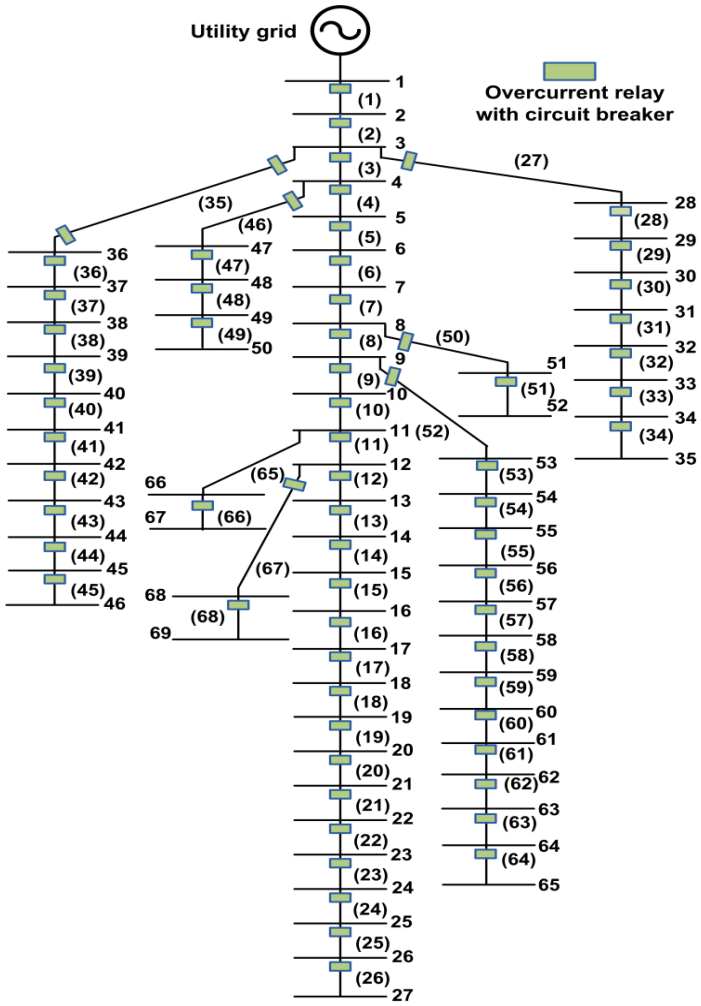

Fig. 6.6: Conventional protection scheme for IEEE-69 bus distribution network with unidirectional power flow.

For large sized distribution network with deeper penetration of renewable generations, the existing MW+MVAr-miles method finds it very difficult in obtaining the DUoS charging calculations by checking power flow path and facilities supporting it. Hence, proposed DUoS charging algorithm based on MW+MVAr-Miles method has been utilised in next sub-section for reflecting the impact of renewable generations on DUoS charges for the users associated with IEEE-33 bus and IEEE-69 bus test systems. With the proposed charging model for use

of network cost calculation, the customers are charged in accordance with the exactly used capacity of the network.

6.3.2 Additional protection cost requirement in the presence of renewable generations.

In this particular sub-section, the impact of renewable generations on the network protection cost requirement has been thoroughly investigated. The IEEE-33 and IEEE-69 bus distribution test systems have been taken into consideration for acquiring the aforementioned objective. The conventional overcurrent protection scheme for IEEE-33 bus and IEEE-69 bus distribution systems are shown in Fig. 6.5 and Fig. 6.6 respectively.

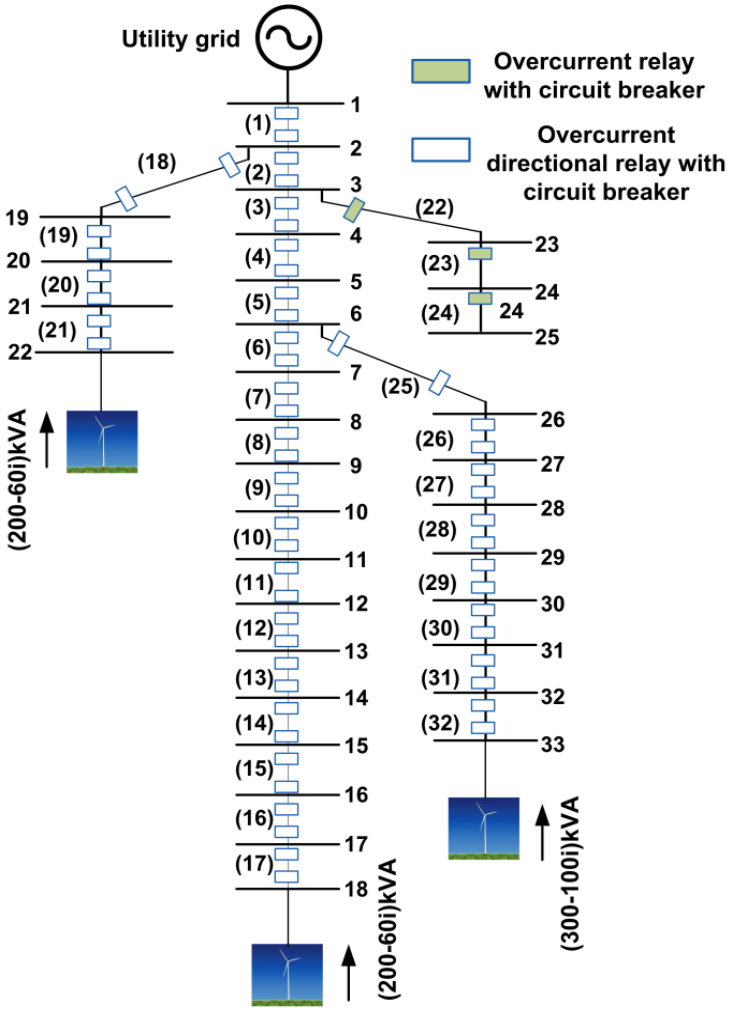

Fig. 6.7: The protection scheme for IEEE-33 bus distribution network in the presence of renewable generations.

Let us consider a scenario in which both the distribution systems are introduced with the wind based renewable generations. The conventional protection schemes that are designed for distribution system protection with radial flow is insufficient for distribution system protection with bidirectional power flow. Hence, a renovated protection scheme is required for successful operation of distribution system in the presence of renewable generations. The directional protection schemes for IEEE-33 bus and IEEE-69 bus distribution systems in the presence of wind generations are shown in Fig. 6.7 and Fig. 6.8 respectively.

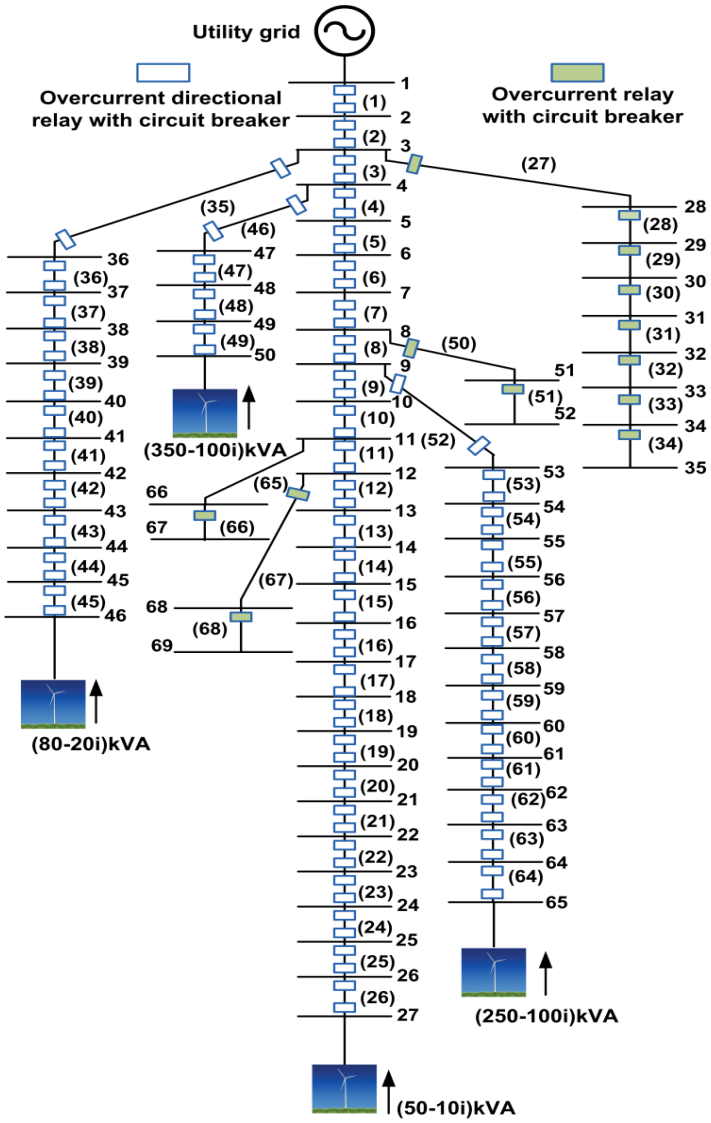

Fig. 6.8: The protection scheme for IEEE-69 bus distribution network in the presence of renewable generations

The renovation required for an existing conventional IEEE distribution systems to meet the requisite protection coordination in the presence of wind generations demands considerable investment. The significant reasons are listed below:

- Fault current is contributed by all connected sources in the system and thereby fault current can be bidirectional. Directional overcurrent relay with associated circuit breaker are required for both ends of a feeder connecting two buses where there is possibility of bidirectional fault current flow {Fig. 6.7 and Fig. 6.8}. As evident form Fig. 6.7 and Fig. 6.8, the line sections {except lines 22-24 in Fig. 6.7 and lines 27-34, 50-51 & 65-68 in Fig. 6.8} requires additional breaker at the remote end to clear the faults from renewable source side. For each breaker in the line except the abovementioned lines, overcurrent relay with directional feature is required. There is no need to change the relay of the mentioned lines {lines 22-24 in Fig. 6.7 and lines 27-34, 50-51 & 65-68 in Fig. 6.8} as they are still radial in nature.
- It is evident from Table 6.3 and Table 6.4 that with the inclusion of renewable generations the short circuit level of the mentioned distribution systems rises and hence enhanced/advanced protection scheme is essentially required. The results shown in Table 6.3 (for Fig. 6.5 and Fig. 6.7) and Table 6.4 (for Fig. 6.6 and Fig. 6.8) are obtained by MVA method [120]. The breakers which do not meet the short circuit demand need to be replaced by higher capacity breakers (as per protection requirement of the system).
- The circuit breaker in the system is controlled by a relay which take signals from C.T and/or P.T. The protection system at each mentioned point needs battery and other accessories for successful operation of the protection system. Thus, the additional relay cost will be required for each facility {except lines 22-24 in Fig. 6.7 and lines 27-34, 50-51 & 65-68 in Fig. 6.8}. The relay embeds C.T/P.T and battery as their major components.

The cost to install one mile of a conventional three phase distribution system varies between $620,000.00 and $1,020,000.00 [121]. In this work the cost of conventional three phase distribution system installation per mile is taken as $720,000. With the inclusion of embedded generations in the IEEE-33 bus and IEEE-69 bus distribution systems, additional cost will be required for renovating the protection schemes for its successful functioning. It is evident from Table 6.5 that protection renovation cost for each facility individually {except

lines 22-24 in Fig. 6.7 and lines 27-34, 50-51 & 65-68 in Fig. 6.8} is 19000 USD. The overall additional network cost requirement is 551000 USD for IEEE-33 bus distribution system and 1026000 USD for IEEE-69 bus distribution system to meet the desired protection coordination in the presence of wind generations (Table 6.6). Hence, inclusion of renewable will significantly impact the distribution use of system charges.

Table 6.3: Short circuit capacity calculation of the distribution system shown in Fig. 6.5 and Fig. 6.7

Facility/ Branch (f)	Length of Facility (Mile)	Max. Capacity (MVA)	Short Circuit MVA(Without DG) (Fig.5)	Short Circuit MVA(With DG at bus18,33 and 22) (Fig.7)
1	0.062	8	350.23	358.79
2	0.310	8	134.63	147.48
3	0.217	5	92.40	108.75
4	0.217	5	69.65	88.64
5	0.497	5	42.92	67.25
6	0.124	3	34.91	53.86
7	0.435	3	28.71	44.98
8	0.621	2.5	22.06	35.80
9	0.621	2.5	17.98	31.96
10	0.124	2.5	17.43	33.03
11	0.217	2.5	16.49	32.25
12	0.932	2.5	13.15	29.06
13	0.341	2	11.98	32.42
14	0.372	2	11.11	34.94
15	0.466	2	10.24	45.95
16	0.808	2	8.66	109.20
17	0.435	2	8.12	120.44
18	0.093	1.5	211.47	223.40
19	0.932	1.2	46.59	101.89
20	0.248	1.2	37.50	118.01
21	0.435	1.2	27.48	152.33
22	0.279	3	83.72	88.31
23	0.560	2.5	46.73	51.30
24	0.560	1.5	32.46	37.71
25	0.124	2.5	39.71	57.19
26	0.186	2.5	35.95	55.31
27	0.621	2.5	25.32	53.58
28	0.497	2.5	20.70	58.62
29	0.310	2.5	18.86	64.56
30	0.590	1.2	15.54	103.76
31	0.186	1.2	14.65	150.18
32	0.217	1.5	13.61	206.50

Table 6.4: Short circuit capacity calculation of the distribution system shown in Fig. 6.6 and Fig. 6.8

Facility/ Branch (f)	Length of Facility (Mile)	Max. Capacity (MVA)	Short Circuit MVA(Without DG) (Fig.6)	Short Circuit MVA (With DG at bus 27,46, 50 and 65) (Fig.8)
1	0.0003	8	497.3284	497.3301
2	0.0003	8	494.6852	494.6912
3	0.001	8	486.9215	486.952
4	0.017	5	421.3722	422.1096
5	0.247	5	173.3799	185.5723
6	0.257	5	107.5009	125.9658
7	0.062	5	98.4492	118.0167
8	0.033	5	94.1886	114.309
9	0.552	2	56.3516	72.2494
10	0.126	2	51.6123	67.4679
11	0.479	1	39.1125	55.783
12	0.694	0.6	28.9591	48.3737
13	0.704	0.6	22.9261	46.8525
14	0.713	0.6	18.9296	50.3685
15	0.132	0.6	18.3356	51.7169
16	0.252	0.5	17.3018	55.1213
17	0.003	0.5	17.2895	55.1725
18	0.221	0.3	16.4771	59.3383
19	0.142	0.35	15.9941	62.7985
20	0.23	0.35	15.2680	70.2561
21	0.009	0.15	15.2396	70.6239
22	0.107	0.15	14.9247	75.2436
23	0.233	0.15	14.2821	89.0711
24	0.505	0.05	13.0659	167.6246
25	0.208	0.05	12.6224	287.652
26	0.117	0.05	12.3867	499.8742
27	0.003	0.2	472.1732	472.1917
28	0.043	0.1	284.4766	284.4834
29	0.268	0.1	143.3116	143.3134
30	0.047	0.1	131.7726	131.7742
31	0.237	0.1	93.9500	93.9506
32	0.565	0.1	55.6855	55.6858
33	1.151	0.05	30.4647	30.4647
34	0.993	0.05	21.9033	21.9033
35	0.003	0.3	472.1732	472.3531
36	0.043	0.25	284.4766	294.8556
37	0.071	0.25	206.0418	226.5143
38	0.02	0.25	190.8526	213.9398
39	0.001	0.2	190.0236	213.2622
40	0.491	0.2	68.8758	164.577
41	0.209	0.25	54.1724	258.7226
42	0.028	0.25	52.6869	290.019
43	0.006	0.15	52.3494	298.8865
44	0.073	0.15	48.6601	496.9224
45	0.001	0.1	48.6308	520.3301
46	0.002	1.5	469.7898	477.3891

Facility/ Branch (f)	Length of Facility (Mile)	Max. Capacity (MVA)	Short Circuit MVA(Without DG) (Fig.6)	Short Circuit MVA (With DG at bus 27,46, 50 and 65) (Fig.8)
47	0.057	1.5	250.7382	280.0259
48	0.195	1.5	96.9079	287.9295
49	0.055	1	82.5454	325.8808
50	0.063	0.1	90.7578	107.258
51	0.224	0.05	71.8820	82.039
52	0.117	3	81.7614	100.5199
53	0.137	3	70.8542	88.8907
54	0.192	3	59.7045	77.5631
55	0.19	3	51.6576	69.8657
56	1.072	3	30.1030	54.2908
57	0.528	3	24.9681	54.6101
58	0.205	3	23.4197	55.8934
59	0.26	2.5	21.7232	58.6133
60	0.342	2.5	19.7081	65.2823
61	0.066	0.5	19.3633	67.0819
62	0.098	0.5	18.8720	70.1761
63	0.479	0.5	16.7846	97.656
64	0.702	1	14.4439	156.4666
65	0.136	1	47.3641	60.4907
66	0.003	0.05	47.2734	60.3447
67	0.498	0.1	29.6020	46.1341
68	0.003	0.05	29.5661	46.0531

Table 6.5: Additional cost requirement for each facility except facilities/lines 22-24 in Fig. 6.7 and facilities/lines 27-34, 50-51 & 65-68 in Fig. 6.8

Equipment Name	Cost($)
Circuit Breaker	15000
Relay+ Battery	4000
Total Additional Cost Requirement for each facility	19000

Table 6.6: Total network cost requirement

Test System	**Protection Scheme**	**Total Network Cost ($)**
IEEE-33 Bus System (Fig. 6.5)	Conventional Overcurrent Protection Scheme	9104329
IEEE-33 Bus System (Fig. 6.7)	Directional Overcurrent Protection Scheme	9655329
Total Additional Cost ($) = IEEE-33 Bus System (Fig. 6.5)- IEEE-33 Bus System (Fig.6.7)		551000
IEEE-69 Bus System (Fig. 6.6)	Conventional Overcurrent Protection Scheme	11464785
IEEE-69 Bus System (Fig. 6.8)	Conventional Overcurrent Protection Scheme	12490785
Total Additional Cost ($) = IEEE-33 Bus System (Fig. 6.6)- IEEE-33 Bus System (Fig. 6.8)		1026000

6.3.3 Impact investigation of renewable generations on the distribution use of system charges

This section in particular investigates the impact of protection system reinforcement costs on the consumers associated with renewable integrated distribution network. The sequential steps required for acquiring the aforementioned objective are as follow:

Step 1. Compute the total network cost and total network annuity costs of conventional distribution network i.e. the distribution network with conventional protection scheme.

Step 2. Subsequently, calculate the additional cost required for revamping the protection system of existing distribution network when renewable generations are being integrated to it (using the methodology developed in section 6.3.2).

Step 3. Compute the total network cost and total network annuity costs of renewable integrated modern distribution network i.e. the distribution network with overcurrent directional protection scheme. (using the methodology developed in section 6.3.2).

Step 4. Compute the DUoS charges considering three different scenarios i.e Case 1, Case 2 and Case3 (using the DUoS charging methodology developed in section 6.2):

Case 1: In the first case, DUoS charges needs to be calculated for the users associated with distribution system incorporating conventional protection scheme (also called as conventional distribution network).

Case 2: In the second case, DUoS charges have been calculated for the users associated with distribution system (incorporating conventional protection scheme) in the presence of renewable generations.

Case 3: In the third case, DUoS charges have been calculated for the users associated with distribution system incorporating directional protection scheme (also called as modern distribution network) in the presence of renewable generations.

Step 5. On comparing and analysing the obtained results, the main objective of this article could be achieved.

The problem solving steps have been explicitly explained through the flowchart embedding complete steps to investigate the impact of protection system reinforcement cost on the consumers associated with renewable integrated distribution network (Fig. 6.9). The test systems are standard IEEE-33 bus system and IEEE-69 bus system. All the aforementioned

steps have been carried out on the IEEE-33 bus and IEEE-69 bus distribution systems. The cost related analysis (i.e total network cost and total network annuity cost calculations) of the conventional distribution networks {distribution system with conventional overcurrent protection scheme} (Fig. 6.5 and Fig. 6.6) and renewable integrated modern distribution networks (Fig. 6.7 and Fig. 6.8) have been explicitly exemplified in section 6.3.2 of this article. It is obvious from Table 6.6, that network cost requirement for IEEE-33 and IEEE-69 bus distribution systems with directional overcurrent protection scheme is significantly higher than the conventional IEEE-33 and IEEE-69 bus distribution systems respectively. The additional cost required for upgrading the protection of existing conventional distribution system is an ample amount and will significantly impact the consumers. Distribution use of system (DUoS) charge is a key factor for scrutinizing the economic impact of renewable generation on distribution network users.

For our purpose, DUoS charges are calculated for the users associated with the mentioned distribution systems considering three different scenarios/cases.

1) **Case 1*:*** In the first case, DUoS charges have been calculated for the users associated with:
   - ✓ Conventional IEEE-33 bus distribution system (Fig. 6.5) .
   - ✓ Conventional IEEE-69 bus distribution system (Fig. 6.6).
2) **Case-2*:*** In the second case, DUoS charges have been calculated for the users associated with:
   - ✓ IEEE-33 bus distribution system (incorporating conventional overcurrent protection scheme) in the presence of wind generations injecting (200-60i) kVA, (200-60i) kVA and (300-100i) kVA at bus number 18,22 and 33 respectively.
   - ✓ IEEE-69 bus distribution system (incorporating conventional overcurrent protection scheme) in the presence of wind generations injecting (50-10i) kVA, (80-20i) kVA, (350-100i) and (250-100i) kVA at bus number 27, 46, 50 and 65 respectively.
3) **Case-3*:*** In the last case, DUoS charges have been calculated for the users associated with
   - ✓ IEEE-33 bus distribution system (with associated directional protection scheme) (Fig. 6.7) in the presence of wind generations injecting (200-60i) kVA, (200-60i) kVA and (300-100i) kVA at bus number 18,22 and 33 respectively.

- ✓ IEEE-69 bus distribution system (with associated directional protection scheme) (Fig. 6.8) in the presence of wind generations injecting (50-10i) kVA, (80-20i) kVA, (350-100i) and (250-100i) kVA at bus number 27, 46, 50 and 65 respectively.

The obtained results and their comprehensive analysis will provide the means to investigate the impact of protect system reinforcement costs on the consumers associated with renewable integrated distribution networks (IEEE 33 and IEEE-69).

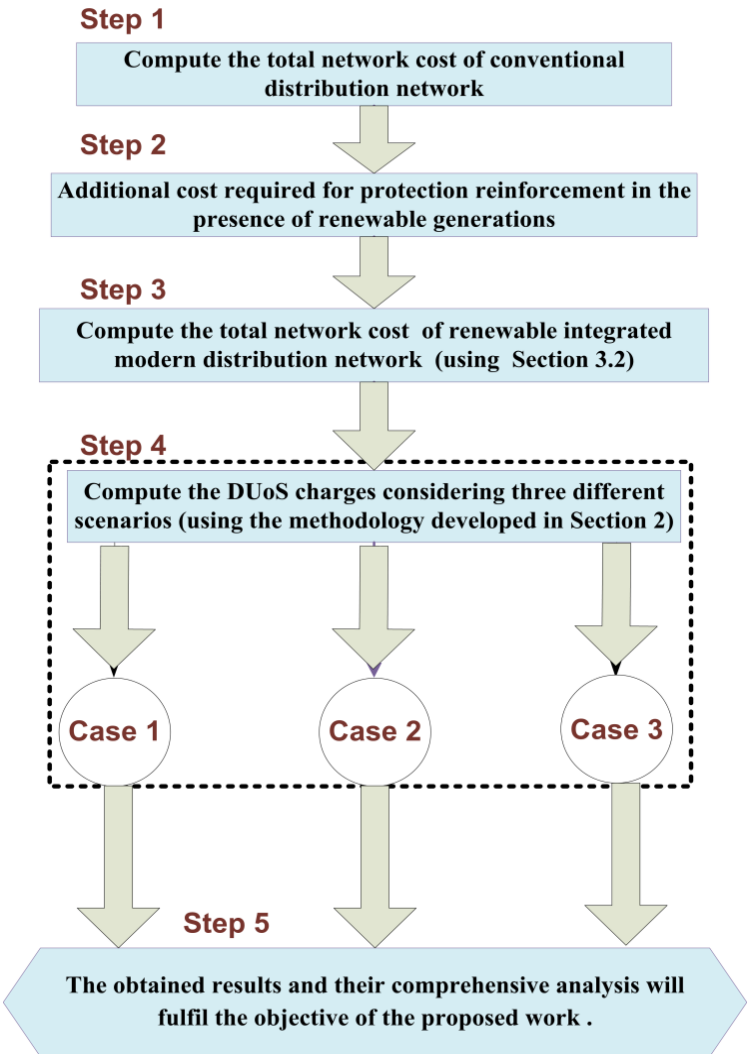

Fig. 6.9: Flowchart for investigating the economic impact of protection system reinforcement cost on the consumers

Table 6.7: Network Annuity Cost, Recovered Cost, Un-recovered Cost and Reconciliation Rate calculated for IEEE-33 bus distribution network.

Case Study	Network Annuity Cost ($)	Recovered Cost (Annually in $)	Un-Recovered Cost (Annually in $)	Reconciliation Rate ($/MWh)
Case-1	965787.3	284434.7	681352.6	20.90
Case-2	965787.3	246942.6	718844.7	18.58
Case-3	1024237	256707.6	767529.4	19.84

Table 6.8: Network Annuity Cost, Recovered Cost, Un-recovered Cost and Reconciliation Rate calculated for IEEE-69 bus distribution network.

Case Study	Network Annuity Cost ($)	Recovered Cost (Annually in $)	Un-Recovered Cost (Annually in $)	Reconciliation Rate ($/MWh)
Case-1	1216184	700030	516154.5	21.96
Case-2	1216184	648896.2	567287.8	14.082
Case-3	1325022	700002	608418.8	15.737

Table 6.9: Use of distribution network charges for IEEE-33 bus network users (loads and generators) due to their real and reactive power

Bus (T)	*CC(TP)* $/MW/hour			*CC(TQ)* $/MVAr/hour		
	Case-1	Case-2	Case-3	Case-1	Case-2	Case-3
1	NA	NA	NA	NA	NA	NA
2	0.166	0.121	0.129	0.105	0.15	0.16
3	0.997	0.731	0.775	0.633	0.904	0.967
4	1.576	1.156	1.225	1.002	1.432	1.532
5	2.159	1.584	1.679	1.37	1.958	2.095
6	3.486	2.556	2.71	2.216	3.168	3.389
7	3.817	2.799	2.968	2.426	3.469	3.711
8	4.978	3.652	3.871	3.165	4.525	4.841
9	6.637	4.868	5.161	4.219	6.033	6.454
10	8.297	6.086	6.452	5.271	7.538	8.064
11	8.629	6.33	6.71	5.483	7.842	8.389
12	9.209	6.755	7.161	5.854	8.372	8.957
13	11.697	8.58	9.096	7.435	10.633	11.376
14	12.612	9.251	9.807	8.017	11.465	12.265
15	13.607	9.981	10.581	8.658	12.381	13.246
16	14.853	4.991	5.235	9.438	13.498	14.44
17	17.007	1.768	1.819	10.813	15.465	16.544

Bus (T)	*CC(TP)* $/MW/hour			*CC(TQ)* $/MVAr/hour		
	Case-1	Case-2	Case-3	Case-1	Case-2	Case-3
18	18.172	0.864/ **-0.864**	0.916/ **-0.916**	11.552	16.518/ **16.518**	17.671/ **17.671**
19	0.416	0.305	0.323	0.264	0.376	0.403
20	2.905	2.503	2.62	1.847	2.64	2.824
21	3.567	1.399	1.45	2.267	3.241	3.467
22	4.73	0.517/ **-0.517**	0.548/ **-0.548**	3.005	4.299/ **4.299**	4.6/ **4.6**
23	1.742	1.278	1.354	1.107	1.583	1.693
24	3.236	2.374	2.516	2.057	2.941	3.146
25	4.73	3.469	3.678	3.007	4.299	4.6
26	3.815	2.798	2.966	2.424	3.467	3.709
27	4.313	3.164	3.354	2.744	3.923	4.197
28	5.974	4.382	4.645	3.794	5.426	5.805
29	7.302	5.356	5.678	4.642	6.638	7.101
30	8.131	5.964	6.323	5.169	7.392	7.908
31	9.709	5.868	6.22	6.172	8.826	9.443
32	10.206	0.826	0.852	6.487	9.276	9.924
33	10.785	0.377/ **-0.377**	0.40/ **-0.40**	6.858	9.805/ **9.805**	10.489/ **10.489**

Table 6.10: Use of distribution network charges for IEEE-69 bus network users (loads and generators) due to their real and reactive power

Customer Bus (T)	*CC(TP)* $/MW/hour			*CC(TQ)* $/MVAr/hour		
	Case-1	Case-2	Case-3	Case-1	Case-2	Case-3
1	NA	NA	NA	NA	NA	NA
2	0	0	0	0	0	0
3	0	0	0	0	0	0
4	0	0	0	0	0	0
5	0	0	0	0	0	0
6	1.575	1.367	1.469	1.07	1.359	1.513
7	3.099	2.691	2.892	2.106	2.675	2.979
8	3.468	3.011	3.236	2.356	2.994	3.333
9	3.666	3.183	3.42	2.49	3.164	3.523
10	6.942	6.028	6.478	4.717	5.993	6.672
11	7.691	6.678	7.177	5.225	6.639	7.392
12	10.537	9.149	9.833	7.159	9.096	10.127
13	14.658	12.727	13.678	9.959	12.653	14.088
14	18.835	16.353	17.575	12.797	16.258	18.102
15	0	0	0	0	0	0
16	23.854	20.711	22.259	16.207	20.591	22.927
17	25.353	22.012	23.657	17.225	21.884	24.366
18	25.371	22.028	23.675	17.237	21.9	24.384
19	0	0	0	0	0	0
20	27.524	23.898	25.684	18.701	23.759	26.454
21	28.891	25.084	26.959	19.629	24.939	27.767

Customer Bus (T)	*CC(TP)* $/MW/hour			*CC(TQ)* $/MVAr/hour		
	Case-1	Case-2	Case-3	Case-1	Case-2	Case-3
22	28.947	25.133	27.012	19.667	24.986	27.82
23	0	0	0	0	0	0
24	30.969	11.177	12.012	21.04	26.731	29.763
25	0	0	0	0	0	0
26	35.201	2.651	2.849	23.916	30.385	33.832
27	35.893	2.049/ **-2.049**	2.202/ **-2.202**	24.387	30.985/ **30.985**	34.499/ **34.499**
28	0.022	0.019	0.02	0.015	0.019	0.021
29	0.278	0.241	0.259	0.189	0.24	0.267
30	0	0	0	0	0	0
31	0	0	0	0	0	0
32	0	0	0	0	0	0
33	6.911	6	6.449	4.696	5.966	6.642
34	13.744	11.933	12.825	9.338	11.864	13.21
35	19.642	17.054	18.328	13.345	16.955	18.878
36	0.022	0.019	0.02	0.015	0.019	0.021
37	0.278	0.241	0.259	0.189	0.24	0.267
38	0	0	0	0	0	0
39	0.821	0.712	0.766	0.558	0.708	0.789
40	0.828	0.719	0.772	0.562	0.715	0.796
41	3.742	3.249	3.491	2.542	3.23	3.596
42	0	0	0	0	0	0
43	5.146	4.468	4.802	3.496	4.442	4.946
44	0	0	0	0	0	0
45	5.618	1.047	1.126	3.817	4.85	5.4
46	5.622	0.001/ **-0.001**	0.0015/ **-0.0015**	3.82	4.853/ **4.853**	5.403/ **5.403**
47	0	0	0	0	0	0
48	0.364	0.316	0.339	0.247	0.314	0.35
49	1.523	1.322	1.421	1.035	1.315	1.464
50	1.852	0.145/ **-0.145**	0.156/ **--0.156**	1.259	1.599/ **1.599**	1.78/ **1.78**
51	3.839	3.334	3.583	2.609	3.314	3.69
52	5.167	4.486	4.822	3.511	4.46	4.966
53	4.362	3.787	4.07	2.963	3.765	4.192
54	5.174	4.492	4.828	3.515	4.466	4.973
55	6.311	5.479	5.889	4.288	5.448	6.065
56	0	0	0	0	0	0
57	0	0	0	0	0	0
58	0	0	0	0	0	0
59	18.15	15.759	16.936	12.331	15.667	17.444
60	0	0	0	0	0	0
61	21.725	18.863	20.273	14.76	18.753	20.88
62	22.115	17.743	19.069	15.025	19.09	21.255
63	0	0	0	0	0	0
64	25.537	6.521	7.008	17.351	22.044	24.544
65	29.702	2.905/ **-2.905**	3.122/ **-3.122**	20.18	25.639/ **25.639**	28.547/ **28.547**
66	8.496	7.376	7.928	5.772	7.334	8.166
67	8.515	7.392	7.945	5.785	7.35	8.184

Customer Bus (T)	*CC(TP)* $/MW/hour			*CC(TQ)* $/MVAr/hour		
	Case-1	Case-2	Case-3	Case-1	Case-2	Case-3
68	13.495	11.717	12.593	9.169	11.649	12.97
69	13.514	11.733	12.611	9.182	11.666	12.989

In case 1, only demand customers are associated with the conventional distribution systems. In cases 2 and 3 both demand and generation customers are associated with the conventional and modern distribution system respectively. For case 1 and case 2, the total network cost calculated is same, whereas, for case 3 the network cost calculated will be higher because of inclusion of advanced directional protection scheme (as evident form Table 6.7 and Table 6.8). The variation in use of network charge for the customers associated with IEEE-33 bus and IEEE-69 bus distribution test systems considering all the three cases are clearly illustrated in Table 6.9 and Table 6.10 respectively. The rate at which wind generators associated with their respective distribution network are being charged have been highlighted in the Table 6.9 and Table 6.10 respectively. With the inclusion of wind generations into the system the network demand users have to pay at the higher rate for drawing reactive power from the network but at lesser rate for their active power.

The *T* vs *X(T) and T* vs *CC(TQ*) graphs have been plotted for both IEEE-33 bus and IEEE-69 bus distribution systems considering all the cases (Fig. 6.10 and Fig. 6.11 respectively).

where,

$$X(T)=\frac{\sum_{f}(MVAr_{f})_{T}\times L_{f}}{\sum_{T}(\sum_{f}(MVAr_{f})_{T}\times L_{f})} \tag{6.27}$$

$$CC(TQ)=\frac{\sum_{f}(MVAr_{f})_{T}\times L_{f}}{\sum_{T}(\sum_{f}(MVAr_{f})_{T}\times L_{f})}\times C_{Q} \tag{6.28}$$

CC(TQ)= Extent of use of network cost for customer T with respect to their reactive power.

T= Customers located at bus number T.

An interesting result is obtained by comparing these two graphs (*T* vs *X(T) and T* vs *CC(TQ*)) plotted for all the cases. On comparing these two graphs for each cases, relation between *X(T) and CC(TQ*) can be obtained. It is evident from these graphs :

$$X(T) \propto CC(TQ) \tag{6.29}$$

Using equations (6.27) and (6.29):

$$\{\sum_{f}(MVAr_{f})_{T}\times L_{f}\}\propto CC(TQ) \tag{6.30}$$

The extent by which system power factor is affected because of customer T depends upon magnitude of reactive power and distance travelled by reactive power to support customer T. If X(T) is higher, then users located at bus T have to pay higher sum of money annually for their reactive power consumption. Hence, customers are being penalised or appraised in accordance they are for affecting system power factor (as evident from Fig 6.10 and Fig. 6.11). Accordingly, the proposed pricing algorithm encourages users to act based on the economic signal generated at each location. Thus, users will try to reduce their reactive power consumptions by investing in reactive power compensating devises, if they are paying decent sum of money annually for their reactive power consumption. By doing this, system power factor will be improved.

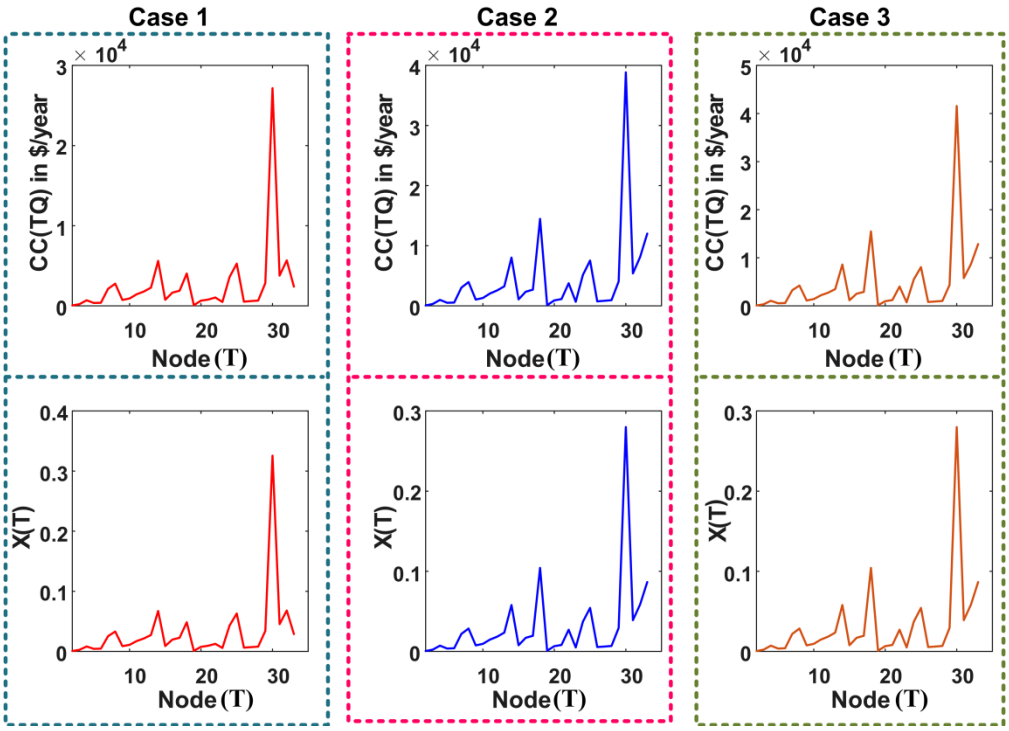

(a) (b) (c)

Fig. 6.10: *T* vs *X(T) and T* vs *CC(TQ) graph of IEEE-33 bus distribution network users considering* (a) Case-1 (b) Case-2 (c) Case-3.

As evident from Table 6.7 and Table 6.8, significant amount of the network revenue has been not recovered. To recover the desired annuity cost of the distribution network, suitable reconciliation approaches need to be applied. The most common reconciliation method that

has been widely adopted is namely, “fixed multiplier” and “fixed adder” [122-123]. The fixed adder technique adds/subtracts a fixed rate to/from the use of network charges to make up for the revenue shortfall/surplus. For our purpose fixed adder method has been adopted for network revenue recovery.

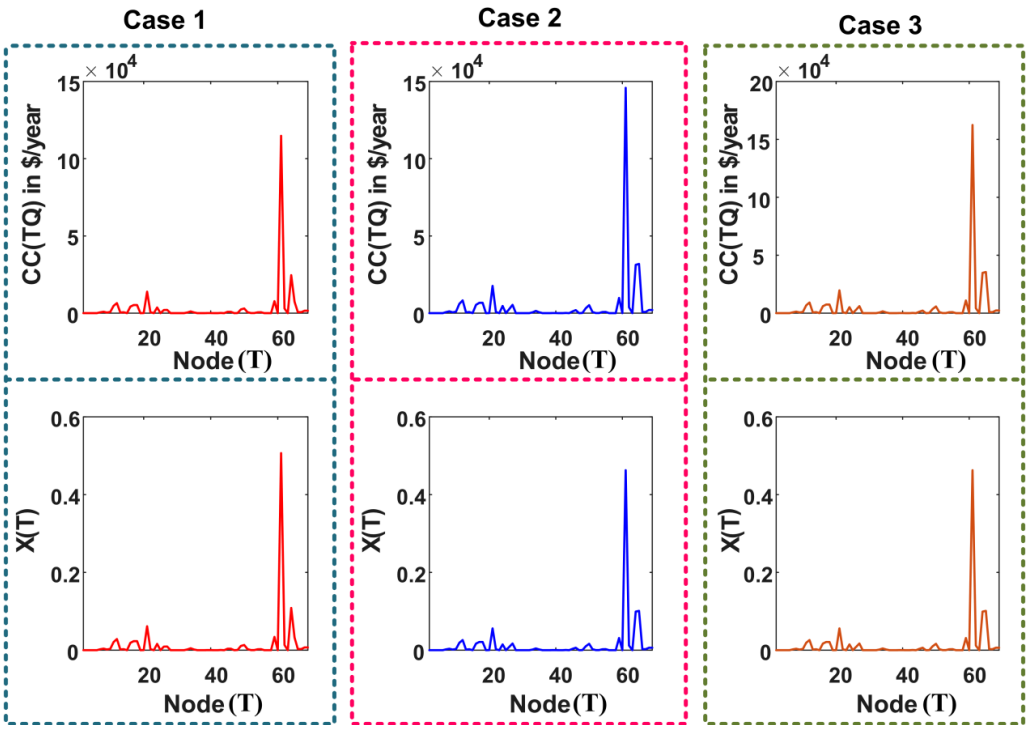

Fig. 6.11: *T* vs *X(T) and T* vs *CC(TQ) graph of IEEE-69 bus distribution network users considering* (a) Case-1 (b) Case-2 (c) Case-3.

6.4 Conclusion

This work comprehensively investigates the impact of renewable generations on the network protection cost requirement and its resulting consequences on DUoS charges. It has been revealed that with the inclusion of renewable generations into the distribution system, conventional overcurrent protection scheme fails to coordinate and hence up-gradation is required. The renovation required for an existing conventional distribution system to meet the requisite protection coordination in the presence of renewable generation demands considerable investment. It is evident from the test results that the capital investment cost required for a distribution system incorporating renewable generations is significantly higher

as compared to distribution system with radial power flow. As a result, distribution use of system charges will significantly vary. In order to calculate distribution use of system (DUoS) charges a DUoS charging algorithm is highly required and hence a power flow based MW+MVAr-Miles methodology has been proposed for charging network users. The developed charging methodology is used for separately pricing real and reactive power, taking into consideration not only the distance and magnitude they travel to support the customers, but also customers impact on system power factor. It is revealed from the load flow results that, the real power flowing through the facilities have been reduced, hence, DG should be credited for its active power injection to the network. On the other hand, charges should be levied on the DG for its reactive power withdrawal. It is precisely depicted that with the inclusion of wind generations into the distribution system, the associated customers have to pay at higher rate for its reactive power drawn from the network and at lower rate for its active power drawn from the network. The obtained DUoS charging results emphasize the significance of associated protection scheme with wind generators in a distribution system.

Chapter-7

Conclusions and Future Scopes

This chapter summarizes major findings of the work presented in this thesis and suggests direction for further investigations in the load flow analysis of AC-DC distribution network.

7.1 Conclusions

Based on the work reported in this thesis, the following conclusions are drawn:

- The algorithm developed for load flow analysis of AC distribution network is utilising the concept of graph theory and matrix algebra for solving load flow problem. Two developed matrices, loads beyond branch matrix [*LB*], the path impedance matrix [*PI*], and simple matrix multiplication are utilized to obtain load-flow solutions. Rest of the other supporting matrices have been derived from above two mentioned matrices. The developed method has been implemented on various unbalanced, balanced and weakly meshed distribution networks. However, in case of meshed &/or ring network it has been converted into its equivalent radial network by splitting the nodes or branches into two parts thus creating a breakpoint. The breakpoint power or current injection is calculated by formulating a breakpoint matrix and injecting the computed breakpoint power or current to one end of a breakpoint and withdrawing from the other end (depending upon the direction of loop current chosen). The load-flow solution of the meshed network is achieved in the same manner as radial distribution systems (after conversion to its equivalent radial network). The convergence characteristics of the proposed algorithm has been thoroughly investigated for various loading conditions. The comparison of the computational performance with already existing methods, in terms of number of iterations and CPU time, gives detail evidence of the efficacy of the proposed method developed in this work.
- The algorithm developed for solving load flow problem of AC distribution network has been further modified for solving the load flow problem of distribution network with distributed generations (DGs). Various models of DGs (PQ and PV) are incorporated in

the proposed load flow model. The DG modelled as PQ bus is included in the proposed load flow algorithm by considering injection by the DG as the negative load. The sensitivity or breakpoint matrix has been utilized to obtain the additional reactive power injection/withdrawal to maintain the specified voltage at each PV nodes. In the case of weakly meshed distribution network with PV type distributed generations, the loop breakpoint injections and PV breakpoint injections have been calculated simultaneously. The net injections is reflected in the *LB* or *LC* matrix of the distribution network. The effectiveness of the proposed solution methodology has been tested on several standard distribution systems and also comparing the convergence speed with the existing methods. Test outcome reveal viability and efficiency of the proposed method.

- The load flow solution for AC-DC radial distribution network has been developed. The concept formulated for AC distribution system load flow has been modified for solving the load flow problem of radial AC-DC distribution network by making use of proposed per-unit equivalent model (or actual phase model) of PWM and other power converters (taking care of enactment of control objectives). For our purpose, the AC-DC distribution network has been subdivided into a number of sub-distribution systems or sub-regions depending on number of bus-bus interfacing converters present in the distribution system. Each sub-region will act as separate distribution system. The relevant matrices formulation (as developed for AC distribution network) has been carried out for each sub-region separately. This algorithm is capable of handling various model of distributed generations. The DGs modelled as PQ and P bus can be included in the proposed load flow algorithm by considering injection by the DG as the negative load. A modified breakpoint matrix or sensitivity matrix (taking care the effect of converters present in the AC-DC distribution network) is formulated to compute the net additional injection by PV and V^{dc} type distributed generations. The net injections is reflected in the LBg or LCg matrix of the distribution network. Due to unavailability of a standard AC-DC distribution system at present, hypothetical test cases (10 bus and 15 bus AC-DC distribution system) have been considered and the performance of the AC-DC load flow algorithm is thoroughly investigated. The effectiveness of the proposed model has been verified against the load flow solution produced by PSCAD and BIBC

method. The test results demonstrate that the proposed load flow algorithm can provide precise solution while also offering the flexibility and speed required for online applications.

- The AC-DC load flow algorithm developed for radial network has been modified in a manner such that it provides the load flow solution for meshed AC-DC distribution systems. For converting meshed network to radial network, the loop breakpoint matrix has been derived for calculating loop breakpoint injections in AC-DC scenario. In the case of weakly meshed distribution network with PV type and V^{dc} type distributed generations, the loop breakpoint injections, PV breakpoint injections and V^{dc} breakpoint injections have been calculated simultaneously. The net injections is reflected in the loads beyond branch matrix or load current matrix of the distribution network. Note that except for some modifications needed to be done for the LB_g or LC_g matrices, the proposed solution techniques require no modification; therefore, the proposed method obtains the load-flow solution for AC-DC distribution system in the presence of distributed generations efficiently. Due to unavailability of a standard AC-DC distribution system at present, hypothetical test cases (33 bus and 13 bus AC-DC distribution system) have been considered and the performance of the AC-DC load flow algorithm is thoroughly investigated. The effectiveness of the proposed model has been verified against the load flow solution produced by PSCAD and reduced gradient approach (implemented in GAMS). The test results demonstrate that the proposed load flow algorithm can provide precise solution while also offering the flexibility and speed required for online applications.
- A study has been carried out to investigate the impact of renewable generations on the network protection cost requirement and its resulting consequences on DUoS charges. It has been revealed that with the inclusion of renewable generations into the distribution system, conventional overcurrent protection scheme fails to coordinate and hence up-gradation is required. The renovation required for an existing conventional distribution system to meet the requisite protection coordination in the presence of renewable generation demands considerable investment. It is evident from the test results that the capital investment cost required for a distribution system incorporating renewable generations is significantly higher as compared to distribution system with

radial power flow. As a result, distribution use of system charges will significantly vary. In order to calculate distribution use of system (DUoS) charges a DUoS charging algorithm is highly required and hence a power flow based MW+MVAr-Miles methodology has been proposed for charging network users. The developed charging methodology is used for separately pricing real and reactive power, taking into consideration not only the distance and magnitude they travel to support the customers, but also customers impact on system power factor. It is revealed from the load flow results that, the real power flowing through the facilities have been reduced, hence, DG should be credited for its active power injection to the network. On the other hand, charges should be levied on the DG for its reactive power withdrawal. It is precisely depicted that with the inclusion of wind generations into the distribution system, the associated customers have to pay at higher rate for its reactive power drawn from the network and at lower rate for its active power drawn from the network. The obtained DUoS charging results emphasize the significance of associated protection scheme with wind generators in a distribution system.

7.2 Future Scopes

The following are presumed as possible future extensions of aforementioned work:

- The proposed load flow analysis method for AC-DC distribution system has been developed only for balanced scenario. The research can be further extended for solving load flow problem of AC-DC distribution system with unbalanced AC parts.
- Development of harmonic Load flow algorithm for AC-DC Radial distribution system.
- Development of harmonic Load flow algorithm for AC-DC meshed distribution system.
- Optimal sitting and sizing of storages in the AC-DC distribution network.
- Optimal sitting and sizing of distributed generations in the AC-DC distribution network.

List of Publications

Journals

I. Krishna Murari and Narayana Prasad Padhy "A Network-Topology Based Approach for the Load Flow Solution of AC-DC Distribution System With Distributed Generations", ***IEEE Transaction on Industrial Informatics (IEEE)***, vol.15, no.3, 2019.

II. Krishna Murari, Narayana Prasad Padhy, Ashok Kumar Pradhan and Furong Li. "Investigating the Impact of Protection System Reinforcement Cost on the Consumers Associated with Renewable Integrated Distribution Network", ***IET Generation Transmission and Distribution (IET),*** vol.13, no.9, pp.1572-1588, 2019.

III. Krishna Murari, Narayana Prasad Padhy " An Efficient Load Flow Algorithm for AC-DC Distribution Systems" in ***Electric Power Component and Systems (Taylor & Francis),*** vol.46, no.8, pp.919-937, 2018.

IV. Krishna Murari and Narayana Prasad Padhy " An Efficient Graphical Method for Load Flow Solutions of Distribution Systems"**,** ***Arabian Journal for Science and Engineering (Springer),*** Vol.44, no.3, pp. 1791-1808, 2019.

Conference

I. Krishna Murari and Narayana Prasad Padhy "Framework for Assessing the Economic Impacts of AC-DC Distribution Network on the Consumer", ***IEEE 59th International Scientific Conference on Power and Electrical Engineering of Riga Technical University***, Latvia, November 2018, pp.1-5.

Bibliography

[1]. A. A. Eajal, M. F. Shaaban, K. Ponnambalam and E. F. El-Saadany, "Stochastic Centralized Dispatch Scheme for AC/DC Hybrid Smart Distribution Systems," in *IEEE Transactions on Sustainable Energy*, vol. 7, no. 3, pp. 1046-1059, July 2016.

[2]. P. Wang, L. Goel, X. Liu, and F. H. Choo, "Harmonizing ac and dc: A hybrid ac/dc future grid solution," IEEE Power Energy Mag., vol. 11, no. 3, pp. 76–83, May/Jun. 2013.

[3]. G. F. Reed, B. M. Grainger, A. R. Sparacino and Z. H. Mao, "Ship to Grid: Medium-Voltage DC Concepts in Theory and Practice, " *IEEE Power and Energy Magazine*, vol. 10, no.6, pp. 70-79, 2012.

[4]. S. Sahoo and S. Mishra, "A Distributed Finite-Time Secondary Average Voltage Regulation and Current Sharing Controller for DC Microgrids," *IEEE Transactions on Smart Grid*, vol. 10, no. 1, pp. 282-292, Jan. 2019.

[5]. T. Adefarati and R. C. Bansal, "Integration of renewable distributed generators into the distribution system: a review," IET Renewable Power Generation, vol. 10, no. 7, pp. 873-884, 7 2016.

[6]. R. K. Sharma and S. Mishra, "Dynamic Power Management and Control of a PV PEM Fuel-Cell-Based Standalone ac/dc Microgrid Using Hybrid Energy Storage," in *IEEE Transactions on Industry Applications*, vol. 54, no. 1, pp. 526-538, Jan.-Feb. 2018.

[7]. C. Zhao, S. Dong, C. Gu, F. Li, Y. Song and N. P. Padhy, "New Problem Formulation for Optimal Demand Side Response in Hybrid AC/DC Systems," *IEEE Transactions on Smart Grid*, vol. PP, no. 99, pp. 1-1.

[8]. F. Blaabjerg, T. Dragievi, S. Doolla, N.Kang, " Recent advances in control, analysis and design of DC distribution systems and microgrids," *Electric Power Components and Systems*, vol. 45, no. 10, pp. 1031, 2017.

[9]. D. J. Hammerstrom, "AC Versus DC Distribution Systems Did We Get it Right?," *Power Engineering Society General Meeting*, Tampa, FL, 2007, pp. 1-5.

[10]. S. K. Chaudhary, J. M. Guerrero, and R. Teodorescu, "Enhancing the capacity of the AC distribution system using DC interlinks–A step toward future DC grid," IEEE Trans. Smart Grid, vol. 6, no. 4, pp. 1722–1729, July 2015.

[11]. K.Kurohane, T.Senjyu, A.Yona, N.Urasaki, T.Goya and T.Funabashi, "A hybrid smart AC/DC power system," IEEE Trans. Smart Grid, vol. 1, no. 2, pp. 199–204, Sept 2010.

[12]. M. Starke, L. M. Tolbert, and B. Ozpineci, "AC vs. DC distribution: A loss comparison," Transmission and Distribution Exposition Conference: IEEE PES Powering Toward the Future, PIMS, 2008.

[13]. A. Gupta, S. Doolla, and K. Chatterjee, “Hybrid AC–DC microgrid: systematic evaluation of control strategies,” IEEE Trans. Smart Grid, vol. 9, no. 4, pp. 3830-3843, Jul. 2018.

[14]. A. Jahangir, V. Nougain and S. Mishra, "Control Topology of Hybrid Energy Storage System for AC-DC Microgrid," *2018 IEEE International Conference on Power Electronics, Drives and Energy Systems (PEDES)*, Chennai, India, 2018, pp. 1-5.

[15]. K. Saxena and A. R. Abhyankar, "Agent based decentralized three-phase load flow computation of unbalanced distribution system," *2017 North American Power Symposium (NAPS)*, Morgantown, WV, 2017, pp. 1-6.

[16]. Hadi Saddat, Power System Analysis. McGraw-Hill, 1999.

[17]. H. K. Kesavan, M. A. Pai and M. V. Bhat, "Piecewise Solution of the Load-Flow Problem," in *IEEE Transactions on Power Apparatus and Systems*, vol. PAS-91, no. 4, pp. 1382-1386, July 1972.

[18]. W. F. Tinney and C. E. Hart, "Power Flow Solution by Newton's Method," in *IEEE Transactions on Power Apparatus and Systems*, vol. PAS-86, no. 11, pp. 1449-1460, Nov. 1967.

[19]. P. W. Sauer and M. A. Pai, "Power system steady-state stability and the load-flow Jacobian," in *IEEE Transactions on Power Systems*, vol. 5, no. 4, pp. 1374-1383, Nov. 1990.

[20]. B. Stott and O. Alsac, "Fast Decoupled Load Flow," in *IEEE Transactions on Power Apparatus and Systems*, vol. PAS-93, no. 3, pp. 859-869, May 1974.

[21]. J. Nanda, D.P. Kothari and S.C. Srivastava, “A Novel Second Order Fast Decoupled Load Flow Method in Polar Coordinates”, *Int. Journal of Electric Machines and Power Systems*, Vol 14, No. 5 , May 1988, pp. 339-351.

[22]. J. Nanda, D.P. Kothari and S.C. Srivastava, “Some Important Observations on Fast Decoupled Load Flow Algorithm”, Proc. of IEEE, Vol. 75, No. 5, May 1987, pp. 932-933.

[23]. Laxmi Srivastava, S.C. Srivastava and L.P. Singh, “Fast Decoupled Load Flow Methods in Rectangular Co-ordinates”, Int. Journal of Electrical Power and Energy Systems”, Vol. 13, No. 3, June 1991, pp. 160-166.

[24]. J. Beerten, S. Cole, and R. Belmans, “Generalized steady-state VSC MTDC model for sequential AC/DC power flow algorithms,” IEEE Trans. Power Syst., vol. 27, no. 2, pp. 821–829, 2012.

[25]. C. Liu, B. Zhang, Y. Hou, F. F. Wu, and Y. Liu, “An improved approach for AC-DC power flow calculation with multi-infeed DC systems,” IEEE Trans. Power Syst., vol. 26, no. 2, pp. 862–869, May 2011.

[26]. F Gonzalez, J. Roldan, C. Charalambous, “Solution of ac/dc power flow on a multiterminal HVDC system: illustrative case supergrid phase I,” International Universities Power Engineering Conference, pp. 1-7, 2012.

[27]. S. Messalti, S. Belkhiat, S. Saadate, D. Flieller, “A new approach for load flow analysis of integrated AC–DC power systems using sequential modified Gauss–Seidel methods, ” European Transactions on Electrical Power, vol. 22, pp. 421–432, 2012.

[28]. O. Osaloni, G. Radman, “Integrated AC/DC systems power flow solution using Newton–Raphson and Broyden approaches.,” Proceedings of the Thirty-Seventh Southeastern Symposium on System Theory, vol. 2, no. 10, pp. 225–229, 2005.

[29]. M. Baradar and M. Ghandhari, “A multi-option unified power flow approach for hybrid AC/DC grids incorporating multi-terminal VSC HVDC,” IEEE Trans. Power Syst., vol. 28, no. 3, pp. 2376–2383, 2013.

[30]. M. El-Hawary, S. Ibrahim, “A new approach to AC–DC load flow analysis, Electric Power Systems Res., ” vol. 33, pp.193-200, 1995.

[31]. E. Acha, B. Kazemtabrizi and L. M. Castro, “A New VSC-HVDC Model for Power Flows Using the Newton-Raphson Method,” in *IEEE Transactions on Power Systems*, vol. 28, no. 3, pp. 2602-2612, Aug. 2013.

[32]. R. Chai, B. Zhang, J. Dou, Z. Hao and T. Zheng, “Unified Power Flow Algorithm Based on the NR Method for Hybrid AC/DC Grids Incorporating VSCs,” *IEEE Transactions on Power Systems*, vol. 31, no. 6, pp. 4310-4318, Nov. 2016.

[33]. J. Lei, T. An, Z. Du and Z. Yuan, “A General Unified AC/DC Power Flow Algorithm With MTDC,” in *IEEE Transactions on Power Systems*, vol. 32, no. 4, pp. 2837-2846, July 2017.

[34]. Xinyi Zhang, Xueshan Han, Ming Yang, Donglei Sun, Yumin Zhang, Wuyang Gai, “A Novel Power Flow Algorithm for Hybrid AC/DC Power Grids,” *Electric Power Components and Systems*, vol. 45, pp. 1607, 2017, ISSN 1532-5008.

[35]. Luis M. Castro, Enrique Acha, Claudio R. Fuerte-Esquivel, “A novel VSC-HVDC link model for dynamic power system simulations, ” Electric Power Systems Research, vol. 126, pp. 111, 2015, ISSN 03787796.

[36]. H. M. A. Ahmed, A. B. Eltantawy and M. Salama, “A Generalized Approach to the Load Flow Analysis of AC-DC Hybrid Distribution Systems,” *IEEE Transactions on Power Systems*, vol. PP, no. 99, pp. 1-1,2017.

[37]. S.Iwamoto and Y.Tamura, “A load flow calculation method for ill conditioned power system,” IEEE Transactions on Power Apparatus and Systems, vol.100, no.4, pp.1736-1743, April 1981.

[38]. Jen-Hao Teng and Chuo-Yean Chang, “A novel and fast three-phase load flow for unbalanced radial distribution systems,” in *IEEE Transactions on Power Systems*, vol. 17, no. 4, pp. 1238-1244, Nov. 2002.

[39]. R. Gnanavignesh, G. Gurrala and U. J. Shenoy, "A piecewise parallel solution of current mismatch based Newton-Raphson power flow," *2017 IEEE PES Asia-Pacific Power and Energy Engineering Conference (APPEEC)*, Bangalore, 2017, pp. 1-6.

[40]. R. D. Zimmerman and Hsiao-Dong Chiang, “Fast decoupled power flow for unbalanced radial distribution systems, ” *IEEE Transactions on Power Systems*, vol. 10, no. 4, pp. 2045-2052, Nov. 1995.

[41]. A. Losi and M. Russo, "Object-oriented load flow for radial and weakly meshed distribution networks," *IEEE Transactions on Power Systems*, vol. 18, no. 4, pp. 1265-1274, Nov. 2003.

[42]. T.Ochi, D. Yamashita, K.Koyanagi and R.Yokoyama, " The development and application of fast decoupled load flow method for distribution systems with high R/X ratio lines," ISGT IEEE PES, pp.1-6, Feb. 2013.

[43]. P. Aravindhababu and R. Ashokkumar, "A fast decoupled power flow for distribution systems, " Electric Power Components and Systems, Vol.36, No.9, pp. 932-940, 2008.

[44]. O. L. Tortelli, E. M. Lourenço, A. V. Garcia and B. C. Pal, "Fast Decoupled Power Flow to Emerging Distribution Systems via Complex pu Normalization," *IEEE Transactions on Power Systems*, vol. 30, no. 3, pp. 1351-1358, May 2015.

[45]. D. Khaniya, A. K. Srivastava and N. N. Schulz, "Distribution power flow for multiphase meshed or radial systems, " *2008 40th North American Power Symposium*, Calgary, AB, 2008, pp. 1-5.

[46]. P. Aravindhababu, "A new fast decoupled power flow method for distribution systems," Electric Power Components and Systems, " Vol.3l, No.9, pp. 869-878, 2003.

[47]. S.Ghosh and D.Das, "Method for load-flow solution of radial distribution networks," IEE Proccedings (GTD), vol.146, no.6,pp.641-648,Nov. 1999.

[48]. G. W. Chang, S. Y. Chu and H. L. Wang, "An Improved Backward/Forward Sweep Load Flow Algorithm for Radial Distribution Systems, " in *IEEE Transactions on Power Systems*, vol. 22, no. 2, pp. 882-884, May 2007.

[49]. Y.Ju, W.Wu and H.Sun, " Loop-analysis based continuation power flow algorithm for distribution networks," IET Gen. Trans. Dist., vol.8, no.7,pp.1284-1292, Jan. 2014.

[50]. T. Alinjak, I. Pavić and M. Stojkov, "Improvement of backward/forward sweep power flow method by using modified breadth-first search strategy," *IET Generation, Transmission & Distribution*, vol. 11, no. 1, pp. 102-109, 5 1 2017.

[51]. Zhuding Wang, Fen Chen and Jingui Li, "Implementing transformer nodal admittance matrices into backward/forward sweep-based power flow analysis for unbalanced radial distribution systems, " *IEEE Transactions on Power Systems*, vol. 19, no. 4, pp. 1831-1836, Nov. 2004.

[52]. M. F. AlHajri and M. E. El-Hawary, "Exploiting the Radial Distribution Structure in Developing a Fast and Flexible Radial Power Flow for Unbalanced Three-Phase Networks, " *IEEE Transactions on Power Delivery*, vol. 25, no. 1, pp. 378-389, Jan. 2010.

[53]. M. R. Shakarami, H. Beiranvand, A. Beiranvand, and E. Sharifipour, "A recursive power flow method for radial distribution networks: Analysis, solvability and convergence," Int. J. Elect. Power Energy Syst., vol. 86, pp. 71–80, Mar. 2017.

[54]. U. Ghatak and V. Mukherjee, "A fast and efficient load flow technique for unbalanced distribution system," Int. J. Electr. Power Energy Syst., vol. 84, pp. 99–110, 2017.

[55]. U. Ghatak and V. Mukherjee, “An improved load flow technique based on load current injection for modern distribution system,” Electrical Power and Energy Systems, vol. 84, pp 168-181,2017.

[56]. M.P. Selvan and K.S. Swarup, “Distribution system load flow using object oriented methodology,” in Proc. Int. Conf. Power System Technology (POWERCON 2004), Singapore, Nov. 2004, vol. 2.

[57]. M P Selvan and K.S.Swarup, “Modelling and Analysis of Unbalanced Distribution System using Object Oriented Methodology, ” Electric Power Systems Research, vol. 76, no. 11, pp.968, 2006..

[58]. S. Khushalani, J. M. Solanki and N. N. Schulz, "Development of Three-Phase Unbalanced Power Flow Using PV and PQ Models for Distributed Generation and Study of the Impact of DG Models," in *IEEE Transactions on Power Systems*, vol. 22, no. 3, pp. 1019-1025, Aug. 2007.

[59]. Khushalani and Schulz, “Unbalanced Distribution Power Flow with Distributed Generation,” *2005/2006 IEEE/PES Transmission and Distribution Conference and Exhibition*, Dallas, TX, 2006, pp. 301-306.

[60]. R. Ranjan and Das, “Simple and efficient computer algorithm to solve radial distribution networks,” Elect. Power Compon. Syst., vol. 31, no. 1, pp. 95–107, 2003.

[61]. C. S. Cheng and D. Shirmohammadi, “A Three-Phase Power Flow Method for Real-Time Distribution System Analysis,” IEEE Trans. Power Systems, vol. 10, no. 2, pp. 671–679, May 1995.

[62]. S. F. Mekhamer, S. A. Soliman, M. A. Moustafa, and M. E. El-Hawary, “Load flow solution of radial distribution feeders: A new contribution,” Int. J. Elect. Power Energy Syst., vol. 24, no. 9, pp. 701–707, Nov. 2002.

[63]. A. Augugliaro, L. Dusonchet, S. Favuzza, M. G. Ippolito, and E. Riva Sanseverino, “A new backward/forward method for solving radial distribution networks with PV nodes,” Elect. Power Syst. Res., vol. 78, pp. 330–336, 2008.

[64]. J. Liu, M. M. A. Salama, R. R. Mansour, "An efficient power flow algorithm for distribution systems with polynomial load", *Int. J. Electr. Eng. Education*, vol. 39, no. 4, pp. 371-386, Oct. 2002.

[65]. D. Shirmohammadi, H. W. Hong, A. Semlyen, and G. X. Luo, “A Compensation-Based Power Flow Method For Weakly Meshed Distribution and Transmission Networks,” IEEE Trans. Power Systems, vol. 3, pp. 753–762, May 1988.

[66]. D. Das, D. P. Kothari, and A. Kalam, “Simple and efficient method for load flow solution of radial distribution networks,” Elect. Power Energy Syst., vol. 17, no. 5, pp. 335–346, 1995.

[67]. J. H. Teng, “A network-topology based three-phase load flow for distribution systems,” Proc. Natl. Sci. Council ROC (A), vol. 24, no. 4, pp. 259–264, 2000.

[68]. J.-H. Teng, “A direct approach for distribution system load flow solutions,” IEEE Transactions on Power Delivery, vol. 18, no. 3, pp. 882–887, July 2003.

[69]. S. Mousavizadeh, M.R. Haghifam, M.H. Shariatkhah, "A new approach for load flow calculation in AC/DC distribution networks considering the control strategies of different converters, " *Int. Trans. Electr. Energy Syst.*, vol. 26, no. 11, pp. 2479-2493, 2016.

[70]. W.H. Kresting, Distribution System Modeling and Analysis. CRC Press, 2016.

[71]. B. Shah, A. Bose and A. Srivastava, "Load modeling and voltage optimization using smart meter infrastructure," *2013 IEEE PES Innovative Smart Grid Technologies Conference (ISGT)*, Washington, DC, 2013, pp. 1-6.

[72]. M.E. Baran, F.F. Wu, "Network reconfiguration in distribution systems for loss reduction and load balancing", *IEEE Trans. Power Deliv.*, vol. 4, no. 2, pp. 1401-1407, 1989.

[73]. M. Baran, F. Wu, "Optimal capacitor placement on radial distribution systems", *IEEE Trans. Power Deliv.*, vol. 4, no. 1, pp. 725-734, 1989.

[74]. J. Subrahmanyam and C. Radhakrishna, "A simple method for feeder reconfiguration of balanced and unbalanced distribution systems for loss minimization", Electrical Power components and Systems, Vol. 38, no. 1, January 2010, pp.72-84.

[75]. W. H. Kersting, "Radial distribution test feeders," IEEE Trans. Power Syst., vol. 6, no. 3, pp. 975–985, Aug. 1991.

[76]. S. R. Behera, S. P. Dash and B. K. Panigrahi, "Optimal positioning and sizing of distributed generations in radial distribution system with consideration of real power loss and short circuit currents," 2017 7th International Conference on Power Systems (ICPS), Pune, 2017, pp. 533-538.

[77]. A. K. Srivastava, A. A. Kumar and N. N. Schulz, "Impact of Distributed Generations With Energy Storage Devices on the Electric Grid," in *IEEE Systems Journal*, vol. 6, no. 1, pp. 110-117, March 2012.

[78]. S. Deshmukh, B. Natarajan and A. Pahwa, "Voltage/VAR Control in Distribution Networks via Reactive Power Injection Through Distributed Generators," in *IEEE Transactions on Smart Grid*, vol. 3, no. 3, pp. 1226-1234, Sept. 2012.

[79]. A. R. Malekpour and A. Pahwa, "Reactive power and voltage control in distribution systems with photovoltaic generation," *2012 North American Power Symposium (NAPS)*, Champaign, IL, 2012, pp. 1-6.

[80]. A. Dubey, "Distributed resource integration analysis and network design of electric power distribution systems, Ph.D Thesis, " The university of Texas at Austin, 2015.

[81]. M. Mukherjee, S. Poudel, A. Dubey and A. Bose, "Distributed Generator Sizing for Joint Optimization of Resilience and Voltage Regulation," *2018 North American Power Symposium (NAPS)*, Fargo, ND, 2018, pp. 1-6.

[82]. A. K. Pradhan, A. Routray and S. Madhan Gudipalli, "Fault Direction Estimation in Radial Distribution System Using Phase Change in Sequence Current," in *IEEE Transactions on Power Delivery*, vol. 22, no. 4, pp. 2065-2071, Oct. 2007.

[83]. A. Zamani, T. Sidhu and A. Yazdani, "A strategy for protection coordination in radial distribution networks with distributed generators," *IEEE PES General Meeting*, Providence, RI, 2010, pp. 1-8.

[84]. A. Fazanehrafat, S. A. M. Javadian, S. M. T. Bathaee and M. -. Haghifamt, "Maintaining The Recloser-Fuse Coordination in Distribution Systems in Presence of DG by Determining DG's Size," *2008 IET 9th International Conference on Developments in Power System Protection (DPSP 2008)*, Glasgow, 2008, pp. 132-137.

[85]. M. Malinowski, A. Milczarek, R. Kot, Z. Goryca and J. T. Szuster, "Optimized Energy-Conversion Systems for Small Wind Turbines: Renewable energy sources in modern distributed power generation systems," in *IEEE Power Electronics Magazine*, vol. 2, no. 3, pp. 16-30, Sept. 2015.

[86]. REN 21 Steering Committee: 'Renewables global status report, 2016'.

[87]. J.C. Hernandez, J.De la Cruz, B. Ogayar, "Electrical protection for the grid-interconnection of photovoltaic-distributed generation, " *Electr. Power Syst. Res*., vol. 89, pp. 85-99, 2012.

[88]. J.C. Hernandez, J.De la Cruz, P.G. Vidal, B. Ogayar, "Conflicts in the distribution network protection in the presence of large photovoltaic plants: the case of ENDESA," *Int. Trans. Electr. Energy Syst*., vol. 23, no. 5, pp. 669–688, 2013.

[89]. A. Kamel, M.A. Alaam, A.M. Azmy, A.Y. Abdelaziz, "Protection Coordination for Distribution Systems in Presence of Distributed Generators," *Electric Power Components and Systems*, vol. 41, no.15, pp. 155-1566, 2013.

[90]. M. Singh, B. Panigrahi, and A. Abhyankar, "Optimal coordination of directional over-current relays using teaching learning-based optimization (TLBO) algorithm," Int. J. Elect. Power Energy Syst., vol. 50, pp. 33–41, 2013.

[91]. N. Hadjsaid, J. -. Canard and F. Dumas, "Dispersed generation impact on distribution networks," *IEEE Computer Applications in Power*, vol. 12, no. 2, pp. 22-28, April 1999.

[92]. F. Li , J. Marangon-Lima, H. Rudnick, L.M.Marangon-Lima. N.P.Padhy, G.Brunekreet, J.Reneses, and C.Kang, "Distribution Pricing: Are We Ready for the Smart Grid?, " *IEEE Power and Energy Magazine*, vol. 13, no. 4, pp. 76-86, July-Aug. 2015

[93]. J. Mutale, G. Strbac and D. Pudjianto, "Methodology for Cost Reflective Pricing of Distribution Networks with Distributed Generation," *2007 IEEE Power Engineering Society General Meeting*, Tampa, FL, 2007, pp. 1-5.

[94]. H. Rudnick, H. Sanhueza and D. Watts, "Discussion of "Distribution pricing based on yardstick regulation, " IEEE Transactions on Power Systems, vol. 18, no. 2, pp. 954-, May 2003.

[95]. H. Rudnick and J. A. Donoso, "Integration of price cap and yardstick competition schemes in electrical distribution regulation," *IEEE Transactions on Power Systems*, vol. 15, no. 4, pp. 1428-1433, Nov 2000.

[96]. J. W. M. Lima, J. C. C. Noronha, H. Arango and P. E. S. dos Santos, "Distribution pricing based on yardstick regulation," *IEEE Transactions on Power Systems*, vol. 17, no. 1, pp. 198-204, Feb 2002.

[97]. J. W. M. Lima, J. C. C. Noronha, H. Arango and P. E. S. dos Santos, "Closure on "Distribution pricing based on yardstick regulation," *IEEE Transactions on Power Systems*, vol. 18, no. 2, pp. 955-, May 2003.

[98]. A. Picciariello, J. Reneses, P. Frias, et al, “Distributed generation and distribution pricing: why do we need new tariff design methodologies?, ” *Electr. Power Syst. Res*., vol.119, pp. 370–376, 2015.

[99]. P. M. Sotkiewicz and J. M. Vignolo, "Nodal pricing for distribution networks: efficient pricing for efficiency enhancing DG," in *IEEE Transactions on Power Systems*, vol. 21, no. 2, pp. 1013-1014, May 2006.

[100]. J. W. Marangon Lima, “Allocation of transmission fixed charges: an overview, ” *IEEE Transactions on Power Systems*, vol. 11, no. 3, pp. 1409-1418, Aug 1996.

[101]. D. Shirmohammadi, C. Rajgopalan, E. R. Alward, and C. L. Thomas, “Cost of transmission transactions: An introduction,” IEEE Trans.Power Syst., vol. 6, no. 3, pp. 1006–1016, Aug. 1991.

[102]. P.Williams and G. Strbac, “Costing and pricing of electricity distribution services,” Power Eng. J., pp. 125–136, Jun. 2001.

[103]. P. Jesus et al., “Uniform marginal pricing for the remuneration of distribution networks,” IEEE Trans. Power Syst., vol. 20, no. 3, pp. 1302–1310, Aug. 2005.

[104]. H. M. Merrill and B. W. Erickson, “Wheeling rates based on marginal cost theory,” IEEE Trans. Power Syst., vol. 4, no. 4, pp. 1445–1451,Nov. 1989.

[105]. D. Shirmohammadi, P. R. Gribik, and E. T. K. Law, “Evaluation of transmission network capacity use for wheeling transactions,” IEEE Trans. Power Syst., vol. 4, no. 4, pp. 1405–1413, Nov. 1989.

[106]. A. M. L. da Silva, J. G. de Carvalho Costa and L. H. Lopes Lima, “A new methodology for cost allocation of transmission systems in interconnected energy markets, ” IEEE Transactions on Power Systems, vol. 28, no. 2, pp. 740-748, May 2013.

[107]. Z. Yang, H. Zhong, Q. Xia, C. Kang, T. Chen and Y. Li, "A Structural Transmission Cost Allocation Scheme Based on Capacity Usage Identification," in *IEEE Transactions on Power Systems*, vol. 31, no. 4, pp. 2876-2884, July 2016.

[108]. K. L. Lo, M. Y. Hassan and S. Jovanovic, "Assessment of MW-mile method for pricing transmission services: a negative flow-sharing approach," *IET Generation, Transmission & Distribution*, vol. 1, no. 6, pp. 904-911, Nov. 2007.

[109]. A. Roy, A. R. Abhyankar, P. Pentayya and S. A. Khaparde, "Electricity transmission pricing: tracing based point-of-connection tariff for Indian power system," *IEEE Power Engineering Society General Meeting*, Montreal, 2006.

[110]. S. Nojeng, M. Y. Hassan, D. M. Said, M. P. Abdullah and F. Hussin, "Improving the MW-Mile Method Using the Power Factor-Based Approach for Pricing the Transmission Services," *IEEE Transactions on Power Systems*, vol. 29, no. 5, pp. 2042-2048, Sept. 2014.

[111]. J. Bialek, “Allocation of transmission supplementary charge to real and reactive power loads,” IEEE Trans. Power Syst., vol. 13, no. 3, pp. 749–754, Aug. 1998.

[112]. F.Li, N.P.Padhy, J.Wang and B.K Kuri, “Cost-benefit reflective distribution charging methodology,” IEEE Trans.Power Syst., vol.23, no. 1, pp.58-64, 2008.

[113]. D. Bhowmik, N. Sinha and A. K. Sinha, "Investigation of multifarious power transferred through the transmission network for all associated generators in the system individually," in *IET Generation, Transmission & Distribution*, vol. 12, no. 8, pp. 1848-1855, 2018.

[114]. A. Enshaee and G. R. Yousefi, "Tracing Reactive Power Flows and Allocating Transmission Lines Losses: An Analytical Method," in *IEEE Systems Journal*, vol. 13, no. 1, pp. 783-791, March 2019.

[115]. A. Enshaee and P. Enshaee, "New reactive power flow tracing and loss allocation algorithms for power grids using matrix calculation," *Int. J. Elect. Power Energy Syst*., vol. 87, pp. 89–98, May 2017.

[116]. C. Achayuthakan, C. J. Dent, J. W. Bialek and W. Ongsakul, "Electricity Tracing in Systems With and Without Circulating Flows: Physical Insights and Mathematical Proofs," in *IEEE Transactions on Power Systems*, vol. 25, no. 2, pp. 1078-1087, May 2010.

[117]. M. De and S. K. Goswami, "Reactive power cost allocation by power tracing based method," *Energy Convers. Mgmt*., vol. 64, pp. 43–51, 2012.

[118]. C. Gu, J. Wu and F. Li, "Reliability-Based Distribution Network Pricing," in *IEEE Transactions on Power Systems*, vol. 27, no. 3, pp. 1646-1655, Aug. 2012.

[119]. F. Li and C. Gu, "Long-Run Incremental Cost Pricing for Negative Growth Rates," in *IEEE Transactions on Power Systems*, vol. 26, no. 4, pp. 2567-2568, Nov. 2011.

[120]. Dennis McKeown, "Simple Methods for Calculating Short Circuit Current without a Computer," GE publication library.

[121]. W.H. Albeck, Jr./Edwards ,Kelcey and Steven Estomin/Exeter Associates, "Cost Benefits for Overhead vs. Underground Utilities, " Maryland State Highway Administration Office of Policy & Research, Rep. SP208B4C , 2003.

[122]. B. H. Kim and M. L. Baughman, "The economic efficiency impacts of alternatives for revenue reconciliation, " *IEEE Transactions on Power Systems*, vol. 12, no. 3, pp. 1129-1135, Aug 1997.

[123]. C. Gu and F. Li, "Long-Run Marginal Cost Pricing Based on Analytical Method for Revenue Reconciliation," in *IEEE Transactions on Power Systems*, vol. 26, no. 1, pp. 103-110, Feb. 2011.